ВЕСТНИК ТРАНСПЛАНТОЛОГИИ И ИСКУССТВЕННЫХ ОРГАНОВ

VESTNIK TRANSPLANTOLOGII I ISKUSSTVENNYKH ORGANOV

RUSSIAN JOURNAL OF TRANSPLANTOLOGY AND ARTIFICIAL ORGANS

УЧРЕДИТЕЛИ: ОБЩЕРОССИЙСКАЯ ОБЩЕСТВЕННАЯ ОРГАНИЗАЦИЯ ТРАНСПЛАНТОЛОГОВ «РОССИЙСКОЕ ТРАНСПЛАНТОЛОГИЧЕСКОЕ ОБЩЕСТВО»

ФГБУ «НМИЦ ТИО ИМЕНИ АКАДЕМИКА В.И. ШУМАКОВА» МИНЗДРАВА РОССИИ

ФГАОУ ВО «ПЕРВЫЙ МГМУ ИМЕНИ И.М. СЕЧЕНОВА» МИНЗДРАВА РОССИИ (СЕЧЕНОВСКИЙ УНИВЕРСИТЕТ)

THE OFFICIAL JOURNAL OF ALL-RUSSIAN PUBLIC ORGANIZATION OF TRANSPLANTOLOGISTS "RUSSIAN TRANSPLANT SOCIETY"

SHUMAKOV NATIONAL MEDICAL RESEARCH CENTER OF TRANSPLANTOLOGY AND ARTIFICIAL ORGANS

I.M. SECHENOV FIRST MOSCOW STATE MEDICAL UNIVERSITY (SECHENOV UNIVERSITY)

2020. Том XXII. № 4

2020. Vol. XXII. № 4

Научно-практический журнал основан в 1999 г.
Регистр. № 018616

Scientific and Practical Journal was founded in 1999
Reg. № 018616

Журнал «Вестник трансплантологии и искусственных органов» включен ВАК РФ в перечень российских рецензируемых научных изданий, в которых должны быть опубликованы результаты диссертационных работ

"Russian Journal of Transplantology and Artificial Organs" is included in the list of leading peer-reviewed scientific publication editions, produced in the Russian Federation and is recommended for publication of primary results of dissertation research

Журнал «Вестник трансплантологии и искусственных органов» индексируется в Scopus и размещен на платформе Web of Science Core Collection: Emerging Science Citation Index

«Russian Journal of Transplantology and Artificial Organs" is indexed in Scopus and in the Emerging Science Citation Index of the Web of Science Core Collection

ISSN 1995-1191

Адрес для корреспонденции:

Россия, 123182, Москва, ул. Щукинская, 1
Тел./факс +7 (499) 193 87 62
E-mail: vestniktranspl@gmail.com
Интернет-сайт журнала: http://journal.transpl.ru
Научная электронная библиотека: http://elibrary.ru

Address for correspondence:

1, Shchukinskaya st., Moscow 123182, Russia
Tel./Fax +7 (499) 193 87 62
E-mail: vestniktranspl@gmail.com
Journal's web site: http://journal.transpl.ru
Scientific eLibrary: http://elibrary.ru

Подписной индекс в каталоге «Газеты и журналы» – 80248

СОДЕРЖАНИЕ

СТРАНИЦА ГЛАВНОГО РЕДАКТОРА

Научная специальность «Трансплантология и искусственные органы»: новое в порядке присуждения ученых степеней 6
С.В. Готье

ТРАНСПЛАНТАЦИЯ ОРГАНОВ

Трансплантация сердца у реципиентов с сахарным диабетом 2-го типа 8
В.Н. Попцов, Е.А. Спирина, Е.Н. Золотова, В.М. Захаревич, Н.Н. Колоскова, Н.П. Можейко, А.А. Сибякина, Я.Л. Поз, А.И. Скокова, В.В. Боронова, В.Ю. Воронков, В.М. Хатуцкий

Диагностическое значение микроРНК-101 и микроРНК-27 при остром отторжении трансплантированного сердца 18
Д.А. Великий, О.Е. Гичкун, С.О. Шарапченко, Н.П. Можейко, Р.М. Курабекова, О.П. Шевченко

Модель оценки донорского сердца, прогнозирующая его использование для трансплантации 24
Э.А. Тенчурина, М.Г. Минина

Особенности вакцинации против гемофильной инфекции типа *b* пациентов листа ожидания трансплантации легких 28
В.Б. Полищук, М.П. Костинов, А.А. Рыжов, О.О. Магаршак, Н.Е. Ястребова, Н.А. Карчевская, Е.А. Тарабрин, Т.Э. Каллагов, А.Е. Власенко

Индукция циркулирующих CD133+ стволовых лимфоцитов, коммитированных к ткани печени, у пациентов из листа ожидания трансплантации 36
А.Н. Шутко, О.А. Герасимова, Н.В. Марченко, Ф.К. Жеребцов

Химиоэмболизация печеночных артерий у больных гепатоцеллюлярным раком на фоне цирроза перед трансплантацией печени: прогностическое значение концентрации альфафетопротеина 43
Д.А. Гранов, А.С. Полехин, П.Г. Таразов, И.О. Руткин, И.И. Тилеубергенов, В.В. Боровик

Лечение кровотечений из варикозно расширенных вен пищевода у больных из листа ожидания трансплантации печени 48
В.Л. Коробка, М.Ю. Кострыкин, А.М. Шаповалов

Клинико-функциональные особенности сквозной кератопластики в Королевстве Иордания. Опыт одного центра 54
М.А. Танаш, М.А. Фролов, П.А. Гончар, Г.Н. Душина, Л.Т. Абабнех

Особенности ведения реципиентов почечного трансплантата с новой коронавирусной инфекцией COVID-19 57
О.Н. Котенко, Л.Ю. Артюхина, Н.Ф. Фролова, Е.С. Столяревич

J-образная стернотомия в хирургии пороков аортального клапана и восходящей аорты. Непосредственные результаты 61
Г.А. Акопов, А.С. Иванов, Т.Н. Говорова, Д.В. Москалев

CONTENTS

EDITORIAL

Scientific specialty "Transplantology and artificial organs": new in the order of awarding academic degrees 6
S.V. Gautier

ORGAN TRANSPLANTATION

Heart transplantation in diabetic recipients 8
V.N. Poptsov, E.A. Spirina, E.N. Zolotova, V.M. Zakharevich, N.N. Koloskova, N.P. Mozheiko, A.A. Sibiakina, I.L. Poz, A.I. Skokova, V.V. Boronova, V.Yu. Voronkov, V.M. Khatutskii

Diagnostic value of miRNA-101 and miRNA-27 in acute heart transplant rejection 18
D.A. Velikiy, O.E. Gichkun, S.O. Sharapchenko, N.P. Mozheiko, R.M. Kurabekova, O.P. Shevchenko

A donor heart scoring model to predict transplant outcomes 24
E.A. Tenchurina, M.G. Minina

Features of *Haemophilus influenzae* type *b* vaccine in patients waitlisted for lung transplantation 28
V.B. Polishchuk, M.P. Kostinov, A.A. Pyzhov, O.O. Magarshak, N.E. Yastrebova, N.A. Karchevskaya, E.A. Tarabrin, T.E. Kallagov, A.E. Vlasenko

Induction of circulating CD133+ stem cells committed to cirrhotic livers in waitlisted patients 36
A.N. Shoutko, O.A. Gerasimova, N.V. Marchenko, F.K. Zherebtsov

Transcatheter hepatic arterial chemoembolization in cirrhotic patients with hepatocellular carcinoma before liver transplantation: the prognostic value of alpha-fetoprotein concentrations 43
D.A. Granov, A.S. Polehin, P.G. Tarazov, I.O. Rutkin, I.I. Tileubergenov, V.V. Borovik

Management of variceal bleeding in the liver transplant waiting list 48
V.L. Korobka, M.Yu. Kostrykin, A.M. Shapovalov

Clinical and functional features of penetrating keratoplasty in the Kingdom of Jordan. A single-center experience 54
M.A. Tanash, M.A. Frolov, P.A. Gonchar, G.N. Dushina, L.T. Ababneh

Clinical course and approaches to therapy in kidney transplant recipients with the novel COVID-19 disease 57
O.N. Kotenko, L.Yu. Artyukhina, N.F. Frolova, E.S. Stolyarevich

J-shaped sternotomy in aortic valve repair and ascending aorta replacement. Short-term results 61
G.A. Akopov, A.S. Ivanov, T.N. Govorova, D.V. Moskalev

ИСКУССТВЕННЫЕ ОРГАНЫ

Проблема биосовместимости и тромбогенности устройств вспомогательного кровообращения
М.О. Жульков, Д.А. Сирота, А.В. Фомичев, А.С. Гренадеров, А.М. Чернявский

РЕГЕНЕРАТИВНАЯ МЕДИЦИНА И КЛЕТОЧНЫЕ ТЕХНОЛОГИИ

Функциональная эффективность клеточно-инженерной конструкции печени на основе тканеспецифического матрикса (экспериментальная модель хронической печеночной недостаточности)
М.Ю. Шагидулин, Н.А. Онищенко, Ю.Б. Басок, А.М. Григорьев, А.Д. Кириллова, Е.А. Немец, Е.А. Волкова, И.М. Ильинский, Н.П. Можейко, В.И. Севастьянов, С.В. Готье

Микроносители в виде волокон из натурального шелка для культивирования клеток
М.М. Боброва, Л.А. Сафонова, А.Е. Ефимов, О.И. Агапова, И.И. Агапов

Биодеградируемые материалы на основе тканей из натурального шелка как перспективные скаффолды для тканевой инженерии и регенеративной медицины
Л.А. Сафонова, М.М. Боброва, А.Е. Ефимов, О.И. Агапова, И.И. Агапов

Исследование микро- и наноструктуры клеток печени, культивированных на биодеградируемых скаффолдах на основе фиброина шелка, методом сканирующей зондовой оптической нанотомографии
О.И. Агапова, А.Е. Ефимов, Л.А. Сафонова, М.М. Боброва, И.И. Агапов

Особенности механизмов реализации дистантного стимулирующего эффекта аутотрансплантации кожного лоскута на перфузию микроциркуляторного русла в условиях локальных и системных нарушений
А.Н. Иванов, Д.Д. Лагутина, Т.В. Степанова

Аутологичные стимуляторы регенерации при имплантации аллогенных костнопластических материалов
К.А. Воробьев, Т.О. Скипенко, Н.В. Загородний, Д.В. Смоленцев, А.Р. Закирова, В.И. Севастьянов

ОБЗОРЫ ЛИТЕРАТУРЫ

Роль эндоваскулярных и эндобилиарных методов в лечении осложнений после трансплантации печени
С.В. Готье, М.А. Восканов, А.Р. Монахов, К.О. Сёмаш

Обзор хирургической техники выполнения лапароскопических донорских резекций фрагментов печени
К.О. Сёмаш, С.В. Готье

Способы артериальной реконструкции трансплантата поджелудочной железы
Н.С. Журавель, И.В. Дмитриев, А.В. Пинчук

ARTIFICIAL ORGANS

67 The problem of biocompatibility and thrombogenicity in mechanical circulatory assist devices
M.O. Zhulkov, D.A. Sirota, A.V. Fomichev, A.S. Grenaderov, A.M. Chernyavsky

REGENERATIVE MEDICINE AND CELL TECHNOLOGIES

72 Functional efficiency of cell-engineered liver constructs based on tissue-specific matrix (experimental model of chronic liver failure)
M.Yu. Shagidulin, N.A. Onishchenko, Yu.B. Basok, A.M. Grigoriev, A.D. Kirillova, E.A. Nemets, E.A. Volkova, I.M. Iljinsky, N.P. Mozheiko, V.I. Sevastianov, S.V. Gautier

78 Natural silk fiber microcarriers for cell culture
M.M. Bobrova, L.A. Safonova, A.E. Efimov, O.I. Agapova, I.I. Agapov

83 Biodegradable materials based on natural silk fabric as promising scaffolds for tissue engineering and regenerative medicine
L.A. Safonova, M.M. Bobrova, A.E. Efimov, O.I. Agapova, I.I. Agapov

91 Investigation of the micro- and nano-structure of liver cells cultured on biodegradable silk fibroin-based scaffolds using scanning probe optical nanotomography
O.I. Agapova, A.E. Efimov, L.A. Safonova, M.M. Bobrova, I.I. Agapov

97 Characteristics of mechanisms of the distant stimulating effect of skin flap autograft on microvascular perfusion in local and systemic microcirculation disorders
A.N. Ivanov, D.D. Lagutina, T.V. Stepanova

105 Autologous regenerative stimulants for bone allograft implantation
K.A. Vorobyov, T.O. Skipenko, N.V. Zagorodniy, D.V. Smolentsev, A.R. Zakirova, V.I. Sevastianov

LITERATURE REVIEWS

110 The role of endovascular and endobiliary methods in the treatment of post-liver transplant complications
S.V. Gautier, M.A. Voskanov, A.R. Monakhov, K.O. Semash

118 Review of surgical techniques for performing laparoscopic donor hepatectomy
K.O. Semash, S.V. Gautier

122 Methods of arterial reconstruction for pancreatic graft
N.S. Zhuravel, I.V. Dmitriev, A.V. Pinchuk

КЛИНИЧЕСКИЕ НАБЛЮДЕНИЯ

Лечение экспираторного стеноза трахеи в сочетании с бронхоэктатической болезнью у реципиента донорских легких (первое наблюдение в Российской Федерации)
И.В. Пашков, А.В. Никулин, Д.О. Олешкевич, М.Т. Беков, Р.А. Латыпов, Е.Ф. Шигаев, А.Г. Сухорукова, В.Н. Попцов, Е.А. Спирина, Е.В. Лебедев, Я.С. Якунин
129

Трансплантация сердца у реципиента с аномальной левой верхней полой веной
Г.В. Анискевич, Г.А. Садриева, В.Н. Попцов, Е.А. Спирина, В.И. Орлов, Р.Ш. Саитгареев
134

Хронический миокардит тяжелого течения, верифицированный как гигантоклеточный: неизбежный выбор в пользу трансплантации сердца
О.В. Благова, Ю.А. Лутохина, Д.Х. Айнетдинова, В.П. Седов, А.Н. Воловченко, Д.А. Парфенов, Н.П. Можейко
138

Случай успешного лечения синдрома исчезающего промежуточного бронха после трансплантации легких
И.В. Пашков, М.Т. Беков, Р.А. Латыпов, Д.О. Олешкевич, Е.Ф. Шигаев, Е.В. Лебедев, К.С. Смирнов, С.В. Готье
146

Морфология трансплантированной печени при возвратном прогрессивном семейном внутрипеченочном холестазе второго типа
И.М. Ильинский, Н.П. Можейко, О.М. Цирульникова
153

Новая коронавирусная инфекция (COVID-19) у больного с декомпенсированным циррозом печени
О.В. Тащян, М.Г. Мнацаканян, А.П. Погромов, И.В. Куприна, Ю.Ф. Шумская
157

ИНФОРМАЦИЯ

Требования к публикациям
161

CLINICAL CASES

Treatment of expiratory tracheal stenosis in combination with bronchiectasis in a lung recipient (initial report in the Russian Federation)
I.V. Pashkov, A.V. Nikulin, D.O. Oleshkevich, M.T. Bekov, R.A. Latypov, E.F. Shigaev, A.G. Suchorukova, V.N. Poptsov, E.A. Spirina, E.V. Lebedev, Ya.S. Yakunin
129

Heart transplant in a patient with persistent left superior vena cava
G.V. Aniskevich, G.A. Sadrieva, V.N. Poptsov, E.A. Spirina, V.I. Orlov, R.Sh. Saitgareev
134

Verified chronic severe giant cell myocarditis: an inevitable choice for heart transplantation
O.V. Blagova, Yu.A. Lutokhina, D.H. Ainetdinova, V.P. Sedov, A.N. Volovchenko, D.A. Parfenov, N.P. Mozheiko
138

Successful treatment of vanishing bronchus intermedius syndrome following lung transplantation
I.V. Pashkov, M.T. Bekov, R.A. Latypov, D.O. Oleshkevich, E.F. Shigaev, E.V. Lebedev, K.S. Smirnov, S.V. Gautier
146

Morphology of transplanted liver in recurrent progressive familial intrahepatic cholestasis type 2
I.M. Iljinsky, N.P. Mozheiko, O.M. Tsirulnikova
153

COVID-19 in decompensated cirrhosis
O.V. Tashchyan, M.G. Mnatsakanyan, A.P. Pogromov, I.V. Kuprina, Yu.F. Shumskaya
157

INFORMATION

Instructions to authors
161

НАУЧНАЯ СПЕЦИАЛЬНОСТЬ «ТРАНСПЛАНТОЛОГИЯ И ИСКУССТВЕННЫЕ ОРГАНЫ»: НОВОЕ В ПОРЯДКЕ ПРИСУЖДЕНИЯ УЧЕНЫХ СТЕПЕНЕЙ

Глубокоуважаемые коллеги!

Перед Вами 4-й, последний в 2020 году, выпуск «Вестника». Традиционно мы вспоминаем и отмечаем наиболее значимые публикации, события и научные результаты года. Закономерно и очевидно, что исследования, посвященные проблемам, связанным с пандемией новой коронавирусной инфекции COVID-19, находились в фокусе всеобщего внимания. Наш журнал не стал исключением: в предыдущем, третьем номере опубликованы результаты национального многоцентрового исследования «Распространенность и Особенности Клинического течения КОРонавирусной инфекции у РЕЦИПИЕНТов сердца, почки, печени» (РОККОР-реципиент). В настоящем выпуске также публикуются работы, посвященные лечению реципиентов солидных органов в условиях пандемии COVID-19.

Однако даже значимые новости и результаты, связанные с работой в условиях пандемии, не могут отвлечь внимание сообщества трансплантологов и близкого к нему круга ученых и специалистов от другого события. По распоряжению Правительства РФ № 2206-р от 31 августа 2020 года НМИЦ ТИО им. ак. В.И. Шумакова вошел в список научных организаций, которые вправе самостоятельно присуждать ученые степени кандидата и доктора наук. Более того, НМИЦ ТИО им. ак. В.И. Шумакова – единственная из подведомственных Минздраву России организация, которой доверена столь почетная и ответственная функция.

Решение об открытии специальности «трансплантология и искусственные органы»

SCIENTIFIC SPECIALTY "TRANSPLANTOLOGY AND ARTIFICIAL ORGANS": NEW IN THE ORDER OF AWARDING ACADEMIC DEGREES

Dear colleagues!

I present to you the 4th and last issue of the Russian Journal of Transplantology and Artificial Organs for the year 2020. Traditionally, we remember and celebrate the most significant publications, events and scientific results of the year. It is logical and obvious that studies on problems associated with the coronavirus disease (COVID-19) pandemic were in the focus of everyone's attention. Our journal is no exception. Our third issue published results from the national multicenter study "Prevalence and Features of the Clinical Course of Coronavirus Infection in Heart, Kidney, and Liver Recipients" (ROCCOR-recipient). This issue also publishes works on the treatment of solid organ recipients in the context of the COVID-19 pandemic.

However, even significant news and results related to works in the context of the pandemic cannot divert the attention of the transplant community and the circle of scientists and specialists close to it from another event. By executive order No. 2206-r of the Russian Government of August 31, 2020, the Shumakov National Medical Research Center of Transplantology and Artificial Organs was included in the list of scientific organizations that can independently award academic degrees (PhD and Doctor of Science). Moreover, Shumakov National Medical Research Center of Transplantology and Artificial Organs is the only organization under the jurisdiction of the Russian Ministry of Health entrusted with such an honorable and responsible function.

The decision to open the "Transplantology and Artificial Organs" discipline and to, at the then Re-

и создании на базе тогда еще Научно-исследовательского института трансплантологии и искусственных органов Министерства здравоохранения СССР диссертационного совета, принимающего к защите диссертации на соискание ученой степени доктора и кандидата наук по этой специальности, было принято в 1986 году, и мы готовимся отметить 35-летие этого знаменательного события.

Через диссертационный совет при НМИЦ ТИО им. ак. В.И. Шумакова проходит подавляющее большинство всех диссертационных работ по нашей специальности. Более того, совет объединяет в своем составе большинство отечественных ведущих специалистов в этой области.

За 35 лет своей истории относительно новая научная специальность «трансплантология и искусственные органы» заняла достойное место на современном научном медицинском поле. Диссертационный совет при ФГБУ «Национальный медицинский исследовательский центр трансплантологии и искусственных органов имени академика В.И. Шумакова» Минздрава России все эти годы успешно выполнял свои функции, продолжал уверенно работать в условиях реформирования системы подготовки и государственной аттестации научных кадров. Хочется выразить уверенность, что право самостоятельного присуждения ученых степеней позволит повысить не только престиж нашего учреждения и специальности, но и качество экспертизы диссертационных работ.

Желаю всем в новом году здоровья, успехов, удачи во всех делах и творческих начинаниях.

С уважением,
академик РАН С.В. Готье

search Institute of Transplantology and Artificial Organs of the USSR Ministry of Health, create a dissertation council hearing the defense of dissertations for PhD and Doctor of Degrees in this discipline was made in 1986. We are preparing to celebrate the 35th anniversary of this landmark event.

The dissertation council at the Shumakov National Medical Research Center of Transplantology and Artificial Organs has been handling a vast majority of all dissertations in our discipline. Moreover, the council brings together most of the Russian leading experts in this field.

Over 35 years of its history, the relatively new scientific discipline "Transplantology and Artificial Organs" has taken its rightful place in the modern scientific medical field. The dissertation council at the Shumakov National Medical Research Center of Transplantology and Artificial Organs has successfully performed its functions all these years and continued to work confidently towards reforming the system of training and state certification of scientific personnel. I would like to express my confidence that the right to independently confer academic degrees will increase not only the prestige of our institution and discipline, but also the quality of examining dissertations.

I'm wishing everyone in this coming new year good health, success, and good luck in all your affairs and creative endeavors.

Sincerely,
S.V. Gautier
Academician, RAS

DOI: 10.15825/1995-1191-2020-4-8-19

HEART TRANSPLANTATION IN DIABETIC RECIPIENTS

V.N. Poptsov, E.A. Spirina, E.N. Zolotova, V.M. Zakharevich, N.N. Koloskova, N.P. Mozheiko, A.A. Sibiakina, I.L. Poz, A.I. Skokova, V.V. Boronova, V.Yu. Voronkov, V.M. Khatutskii

Shumakov National Medical Research Center of Transplantology and Artificial Organs, Moscow, Russian Federation

Introduction. Heart transplantation (HT) in patients with preexisting type 2 diabetes (T2D) is associated with high risk of infectious and non-infectious complications (renal dysfunction, multifocal atherosclerosis, transplant coronary artery disease, etc.) that can negatively affect recipient survival in the early and late periods after HT. **Objective:** to assess the effect of pre-transplant T2D on early and long-term outcomes of HT based on a single-center retrospective study. **Materials and methods.** The study enrolled 891 recipients who underwent HT within the period 2011 to 2018, and were divided into two groups: main group (T2D) – recipients with pretransplant T2D (n = 80, 9.0%) and the control group (T2D-free) – recipients without T2D (n = 811, 91.0%). Recipients from both groups did not differ in terms of HT urgency (UNOS status) and the need for pre-transplant mechanical circulatory support (MCS). **Results.** At the time of the HT, recipients from the T2D group were older than the T2D-free recipients (54 [46; 59] years *vs* 48 [35; 56] years, $p < 0.001$), they had a higher weight ($p < 0.001$) and body mass index ($p < 0.001$), coronary heart disease was more often their main disease (65.0% *vs* 36.5%, $p < 0.001$), they had higher transpulmonary gradient (10.0 [7.0; 12.0] mmHg *vs* 9.0 [6.0; 12.0] mmHg, $p = 0.024$) and pulmonary vascular resistance (2.9 [2.2; 4.0] Wood units *vs* 2.5 [1.8; 3.4] Wood units, $p = 0.038$). In the pre-transplant period, the T2D group had pronounced manifestations of renal dysfunction and increased comorbidity. Recipients in both groups did not differ in terms of cardiac donor parameters, graft ischemia time, cardiopulmonary bypass time, and incidence of severe early heart graft dysfunction requiring MCS (12.5% *vs* 10.7%, $p = 0.74$). In the early post-transplant period, the T2D group had high requirements (100% *vs* 28.0%, $p < 0.001$) and higher doses of insulin therapy. More pronounced manifestations of renal dysfunction and a greater need for renal replacement therapy (51.4% *vs* 27.9%, $p = 0.003$) did not affect artificial ventilation and ICU duration (6 [5; 10] days *vs* 6 [5; 10] days, $p = 0.098$), as well as hospital mortality (8.8% *vs* 8.5%, $p = 0.895$). The presence of pre-transplant T2D had no negative effect on the incidence of acute cardiac graft rejection, progression of transmissible coronary atherosclerosis, incidence and severity of cardiac graft vasculopathy, structure and severity of distant infectious and non-infectious complications, and post-transplant survival. **Conclusion.** With correct selection of recipients and choice of optimal tactics for their post-transplant management, the presence of pre-transplant T2D has no negative effect on early and long-term outcomes of HT.

Keywords: heart transplantation, diabetes mellitus.

INTRODUCTION

Heart transplantation (HT) remains the most effective method of treating patients with end-stage congestive heart failure (CHF) developing against the background of various acquired or congenital heart conditions. Many patients with end-stage CHF have concomitant diseases that can act as an absolute or relative contraindication to HT or be a factor negatively affecting early and long-term HT outcomes [1; 2; 3].

Diabetes mellitus, especially type 2 diabetes (T2D), not only often contributes to the course of CHF, but also promotes its development and progression [4; 5]. There is a 12% prevalence of type 2 diabetes among CHF patients, reaching 24% among patients with its most severe clinical manifestations [4; 5]. Many patients considered as possible heart recipients have T2D, which is still considered a relative contraindication to HT [1; 2; 6; 7]. Surgeons are always extremely cautious in performing HT in patients with preexisting T2D due to increased risk of infectious and non-infectious complications (renal dysfunction, multifocal atherosclerosis, transplant coronary artery disease, etc.), as well as difficulties in selecting the optimal immunosuppressive therapy tactics for this carbohydrate metabolism disorder. In spite of the fact that some studies have shown satisfactory early and long-term post-transplant survival, effective implementation of HT in patients with concomitant T2D is still a challenging clinical task and is the subject of scientific discussion and research [1; 3; 8]. In recent years, development of an HT program at Shumakov National

Corresponding author: Vitaliy Poptsov. Address: 1, Schukinskaya str., Moscow, 123182, Russian Federation. Phone: (963) 644-96-39. E-mail: poptsov_vit@mail.ru

Medical Research Center of Transplantology and Artificial Organs is associated, among other things, with increased number of HT in recipients with comorbid diseases, including T2D [9; 10].

The **aim** of the study is to evaluate the early and long-term outcomes of HT in patients with end-stage CHF and concomitant T2D.

MATERIALS AND METHODS

Between 2011 and 2018, 891 heart transplantations were performed at the Shumakov National Medical Research Center of Transplantology and Artificial Organs. This included 80 (9.0%) recipients – 74 (92.5%) men and 6 (7.5%) women, median age 54 [46; 59] with pre-existing (pre-transplant) T2D. The weight of a recipient in this cohort was 85.0 [78.3; 95.0] kg, body mass index (BMI) 28.3 [25.2; 31.5] kg/m^2. There were 28 (35%) recipients with BMI ≥30.0 kg/m^2.

The main diseases leading to end-stage CHF were: ischemic cardiomyopathy (ICMP) in 52 (65.0%) recipients, dilated cardiomyopathy (DCM) in 27 (33.8%), decompensated atherosclerotic aortic valve disease in 1 (1.2%). The severity of clinical manifestations of CHF corresponded to the NYHA functional class 3.1 ± 0.4.

The urgency of performing HT corresponded to UNOS status 1A in 20 (25.0%), status 1B in 18 (22.5%), and status 2 in 42 (52.5%) recipients. Pre-transplant mechanical circulatory support (MCS) was used in 20 (25.0%): intra-aortic balloon counterpulsation (n = 1 (1.3%)), peripheral venoarterial extracorporeal membrane oxygenation (VA ECMO) (n = 19 (23.8%)). Pre-transplant MCS lasted for 4.1 [3.5; 5.5] days.

Correction of carbohydrate metabolism disorders in the pre-transplant period was achieved via diet therapy in 16 recipients (20.0%), via oral anti-diabetic medication in 44 (55.0%), and via insulin therapy in 20 (25.0%). At the time of HT, one oral anti-diabetic medication was used for T2D drug therapy in 27 (61.4%) of 44 recipients who did not need insulin therapy, a combination of two oral anti-diabetic medications was used in 15 (34.1%) recipients, and a combination of three oral anti-diabetic medications was used in 2 (%) recipients. The following oral medications were used for blood glucose-lowering therapy: glimeperide in 22 (27.5%) recipients, gliclazide in 6 (7.5%), vildagliptin in 43 (53.8%), sitagliptin in 2 (2.5%), metformin in 6 (7.5%), and empagliflozin in 2 (2.5%). Oral anti-diabetic medications were continued in all patients (20 (25.0%)), who needed insulin therapy. The level of glycated hemoglobin (HbA1c) at the time of HT was 7.4%, including 51 (63.8%) with less than 7.4%, and 29 (36.2%) with more than 7.4%. The structure of diabetes-related complications in recipients with pre-transplant T2D was as follows: atherosclerotic coronary artery disease in 53 (66.3%) recipients, chronic obliterating peripheral artery disease in 15 (18.8%), cerebral ischemia in 14 (17.5%), peripheral diabetic neuropathy in 10 (12.5%), and diabetic nephropathy in 9 (11.3%). Chronic kidney disease (CKD) stage 3A and higher was diagnosed in 9 (11.3%) recipients with T2D.

Management of recipients in early and late post-transplant periods was carried out in accordance with the ISHLT Guidelines (2010) [11]. To diagnose and determine the severity (0R, 1R, 2R and 3R degrees) of acute cellular rejection of a heart transplant, the 2004 ISHLT standardized morphological classification was used (Cardiac biopsy grading of cellular rejection revised and standardized International Society for Heart and Lung Transplantation (ISHLT)) [12]. To diagnose and determine the severity of histological and immunopathological manifestations (pAMR 0, pAMR 1 (H+), pAMR 1 (I+), pAMR 2, pAMR 3) of antibody-related (humoral) heart transplant rejection, the 2013 ISHLT working formulation for pathology diagnosis of cardiac antibody-mediated rejection) was used [13]. The paper presents the outcomes of cellular and humoral rejection of recipients who survived up to the first biopsy – 857 recipients (96.2% of 891) in two compared groups. The classification proposed by Gao S.Z. et al. in 1988 was used to determine the degree of damage in transplant coronary artery disease (TCAD) [14]. TCAD was diagnosed based on the 2010 ISHLT Guidelines for the care of heart transplant recipients [11]. CKD diagnosis and severity were established by the degree of decrease in glomerular filtration rate according to the KDIGO 2012 classification [15].

Research data was statistically processed using Microsoft Excel spreadsheets and SPSS Statistics 20 software. All the studied parameters were tested for normal distribution using the Kolmogorov–Smirnov test. Arithmetic mean and standard deviation (M ± SD), upper and lower bounds, were used to represent parametric data. Median and interquartile range (interval between 25% and 75% percentiles) were used to describe nonparametric variables. Significance of differences in quantitative parameters in the two groups was determined via Fisher's exact test. Mann–Whitney U test and the Student's t test were used to compare variables in the study groups. Survival analysis was performed using the Kaplan–Meier estimate. Differences were considered statistically significant if the probability of error was less than 0.05 ($p < 0.05$).

STUDY RESULTS

Analysis of the pre-transplant examination data that was included in the study of heart recipients revealed that patients in the diabetes group were older ($p < 0.05$) by age (Table 1). Weight and body mass index were significantly ($p < 0.05$) higher in the study group.

Table 1

Comparative preoperative clinical characteristics of diabetic and nondiabetic heart recipients (n = 891)

Indicator	T2D in recipients		p
	T2D (n = 80)	T2D-free (n = 811)	
Age	54 [46; 59]	48 [35; 56]	**<0.001**
Height	175 [170; 180]	175 [170; 180]	0.969
Gender men (n/%) women (n/%)	 74/92.5 6/7.5	 683/84.2 129/15.9	 0.067
Weight, kg	85.0 [78.3; 95.0]	75.0 [65.0; 89.0]	**<0.001**
BMI, kg/m²	28.3 [25.2; 31.5]	24.7 [22.0; 28.4]	**<0.001**
BMI≥30.0, kg/m² (n/%)	28/35.0	163/20.1	**0.004**
DCM (n/%)	27/33.8	464/57.2	**<0.001**
ICMP (n/%)	52/65.0	296/36.5	**<0.001**
MAP, mmHg	79.5 [73.0; 89.5]	78.0 [69.0; 87.0]	0.144
RAP, mmHg	8.0 [6.0; 12.8]	8.0 [5.0; 12.0]	0.140
mPAP, mmHg	32.0 [25.0; 42.0]	28.0 [20.0; 37.0]	**0.004**
PWP, mmHg	22.5 [16.0; 29.8]	19.5 [13.0; 28.0]	**0.010**
CI, l/min/m²	1.9 [1.5; 2.2]	2.0 [1.6; 2.2]	**0.047**
TPG, mmHg	10.0 [7.0; 12.0]	9.0 [6.0; 12.0]	**0.024**
PVR, Wood units	2.9 [2.2; 4.0]	2.5 [1.8; 3.4]	**0.038**
PVR >4.0, Wood units (n/%)	25/31.3	122/15.0	**<0.001**
HT urgency by UNOS Status 1A (n/%) Status 1B (n/%) Status 1A–1B (n/%) Status 2 (n/%)	 20/25.0 18/22.5 38/47.5 42/52.5	 151/18.6 194/23.9 345/42.5 467/57.5	 0.216 0.888 0.456 0.456
Total bilirubin, μmol/L	20.3 [13.3; 36.5]	25.0 [15.6; 50.0]	**0.042**
Urea, mmol/L	8.3 [6.0; 10.0]	6.7 [5.6; 10.2]	**0.036**
Creatinine, μmol/L	105.2 [82.4; 110.0]	90.0 [77.0; 112.8]	**0.042**
GFR, mL/min	67.5 [62.7; 88.7]	79.9 [60.4; 95.7]	**0.046**
Total protein, g/L	72.0 [68.5; 76.3]	71.8 [65.5; 76.3]	**0.020**
ALT, U/L	21.0 [14.0; 35.0]	24.0 [15.6; 42.2]	0.147
AST, U/L	24.0 [19.0; 30.0]	27.0 [20.0; 39.0]	0.145
Prothrombin index, %	84.0 [69.0; 91.5]	78.0 [65.0; 88.0]	**0.025**
INR	1.2 [1.0; 1.6]	1.4 [1.1; 1.7]	**0.047**
White blood cells	7.8 [6.7; 9.4]	7.5 [6.0; 8.9]	0.095
Platelets	188.5 [142.0; 237.0]	192.0 [134.0; 243.0]	0.694
Glucose level (at any time), mmol/L	7.9 [6.4; 9.2]	6.1 [5.4; 6.9]	**<0.001**

Note: BMI – body mass index, DCM – dilated cardiomyopathy, ICMP – ischemic cardiomyopathy, mAP – mean arterial pressure, RAP – right atrial pressure, mPAP – mean pulmonary artery pressure, PWP – pulmonary wedge pressure, CI – cardiac index, TPG – transpulmonary gradient, PVR – pulmonary vascular resistance, HT – heart transplantation, GFR – glomerular filtration rate, ALT – alanine aminotransferase, AST – aspartate aminotransferase, INR – international normalized ratio.

The ratio of recipients with DCM and ICMP was multidirectional between the main and control groups. Recipients diagnosed with pretransplant ICMP (65.0%) prevailed in the main group ($p < 0.001$), while those diagnosed with DCM (57.2%) predominated in the control group. Hemodynamic manifestations of CHF and concomitant pulmonary hypertension (PH) were pronounced in the main group, as manifested by lower ($p < 0.05$) cardiac index (CI), higher ($p < 0.05$) mean pulmonary artery pressure (mPAP), transpulmonary gradient (TPG) and pulmonary vascular resistance (PVR). The proportion of patients with pre-transplant PVR level >4 Wood units (27.5%) was also higher ($p < 0.05$) in the main group. Recipients in both groups did not differ in terms of urgency of performing HT. Biochemical manifestations of pre-transplant renal dysfunction (urea, blood creatinine, glomerular filtration rate (GFR)) were more ($p < 0.05$) pronounced in the main group, hepatic dysfunction (total bilirubin, prothrombin index (PI) and international normalized ratio (INR)) – in the main groups. Naturally, pre-transplant blood glucose level was higher ($p < 0.05$) in the main group.

The nature and incidence of coexisting conditions at the time of HT in the main and control groups are presented in Table 2.

The main group was characterized by a larger proportion (3.8% to 17.5%) of recipients with stage 2/3 hypertension, stage 2/3 dyscirculatory encephalopathy, multifocal atherosclerosis, urolithiasis, subclinical hypothyroidism, and CKD stage 3 and higher ($p < 0.05$). In the control group, incidence of the same concomitant diseases ranged from 0.6% to 5.5%.

There were no differences in the main clinical, laboratory and imaging parameters of heart donor between the main and control groups, except for the "donor/recipient body weight ratio" indicator (Table 3).

The main and control groups did not differ in terms of incidence of early graft dysfunction, requiring post-transplant MCS – 12.5% versus 10.7%, respectively ($p = 0.764$) (Table 4). Clinical and biochemical manifestations of acute kidney injury in the early post-transplant period were more ($p < 0.05$) pronounced in the main group, which led to 1.8 times greater ($p < 0.05$) need for renal replacement therapy (RRT). The duration of the use of continuous RRT methods (continuous veno-venous hemofiltration (CVVH)) was longer ($p < 0.05$)

Table 2

Preoperative morbidity in diabetic and nondiabetic heart transplant recipients (n = 891)

Comorbidities (n/%)	T2D in recipients		Chi-square	p
	T2D (n = 80)	T2D-free (n = 811)		
Arterial hypertension, stage 2/stage 3	14/17.5	45/5.5	14.979	**<0.001**
DEP, stage 2/stage 3	11/13.8	19/2.3	23.767	**<0.001**
Multifocal atherosclerosis	11/13.8	10/1.2	44.349	**<0.001**
CKD, stage 3 and above, (n/%)	9/11.3	11/1.4	28.175	**<0.001**
Brachiocephalic artery atherosclerosis with carotid stenosis >50%	8/10.0	9/1.1	26.225	**<0.001**
Non-drug-induced clinical/subclinical hypothyroidism	7/8.8	14/1.7	12.731	**<0.001**
Obliterating atherosclerosis of the lower extremities	6/7.5	10/1.2	12.881	**<0.001**
Kidney stone disease	3/3.8	5/0.6	4.909	0.027

Note. DEP – dyscirculatory encephalopathy, CKD – Chronic kidney disease.

Table 3

Clinical characteristics of heart recipients (n = 891)

Indicator	T2D in recipients		p
	T2D (n = 80)	T2D-free (n = 811)	
Age (years)	45.0 [34.0; 55.5]	44.0 [34.0; 53.0]	0.441
Sex Female, (n/%) Male, (n/%)	 15/18.8 65/81.2	 160/19.7 652/80.3	 0.955
Female donor/male recipient pair (n/%)	13/16.3	124/15.3	0.945
Donor weight (kg)	85 [75; 90]	80 [70; 90]	0.143
Donor/recipient body weight ratio	0.95 [0.85; 1.1]	1 [0.86; 1.2]	**0.010**
Non-traumatic brain injury in the donor, (n/%)	48/60	522/64.4	0.523
Cardiopulmonary resuscitation, (n/%)	3/3.8	32/3.9	0.828
MV (days)	2 [1; 3]	2 [1; 3]	0.562
Hemoglobin, g/L	120 [92; 142]	113 [89; 138]	0.168
Total protein, g/L	60 [52; 70]	60.5 [52; 67]	0.542
Blood sodium, mmol/L	148 [141; 157]	147 [140; 156]	0.298
Blood sodium >160 (mmol/L), (n/%)	13/16.3	82/10.1	0.131
Sympathomimetic therapy, (n/%)	63/78.8	572/70.5	0.156
Norepinephrine (n/%, ng/kg/min) (max.)	44/55 300 [167; 550]	458/56.5 340 [180; 600]	0.902 0.194
Dopamine (n/%, μg/kg/min) (max.)	19/23.8 6 [3.5; 13.5]	279/34.4 7 [4; 12]	0.073 0.184
Troponin T, (pg/ml)	0.17 [0.1; 0.7]	2 [0.2; 62.1]	**0.049**
CK-MB, ng/mL	37 [32; 65]	33 [5.5; 54.5]	0.161

Note. MV – mechanical ventilation, CK-MB – creatine kinase-MB.

Table 4

Early posttransplant clinical characteristics of diabetic and nondiabetic recipients (n = 891)

Indicator	T2D in recipients		P
	T2D (n = 80)	T2D-free (n = 811)	
Graft ischemia, min.	154 [133; 185]	159 [131; 194]	0.597
AC duration, min.	119 [100; 142]	120 [93; 152]	0.878
Dopamine			
n/%	76/95.0	632/78.0	**<0.001**
μg/kg/min (max.)	6 [4;10]	6 [4; 8]	0.184
Dobutamine			
n/%	54/67.5	457/56.4	0.072
μg/kg/min (max.)	4.0 [3.5; 6.0]	5.0 [4.0; 6.0]	0.769
Adrenalin			
n/%	78/97.5	625/77.1	**<0.001**
ng/kg/min (max.)	40.0 [60.0; 80.0]	43.0 [60.0; 80.0]	0.299
Post OHT – MCS, n/%	10/12.5	87/10.7	0.764
Post-transplant MCS (days)	3.5 [1.5; 5.5]	3 [2; 5]	0.524
Postoperative MV, hours	8.5 [6; 13]	9 [6; 14.5]	0.831
Total bilirubin (max.), (mmol/L)	43 [31.7; 69.4]	47 [30.7; 77.8]	0.888
ALT (max.), U/L	42 [30; 54]	42 [31; 81]	0.770
AST (max.), U/L	129 [98; 236]	108 [143; 193]	0.585
Urea (max.), (mmol/L)	16.7 [12.2; 22.2]	14 [10.1; 18.8]	**0.022**
Creatinine (max.), (mmol/L)	151.2 [115.6; 218.7]	133.9 [100.1; 174]	**0.019**
Total protein (min.), G/l	58 [54; 62]	66 [63; 68]	**<0.001**
PT (min.), %	67 [60; 74]	71 [63; 77]	**0.016**
White blood cells (max.)	20.2 [17.4; 23]	18.1 [15.2; 22.3]	**0.028**
Platelets (min.)	76 [56; 103.5]	74.5 [51; 107]	0.871
Procalcitonin (max.)	8.8 [2.7; 23.9]	6.4 [2.6; 17.7]	0.159
Postoperative delirium, n/%	19/27.1	101/12.5	0.008
Renal replacement therapy: CVVH, (n/%)	36/51.4	226/27.9	**0.003**
Start of CVVH, days after surgery	1.5 [1; 2]	4 [2; 12]	**0.002**
Transition from CVVH to intermittent HDF, (n/%)	13/18.6	85/10.5	0.165
Number of patients receiving insulin pump therapy after HT, n/%	80/100	227/28.0	**<0.001**
Intravenous insulin, units/day	66.7 [50; 89.3]	50 [33.3; 66.7]	**<0.001**
Intravenous insulin, duration of days	2 [1; 5]	1 [0.5; 2]	**<0.001**
ICU (days)	6 [5; 10]	6 [4; 8]	0.098
Hospital survival, n/%	73/91.2	742/91.5	0.895

Note. AC – assisted circulation, OHT – orthotopic heart transplantation, MCS – mechanical circulatory support, MV – mechanical ventilation, ALT – alanine aminotransferase, AST – asprat aminotransferase, PT – prothrombin time, CVVH – continuous veno-venous hemofiltration, HDF – hemodiafiltration, HT – heart transplant, ICU – intensive care unit.

in the study group. Recipients in the main group were characterized by a more frequent (2.2 times) occurrence of postoperative delirium (27.1% versus 12.4%). The leading in-hospital infectious complications in both the main and control groups were pneumonia (mainly of bacterial etiology) and purulent mediastinitis, whose incidence was, respectively, 18.8% (T2D group) versus 19.0% (T2D-free group) (p = 0.919) and 2.5% (T2D group) versus 2.1% (T2D-free group) (p = 0.86). There were no significant differences in the incidence of these infectious complications among both groups.

In the early periods after HT, the need and average daily doses of insulin were higher (p < 0.05) in the main group (Table 5). In the control group, 227 patients (28%) received continuous intravenous insulin infusion via a medication dispenser. In our study, the target blood glucose level was 5–10 mmol/L.

77 (96.3%) of 80 recipients from the T2D group and 780 (96.2%) of 811 recipients from the T2D-free group survived up to the first endomycardial biopsy. The groups did not differ significantly in terms of incidence of acute cellular rejection: (1) grade 1R rejection – 45.5% (T2D group) versus 42.9% (T2D-free group) (p = 0.76); (2) grade 2R rejection – 0.0% (T2D group) versus 1.0% (T2D-free group) (p = 1.00); (3) grade 3R rejection – 2.6% (T2D group) versus 2.1% (T2D-free group) (p = 0.92). In terms of incidence of antibody-mediated rejection, there were no significant differences between reci-

Table 5

Daily intravenous insulin doses (U/day) at early postoperative period in diabetic and non-diabetic recipients (n = 307)

Study phase (after HT)	Recipient group		Chi-square / Fisher's exact test	p
	T2D group (n = 80)	T2D-free group (n = 227)		
12 hours	115.5 ± 47.1	110.3 ± 35.5	1.1871	0.236
Day 1	89.3 ± 33.7	55.3 ± 29.3	9.6193	0.0001
Day 2	63.9 ± 25.1	47.1 ± 15.3	8.5071	0.0001
Day 3	52.3 ± 17.1	37.5 ± 12.1	9.7958	0.0001
Day 4	48.9 ± 16.3	23.3 ± 7.1	25.3178	0.0001
Day 5	35.7 ± 15.0	14.4 ± 5.3	26.2307	0.0001

Note. HT – heart transplantation.

Table 6

Causes of post-transplant in-hospital mortality (n = 76)

Cause of death	Pre-transplant T2D in recipients who died in the early post-HT period		Chi-square / Fisher's exact test	p
	T2D (n = 7)	T2D-free (n = 69)		
Multiple organ failure not associated with primary graft dysfunction	4/57.1	28/40.6	0.273	0.603
Multiple organ failure associated with primary graft dysfunction	2/28.6	19/27.5	0.148	0.701
Acute rejection crisis	1/14.3	15/21.7	0.004	0.951
Other reasons	0	7/10.1	0.039	0.843

pients from both groups. In all cases, antibody-mediated rejection pAMR 2 was diagnosed – 3.9% (T2D group) versus 4.7% (T2D-free group), respectively (p = 0.96).

The presence of pre-transplant T2D had no adverse effect on length of stay in intensive care unit (ICU) and hospital mortality, which was, respectively, 8.8% (T2D group) versus 8.5% (T2D-free group) (p = 0.895). There was no difference in hospital mortality between the groups (Table 6).

In the long term post-HT period, the leading infectious complication in both groups was community-acquired pneumonia (mainly of mixed bacterial-viral etiology), whose incidence was 12.5% (T2D group) versus 10.9% (T2D-free group) (p = 0.793).

The incidence of donor-transmitted coronary atherosclerosis (DTCA) (developed during the lifetime of the heart donor) in both groups of recipients did not differ significantly – respectively 22.5% (T2D group, n = 18) versus 26.1% (T2D-free group, n = 212) (p = 0.569), as well as the number of initially detected affected coronary arteries – respectively 1.4 ± 0.4 (T2D group) versus 1.3 ± 0.5 (T2D-free group, n = 212) (p = 0.071). The groups also did not differ significantly in the frequency of percutaneous coronary intervention in the early post-HT period in recipients with DTCA – respectively 45.0% (9 of 20, T2D group) vs. 63.1% (159 of 252, T2D-free group) (p = 0.173). In the late posttransplant period, repeated coronary angiographic studies in 14 (70%) of 20 recipients of the T2D group revealed the progression of DTCA, which required additional percutaneous coronary intervention. In the T2D-free group, additional percutaneous coronary intervention was required for 177 (70.2%) of 252 patients with identified DTCA (p = 0.817).

There was no significant difference in the incidence of TCAD diagnosed at different times after HT in recipients from both groups discharged from the hospital – respectively 45.2% (33 out of 73, T2D group) versus 39.6% (294 out of 742, T2D-free group) (p = 0.417). According to the classification by Gao S.Z. et al. (1988), the groups did not differ significantly in terms of frequency of detection of various types of stenotic coronary artery lesions in TCAD: (1) type A – 39.4% (T2D group) versus 54.8% (T2D-free group) (p = 0.136); (2) type B1/B2 – 42.4% (T2D group) versus 33.0% (T2D-free group) (p = 0.373); (3) type C – 18.2% (T2D group) versus 12.2% (T2D-free group) (p = 0.489).

Outpatient renal replacement therapy by long-term hemodialysis was required in 11 (1.3%) out of all the 816 recipients discharged from the hospital after HT. Recipients in both groups did not differ in the incidence of "chronicity" of renal failure requiring outpatient long-term hemodialysis – respectively 1.4% (1 out of 73, T2D group) versus 1.3 (10 out of 743, T2D-free group) (p = 0.606).

During the analyzed period, 145 of 816 heart recipients who were discharged from the hospital died, including 13 (17.8%) of 73 (T2D group) and 132 (17.8%) of 743 (T2D-free group). There were no significant diffe-

rences in the structure of long-term mortality in recipients discharged after HT (Table 7).

The presence of pre-transplant T2D did not significantly affect both early and long-term survival of heart recipients (Fig.).

DISCUSSION

Frequent combination of cardiovascular conditions and carbohydrate metabolism disorders accounts for the high prevalence of T2D among patients with heart diseases, accompanied by development of CHF [4; 5]. This, in turn, explains the presence of T2D in many patients with end-stage CHF, some of whom are indicated for HT [3; 4; 5; 16; 17]. Despite the fact that many years of experience with HT in patients with concomitant T2D have been accumulated abroad, the intervention continues to be associated with increased risk of early and long-term complications that may negatively affect the post-transplant survival of recipients [2; 6; 7; 18]. According to a single-center study, Ram E. et al. (2020), the presence of pre-transplant T2D in heart recipients increases the risk of post-HT death by 1.8 times [19].

According to multicenter studies, the proportion of HT in recipients with pre-transplant T2D ranges from 13.6% to 28.2% [20; 21]. In our study, the proportion of HT in recipients with pre-transplant diabetes was 9.0% of the total number of heart transplants performed during the analyzed 8-year period. The initiation of regular HT in recipients with pre-transplant T2D since 2011 coincided with an increase in the number of heart transplants performed annually over 30 per year. An increase in the proportion of HT in recipients with pre-transplant diabetes was also associated with increased proportion of heart transplants in older patients, which led to an increase in the average age of the heart recipient [22].

A comparative study revealed that pre-transplant T2D recipients were older in age, had a higher weight and BMI compared to recipients without pre-transplant

Table 7

Causes of long-term post-transplant post-discharge mortality (n = 145)

Cause of death	T2D in recipients		Chi-square / Fisher's exact test	p
	T2D (n = 13)	T2D-free (n = 132)		
Infectious complications	5/38.5	22/16.7	2.411	0.121
Rejection	3/23.1	32/24.2	0.060	0.806
CAV	2/15.4	25/18.9	0.004	0.953
Sudden death	1/7.6	30/22.7	0.823	0.365
Cancer	0	8/6.1	0.076	0.783
Unknown cause	2/15.4	15/11.4	0.000	0.983

Note: CAV – cardiac allograft vasculopathy.

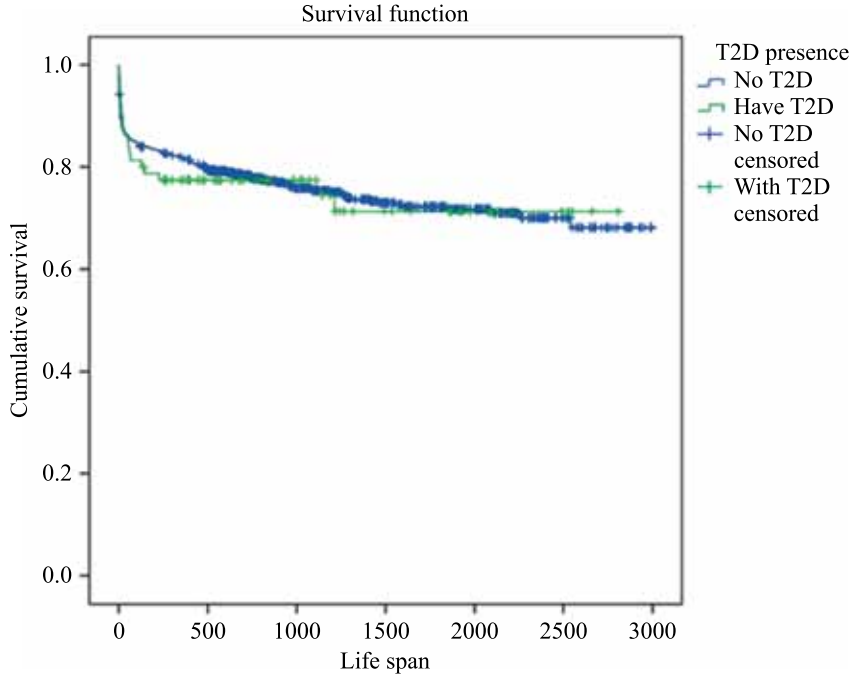

Fig. The effect of pre-transplant T2D on early and long-term survival in heart recipients

carbohydrate metabolism disorders. Coronary heart disease (CHD) was the leading cause of end-stage CHF in recipients with pre-transplant T2D. Predominant impairment of left ventricular (LV) systolic and diastolic function resulted in more pronounced manifestations of pre-transplant PH in this cohort of heart recipients. Nearly 1/3 were recipients with pre-transplant PVR levels above 4 Wood units. In addition, as this study has shown, when preparing and performing HT in recipients with pre-transplant T2D, it is necessary to take into account more pronounced manifestations of preoperative renal dysfunction and the presence of concomitant conditions (arterial hypertension (AH), multifocal atherosclerosis, CKD stage 3 and higher, etc.), which can negatively affect the course of early and long-term post-transplant periods.

Almost half of patients with pre-transplant T2D required urgent HT. This included 25% with pre-transplant MCS using peripheral venoarterial extracorporeal membrane oxygenation (VA ECMO), which could negatively affect the course of the perioperative period and be a risk factor for adverse outcomes in the early post-transplant period.

The median age of the heart donor did not differ significantly between the two studied groups of recipients – within 44–45 years – which fully corresponds to the median age of the heart donor in Europe and reflects the current trends towards an increase in the age of the heart donor due to pronounced reduction in the pool of donors under 40 years old [23]. In both groups, heart donors, whose cause of death was irreversible non-traumatic brain injury, which is considered a possible risk factor for early graft dysfunction, prevailed (60.0–64.4%) [24; 25]. Significantly lower need and doss of sympathomimetic support, as well as the value of the marker for myocardial injury troponin T during cardiac donor conditioning could positively affect the nature of restoration of initial cardiac graft function in the main group [24; 26].

Despite the absence of differences in the frequency of MCS use in the early post-transplant period, the intensity of sympathomimetic therapy, and the duration of postoperative mechanical ventilation, the main group showed more pronounced manifestations of multiple organ failure, mainly kidney-liver failure. Moreover, postoperative delirium was 2.2 times more frequent. Renal replacement therapy was used 1.8 times more often. These features are worth considering when managing recipients with pre-transplant T2D in the perioperative period. It is expected that this category of patients had a significantly greater need for insulin therapy. At the same time, as our study showed, the above facts did not have a negative impact on the duration of postoperative treatment of recipients with T2D in the ICU and on hospital mortality. In both study groups, the leading cause of death was multiple organ failure syndrome.

The study revealed no negative effect of pre-transplant T2D on the incidence of early and late infectious complications, which we attribute to a "more aggressive" postoperative antimicrobial chemoprophylaxis (early complications) and a personalized approach in determining the optimal immunosuppressive therapy scheme (early and late complications) [27; 28; 29].

Our study did not find any significant negative effect of pre-transplant T2D on DTCA in the post-transplant period, as well as on incidence and severity of TCAD. Early studies demonstrate the ambiguous effect of pre-transplant T2D on development and progression of pre-existing or de novo emerging transplant coronary artery disease [16; 19; 30]. The presence of pre-transplant T2D did not negatively affect the incidence and severity of TCAD, which was also revealed in other studies [27].

There was no significant effect of pre-transplant T2D on the incidence and severity of other non-infectious non-lethal and lethal complications (chronic renal failure, oncopathology, acute graft rejection, etc.).

Early and long-term survival rates in recipients with and without T2D were comparable, indicating that with the correct selection of recipients and choice of an optimal management strategy in the post-transplant period, high HT outcomes are achieved even in recipients with a high risk of early and long-term complications [6; 17; 31]. A possible explanation for the results obtained in the study is that HT in recipients with pre-transplant T2D was performed in the absence of significant manifestations of diabetes-dependent and diabetes-associated complications that could affect the survival of recipients. Besides, the presence and significance of the influence of other comorbidities on HT outcomes were taken into account [7].

CONCLUSION

With the correct selection of recipients and choice of an optimal management strategy in the post-transplant period, pre-transplant type 2 diabetes does not have a negative effect on early and long-term outcomes of heart transplantation.

The authors declare no conflict of interest.

REFERENCES

1. *Mehra MR, Canter CE, Hannan MM, Semigran MJ, Uber PA, Baran DA et al.* The 2016 international society for heart lung transplantation listing criteria for heart transplantation: A 10-year update. *The Journal of Heart and Lung Transplantation.* 2016; 3: 1–23.
2. *Marelli D, Laks H, Patel B, Kermani R, Marmureanu A, Patel J et al.* Heart transplantation in patients with diabe-

tes mellitus in the current era. *The Journal of Heart and Lung Transplantation.* 2003; 22 (10): 1091–1097.
3. *Mehra MR, Kobashigawa J, Starling R, Russel S, Uber PA, Parameshwar J et al.* Listing criteria for heart transplantation: international society for heart and lung transplantation guidelines for the care of cardiac transplant candidates – 2006. *The Journal of Heart and Lung Transplantation.* 2006; 25 (9): 1024–1042.
4. *Obrezan AG, Kulikov NV*. Chronic Heart Failure and Diabetes Mellitus: Pathogenesis and Possibilities of Treatment. *Kardiologiia*. 2018; 58 (7): 85–94. (In Russ.). doi: 10.18087/cardio.2018.7.10156.
5. *Pochinka IG, Strongin LG, Botova SN, Razumovsky AV, Baranova AA, Dvornikova MI et al*. Effect of Type 2 Diabetes Mellitus on Five-Year Survival of Patients Hospitalized Because of Acute Decompensated Heart Failure. *Kardiologiia*. 2017; 57 (9): 14–19. doi: 10.18087/cardio.2017.9.10027.
6. *Schulze PC, Jiang J, Yang J, Cheema FH, Schaeffle K, Kato TS et al.* Preoperative assessment of high-risk candidates to predict survival after heart transplantation. *Circulation: Heart Failure.* 2013; 6: 527–534.
7. *Gomis-Pastor M, Mingell EU, Perez SM, Loidi VB, Lopez LL, Bassons AD et al.* Multimorbidity and medication complexity: New challenges in heart transplantation. *Clinical Transplantation.* 2019; 33: 1–14.
8. *Morgan JA, John R, Weinberg AD, Colletti NJ, Mancini DM, Edwards NM.* Heart transplantation in diabetic recipients: a decade review of 161 patients at Columbia Presbyterian. *The Journal of Thoracic and Cardiovascular Surgery.* 2004; 127 (5): 1486–1492.
9. *Gautier SV, Shevchenko AO, Kormer AY, Poptsov VN, Shevchenko OP*. Prospects to improve long-term outcomes of cardiac transplantation. *Russian Journal of Transplantology and Artificial Organs*. 2014; 16 (3): 23–30. (In Russ.) https://doi.org/10.15825/1.
10. *Meboniya NZ, Poptsov VN.* Transplantatsiya serdtsa u retsipientov 60 let i starshe. *Transplantology: results and prospects*. Vol. X. 2018 / Ed. by S.V. Gautier. M.–Tver: Triada, 2019: 504, 335.
11. *Costanzo MR, Dipchand A, Starling R, Anderson A, Chan M, Desai S et al.* ISHLT Guidelines for the care of heart transplant recipients. *The Journal of Heart and Lung Transplantation.* 2010; 29 (8): 914–956.
12. *Stewart S, Winters GL, Fishbein MC, Tazelaar HD, Kobashigawa J, Abrams J et al.* Revision of the 1990 working formulation for the standartization of nomenclature in the diagnosis of heart rejection. *The Journal of Heart and Lung Transplant.* 2005; 24 (11): 1710–1720.
13. *Berry GJ, Burke MM, Andersen C, Bruneval P, Fedrigo M, Fishbein MC et al.* The 2013 international society for heart and lung transplantation working formulation for the standartization of nomenclature in the pathologic diagnosis of antibody-mediated rejection in heart transplantation. *The Journal of Heart and Lung Transplantation.* 2013; 32 (12): 1147–1162.
14. *Gao SZ, Alderman EL, Schroeder JS, Hunt SA*. Accelerated coronary vascular disease in the heart transplant patient: coronary arteriographic finding. *Journal of the American College of Cardiology.* 1988; 12: 334–340.
15. *Eknoyan G, Lameire N, Eckardt K-U, Kasiske BL, Wheeler DC, Abboud OI et al.* KDIGO 2012 Clinical practice guideline for the evaluation and management of chronic kidney disease. *Official Journal of the International Society of Nephrology.* 2013; 3 (1): 1–150.
16. *Chen JM, Russo MJ, Hammond KM, Mancini DM, Kherani AR, Fal JM et al.* Alternate waiting list strategies for heart transplantation maximize donor organ utilization. *The Annals of Thoracic Surgery.* 2005; 80 (1): 224–228.
17. *Hong KN, Iribarne A, Worku B, Takayama H, Gelijns AC, Naka Y et al.* Who is the high-risk recipient? Predicting mortality after heart transplant using pretransplant donor and recipient risk factors. *The Annals of Thoracic Surgery.* 2011; 92: 520–527.
18. *Szabo Z, Hakanson E, Svedjeholm R.* Early postoperative outcome and medium-term survival in 540 diabetic and 2239 nondiabetic patients undergoing coronary artery bypass grafting. *The Annals of Thoracic Surgery.* 2002; 74 (3): 712–719.
19. *Ram E, Lavee J, Sternik L, Segev A, Peled Y.* Relation of age of major rejections, allograft vasculopathy, and long-term mortality in a contemporary cohort of patients undergoing heart transplantation. *Israel Medical Association Journal.* 2020; 22: 486–490.
20. *Lund LH, Khush KK, Cherikh WS, Goldfarb S, Kucheryavaya AY, Levvey BJ et al.* The registry of the international society for heart and lung transplantation: thirty-fourth adult heart transplantation report – 2017; focus theme: allograft ischemic time. *The Journal of Heart and Lung Transplantation.* 2017; 26 (10): 1037–1046.
21. *Cehic MG, Nundall N, Greenfield JR, Macdonald PS.* Management strategies for posttransplant diabetes mellitus after heart transplantation: a review. *Journal of Transplantation.* 2018: 1–14.
22. *Poptsov VN, Spirina EA, Ukhrenkov SG, Ustin SYu, Aliev EZ, Masyutin SA et al.* Early Postoperative Period After Orthotopic Heart Transplantation in Recipients of 60 Years and Older. *Russian Journal of Transplantology.* 2016; 18 (4): 56–65. (In Russ.) doi: 10.15825/1995-1191-2016-4-56-65.
23. *Khust KK, Cherikh WS, Chambers DC, Harhay MO, Hayers DJ, Hsich E et al.* The international thoracic organ transplant registry of the international society for heart and lung transplantation: thirty-sixth adult heart transplantation report – 2019; focus theme: donor and recipient size match. *The Journal of Heatr and Lung Transplantation.* 2019; 38: 1056–1066.
24. *Peled Y, Kassif Y, Raichlin E, Kogan A, Har-Zahav Y, Nachum E et al.* Improved long-term outcomes after heart transplantation utilizing donors with traumatic mode of brain death. 2019; 14 (138): 1–9.
25. *Samsky M, Patel CB, Owen A, Schulte PJ, Jentzer J, Rosenberg PB et al.* Ten year experience with extended criteria cardiac transplantation. *Circulation: Heart Failure.* 2013; 6 (6): 1230–1238.

26. *Nakamura Y, Saito S, Miyagawa S, Yoshikawa Y, Hata H, Yoshioka D et al.* Perioperative ischaemic reperfusion injury and allograft function in the early post-transplantation period. *Interactive CardioVascular and Thoracic Surgery.* 2019; 29: 230–236.
27. *Russo MJ, Chen JM, Hog KM, Stewart AS, Ascheim DD, Argenziano M et al.* Survival after heart transplantation is not diminished among recipients with uncomplicated diabetes mellitus (an analysis of the United Network of Organ Sharing database). *Circulation.* 2006; 114: 2280–2287.
28. *Subramanian S, Trence DL.* Immunosuppressive agents: effects on glucose and lipid metabolism. *Endocrinology and MetabolismClinics of North America.* 2007; 36: 891–905.
29. *Pirsch JD, Henning AK, First MR, Fitzsimmons W, Gaber AO, Reisfield R et al.* New-onset diabetes after transplantation: results from a double-blind early corticosteroid withdrawal trial. *American Journal of Transplantation.* 2015; 20: 1–9.
30. *Ram E, Lavee J, Tenenbaum A, Klempfner R, Fishman EZ, Maor E et al.* Metformin therapy in patients with diabetes mellitus is associated with a reduced risk of vasculopathy and cardiovascular mortality after heart transplantation. *Cardiovascular Diabetology.* 2019; 18 (118): 1–8.
31. *Chambers DC, Cherikh WS, Goldfarb SB, Hayers JD, Kucheryavaya AY, Toll AE et al.* The International Thoracic Organ Transplant Registry of the International Society for Heart and Lung Transplantation: Thirty-Fifth Adult Heart Transplantation Report – 2018; Focus Theme: Multiorgan Transplantation. *Journal of Heart and Lung Transplantation.* 2018; 37 (10): 1169–1183.

The article was submitted to the journal on 7.05.2020

DOI: 10.15825/1995-1191-2020-4-20-26

DIAGNOSTIC VALUE OF MIRNA-101 AND MIRNA-27 IN ACUTE HEART TRANSPLANT REJECTION

D.A. Velikiy[1], O.E. Gichkun[1, 2], S.O. Sharapchenko[1], N.P. Mozheiko[1], R.M. Kurabekova[1], O.P. Shevchenko[1, 2]

[1] Shumakov National Medical Research Center of Transplantology and Artificial Organs, Moscow, Russian Federation

[2] Sechenov University, Moscow, Russian Federation

Objective: to determine the diagnostic value of miRNA-101 and miRNA-27 expression levels for acute heart transplant rejection. **Materials and methods.** The study enrolled 46 heart recipients, among whom were 36 men (78.3%); the average age of recipients was 47.7 = 10.8 (16 to 67) years. Serum microRNA expression levels were measured via quantitative polymerase chain reaction (PCR). Graft rejection was verified through morphological analysis of endomyocardial biopsy specimens. **Results.** The expression levels of miRNA-101 and miRNA-27 in recipients with acute graft rejection are significantly lower than in recipients without rejection ($p = 0.04$ and $p = 0.03$, respectively). When the miRNA-101 expression level is below the determined threshold value, the risk of developing acute graft rejection increases 1.8 times (RR = 1.8 [95% CI 1.13–3.01]). When the miRNA-27 expression level is below the determined threshold value, the risk of developing acute graft rejection increases 1.9 times (RR = 1.9 [95% CI 1.12–3.37]). Simultaneous decrease in the expression levels of miRNA-101 and miRNA-27 below the determined threshold values increases the likelihood of acute graft rejection by 2.0 times (RR = 2.0 [95% CI 1.16–3.36]). **Conclusion.** The serum miRNA-101 and miRNA-27 expression levels are of diagnostic value for acute graft rejection in heart recipients.

Keywords: heart transplantation, miRNA-101, miRNA-27, acute rejection, biomarkers.

Acute transplant rejection is one of the major factors affecting survival in heart recipients. The risk of developing acute heart transplant rejection is higher in the early postoperative period, although acute rejection crises can occur at any time after transplantation. Late rejection crises often occur where there are insufficient doses of immunosuppressive therapy or non-compliance with the prescribed medication regimen, as well as in cases of viral infections leading to activation of the patient's immune system [1, 2].

Endomyocardial biopsy, which is used to verify and control the treatment of acute rejection, is an invasive procedure that is laborious and risky for patients. Biopsy results can be influenced by sampling errors and variability in the assessment of the obtained preparations [3]. In order to improve preclinical diagnostics and reduce the number of repeated invasive diagnostic interventions, there has recently been active development of minimally invasive methods for diagnosing post-transplant complications, which can not only reveal the presence of acute graft rejection, but also control the effectiveness of recipient treatment [4].

To solve this problem, the relationship of various biomarkers, including factors and mediators of inflammation, neoangiogenesis, tissue destruction, thrombus formation, etc., with the risk of cardiovascular diseases and post-transplant complications, is being actively studied all over the world [5–9]. The study of microRNAs (small, non-coding RNAs that repress gene expression) as well as search and validation of new biomarkers for their diagnosis represent a separate subject of research aimed at understanding the pathogenesis of pathological processes in the myocardium. Due to the variety of regulatory functions, miRNAs are a promising group of biomarkers, potentially significant both for diagnosis and for monitoring the progression of post-transplant complications [10–12]. In our previous work, a comparative analysis of miRNA expression in heart recipients found that the expression levels of miRNA-101 and miRNA-27 significantly differed acute graft rejection and without rejection [13].

The objective of this work was to determine the diagnostic accuracy of miRNA-101 and miRNA-27 with respect to acute graft rejection in cardiac recipients.

MATERIALS AND METHODS

The study enrolled 46 patients who, between 2013 and 2016, underwent a heart transplant (HT) surgery at the Shumakov National Medical Research Center of Transplantology and Artificial Organs. Among the pati-

Corresponding author: Dmitriy Velikiy. Address: 1, Shchukinskaya str., Moscow, 123182, Russian Federation. Phone: (499) 193-87-62. E-mail: dim_vel@mail.ru

ents were 36 men (78.3%). The mean age of recipients was 47.7 ± 10.8 (16 to 67) years. Before the HT, 29 (63%) recipients were diagnosed with dilated cardiomyopathy (DCM), 12 (26%) recipients were found to have coronary heart disease (CHD), while 5 (11%) recipients were diagnosed with other conditions. The maximum follow-up period after HT was 2215 days (median 264.5 [32; 785.3]).

All patients with indications for HT underwent a routine examination according to the National Clinical Guidelines '*Heart Transplantation and Mechanical Circulatory Support*' and the patient management protocol at the Shumakov National Medical Research Center of Transplantology and Artificial Organs. After transplantation, routine examinations of the recipient included clinical assessment of the state, general and biochemical blood tests to determine tacrolimus levels, 24-hour blood pressure monitoring (to correct antihypertensive therapy), echocardiographic examination, repeated myocardial biopsies, and annual coronary angiogram. All recipients received a three-component immunosuppressive therapy, including a combination of calcineurin inhibitors (tacrolimus) and cytostatics (mycophenolate mofetil or mycophenolonic acid), as well as varying doses of oral prednisolone, depending on the time after surgery and the frequency of graft rejection episodes and adjuvant medication as indicated [1].

The material for the study of microRNA expression was venous blood plasma (1 to 3 samples from each patient, mean 1.22). Patients' peripheral blood samples were collected in disposable tubes with anticoagulant ethylenediaminetetraacetic acid (EDTA), centrifuged for 10 minutes at 3000 rpm, after which blood plasma was separated from the cell sediment and immediately frozen at –20 °C. Total RNA was isolated from 100 μL of blood plasma using Serum Plasma kits (Qiagen, USA) with preliminary addition of 1.6×10^8 copies of synthetic cel-miR-39 microRNA (Qiagen) after plasma incubation with Qiazol phenolic mixture. Cel-miR-39 was used as an internal control for the efficiency of RNA isolation, complementary DNA (cDNA) synthesis, and quantitative polymerase chain reaction (PCR) in real time. The intensity of miRNA expression was calculated using the 2-ΔCT method [14] and was expressed in relative units equivalent to $\log_2 (2^{-\Delta Ct})$, where ΔCt are the working values of the change in the product production cycle relative to the internal control of cel-miR-39 miRNA expression.

Acute cellular rejection (ACR) and antibody-mediated rejection (AMR) were verified by examining endomyocardial biopsy specimens. For histological examination, endomyocardial pieces were fixed in 10% formalin, then washed with water, dehydrated and embedded in paraffin. 3–4 μm thick slices were prepared on a microtome. To diagnose ACR, the slices were stained with hematoxylin and eosin; to diagnose AMR, an immunohistochemical study was used. The degree of ACR and AMR was assessed according to the recommended classifications adopted by the International Society for Heart and Lung Transplantation (ISHLT-2004 and ISHLT-2013).

Statistical data processing

Sensitivity and specificity were measured using ROC analysis. To assess the diagnostic significance of miRNA-101 and miRNA-27, a relative risk index was used. The Youden's index was calculated to determine the threshold level of microRNA expression. The test's sensitivity (Se) is represented by the proportion of true positive cases, while specificity (Sp) is the proportion of true negative cases. The test's diagnostic accuracy (De) is expressed as the percentage ratio of the sum of all true cases to the total number of results obtained. Statistical analysis of results obtained was done using software and standard statistical processing methods of the applied software package Statistica v.13.0 from StatSoftInc. (USA). Obtained data was statistically processed by nonparametric methods: for comparison of dependent samples, the paired Wilcoxon test was calculated, and the Mann–Whitney U test was used to compare the independent variables. The critical level of significance was assumed to be 5%, i.e. the null hypothesis was rejected at $p < 0.05$.

RESULTS AND DISCUSSION

The miRNA-101 and miRNA-27 expression indicators in heart recipients are presented as a median of concentrations [interquartile range] with an indication of the significance of differences, which is due to the distribution of values other than normal.

During the entire follow-up period after transplantation, signs of acute rejection were verified in 27 recipients in 31 endomyocardial biopsy specimens. Among them, ACR (grades R1G–R3G according to ISHLT-2004 classification) was observed in 23 recipients in 24 samples, and AMR in 6 recipients in 6 samples, and mixed acute rejection in 1 sample.

Fig. 1 shows the morphological picture of endomyocardial biopsy specimens of the transplanted heart, in which ACR and AMR signs were detected.

Recipients with and without acute graft rejection did not differ significantly by age ($p = 0.84$), sex ($p = 0.07$), and pre-transplant diagnosis ($p = 0.51$). When we analyzed tacrolimus blood levels in cardiac recipients, no significant differences were found in the group of patients with and without acute rejection – 8.1 [6.7; 10.7] and 9.9 [6.1; 12] ng/mL, respectively ($p = 0.75$).

It was found that the miRNA-101 and miRNA-27 expression levels in recipients with acute graft rejection was significantly lower than in recipients without rejec-

tion (p = 0.04 and p = 0.03, respectively, Fig. 2). The results obtained are consistent with available reports on the inhibitory effect of miRNA-101 [15–17] and miRNA-27 [18, 19] on the development of fibrotic processes in the heart and other organs.

We used the ROC-curve analysis to determine the diagnostic significance of miRNA-101 and miRNA-27 as a marker of acute rejection of transplanted heart (Fig. 3).

Calculations showed that the area under the ROC curve of miRNA-101 and miRNA-27 in heart recipients

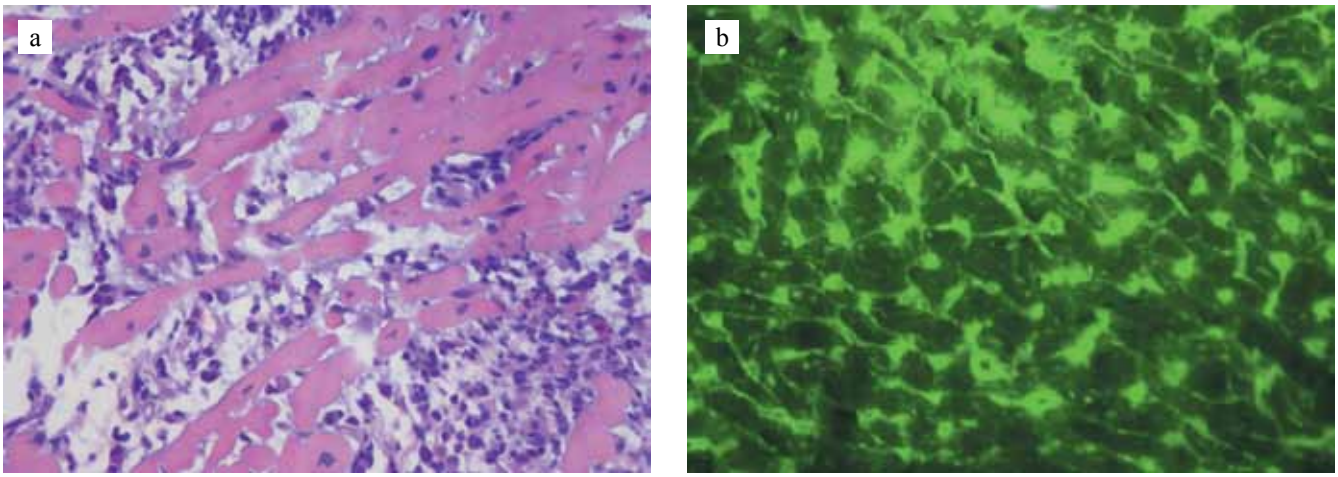

Fig. 1. Study of endomyocardial biopsy specimens. (a) multifocal moderate ACR of a heart transplant (R2G grade according to ISHLT-2004 classification). H&E stain. 400×. (b) fixation of the C4d fragment of the complement in the myocardial capillary wall in AMR. Immunohistochemistry analysis

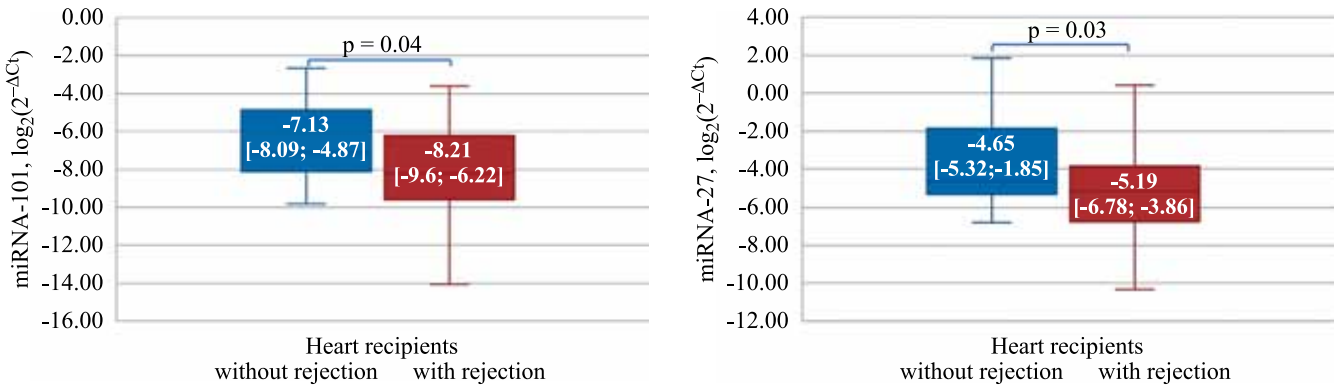

Fig. 2. miRNA-101 and miRNA-27 expression levels in heart recipients with and without graft rejection ($\log_2(2^{-\Delta Ct})$)

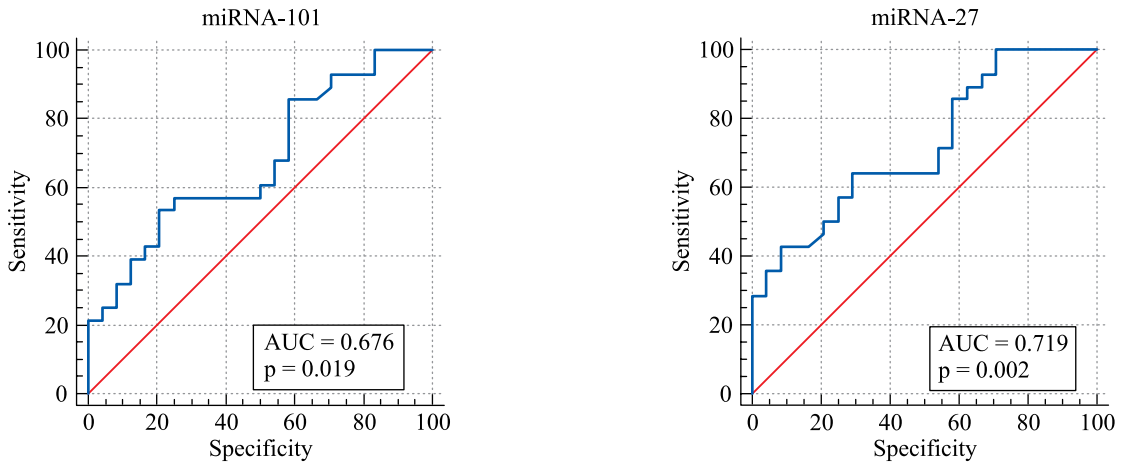

Fig. 3. ROC curves of miRNA-101 and miRNA-27 in heart recipients with acute transplant rejection

with acute graft rejection is 0.676 and 0.719 (p = 0.02 and p = 0.002, respectively).

The threshold expression levels of miRNA-101 and miRNA-27, significant for the diagnosis of acute graft rejection in cardiac recipients, were determined by optimal combination of sensitivity and specificity values corresponding to the highest Youden's index [20].

Fig. 4 shows a graph of sensitivity and specificity dependence on the miRNA-101 and miRNA-27 expression levels in blood plasma in relation to acute graft rejection in cardiac recipients.

The threshold of miRNA-101 expression, which is a significant factor for diagnosis of acute graft rejection in cardiac recipients, was –8.36. When the miRNA-101 expression level is below this threshold, the likelihood of the risk of developing acute graft rejection is 1.8 times higher than in recipients with miRNA-101 expression level above this threshold (sensitivity 53.6%, specificity 79.2%). The diagnostic accuracy of the test was 65.4%. The threshold value of miRNA-27 expression, which is a significant factor for diagnosis of acute graft rejection in cardiac recipients, was –5.07. When the miRNA-27

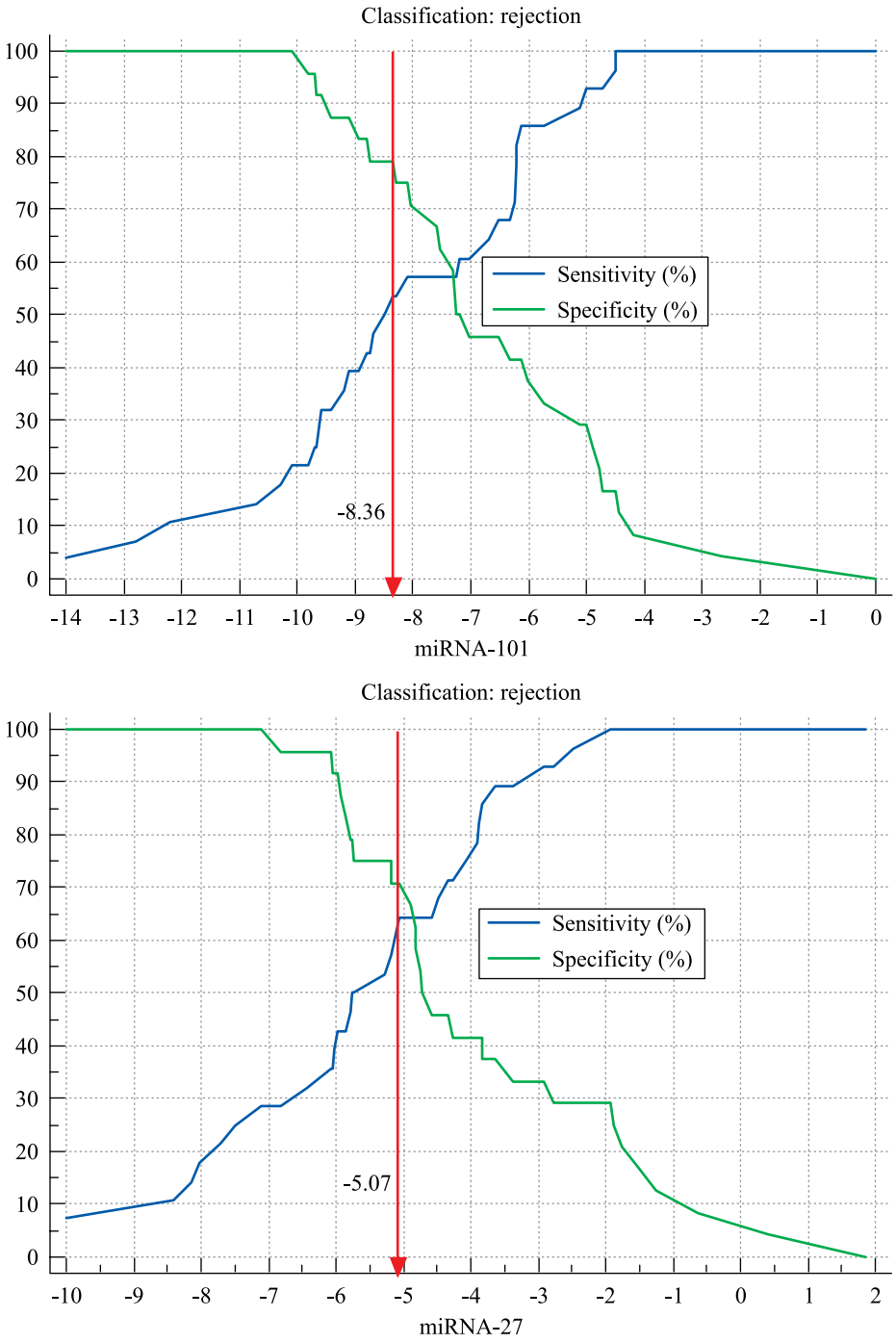

Fig. 4. Diagnostically significant threshold expression levels of miRNA-101 and miRNA-27 in heart recipients with acute transplant rejection

Table

The diagnostic significance of the expression levels of miRNA-101 and miRNA-27 is below the thresholds in heart recipients with acute transplant rejection

miRNA	RR	95% CI	Se	Sp	De
miRNA-101	1.8	[1.132–3.012]	53.6%	79.2%	65.4%
miRNA-27	1.9	[1.122–3.367]	64.3%	70.8%	67.3%
miRNA-101 + miRNA-27	2.0	[1.158–3.364]	60.0%	78.9%	68.2%

expression level is below this threshold, the probability of the risk of developing acute graft rejection is 1.9 times higher than in recipients with miRNA-27 expression level above this threshold (64.3% sensitivity, 70.8% specificity). The test's diagnostic accuracy was 67.3% (Table).

When assessing the diagnostic significance of combined measurement of microRNA-101 and microRNA-27 with respect to acute graft rejection in heart recipients, it was found that when the expression level of these microRNAs is below the thresholds determined, the probability of the risk of developing acute graft rejection is twice as high (60.0% sensitivity, 78.9% specificity). The test's diagnostic accuracy is 68.2%.

CONCLUSION

In heart recipients, the miRNA-101 and miRNA-27 expression levels are of diagnostic significance with respect to acute graft rejection. With microRNA-101 expression level ≤–8.63 units ($\log_2(2^{-\Delta Ct})$), the risk of acute graft rejection in heart recipients is 1.8 times higher than in recipients with microRNA-101 expression level above the threshold. At a microRNA-27 expression level ≤–5.07 arbitrary units ($\log_2(2^{-\Delta Ct})$), the risk of developing acute graft rejection in heart recipients is 1.9 times higher than in recipients with the miRNA-27 expression level above the threshold. When the miRNA-101 and miRNA-27 expression levels below the thresholds simultaneously, the risk of developing acute graft rejection doubles.

This work was supported by a grant (No. NSh-2598.2020.7) of the President of the Russian Federation for government support of leading Russian research schools.

The authors declare no conflict of interest.

REFERENCES

1. *Gautier SV, Shevchenko AO, Popcov VN*. Pacient s transplantirovannym serdcem: rukovodstvo dlya vrachej po vedeniyu pacientov, perenesshih transplantaciyu serdca. M.: Triada, 2014. 144.
2. *Shevchenko AO, Nikitina EA, Koloskova NN, Shevchenko OP, Gautier SV*. Kontroliruemaja arterial'naja gipertenzija i vyzhivaemost' bez nezhelatel'nyh sobytij u recipientov serdca. *Kardiovaskuljarnaja terapija i profilaktika*. 2018; 17 (4): 4–11. [In Russ, English abstract].
3. *Stehlik J, Starling RC, Movsesian MA, Fang JC, Brown RN, Hess ML et al.* Cardiac Transplant Research Database Group. Utility of long-term surveillance endomyocardial biopsy: a multi-institutional analysis. *J Heart Lung Transplant*. 2006; 25 (12): 1402–1409.
4. *Crespo-Leiro MG, Barge-Caballero G, Couto-Mallon D*. Noninvasive monitoring of acute and chronic rejection in heart transplantation. *Curr Opin Cardiol*. 2017; 32 (3): 308–315.
5. *Shumakov VI, Shevchenko OP, Hubutiya MSh, Orlova OV, Kazakov EN, Kormer AYa, Olefirenko GA*. Vaskulopatiya transplantirovannogo serdca: sinergizm provospalitel'nyh, proaterogennyh faktorov i virusnoj infekcii. *Vestnik Rossijskoj akademii medicinskih nauk*. 2006; 11: 8–14.
6. *Savic-Radojevic A, Pljesa-Ercegovac M, Matic M et al*. Novel biomarkers of heart failure. *Advances In Clinical Chemistry*. 2017; 79: 93–152.
7. *Kransdorf EP, Kobashigawa JA*. Novel molecular approaches to the detection of heart transplant rejection. *Per Med*. 2017 Jul; 14 (4): 293–297.
8. *van Gelder T*. Biomarkers in solid organ transplantation. *Br J Clin Pharmacol*. 2017 Dec; 83 (12): 2602–2604.
9. *Starling RC, Stehlik J, Baran DA et al*. Multicenter analysis of immune biomarkers and heart transplant outcomes: results of the clinical trials in organ transplantation-05 study. *American Journal of Transplantation*. 2016; 16: 121–136.
10. *Di Francesco A, Fedrigo M, Santovito D, Natarelli L, Castellani C, De Pascale F et al*. MicroRNA signatures in cardiac biopsies and detection of allograft rejection. *J Heart Lung Transplant*. 2018 Nov; 37 (11): 1329–1340.
11. *Shah P, Bristow MR, Port JD*. MicroRNAs in Heart Failure, Cardiac Transplantation, and Myocardial Recovery: Biomarkers with Therapeutic Potential. *Curr Heart Fail Rep*. 2017 Dec; 14 (6): 454–464.
12. *Khush K, Zarafshar S*. Molecular Diagnostic Testing in Cardiac Transplantation. *Curr Cardiol Rep*. 2017 Oct 13; 19 (11): 118.
13. *Velikiy DA, Gichkun OE, Sharapchenko SO, Shevchenko OP, Shevchenko AO*. Uroven' ekspressii mikroRNK v rannie i otdalennye sroki posle transplantacii u recipientov serdca. *Vestnik transplantologii i iskusstvennyh organov*. 2020; 22 (1): 26–34.
14. *Livak KJ, Schmittgen TD*. Analysis of relative gene expression data using real-time quantitative PCR and the

2(-Delta Delta C(T)) Method. *Methods*. 2001 Dec; 25 (4): 402–408.
15. *Li X, Zhang S, Wa M, Liu Z, Hu S.* microRNA-101 Protects Against Cardiac Remodeling Following Myocardial Infarction via Downregulation of Runt-Related Transcription Factor 1. *J Am Heart Assoc*. 2019 Dec 3; 8 (23): e013112.
16. *Huang C, Xiao X, Yang Y, Mishra A, Liang Y, Zeng X et al*. MicroRNA-101 attenuates pulmonary fibrosis by inhibiting fibroblast proliferation and activation. *J Biol Chem*. 2017 Oct 6; 292 (40): 16420–16439.
17. *Meroni M, Longo M, Erconi V, Valenti L, Gatti S, Fracanzani AL, Dongiovanni P.* Mir-101-3p Downregulation Promotes Fibrogenesis by Facilitating Hepatic Stellate Cell Transdifferentiation During Insulin Resistance. *Nutrients*. 2019 Oct 29; 11 (11): 2597.
18. *Zhang XL, An BF, Zhang GC*. MiR-27 alleviates myocardial cell damage induced by hypoxia/reoxygenation via targeting TGFBR1 and inhibiting NF-κB pathway. *Kaohsiung J Med Sci*. 2019 Oct; 35 (10): 607–614.
19. *Wang Y, Cai H, Li H, Gao Z, Song K*. Atrial overexpression of microRNA-27b attenuates angiotensin II-induced atrial fibrosis and fibrillation by targeting ALK5. *Hum Cell*. 2018 Jul; 31 (3): 251–260.
20. *Hughes G*. Youden's Index and the Weight of Evidence Revisited. *Methods Inf Med*. 2015; 54 (6): 576–577.

The article was submitted to the journal on 9.10.2020

DOI: 10.15825/1995-1191-2020-4-27-31

A DONOR HEART SCORING MODEL TO PREDICT TRANSPLANT OUTCOMES

E.A. Tenchurina[1], M.G. Minina[1, 2]

[1] Botkin City Clinical Hospital, Moscow, Russian Federation
[2] Shumakov National Medical Research Center of Transplantology and Artificial Organs, Moscow, Russian Federation

Selection of heart donors is the most important stage on which the success of heart transplantation depends. **Objective:** to create a donor heart scoring model based on a number of donor characteristics. **Materials and methods.** The study used data from 650 brain-dead donors who underwent organ explantations between January 1, 2012 and December 31, 2017. In binomial logistic regression, non-selection of heart donor was used as a dependent variable, while donor characteristics were used as factor features. In regression model, the odds ratio was determined for each donor factor, which was transformed into points. The sum of the points of each of the donor factors included in the model was taken as the score of the donor heart. The proposed model was validated on a sample of donors for the period from January 1, 2019 to December 31, 2019; n = 218. **Results.** The model includes donor characteristics, such as age, cause of death (traumatic brain injury (TBI)/stroke), history of hypertension and diabetes, cardiac arrest with subsequent recovery, own pathology and traumatic heart disease, as well as heart rate, systolic blood pressure, arterial lactate, and need for norepinephrine immediately before organ harvesting. Based on the average value of the sum of points, low-risk donors (LRD ≤17 points) and high-risk donors (HRD ≥18 points) were identified. In the validation pool of donors, the proportion of heart failure among LRD and HRD was 4.1% and 78.6%, respectively, $p < 0.0001$, Pearson's χ^2 – 130.9. **Conclusion.** The presented donor heart scoring model accurately reflects the probability of using a donor's heart for transplantation and creates conditions for optimal distribution of heart transplants, especially from high-risk donors.

Keywords: donor heart scoring model, donor heart risk factors.

INTRODUCTION

When deciding on the suitability of a donor heart for transplantation, the specialists need to consider a large number of both donor and recipient factors in order to achieve optimal outcomes. It is often difficult to subjectively determine the total risk of heart transplantation, especially when it involves expanded criteria donors. In the world, there is a practice of using statistical models that determine the relationship between initial factors and final outcome to make an objective decision. In such models, the donor heart score is usually measured by the sum of the scores determined for each factor. The most famous models of this kind are the European model [1] and the model created by American researchers using the UNOS database [2]. Improving the assessment of the state of the donor heart, as well as standardizing the risk factors, are extremely pressing issues for improving the efficiency of heart transplantation [3].

MATERIALS AND METHODS

We used data from 650 brain-dead donors who underwent organ explantations from January 1, 2012 to December 31, 2017. In 198 (30.5%) donor cases, it was decided not to use the donor heart for transplantation. At the initial stage, a general analysis of the reasons for non-selection of a donor heart was conducted, taking into account the age category of donors. A comparative analysis of indicators between donor groups who died from traumatic brain injury (TBI) and stroke was carried out. Binary logistic regression was used to estimate the cumulative risk of using a donor heart for transplantation, the end point of which was non-selection of the donor heart. Independent factors were donor characteristics – age, sex, cause of death, high blood pressure, diabetes, circulatory arrest, lifetime heart disease and acute traumatic cardiac injury. The following indicators were considered in two values – mean arterial pressure (MAP), heart rate (HR), hemoglobin, pH, lactate, Na, glucose, norepinephrine need, and creatinine. The odds ratio (OR) obtained in the regression model was assigned, as a score, to each donor factor included in the model. The donor heart score was obtained by summing the scores of the factors encountered in a particular donor. Based on the mean value of the sum of scores, low-risk donors (LRD ≤17 points) and high-risk donors (HRD ≥18 points) were identified. A pool of 218 donors from January 1 to December 31, 2019 was used to validate the model presented. Verification of the model revealed

Corresponding author: Elmira Tenchurina. Address: 5, Vtoroy Botkinsky Proezd, Moscow, 125284, Russian Federation. Phone: (967) 113-87-64. E-mail: arimle@inbox.ru

a significant difference in the proportion of donor heart non-selection, depending on the donor heart score.

Data was processed using the SPSS23.0 software for Windows.

DISCUSSION AND RESULTS

The clinical characteristics of 650 donors were studied from January 1, 2012 to December 31, 2017 (Fig. 1). Heart explantation was performed in 452 (69.5%) donors, the heart was not used for transplantation in 198 (30.5%) cases. The distribution of reasons for non-selection of a donor heart are given in Fig. 2. It is noteworthy that in the older group of donors, own disease and heart injuries, high blood pressure, diabetes come out on top as the reasons for non-selection of a donor heart for transplantation.

In a group of donors under 50, non-selection due to severe concomitant injuries, including those affecting the chest organs, predominate. The number of rejections associated with poor donor homeostasis was comparable in both age groups.

Among all donors whose hearts were not used for transplantation, the number of those who died from stroke was 2.3 times higher than those who died from traumatic brain injury. Donors with stroke are significantly older than donors with traumatic brain injury ($p < 0.0001$). At the same time, donors with traumatic brain injury have worse homeostasis indicators than donors with vascular lesions due to the higher frequency of traumatic and hemorrhagic shock symptoms and severe hemodynamic disorders in donors with brain injury (Table 1).

Multivariate regression model of donor heart evaluation

Table 2 presents the donor factors significantly influencing the decision to reject a donor heart. Factors that did not demonstrate statistically significant influence on the decision to reject a donor heart were excluded from the model – donor gender, MAP, HR, hemoglobin, pH, lactate, Na, blood glucose and creatinine, and norepinephrine requirements recorded during the initial examination of a potential heart donor. Two factors showed possible credibility, lactate 2 ($p = 0.060$) and norepinephrine requirement – 2 (0.061), and we considered it possible to include them in the regression model.

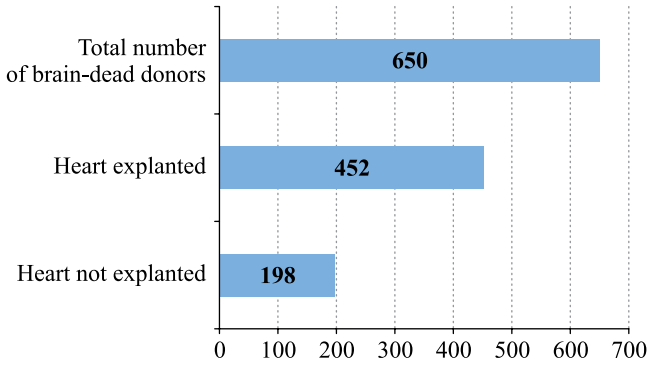

Fig. 1. Distribution of a pool of brain-dead donors included in the study

The degree of influence of each of the factors, determined by the OR value, was converted into scores. The ORs obtained from the regression model reflect the probability of donation depending on the presence/absence of a particular factor in the donor in comparison with the baseline values of donor factors. For example, the chance of refusing to use a heart for transplantation from a 56-year-old donor was 1.85 times greater than for a 46-year-old donor, whose OR value was taken as the baseline and was 1 point (Table 2). Table 3 shows how heart donor scores are calculated. A 46-year-old donor who died from cerebrovascular disease and had concomitant diseases with a score of 19 is considered a high-risk heart donor, while a 56-year-old donor,

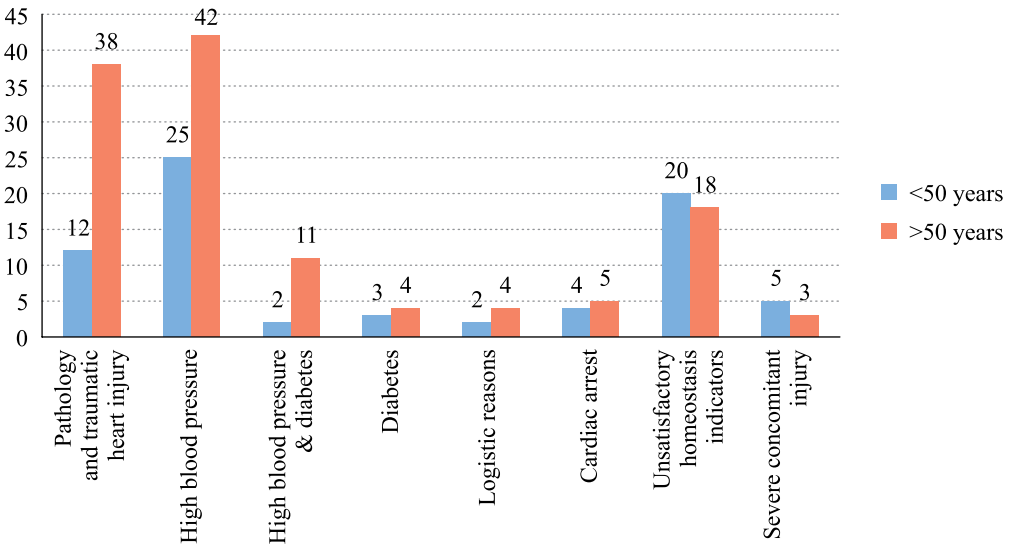

Fig. 2. Reasons for non-selection of donor heart

Table 1

Comparative analysis of donors whose hearts were not used for transplantation

Factor	TBI (n = 60)		Stroke (n = 138)		p
	Mean value	Min–Max	Mean value	Min–Max	
Age, years	46.4 (n = 60)	19–64	52.5 (n = 138)	27–67	<0.0001
pH, unit pH	7.38 (n = 49)	6.97–7.60	7.39 (n = 129)	6.90–7.62	0.47
Lactate, mmol/L	4.72 (n = 34)	0.7–22	2.74 (n = 94)	0.2–9.2	0.001
Na, mmol/L	149.7 (n = 49)	123–178	144.8 (n = 130)	131–183	0.007
Hb, g/L	102.9 (n = 48)	56–156	136.5 (n = 128)	48–186	<0.0001
Glucose, mmol/L	11.5 (n = 48)	6.0–31.0	10.3 (n = 127)	3.0–22.8	0.082
Creatinine, μmol/L	99.9 (n = 60)	47.0–239.0	103.0 (n = 136)	37.0–549.0	0.676
HA, ng/kg/min	560.4 (n = 60)	0.0–2000	442.9 (n = 134)	0.0–2500	0.125

Table 2

Regression model for evaluating donor heart. Dependent variable – non-selection of donor heart; 650 donors; January 1, 2012 to December 31, 2017

Factors	OR	Confidence interval	Points*	p
Age				
<45	0.35	0.237–0.504	1	
45–54	1.22	0.86–1.74	1	<0.0001
55–59	1.85	1.24–2.77	2	
>60	2.81	0.86–1.74	3	
Cause of death				
Stroke	1.51	1.06–2.16	2	0.024
TBI	0.66	0.46–0.95	1	
Hypertension				
Yes	1.96	1.39–2.8	2	0.001
No	0.506	0.36–0.72	1	
Diabetes				
Yes	1.97	1.19–3.26	2	0.009
No	0.51	0.31–0.843	1	
Circulatory arrest**				
Yes	23.99	3.05–188.72	24	<0.0001
No	0.042	0.005–0.33	1	
Pathology and traumatic heart injury***				
Yes	14.61	6.39–33.43	15	<0.0001
No	0.68	0.30–0.157	1	
Heart rate-2, beats/min				
<60	7.45	0.77–72.1	7	<0.0001
60–90	0.51	0.36–0.74	1	
>90	1.83	1.27–2.63	2	
SBP-2, mmHg				
<70	0.57	0.06–5.12	1	
70–110	0.63	0.44–0.91	1	<0.0001
110–150	1.42	0.97–2.10	1	
>150	3.03	1.11–8.25	3	
Lactate-2, mmol/L				
<2	0.58	0.37–0.89	1	0.060*
>2	1.72	1.13–2.64	2	
Norepinephrine-2, ng/kg/min				
<100	1.23	0.85–1.77	1	
100–600	0.785	0.56–1.10	1	0.061**
600–1000	0.813	0.45–1.46	1	
>1000	2.615	1.09–6.26	3	

Note. * Maximum 63 points, minimum 10 points. Low-risk donor ≤17 points, high risk donor ≥18 points. ** Circulatory arrest at pre-hospital or hospital stages. *** CHD, rhythm disturbances, pathology and valve replacement, traumatic heart injury.

without concomitant diseases, whose cause of death was traumatic head injury is regarded as a low-risk heart donor according to the proposed model. Rejection rate of donors who scored 19 and 13 points in the verification pool was 100% and 2.8% respectively.

The functionality of the proposed model was assessed using donor pool validation. The proportion (%) of rejections increased significantly, with total donor attainment of 18 points or more (Fig. 3). Rejections for LRDs and HRDs were 4.1% and 78.6% respectively. The difference is statistically significant ($p < 0.0001$), Pearson's chi-squared was 130.9.

CONCLUSION

We obtained an objective tool for primary assessment of a donor heart in the context of donor risk factors. The regression model reflects the evolution in the assessment of heart donors observed in Moscow over the past 10 years. Instead of a subjective assessment of each of the donor factors and their associated risks of poor transplant outcome, we have developed an evidence-based assessment system for donor heart refusal. The regression model can be used in the earliest stages of heart donor assessment as a tool for identifying high-risk donors. Undoubtedly, the final decision on the suitability of a donor heart for transplantation rests on specialists providing transplant care, based on, among other things, the results of invasive high-tech imaging studies, if necessary. However, at the initial stage of selection of a donor heart for transplantation, a simple and affordable tool that allows you to quickly present objective information about the donor to all interested transplant centers for preliminary selection of a recipient is needed.

Table 3

Example of how scores for heart donors are calculated

Factor	Donor 1	Points	Donor 2	Points
Age	46	1	56	2
Cause of death	Stroke	2	TBI	1
Hypertension	Yes	2	No	1
Diabetes	Yes	2	No	1
Circulatory arrest	No	1	No	1
Pathology and traumatic heart injury	No	1	No	1
Heart rate-2, beats/min	56	7	96	2
SBP-2, mmHg	103	1	89	1
Lactate-2, mmol/L	0.8	1	2.1	2
Norepinephrine-2, ng/kg/min	270	1	100	1
Total score		19		13

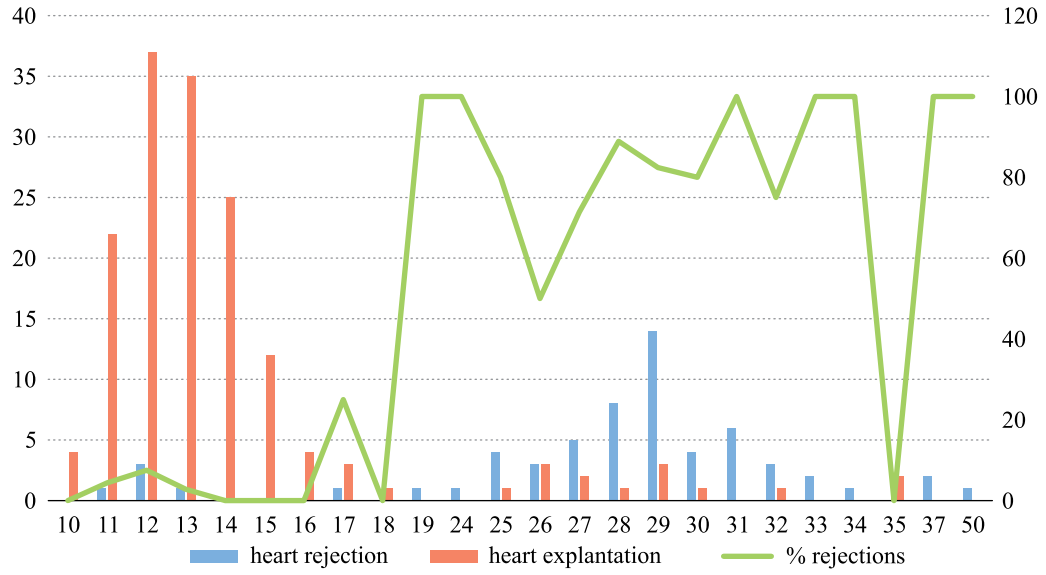

Fig. 3. Heart donor scores and proportion of rejection (%) in the validation pool of brain-dead donors

The authors declare no conflict of interest.

REFERENCES

1. *Smits JM, De Pauw M, de Vries E et al.* Donor scoring system for heart transplantation and the impact on patient survival. *J Heart Lung Transplant*. 2012; 31: 387–397.
2. *Weiss ES, Allen JG, Kilic A et al.* Development of a quantitative donor risk index to predict short-term mortality in orthotopic heart transplantation. *J Heart Lung Transplant*. 2012; 31: 266–273.
3. *Dorent R, Gandjbakhch E, Goéminne C et al.* Assessment of potential heart donors: A statement from the French heart transplant community. *Arch Cardiovasc Dis*. 2018 Feb; 111 (2): 126–139.

The article was submitted to the journal on 9.09.2020

DOI: 10.15825/1995-1191-2020-4-32-42

FEATURES OF HAEMOPHILUS INFLUENZAE TYPE *b* VACCINE IN PATIENTS WAITLISTED FOR LUNG TRANSPLANTATION

V.B. Polishchuk[1], M.P. Kostinov[1, 2], A.A. Pyzhov[1], O.O. Magarshak[1], N.E. Yastrebova[1], N.A. Karchevskaya[3], E.A. Tarabrin[3], T.E. Kallagov[3], A.E. Vlasenko[4]

[1] Mechnikov Research Institute of Vaccines and Sera, Moscow, Russian Federation
[2] Sechenov University, Moscow, Russian Federation
[3] Sklifosovsky Research Institute of Emergency Care, Moscow, Russian Federation
[4] Novokuznetsk State Institute for Advanced Training of Physicians, Novokuznetsk, Russian Federation

Objective: to evaluate the immunological efficacy of *Haemophilus influenzae* type b (*Hib*) vaccine in patients with severe bronchopulmonary condition waitlisted for lung transplantation. **Materials and methods.** 16 patients (age 22–61 years) with severe bronchopulmonary diseases were vaccinated once against *Hib* infection. IgG antibody concentrations to *Hib* capsular polysaccharide before vaccination and 1 month after was measured by ELISA using a test system developed at Mechnikov Research Institute of Vaccines and Sera. Statistical data processing was carried out using stats (v.3.6.2), lme4 (v.1.1 – 21), and lmerTest (v.3.1 – 1) packages. **Results.** *Hib* vaccine in patients with severe bronchopulmonary condition did not elicit any local or systemic reactions. The proportion of patients whose antibody (Ab) concentrations to *Hib* capsular polysaccharide exceeded the long-term protection threshold was 69% and 100% before and after vaccination, respectively (p = 0.02). There were differences in the formation of post-vaccination immunity depending on the nosological forms of patients' diseases. In the group of patients with obstructive pulmonary diseases, the geometric mean level of antibodies to the *Hib* capsular polysaccharide after vaccination increased as compared to the baseline value – from 1.3 [0.6–2.8] to 5.5 [1.9–15.4] AU/mL, (p = 0.05). In the group of patients with restrictive lung diseases, the level did not change – 2.8 [0.6–14.1] AU/mL before vaccination and 3.4 [1.3–8.5] AU/mL 1 month after vaccination. In the group of patients taking glucocorticosteroids, there was no increase in the level of antibodies to *Hib* capsular polysaccharide (2.7 [0.8–9.3] AU/mL before and 2.8 [1.2–6.5] AU/mL after vaccination). In the group of patients who did not take hormones, antibody concentrations to *Hib* capsular polysaccharide increased from 1.2 [0.7–2.1] AU/mL to 4.8 [2.2–10.1] AU/mL (p = 0.006). **Conclusion.** *Hib* vaccination of waitlisted patients with severe bronchopulmonary disease is safe and immunologically effective.

Keywords: Haemophilus influenzae type b, IgG, vaccine prophylaxis, adults, bronchopulmonary diseases.

Haemophilus influenzae type b (Hib) vaccination is a good example of the efficacy of this method in preventing infectious diseases. The introduction of vaccination using first a polysaccharide and later a conjugate vaccine significantly reduced the incidence of Hib infection, especially in children younger than 5 years old. It was in this age group that severe invasive forms of the disease, such as meningitis and pneumonia, were most often noted, which in many cases ended in death or disability [1–3]. WHO is currently recommending the inclusion of Hib vaccination in routine prevention programs for children. In 2018, vaccination against this infection was included in national vaccination calendars across 191 countries around the world [4, 5].

Healthy adults usually do not receive Hib vaccine, since most of them are carriers of the bacteria, or the disease proceeds as acute respiratory infections, mainly in mild and clinically not pronounced forms. The risk group for invasive Hib infection primarily includes patients with functional and anatomic asplenia. However, according to a study by D.C. Cassimos et al., out of 42 European countries, only 5 have included Hib vaccination for adults at risk in their national vaccination policies; the vaccination is recommended in 3 countries and is compulsory in 2 countries [6]. This being said, the risk groups for severe Hib infection in some countries include patients with HIV infection, patients with malignant tumors, and solid organ recipients [7].

The aim of the study was to evaluate the immunological efficacy of Hib vaccination in patients with severe bronchopulmonary condition waitlisted for lung transplantation.

MATERIALS AND METHODS

The study included 16 patients with severe bronchopulmonary diseases aged 22 to 61 years (median 42 [41–47] years). Among those examined were 81.3% (13/16) women and 18.8% (3/16) men. There were 44%

Corresponding author: Valentina Polishchuk. Address: 5a, Malyj Kazennyj pereulok, Moscow, 105064, Russian Federation. Phone: (495) 917-41-49. E-mail: polischook@mail.ru

(7/16) of patients with chronic obstructive pulmonary diseases (COPD, lymphangioleiomyomatosis, emphysema), 31% (5/16) with restrictive lung disease (idiopathic pulmonary fibrosis, fibrosis resulting from exogenous allergic alveolitis, nonspecific interstitial pneumonia), 3 patients had pulmonary vascular diseases (pulmonary hypertension of various origins) and one with cystic fibrosis. Patients with obstructive diseases received therapy with bronchodilators, mucolytics, while the patient with cystic fibrosis also received antibiotic therapy. Patients with idiopathic pulmonary fibrosis were treated with fibrostatics. In other types of interstitial lung diseases (fibrosis resulting from exogenous allergic alveolitis, nonspecific interstitial pneumonia), the patients received small doses of systemic glucocorticoids. Patients with pulmonary hypertension were on PAH-specific therapy with endothelin receptor antagonists, guanylate cyclase stimulants, and prostacyclin drugs. At the time of vaccination, 38% (6/16) of patients were taking glucocorticoids. The patients had not previously been vaccinated against Hib.

Hib vaccination was carried out in the absence of an exacerbation of the underlying disease and signs of respiratory infection. A single 0.5 mL intravenous Hiberix vaccine (manufactured by GlaxoSmithKline) was administered. Before vaccination and 1 month after, there was blood sampling, followed by measurement of the IgG antibody (Ab) concentrations against the Hib capsular polysaccharide.

The serum Ab concentrations (IU/mL) in the examined were determined by enzyme-linked immunosorbent assay (ELISA) using a test system developed at the Mechnikov Research Institute of Vaccines and Sera, Moscow [8]. A ≥0.15 IU/mL concentration was conventionally regarded as the antibody concentration providing short-term protection, while ≥1 IU/mL was considered the threshold for long-term protection.

STATISTICAL ANALYSIS

Descriptive statistics of quantitative features were represented by the geometric mean and 95% confidence interval (95% CI) for Ab, and for median and interquartile range for the age of the subjects. Qualitative traits were represented by the proportion with 95% CI, calculated by the Clopper-Pearson method, and the absolute number of subjects with the trait under study in the total group population (n/N). Initial quantitative data were pre-logarithmized and checked for compliance with normal distribution (Shapiro-Wilk test was used). The check showed that all the logarithmic features corresponded to normal distribution. All calculations were performed on the transformed data, with reverse transformation of results obtained.

Two related samples (before/after vaccination) were compared based on quantitative criteria by the Student's t-test for related samples, and based on qualitative criteria by McNemar's test. Two independent samples were compared under qualitative criteria by Fisher's exact test. A mixed-effects model was used to analyze the change in Ab levels depending on the period and study group. The prerequisites for use were tested by the Levene's test (homoscedasticity of residuals) and the Shapiro-Wilk test (normal distribution of standardized residuals). Post-hoc tests were performed using Tukey Test. The relationship between the two quantitative traits was calculated using Spearman's correlation. All calculations were performed in free statistical environment R (v.3.6, GNU GPL2 license). Packages stats (v.3.6.2), lme4 (v.1.1 – 21), and lmerTest (v.3.1 – 1) were used.

RESULTS

Administration of the Hib vaccine in patients with severe bronchopulmonary disease was not accompanied by local and systemic reactions, although in childhood immunization, it can rarely lead to such phenomena.

In all patients enrolled in the study, antibody concentrations against the Hib capsular polysaccharide before vaccination exceeded 0.15 IU/mL. The proportion of subjects with Ab concentrations exceeding the long-term protection threshold before and after vaccination was 69 [41–89]% (11/16) and 100 [79–100]% (16/16) respectively, the differences tending to be statistically significant (p = 0.06 – McNemar's exact test).

The geometric mean of Ab concentrations against the Hib capsular polysaccharide before and after vaccination was 1.7 [1.0–2.8] IU/mL and 3.9 [2.3–6.6] IU/mL respectively. So, the indicator increased 2.3 [1.2–4.6] times, and this increase was statistically significant (p = 0.02) (Fig. 1).

Among the patients enrolled in the study, 7 had obstructive pulmonary disease, 5 had restrictive lung disease, 3 had vascular pulmonary disease and one had cystic fibrosis. Among patients with vascular pulmonary disease, 2 out of 3 people had a protective threshold for Ab concen-

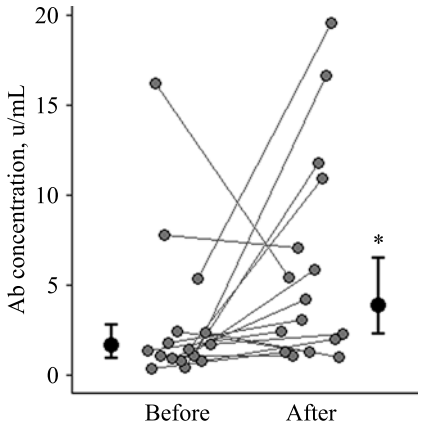

Fig. 1. Geometric mean of antibody concentrations against the Hib capsular polysaccharide before and after vaccination. Individual values, geometric mean and 95% CI are shown

trations against the Hib capsular polysaccharide, which is necessary for long-term protection against infection. Before vaccination, 2 out of 3 people had protective Ab concentrations while after vaccination, all 3 patients had protective Ab levels. In a patient with cystic fibrosis, the baseline antibody concentrations against the Hib capsular polysaccharide exceeded the threshold required for long-term protection against infection. The proportion of subjects with Ab concentrations against the Hib capsular polysaccharide required for long-term protection against infection among patients with obstructive and restrictive lung diseases before and after vaccination is shown in the table (Table 1).

The study revealed an increase in the proportion of patients with Ab concentrations against the Hib capsular polysaccharide in both groups at the necessary long-term protection levels. This increase was not statistically significant, probably due to the small sample size.

A linear mixed effect model was used to analyze the change in the Ab concentrations against the Hib capsular polysaccharide depending on the period and study group. The study period and the group were the fixed effects, individual changes for each subject were considered as random effects. The prerequisites for application of the method were met: homoscedasticity of residuals was tested by the Levene's test ($p = 0.15$), while the normality of distribution of standardized residuals was tested by the Shapiro-Wilk test ($p = 0.59$). The analysis revealed that the average Ab concentrations against the Hib capsular polysaccharide did not differ between patients with obstructive and restrictive lung diseases ($p = 0.22$). The study period (before/after vaccination) had a statistically significant effect ($p = 0.01$), and the change in Ab concentrations against the Hib capsular polysaccharide resulting from vaccination may differ between groups of subjects with different diseases ($p = 0.07$, trending toward statistical significance). The geometric mean Ab concentrations against the Hib capsular polysaccharide in the study groups before and after vaccination, as well as post-hoc test results, are shown in Table 2.

Individual data on the dynamics of Ab concentrations against the Hib capsular polysaccharide before and after vaccination in vaccinated patients are clearly presented in Fig. 2.

In the group of patients with obstructive pulmonary diseases, the geometric mean Ab concentrations against the Hib capsular polysaccharide after vaccination increased by 4.1 [1.1–14.7] times compared with the baseline: from 1.3 [0.6–2.8] IU/mL to 5.5 [1.9–15.4] IU/mL, the increase is statistically significant ($p = 0.05$). In the group with restrictive diseases, the geometric mean Ab concentrations against the Hib capsular polysaccharide did not change statistically significantly after vaccination ($p = 0.99$) – 2.8 [0.6–14.1] IU/mL before vaccination and 3.4 [1.3–8.5] IU/mL 1 month after the procedure. There were no statistically significant differences between the study groups with different lung diseases, both before vaccination ($p = 0.63$) and after vaccination ($p = 0.89$).

The next stage of the study was to evaluate the effect of taking glucocorticoid on changes in Ab to the Hib capsular polysaccharide during vaccination. A mixed-effects model was used, with the study period and the presence/absence of hormones used as fixed factors, individual changes for each subject were taken as random factors. The prerequisites for application of the method were met (Levene's test – $p = 0.94$, Shapiro-Wilk test – $p = 0.22$). As a result, it was found that, on average, Ab concentrations against the Hib capsular polysaccharide

Table 1

Percentage of patients with Hib capsular polysaccharide antibodies required for long-term protection against infection, before and after vaccination, depending on the study group

Study groups	Before vaccination		1 month after vaccination		Dynamics analysis[1]
	Abs.	%	Abs.	%	
Obstructive diseases	4	57.1 [18–90]	7	100 [59–100]	p = 0.25
Restrictive diseases	4	80.0 [28–99]	5	100 [48–100]	p = 1.00
Differences between groups[2]	p = 0.58		p = 1.00		–

Note: [1] – McNemar's test was used; [2] – Fisher's exact test was used.

Table 2

Geometric mean of IgG antibody concentrations against the Hib capsular polysaccharide before and after vaccination, depending on the study group

Study groups	Geometric mean of antibody concentrations and 95% CI		Dynamics analysis[1]
	Before vaccination	1 month after vaccination	
Obstructive diseases	1.3 [0.6–2.8]	5.5 [1.9–15.4]	p = 0.05
Restrictive diseases	2.8 [0.6–14.1]	3.4 [1.3–8.5]	p = 0.99
Differences between groups[2]	p = 0.63	p = 0.89	–

Note: [1, 2] – Tukey's post hoc test was used.

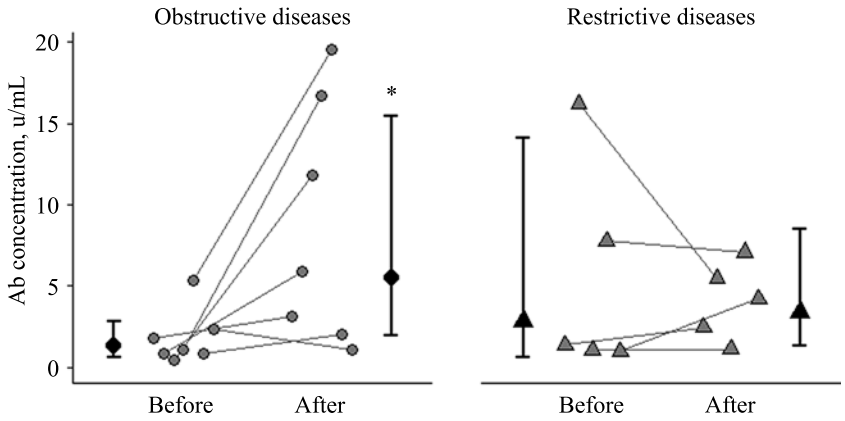

Fig. 2. Antibody concentrations against the Hib capsular polysaccharide before and after vaccination, depending on the disease. Individual values, geometric mean and 95% CI are shown

is independent of hormone intake (p = 0.12), and the Ab concentration changes statistically significantly after vaccination (p = 0.002), but the intensity of this change differs depending on hormone intake (p = 0.03). The geometric mean of Ab concentrations against the Hib capsular polysaccharide before and after vaccination, depending on hormone intake, as well as the results of post-hoc tests, are given in Table 3.

Individual data on changes in Ab concentrations in vaccinated patients with and without hormone therapy are shown in Fig. 3.

There was no statistically significant increase in Ab concentrations against the Hib capsular polysaccharide in the group of patients taking glucocorticoid, the geometric mean level was 2.7 [0.8–9.3] IU/mL before vaccination and 2.8 [1.2–6.5] IU/mL after (p = 1.00). Whereas in the hormone-free patient group, the geometric mean Ab concentration increased 3.9 [1.7–9.0] times as a result of vaccination: from 1.2 [0.7–2.1] IU/mL to 4.8 [2.2–10.1] IU/mL, the change is statistically significant (p = 0.006). There were no statistically significant differences between the study groups, either before vaccination (p = 0.39) or after (p = 0.73).

Table 3

Geometric mean of antibody concentrations against the Hib capsular polysaccharide before and after vaccination, depending on hormone intake

Took hormone	Geometric mean of antibody concentrations and 95% CI		Dynamics analysis[1]
	Before	After	
No	1.2 [0.7–2.1]	4.8 [2.2–10.1]	p = 0.006
Yes	2.7 [0.8–9.3]	2.8 [1.2–6.5]	p = 1.00
Differences between groups[2]	p = 0.39	p = 0.73	–

Note: [1, 2] – Tukey's post hoc test was used.

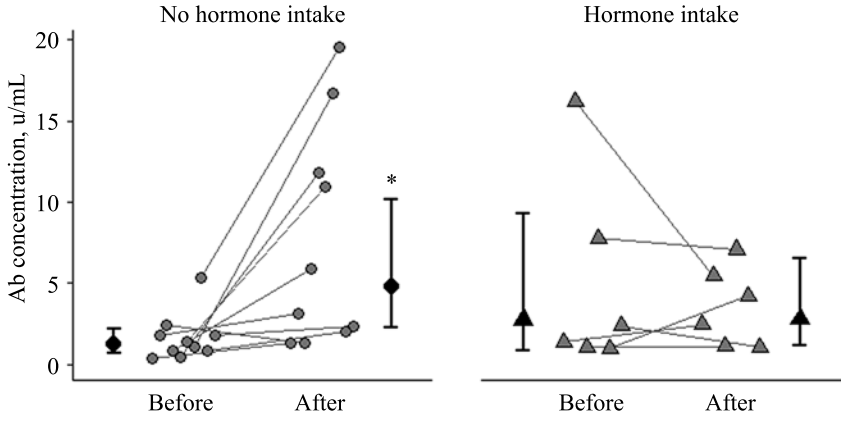

Fig. 3. Antibody concentrations against the Hib capsular polysaccharide before and after vaccination, depending on GCs intake. Individual values, geometric mean and 95% CI are shown

It should be noted that hormone intake is very strongly associated with restrictive lung diseases: 83% (5/6) of all cases of hormone intake occur in the patients of this group.

Next, we analyzed the effect of the age of the subjects on changes in Ab concentrations against the Hib capsular polysaccharide during vaccination. A mixed-effects model was used, the study period and the subject's age were the fixed factors, while the individual changes for each subject were taken as random factors. The prerequisites for applying the method were met (Levene's test – p = 0.83, Shapiro-Wilk test – p = 0.51). Regression curves characterizing the dependence of Ab concentrations against the Hib capsular polysaccharide on the subject's age, estimated using the linear mixed effects models (LMEM), are shown in Fig. 4.

There was a statistically significant increase in concentrations of Hib capsular polysaccharide antibodies after vaccination (p = 0.02), and the intensity of the increase was independent of age (p = 0.84). The relationship between the Ab concentration and age of the subject (p = 0.02) was also established. This relationship manifests itself only after vaccination (correlation coefficient of age and Ab concentrations – rs = 0.48, p = 0.05), before vaccination the relationship was weak and statistically insignificant (rs = 0.26, p = 0.34). This may be a consequence of the different immune response to vaccination in subjects with different lung diseases, as well as the fact that the group of subjects with obstructive diseases is somewhat older than restrictive diseases: 43 [41–49] years versus 32 [32–43] years (differences were not statistically significant p = 0.25).

Subsequently, we analyzed the relationship between the age of vaccinated patients and changes in Hib capsular polysaccharide antibody concentrations after vaccination within certain groups of lung diseases. For the analysis, a mixed-effects model was applied separately for patients with obstructive and restrictive diseases. The period and age of the subjects were the fixed factors; individual changes of each member of the group served as random factors. The prerequisites for application of the method were met in both groups (p = 0.16 – Levene's test, p = 0.41 – Shapiro-Wilk test in the obstructive pulmonary disease group; p = 0.45 – Levene's test, p = 0.52 – Shapiro-Wilk test in the restrictive lung disease group). Regression curves characterizing the dependence of Hib capsular polysaccharide anybody concentrations on the subject's age, estimated using the linear mixed effects model (LMEM) separately for each group of lung diseases, are shown in Fig. 5.

Analysis found no relationship between age and Ab concentrations against the Hib capsular polysaccharide in any of the groups (p = 0.29 in the obstructive pulmonary disease group, p = 0.15 in the restrictive lung disease group). In the group with restrictive lung diseases, there were no statistically significant changes in Hib capsular polysaccharide antibody concentrations after vaccination (p = 0.14). At the same time, the absence of changes in Ab concentrations is characteristic of all ages (no correlation between age and intensity of change, p = 0.16). While in the group of subjects with obstructive pulmonary diseases, there is a statistically significant increase in the Ab concentration after vaccination (p = 0.02), the intensity of increase was independent of age (p = 0.82).

DISCUSSION

Lung transplantation is the only treatment for end-stage lung diseases. The lung transplantation waiting list includes patients with severe bronchopulmonary conditions, for whom all other treatments have proved ineffective. The main nosologies of waitlisted candidates are obstructive pulmonary diseases, cystic fibrosis,

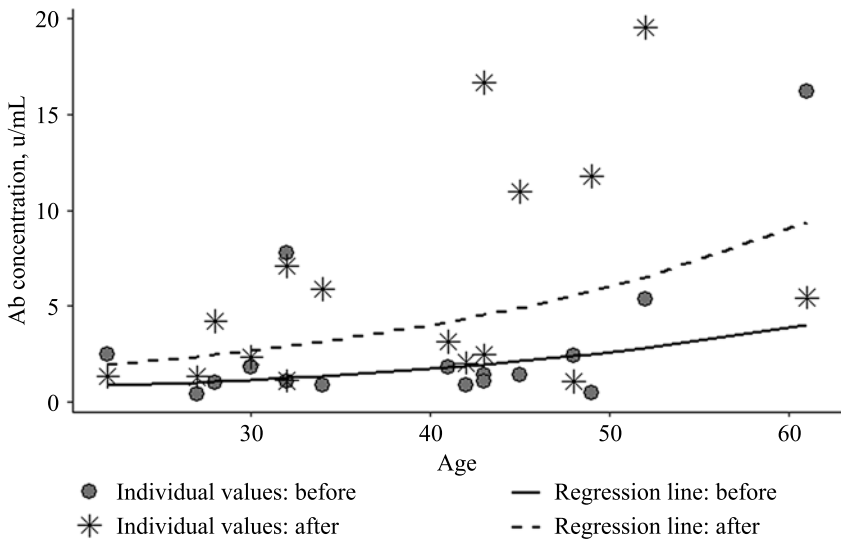

Fig. 4. Antibody concentrations against the Hib capsular polysaccharide before and after vaccination, depending on the age of the subjects. Individual values and regression curves estimated using the LMEM are shown

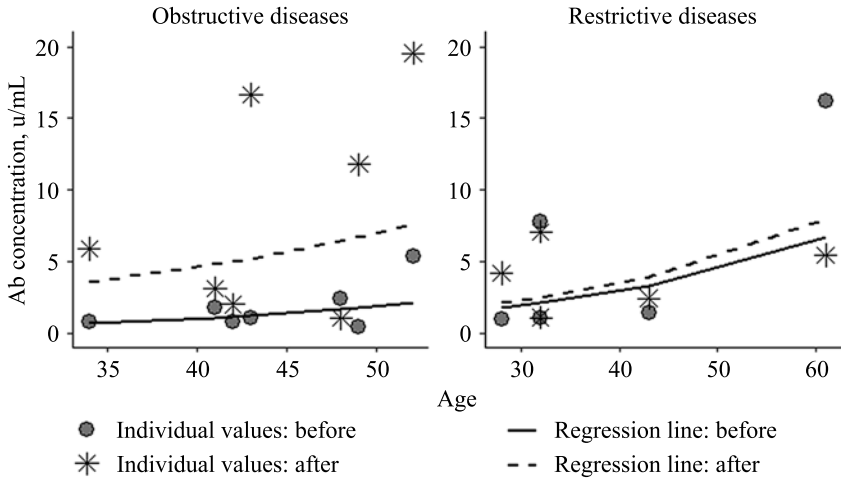

Fig. 5. Antibody concentrations against the Hib capsular polysaccharide before and after vaccination, depending on the age of the subjects and their disease. Individual values and regression curves estimated using the LMEM are shown

restrictive diseases and pulmonary vascular disease. After lung transplantation, patients undergo lifelong immunosuppressive therapy, in most cases including calcineurin inhibitors, glucocorticoids and antimetabolites, which dramatically increases the risk of infectious complications [9]. In addition, the predisposing factors for development of infectious processes in this category of patients are constant exposure of the allograft on environmental factors and violation of natural defense mechanisms (impaired mucociliary clearance, allograft denervation, inhibition of cough-reflex sensitivity [10]. As a result, infectious complications occur 2 times more often after lung transplantation than after heart transplantation. The most common site of infection is the transplanted lung itself [11–12]. All this points to the importance of prevention (vaccine-preventable, primarily respiratory) of infections in terms of management of waitlisted patients. Vaccination should be started as early as possible, since immunosuppressive therapy, initiated after transplantation, disrupts innate and acquired immunity mechanisms, and reduces the effectiveness of post-vaccination immunity [13–16].

Together with pneumococcal, meningococcal infections and influenza, Hib is one of the infections posing a danger to patients with lung diseases [16–22]. In the pre-vaccination era, the most vulnerable age group was children younger than 5 years old. The disease overwhelmingly proceeded in the form of meningitis [23–25]. At present, after the introduction of childhood vaccination against Hib into the national vaccination calendars of most countries, invasive forms of infection are increasingly described in adults, while the clinical disease in most cases proceeds in the form of pneumonia. Unencapsulated types of the pathogen prevail [26]. Nevertheless, the proportion of Hib in invasive forms of disease is 1.6% of all isolated *Haemophilus influenzae* strains, while over 60% of adult patients have chronic diseases [27].

Undoubtedly, invasive forms of *Haemophilus influenzae* infection are particularly severe in immunocompromised patients, which include waitlisted patients, primarily for lung transplantation. It should be noted that in COPD patients, about 75–80% of exacerbations of the disease are infectious in nature, with bacterial pathogens isolated from the sputum or bronchial secretions of patients in 40–50%, of which 13–46% are found in the culture of *Haemophilus influenzae* [28, 29]. At the same time, most patients with restrictive lung diseases receive glucocorticoids in the course of therapy even before transplantation, as well as, in some cases, cytostatic therapy, i.e. they are immunosuppressed, which significantly increases the risk of developing infectious complications. Hib vaccination in these patients can reduce the risk of infectious complications and increase the chances of remaining alive till transplantation.

Literature data on antibody concentrations against the Hib capsular polysaccharide in healthy individuals vary. In a study by Ladhani S.N. et al. in a cohort of persons aged 25 to 85 years, Ab concentrations exceeding the short-term and long-term protective thresholds were noted in 41–57% and 8–21% of cases, respectively [30]. These figures differ from those obtained by Nix E.B. et al., who noted Ab concentrations exceeding the short-term protective threshold in 97% of healthy controls [31]. In our study, all patients had Ab concentrations against the Hib capsular polysaccharide that exceeded the short-term protective threshold, while the proportion of patients with Ab concentrations exceeding the long-term protective threshold was 69%. This data can be compared with the results obtained by Nix E.B. et al. showing that the proportion of patients with a protective Ab level (≥0.15 μg/mL) among patients with COPD was 86%; among patients with chronic renal failure, 71% had protective antibody concentrations, 80% with diabetes, and 45% with melanoma [31].

One month after vaccination, the proportion of patients with long-term Ab protective levels was 100%. There was a statistically significant increase (by 2.3 times) in the geometric mean Ab concentrations against the Hib capsular polysaccharide as compared to the initial values ($p = 0.02$). Moreover, in 7 patients (44.8%), Ab concentrations exceeded 5 IU/mL, which also protects against bacterial carriers. Similar data were obtained during Hib vaccination in both adults and children with various bronchopulmonary conditions. Thus, during combined vaccination of COPD patients against influenza, pneumococcal and hemophilic type b infections, concentrations of post-vaccination antibodies to the Hib capsular polysaccharide remained significantly higher than the initial values at 3, 6 and 12 months after vaccination [32]. Similar data were obtained for vaccination of children with pulmonary malformations and bronchial asthma [33–35].

We found that a more pronounced increase in Ab concentrations against the Hib capsular polysaccharide was noted in the group of patients with obstructive pulmonary diseases as compared to the group with restrictive diseases. This is probably due to ongoing therapy, since patients in this group received hormonal therapy. In this regard, it is necessary to once again note the importance of early vaccination, since with progression of the disease, hormone dose increases, and this negatively affects formation of post-vaccination immunity. It is possible that this patient group needs to be re-vaccinated against Hib. A similar approach is used in the Serbian national guidelines on vaccination against Hib for at-risk groups. Under these guidelines, patients vaccinated against Hib before surgery are given the drug once, and 2 or more times in the post-transplant period (i.e., in immunosuppressive therapy) [7].

The study did not reveal any correlation between the age of the patients and antibody concentrations against the Hib capsular polysaccharide. Consequently, formation of antibodies is influenced by the ongoing therapy, which is in direct proportion to the severity of the disease.

So, Hib vaccination should be considered as an integral part of prevention of infectious complications in patients with severe bronchopulmonary diseases. The vaccine is not only safe, but also immunologically effective in lung-transplant waitlisted candidates with severe bronchopulmonary conditions.

The authors declare no conflict of interest.

REFERENCES

1. Epidemiologiya i vaktsinoprofilaktika infektsii, vyzyvaemoy *Haemophilus influenzae* tipa b: Metodicheskie rekomendatsii. M.: Federal'nyy tsentr gigieny i epidemiologii Rospotrebnadzora, 2010. 32. [In Russ].
2. *Namazova LS, Kostinov MP, Volkova ON, Tatochenko VK, Galitskaya MG, Izvol'skaya ZA et al.* Profilaktika grippa, ORI, pnevmokokkovoy, meningokokkovoy i Hib-infektsii y chasto boleyushchikh detey (posobie dlya vrachey). M.: Federal'noe agentstvo po zdravookhraneniyu i sotsial'nomu razvitiyu, 2006. 43. [In Russ].
3. *Kostinov MP, Lavrov VF.* Vaktsiny novogo pokoleniya v profilaktike infektsionnykh zabolevaniy (izdanie 2-e, dopolnennoe). M.: MDV, 2010. 192. [In Russ].
4. *Haemophilus influenzae type b (Hib)* Vaccination Position Paper. *Weekly epidemiological record.* 2013; 88, 39: 413–428. http://www.who.int/wer.
5. WHO Immunization coverage. https://www.who.int/en/news-room/fact-sheets/detail/ immunization-coverage
6. *Cassimos DC, Effraimidou E, Medic S, Konstantinidis T, Theodorido M, Maltezou HC.* Vaccination Programs for Adults in Europe, 2019. *Vaccines (Basel)*. 2020; 8 (1): 34. doi: 10.3390/vaccines8010034. doi: 10.3390/vaccines8010034.
7. Professional methodical introduction for implementation mandatory and recommended immunization of active population [In Serbian]. http://www.batut.org.rs/download/publikacije/SMU%20imuinizacija.pdf 6.
8. *Yastrebova NE, Vaneeva NP, Markina OA, Orlova OE, Elkina SI, Kostinov MP et al.* Sposob opredeleniya antitel k kapsul'nomu polisakharidu *Haemophilus influenzae* tipa *b.* Patent na izobretenie RUS № 2331075. Zayavka № 2006133787/15 ot 22.09.2006. Opubl. 10.08.2008. [In Russ].
9. *Duchini A, Goss JA, Karpen S, Pockros PJ.* Vaccinations for Adult Solid-Organ Transplant Recipients: Current Recommendations and Protocols. *Clin Microbiol Rev*. 2003; 16 (3): 357–364. doi: 10.1128/CMR.16.3.357-364.2003.
10. *Speich R, van der Bij W.* Epidemiology and management of infections after lung transplantation. *Clin Infect Dis*. 2001; 33 Suppl 1: 58–65. doi: 10.1086/320906.
11. *Remund KF, Best M, Egan JJ.* Infections relevant to lung transplantation. *Proc Am Thorac Soc*. 2009; 6 (1): 94–100. doi: 10.1513/pats.200809-113GO.
12. *Arcasoy SM, Kotloff RM*. Lung transplantation. *N Engl J Med*. 1999; 340 (14): 1081–1091. doi: 10.1056/NEJM199904083401406.
13. *Kostinov MP, Kostinov AM, Pakhomov DV, Polishchuk VB, Kostinova AM, Shmitko AD et al.* Efficacy of pneumococcal vaccine in immunocompetent and immunocompromised patients. *Journal of Microbiology Epidemiology Immunobiology.* 2019; 5: 72–83. [In Russ, English abstract]. doi: 10.36233/0372-9311-2019-5-72-83.
14. *Chuchalin AG, ed.* Respiratornaya meditsina. Rukovodstvo v 3 tomakh. 2-e izdaniye, pererabotannoye i dopolnennoye. T. 2. M.: Litterra, 2017. 544. [In Russ].
15. *Kostinov MP, Zverev VV, eds.* Vaktsinatsiya protiv gepatita B, grippa i krasnukhi vzroslykh patsientov s khronicheskimi zabolevaniyami. Prakticheskoe rukovodstvo. M.: MDV, 2009. 196. [In Russ].
16. *Kostinov MP, Chuchalin AG, eds.* Rukovodstvo po klinicheskoj immunologii v respiratornoj medicine. 1st ed. M.: ATMO, 2016. 128. [In Russ].

17. *Briko NI, Simonova EG, Kostinov MP, Zhirova SN, Kozlov RS, Murav'yev AA.* Immunoprofilaktika pnevmokokkovykh infektsiy. Uchebno-metodicheskoye posobiye. N.N.: Remedium Privolzh'ye, 2013. 278. [In Russ].
18. *Chuchalin AG, Bilichenko TN, Osipova GL, Kurbatova EA, Egorova NB, Kostinov MP.* Vaccine prevention of respiratory diseases in the framework of primary health care to the population. Russian Pulmonology. Supplement. 2015; 2 (25): 1–19. [In Russ.].
19. *Ryzhov AA, Kostinov MP, Magarshak OO.* Primeneniye vaktsin protiv pnevmokokkovoy i gemofil'noy tipa b infektsiy u lits s khronicheskoy patologiyey. *Epidemiologiya i vaktsinoprofilaktika.* 2004; 6 (19): 24–27. [In Russ].
20. *Markelova EV, Gushchina YaS, Kostinov MP, Zhuravleva NV.* Clinical and immunological effect produced by vaccination with "Pneumo 23" of children with atopic bronchial asthma. *Journal of Microbiology Epidemiology Immunobiology.* 2005; 2: 83–85. [In Russ, English abstract].
21. *Protasov AD, Zhestkov AV, Lavrenteva NE, Kostinov MP, Ryzhkov AA.* Effect of complex vaccination against pneumococcal, haemophilus type b infections and influenza in patients with chronic obstructive pulmonary disease. *Journal of Microbiology Epidemiology Immunobiology.* 2011; 4: 80–84. [In Russ, English abstract].
22. *Kostinov MP, ed.* Novoye v klinike, diagnostike i vaktsinoprofilaktike upravlyayemykh infektsiy. M.: Meditsina, 1997. 110.
23. *Garashchenko TI, Kostinov MP, Ilienko LI, Kyt'ko OV, Garashchenko MV, Foshina YeP et al.* Preventive and therapeutic application of Hib and pneumococcal vaccines among children, who are prone to frequent and prolonged recurrent otitis media. *Current Pediatrics*. 2006; 5 (5): 24–28. [In Russ, English abstract].
24. *Ilienko LI, Kostinov MP, Garashchenko MV, Kyt'ko OV, Ovechkina NV, Kats TP.* Vaccine immunization for prevention of pneumococcal, haemophilus influenzae and flu among sickly children, who often suffer from persistent heterospecific infectious pathology of the bronchopulmonary system. *Current Pediatrics* 2006; 5 (4): 27–30. [In Russ, English abstract].
25. *Kostinov MP, Maleev VV.* Hib-infektsiya: voprosy vaktsinoprofilaktiki. M.: Meditsina dlya vsekh, 1998. 90. [In Russ].
26. *Livorsi DJ, MacNeil JR, Cohn AC, Bareta J, Zansky S, Petit S et al.* Invasive *Haemophilus influenzae* in the United States, 1999–2008: Epidemiology and Outcomes. *J Infect*. 2012; 65 (6): 496–504. doi: 10.1016/j.jinf.2012.08.005.
27. *Soeters HM, Blain A, Pondo T, Doman B, Farley MM, Harrison LH et al.* Current Epidemiology and Trends in Invasive Haemophilus Influenzae Disease-United States, 2009–2015. *Clin Infect Dis.* 2018; 67 (6): 881–889. doi: 10.1093/cid/ciy187.
28. Infektsionnoe obostrenie KhOBL: Prakticheskie rekomendatsii po diagnostike, lecheniyu i profilaktike. Posobie dlya vrachey. M., 2005. 37.
29. *Kostinov MP, ed.* Vaktsinatsiya vzroslykh s bronkholegochnoy patologiey. Rukovodstvo dlya vrachey. M.: Sozvezdie, 2013. 112.
30. *Ladhani SN, Ramsay ME, Flood JS, Campbell H, Slack MP, Pebody R et al. Haemophilus influenzae serotype b (Hib)* seroprevalence in England and Wales in 2009. *Euro Surveill.* 2012; 17 (46): 20313. doi: 10.2807/ese.17.46.20313-en.
31. *Nix EB, Hawdon N, Gravelle S, Biman B, Brigden M, Malik S et al*. Risk of Invasive *Haemophilus influenza type b (Hib)* Disease in Adults with Secondary Immunodeficiency in the Post-Hib Vaccine Era. *Clin Vaccine Immunol*. 2012; 19 (5): 766–771. doi: 10.1128/CVI.05675-11.
32. *Kostinov MP, Protasov AD, Zhestkov AV, Pakhomov DV, Chebykina AV, Kostinova TA.* Post-vaccination Immunity to Pneumococcal, Haemophilus Influenzae type b Infection and Influenza in Patients with Chronic Obstructive Pulmonary Disease (COPD). *J Vaccines Vaccin.* 2014; 5: 2. doi: 10.4172/2157-7560.1000221.
33. *Kostinov MP, red.* Primenenie vaktsin "PNEVMO 23" i "Akt-KhIB" v komplekse lechebno-profilakticheskikh meropriyatiy pri khronicheskikh vospalitel'nykh zabolevaniyakh legkikh u detey: posobie dlya vrachey. M.: Meditsina dlya vsekh, 2004. 46.
34. *Kostinov MP, ed.* Rasshirenie kompleksa lechebno-profilakticheskikh meropriyatiy pri bronkhial'noy astme u detey s primeneniem vaktsin "PNEVMO-23" i "Act-KhIB". Posobie dlya vrachey. M.: Meditsina dlya vsekh, 2004. 36. [In Russ].
35. *Korovkina ES, Krakovskaya AV, Kostinov MP, Kozlov VK, Jastrebova NE, Magarshak OO et al.* Dynamics in IgM and IgG antibodies against a polysaccharide capsule-containing complex of various *S. pneumoniae* and *H. influenzae* type b serotypes in children with chronic lung and bronchial inflammatory diseases after vaccination with "Pneumo-23" and "Act-HIB". *Russian Journal of Infection and Immunity* (2019), 9 (5–6): 713–722. [In Russ, English abstract]. doi: 10.15789/2220-7619-2019-5-6-713-722.

The article was submitted to the journal on 16.05.2020

DOI: 10.15825/1995-1191-2020-4-43-51

INDUCTION OF CIRCULATING CD133+ STEM CELLS COMMITTED TO CIRRHOTIC LIVERS IN WAITLISTED PATIENTS

A.N. Shoutko[1], O.A. Gerasimova[1, 2], N.V. Marchenko[1, 2], F.K. Zherebtsov[1]

[1] Granov Russian Scientific Center of Radiology and Surgical Technology, St. Petersburg, Russian Federation

[2] St. Petersburg State University, St. Petersburg, Russian Federation

Studies on the regenerative capabilities of tissues have shown that damaged liver can recover using hematopoietic stem cells (HSCs), which are able not only to replace cells in the target organ, but can also deliver trophic factors that support endogenous liver regeneration. There is practically no data on how organ-derived humoral signals involve such morphogenic/trophic cells in circulation. **Objective:** to investigate the role of non-invasive vibromechanical percutaneous action on the liver in cirrhosis by quantification of CD133+ lymphoid HSCs with specific hepatic marker alpha-fetoprotein (AFP) in patients awaiting liver transplantation. **Materials and methods.** In order to increase the number of AFP+ part of CD133+ stem lymphoid cells in the blood, the patient's cirrhotic liver was mechanically activated by transcutaneous microvibration using electromagnetic vibrophones in contact with the skin. This generated mechanical impulses with a 10 μm amplitude and a smoothly varying frequency from 0.03 kHz to 18 kHz and back to within one cycle lasting 1 minute. The amount of AFP+ lymphocyte fraction in the total content of CD133+ HSCs in lymphocytes of potential recipients was monitored by flow cytometry before and during daily 15-minute sonication of the skin zone corresponding to the liver projection for three weeks with eight synphased vibraphones. **Results.** Sonication of the liver projection zone significantly increased the number of liver-specific CD133+ AFP+ lymphocytes by 2–3 times compared to the baseline values. Repeated similar sonication of the same site after a three-week break showed a statistically insignificant increase from the initial level. With a similar effect on the spinal projection in the control group of waitlisted patients with cirrhosis, there was no increase in CD133+ AFP+ lymphocytes. **Conclusion.** Mechanical stress prompts the organ to secrete specific humoral signals that provoke the bone marrow to produce additional lymphoid stem cells committed to the liver and recruit them into circulation.

Keywords: hematopoietic stem cells, cirrhosis, regeneration, waiting list, mechanical microvibration.

INTRODUCTION

Hematopoiesis and normal tissues

Most primitive mononuclear cells in the bone marrow and blood of adults are represented by CD133+CD34–, CD133+CD34+, and CD133–CD34+ markers, with the CD133 marker being earlier than CD34. Intensively proliferating CD133+ cells are capable of differentiating into cells with meso-, endo- and neurodermal layer characteristics, namely: endothelial progenitor cells, neural progenitor cells, astrocytes, oligodendrocytes, renal proximal tubule cells, mammary duct cells, cells of the prostate gland, skin, lungs, intestines, hepatocytic cells and skeletal muscle cells, expressing basic tissue proteins [1, 2]. Primitive bone marrow cells migrate through the blood to various tissues and organs, especially after damage [3]. There is abundant evidence of increased tissue regeneration resulting from stimulation of primitive bone marrow cells or their introduction into the body [4–6]. So, the idea of bone marrow as a source of circulating tissue-committed morphogenic stem cells is confirmed. Vascular endothelium is renewed with the help of circulating CD133+ progenitor cells from the bone marrow [7]. Even if primitive bone marrow cells do not transdifferentiate, as some researchers suggest, they aggregate with other host cells (the fusing phenomenon), or release regenerative cytokines and nutrients [8], thus supporting target tissue regeneration. The earliest lymphocytes, as well as mononuclear stem and progenitor cells, penetrate the capillary walls into the interstitial non-lymphoid tissues, including the liver in order to maintain dynamic proliferative balance, that is, homeostasis under normal conditions [9]. Such cells sacrifice themselves to support the function of surrounding cells with a different phenotype. For example, TDT+ prolymphocytes, γδ-T cells (CD4−CD8–) [10] and CD3+CD31+CXCR4+ angiogenic T lymphocytes [11] are directly involved in tissue cellular renewal by producing growth factors and nutrients, and maintaining angiogenesis processes. All these cells, according to Fiedler's prediction [12], are not immunocytes, but rather trophocytes feeding the feeder lymphocytes.

Corresponding author: Olga Gerasimova. Address: 70, Leningradskaya str., Pesochnyy town, St. Petersburg, 197758, Russian Federation. Phone: (812) 439-66-40. E-mail: ren321@mail.ru

Stem cells and liver

It is known that chronic liver disease leads to non-functional regeneration, which is controlled by interaction between liver tissue cells (hepatocytes, hepatic stellate cells, inflammatory cells, biliary epithelial cells, sinusoidal endothelial cells), in the end fibrosis-cirrhosis is formed [13]. Along with the actual liver cells, recruited from the circulation of hematopoietic stem cells (HSCs) from the bone marrow, they can also promote liver regeneration by fusion with damaged hepatocytes or by differentiation into hepatocyte-like cells, or through their morphogenic and pro-angiogenic growth factors [14–16]. Lymphocyte colony-stimulating factors, modulating hematopoiesis, are used to mobilize HSCs into the bloodstream in order to reverse induced chronic liver damage. However, the approach has standard limitations on the number of cycles and hematological toxicity of agents [17]. Intraportal infusions of autologous HSCs isolated from a pre-aspirated bone marrow volume represent another invasive approach to artificial enrichment of the cirrhotic liver microenvironment with cellular elements of autologous HSCs [18].

A liver transplant in patients with cirrhosis may itself be a natural long-term stimulus for recruitment of additional HSCs into the peripheral blood [19], confirming the existence of a humoral information pathway (axis) between these two tissues. Interestingly, HSCs produced during embryonic liver development can traffic between different tissues, just like HSCs in adults, and in both cases, they are provided with humoral signals, regulated tightly enough to reach their final destinations [20, 21].

While waiting for liver transplantation, it seems extremely interesting to find an opportunity to induce pro-regenerative paracrine signals emanating from the organ parenchyma in the liver-bone marrow axis.

Having had a positive experience in remote non-invasive recruitment of HSCs into the blood by means of moderate percutaneous mechanical microvibration of cancellous bones containing active ("red") bone marrow [22–24], we suggested that a similar mechanical effect (stress) on altered liver tissue would probably open additional up additional opportunities for a positive interaction between AFP+ morphogenic HSCs and liver cells.

The **aim** of the study was to study the effect of percutaneous mechanical microvibration on mobilization of liver-committed HSCs from the bone marrow via humoral signals.

MATERIALS AND METHODS

The study included 9 patients aged 53 to 61 years with cirrhosis awaiting liver transplantation. Six out of the 9 patients received mechanical vibration courses through skin-contact vibraphones on the projection area of the liver. Three patients received vibration in the spine projection in a similar manner. Certified serial device Vitafon-5 (GOST 50444-92 and TU9444-009-23138557-2009 RF) was used as the electromechanical vibration source for vibroacoustic impact. In addition, data obtained from 6 healthy volunteers, whose age did not differ from the subjects, were used for comparison. produced synchronous and in-phase mechanical vibrations in cyclic mode. During one cycle (60 seconds), the vibration frequency varied from 0.03 Hz to 18 kHz and in reverse sequence at about 10 μm constant vibration amplitude. The block of vibraphones (45 mm diameter each) consisted of two rows (four in a row) with 75 mm distance between the centers of the rows and 55 mm distance between the centers of vibraphones within each row. Thus, the block formed an active rectangular field of mechanical microvibrations 12 × 22 cm, held by a flat fabric frame with eight fastening sockets and soft fasteners for tight fixation on the human body.

Before exposure, all patients had blood sampling for clinical and biochemical analysis. Vibration exposure was performed once a day for 15 minutes while sitting in an armchair (reclining position). Two exposure modes were used: the first (I) included 15 minutes of exposure daily for three weeks, the second (II) – 15 minutes daily for three weeks, then a break for three weeks and repeated exposure.

The control scheme (III) consisted of simultaneous mechanical microvibrations on 8 pairs of equidistant points along the spine with 0.5 cm distance between vibraphones in each pair, for 3 weeks (2nd, 3rd, and 4th) 15 minutes daily.

Once a week, we determined the proportions of circulating lymphocytes in the synthetic phase of S+, CD133+, CD31+ cells in the lymphoid fraction, the proportion of double positive cells AFP+CD133+, AFP+CD31+, and the derived ratios (AFP+CD133+)/CD133+, (AFP+CD31+)/CD31+ and AFP+CD133+/AFP+CD31+. For this purpose, a mononuclear cell (MNC) fraction was isolated from peripheral blood by classical separation on a Ficoll density gradient, omitting the final enrichment stage. [25]. Viability of MNCs was assessed using the trypan blue exclusion test. Cells from two equal parts of the MNC fraction were stained for analysis on an LSR Fortessa flow cytometer (Becton-Dickinson). Hoechst 33342 staining was used for cell cycle analysis as previously described [26] with slight modifications.

The phenotypes of circulating cells in the lymphocytic part of MNCs were assessed using monoclonal antibodies to markers CD133/2, CD31, AFP (α-fetoprotein) conjugated with allophycocyanine (APC), fluorescein isothiocyanate (FITC), and phycoerythrin (PE), respectively.

The parameters were evaluated statistically by calculating the mean (M) and standard error (SE). M values were compared using the t-test and p probability. Kinetic tendencies of the parameters before and after scoring were characterized by mathematical functions generated automatically using nonlinear approximations in Excel. The R-squared was used as a statistical goodness-of-fit

measure of the regression line to the data. Satisfactory R-squared values were confirmed using the t-parameter equation: t = R2 × (n – 2) (1 – R2) [27].

RESULTS

A relative decrease in S+, CD31+ cells and a minor increase in CD133+ cells are characteristic of patients awaiting liver transplantation as compared to healthy volunteers (Table, Fig. 1).

As a result of the acoustic effect on the liver area according to two schemes, the S+, CD31+, and CD133+ content before treatment was normalized by 4–5 weeks (Fig. 2). In addition, the number of double-positive liver-committed CD133+AFP+ cells increased. This effect can be considered specific for the effect on the liver area, since only the CD133+ population increased in the spine projection when using the third sound exposure scheme (Fig. 3). Spine vibration stress significantly increased the count of uncommitted CD133+ cells in circulation, exceeding not only their number before exposure, but also the level of these cells after the first course of exposure to the liver (Fig. 3).

The real concentrations corresponding to Fig. 2 are 0.07 ± 0.022 ± 0.0125 (Scheme 1) and 0.079 ± 0.037 ± 0.0099 (Scheme 2). These mean values increased 1.95 times (p = 0.006) and 1.75 times (p = 0.008), respectively for spine exposure based on Scheme 3.

No specific changes were found at week 10–12 of exposure compared to the data before it (Fig. 4). The increase in the CD133+AFP+ cell count and the CD133+AFP+/CD133 ratio obtained at week 4–5 according to scheme 1 (Fig. 2) lost its statistical significance by week 10–12 (Fig. 4). After repeated exposure to the liver area according to scheme 2, the specific increase in CD133+AFP+ cell count disappeared at week 10–12, but the cells were replaced by nonspecific CD133+ cells, whose increased level remained (Fig. 1, dashed line, left column for CD133+).

Table

Baseline indicators of circulating lymphocytes in healthy volunteers

Parameters	CD133+	CD133+ AFP+	CD31+	CD31+ AFP+	s	CD133+/ CD31+	CD133+AFP+/ CD31+AFP+	CD133+AFP+/ CD133+	CD31+AFP+/ CD31+
M	0.037	0.0052	40.1	0.39	0.95	0.101*	1.64*	12.36*	0.97*
SD	0.012	0.0044	9.2	0.36	0.98	0.037	1.25	8.22	0.74
SE	0.004	0.0015	3.1	0.12	0.28	0.013	0.44	2.90	0.24
KV	0.32	0.84	0.23	0.92	1.03	0.37	0.76	0.66	0.76

Note. * Obtained by averaging personal odds.

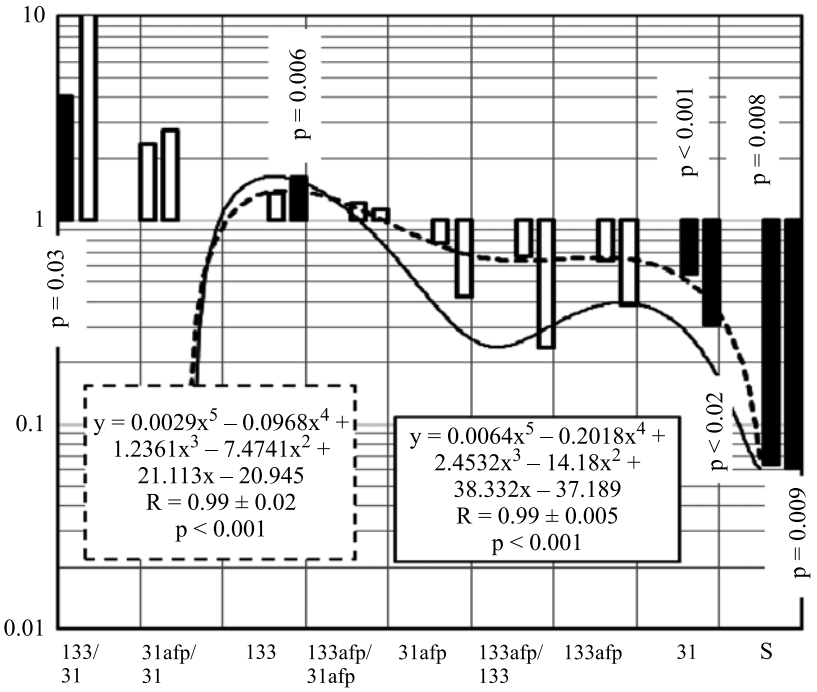

Fig. 1. Changes in mean parameters (M) in cirrhosis relative to mean parameters for healthy volunteers, taken as 1.0. The right-hand columns represent the data obtained in the first week before sonication based on Scheme 1 (solid approximation line). The left-hand columns represent the data obtained before sonication based on Scheme 2 and Scheme 3 (dashed line). Statistically significant deviations are shown in black

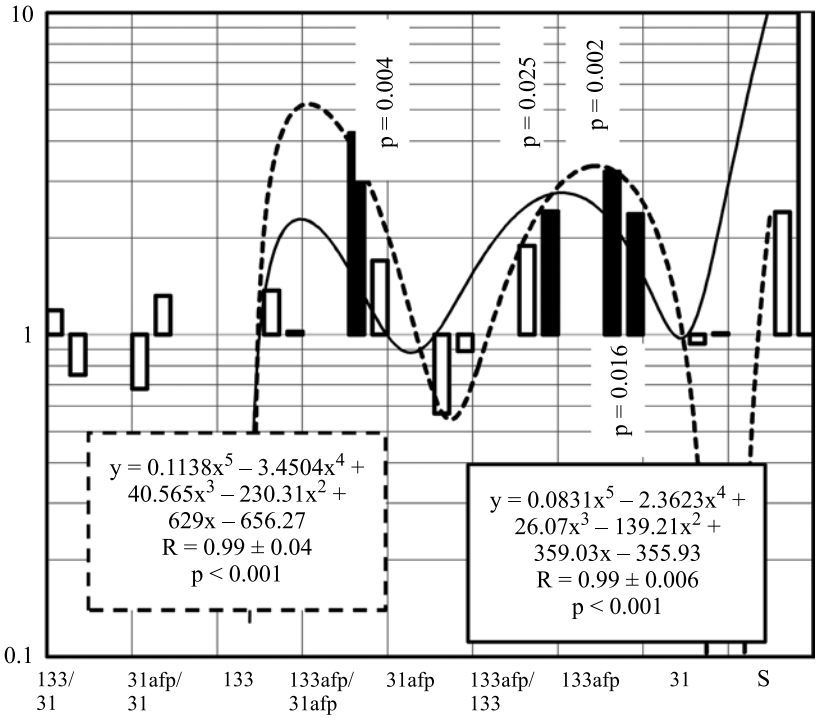

Fig. 2. Changes in mean parameters (M) by 4–5 weeks of sonication compared to the liver area relative to mean parameters for patients in Fig. 1, taken as 1.0. The right and left columns represent the relative data obtained by 4–6 weeks after the start of sonication based on Scheme 1 (solid line, right columns) and Scheme 2 (dashed line, left columns). Statistically significant deviations are shown in black

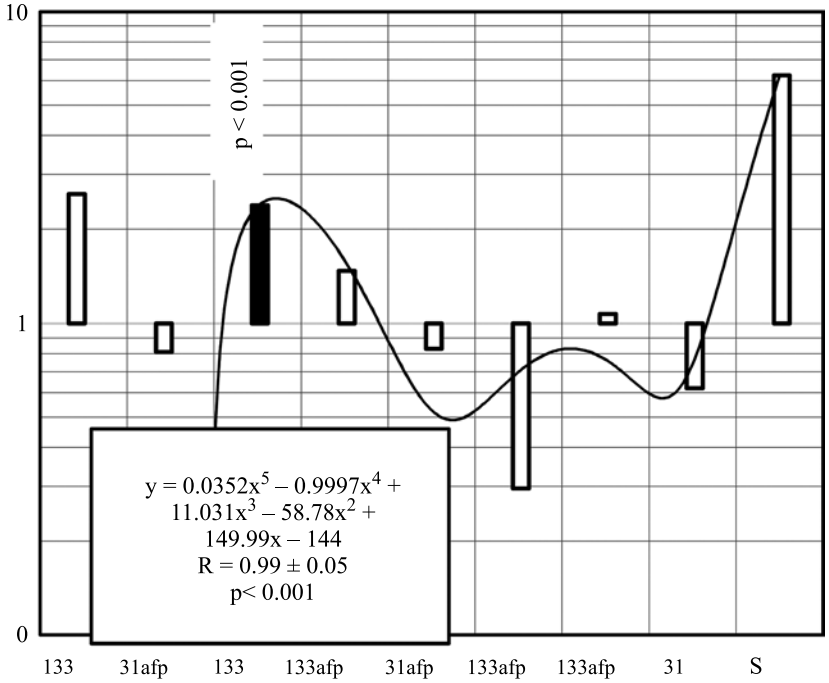

Fig. 3. Changes in mean cell parameters after sonication of the spine (Scheme 3) relative to the parameters in healthy people (Fig. 1), taken as 1.0. The columns show the relative data obtained at 4–6 weeks

Thus, indirect percutaneous mechanical mobilization of liver-committed CD133+AFP+ stem cells in the lymphocyte pool occurs within week 4–6 of exposure and is weakened at week 10–12, regardless of continuation of exposure (scheme 2) or its termination (scheme 1).

DISCUSSION

Physical factors obviously play an important role in biological processes. Application of tissue tensile stress, shear stress, electromagnetic fields, and ultrasound induces variants of enhancement of osteogenesis and chon-

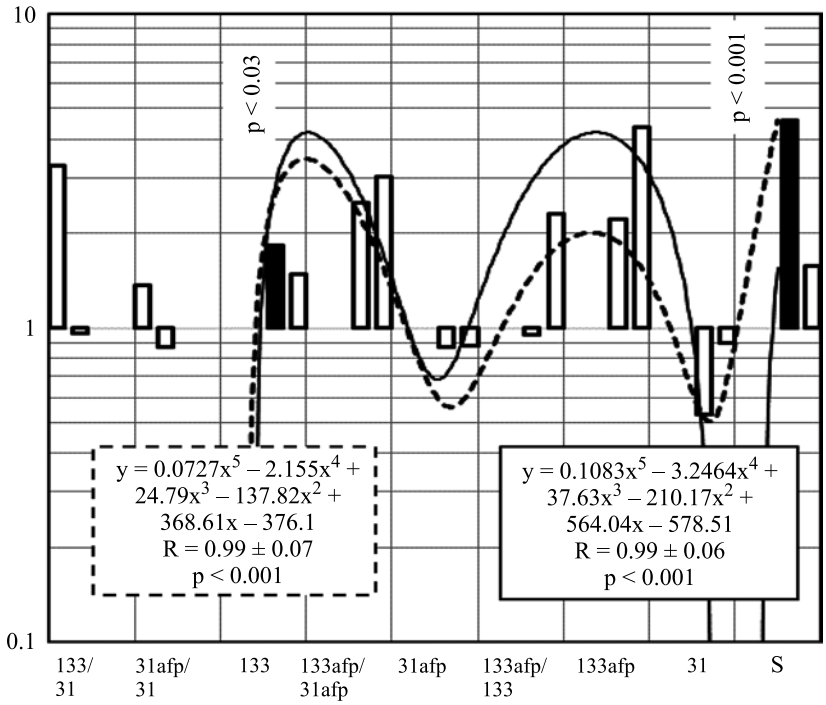

Fig. 4. Changes in mean cell parameters (M) over 10–12 weeks compared to baseline (right-hand columns with solid approximation line). The columns show the relative data obtained at 10–12 weeks after the start of sonication based on Scheme 1 (solid line, right columns) and Scheme 2 (dashed line, left columns)

drogenesis, involving human stem cells in the process. Therefore, direct physical intervention appears to be a potentially attractive approach and can be used to support tissue regeneration.

Application of acoustic non-invasive effect on the liver in compensated cirrhosis seems to be a promising method. Some researchers have previously reported that the liver exhibits mechanical resonance within a registered frequency of 30–400 Hz, depending on the odd harmonics of 1–3 orders [28]. The liver tissue itself has its own natural frequency of about 55–60 MHz [29]. For non-invasive effect on this complex system with little-known physical properties, mechanical vibrations seemed promising, as they can essentially produce stochastic resonance (SR) in nonlinear biological systems, amplifying subthreshold stimuli in metabolic pathways [30, 31]. We expected that humoral signals of a still unknown nature from artificial liver tissue tension would reach the lymphopoietic niches of the bone marrow and intensify either the natural production of morphogenic liver-committed CD133+AFP+ lymphocytes, or enhance their recruitment into circulation, against the background of initial suppression in cirrhosis. If this assumption is correct, we could get a new approach for non-invasive and long-term support of liver function in waitlisted patients. To increase the likelihood of resonance processes in liver tissues, we chose a source of mechanical vibrations in a wide frequency range [24].

Circulating lymphocytes were chosen as objects of this study for several reasons. First, lymphoid cells have the most developed and flexible mechanisms of navigation to various tissues or tropism, and contain fractions of morphogenic/trophic cells, such as CD133+, CD34+ stem cells, lymphoid TdT+ stem cells, angiogenic CD31 T+ cells, and other trophic lymphocytes of intermediate degree of differentiation, which are usually called regulatory cells. Secondly, lymphocytopoiesis is the most damaging process, and lymphoid tissue is characterized by the highest depreciation, that is, loss of actual and functional mass during the lifetime of the organism [32]. Thirdly, in various organ diseases, including liver diseases, the worst forecasts are associated with a high ratio of neutrophil count to blood lymphocyte count (the so-called neutrophil-lymphocyte ratio), which emphasizes the role of weakening of lymphopoiesis in the loss of vitality of the organism as a whole [33].

A study of blood samples from cirrhotic patients revealed a deficiency of naive CD31+ lymphocytes with angiogenic properties [11, 34], as well as a deficiency of lymphocytes in the S-phase of DNA synthesis. The first course of action on the liver or spine normalized both deficiencies. Thus, this was an argument against the specificity of these two effects.

On the contrary, the first exposure to the liver increases the number of committed CD133+AFP+ cells, which seems to be quite specific for liver tissue. We interpret the increasing number of CD133+AFP+ cells as a distant result of specific paracrine stimulation occurring remotely as a result of mechanical resonance strained liver parenchyma. A humoral stimulus targeted on the bone marrow reproductive system specifically activates it, recruiting trophic/morphogenic lymphoid bone mar-

row stem cells for targeted maintenance of the function of the damaged liver [35]. Signals can be either easily soluble molecular substances in plasma, or circulating extracellular vesicles measuring tenths of microns, recently discovered [36]. In any case, mechanical vibration is likely to simulate liver injury perceived as real by the physiological "lymphopoiesis – liver" axis effector.

Several liver cell types can be targets for such interaction with CD133+AFP+ lymphocytes. Among the parenchymal cells of the organ, there is a CD133+ oval cell population with the function of primitive, "bipotent" liver stem cells [37, 38], but they do not carry the AFP marker [39]. That is why the youngest type of hepatic stem cells (HepSCs) are hardly a target for AFP+CD133+ lymphocytes. Immature "unipotent" hepatoblasts arising during regenerative processes in the liver, have an antigenic profile with strongly positive expression of both CD133 and the liver-specific AFP marker [40, 41]. Thus, they are probably more likely to be considered as targets for CD133+AFP+ migrants [5].

This agreement may be an additional argument backing the fact that hepatocytes are the most likely inducer of humoral stimuli, as well as a target for committed lymphoid cells. Notably, the second course of exposure to the liver area (scheme 2) did not alter the attenuation effect of the first course in the CD133+AFP+ subpopulation. The reasons for this are not completely clear, but the general inhibition of lymphocytopoiesis in cirrhotic patients, and the associated instability/turbulence of hematopoiesis [5, 20], may be one of the possible causes. On the other hand, the initially depleted/amortized natural ability of the cirrhotic parenchyma to produce paracrine signals may also be responsible for altered sensitivity to mechanical stress as compared to an intact organ.

CONCLUSION

The study confirms that the number of trophic lymphoid stem cells committed to the liver in patients with cirrhosis can be increased indirectly and non-invasively. The new technique proposed by us is specific and has no restrictions in re-use. We consider our results only as a therapeutic roadmap for non-invasive support of liver regeneration in cirrhosis in patients waitlisted for liver transplantation. Further studies are needed to evaluate the clinical effects.

The authors declare no conflict of interest.

REFERENCES

1. *Drapeau C*. Cracking the Stem Cell Code: Demystifying the most dramatic scientific breakthrough of our times. Sutton Hart Press, Hillsboro; 2010.
2. *Kucia M, Ratajczak J, Ratajczak MZ*. Bone marrow as a source of circulating CXCR4+ tissue-committed stem cells. *Biol Cell*. 2005; 97 (2): 133–146. doi: 10.1042/BC20040069.
3. *Stroo I, Stokman G, Teske GJ, Florquin S, Leemans JC*. Haematopoietic stem cell migration to the ischemic damaged kidney is not altered by manipulating the SDF-1/CXCR4-axis. *Nephrol Dial Transplant*. 2009; 24: 2082–2088. doi: 10.1093/ndt/gfp050.
4. *Kolvenbach R, Kreissig C, Cagiannos C, Afifi R, Schmaltz E*. Intraoperative adjunctive stem cell treatment in patients with critical limb ischemia using a novel point-of-care device. *Ann Vasc Surg*. 2010; 24: 367–372. doi: 10.1016/j.avsg.2009.07.018.
5. *Shoutko AN, Gerasimova OA, Ekimova LP, Zherebtsov FK, Mus VF, Granov DA*. Long-term activation of circulating liver-committed mononuclear cells after OLT. *Jacobs Journal of Regenerative Medicine*. 2016; 1 (3): 1–9. https://jacobspublishers.com/.
6. *Halin C, Mora J, Sumen C, von Andrian UH. In vivo* imaging of lymphocyte trafficking. *Ann Rev Cell Dev Biol*. 2005; 21: 581–603. doi: 10.1146/annurev.cellbio.21.122303.133159.
7. *Wassmann S, Werner N, Czech T, Nickenig G*. Improvement of endothelial function by systemic transfusion of vascular progenitor cells. *Circ Res*. 2006; 99: 74–83. doi: 10.1161/01.RES.0000246095.90247.d4.
8. *Burchfield JS, Dimmeler S*. Role of paracrine factors in stem and progenitor cell mediated cardiac repair and tissue fibrosis. *Fibrogenesis Tissue Repair*. 2008; 1: 1–11. doi: 10.1186/1755-1536-1-4.
9. *Strick-Marchand H, Masse GX, Weiss MC, Di Santo JP*. Lymphocytes support oval cell dependent liver regeneration. *J Immunol*. 2008; 181: 2764–2771. doi: 10.4049/jimmunol.181.4.2764.
10. *Roullet M, Gheith SMF, Mauger J, Junkins-Hopkins JM, Choi JK*. Percentage of {gamma} {delta} T cells in panniculitis by paraffin immunohistochemical analysis. *Am J Clin Pathol*. 2009; 13: 1820–1826.
11. *Hur J, Yang H-M, Yoon C-H, Lee C-S, Park K-W et al*. Identification of a novel role of T cells in postnatal vasculogenesis. Characterization of endothelial progenitor cell colonies. *Circulation*. 2007; 116: 1671–1682. doi: 10.1161/CIRCULATIONAHA.107.694778.
12. *Shoutko A., Shatinina N*. Chronic cancer could it be? *Coherence Int J Integrated Med*. 1998; 2: 36–40.
13. *Ding B-S, Cao Z, Lis R, Nolan DJ, Guo P, Simons M et al*. Divergent Angiocrine Signals from vascular niche balance liver regeneration and fibrosis. *Nature*. 2014; 505: 97–102. doi: 10.1038/nature12681.
14. *Woo DH, Kim SK, Lim HJ, Heo J, Park HS, Kang GY et al*. Direct and indirect contribution of human embryonic stem cell-derived hepatocyte-like cells to liver repair in mice. *Gastroenterology*. 2012; 142: 602–611. doi: 10.1053/j.gastro.2011.11.030.
15. *Ratajczak J, Kucia M, Mierzejewska K, Marlicz W, Pietrzkowski Z, Wojakowski W et al*. Paracrine proangiopoietic effects of human umbilical cord blood-derived purified CD133+ cells – implications for stem cell therapies in regenerative medicine. *Stem Cells and Dev*. 2013; 22: 422–430. doi: 10.1089/scd.2012.0268.
16. *Liu W-H, Ren L-N, Wang T, Navarro-Alvarez N, Tang L-J*. The involving roles of intrahepatic and extrahepatic stem/progenitor cells (SPCs) to liver regeneration. *Int J Biol Sci*. 2016; 12: 954–963. doi: 10.7150/ijbs.15715.
17. *Tsolaki E, Athanasiou E, Gounari E, Zogas N, Siotou E, Yiangou M et al*. Hematopoietic stem cells and liver re-

generation: differentially acting hematopoietic stem cell mobilization agents reverse induced chronic liver injury. *Blood Cells Mol Dis*. 2014; 53: 124–132. doi: 10.1016/j.bcmd.2014.05.003.

18. *Mohamadnejad M, Vosough M, Moossavi S, Nikfam S, Mardpour S, Akhlaghpoor S et al.* Intraportal infusion of bone marrow mononuclear or CD133+ cells in patients with decompensated cirrhosis: a double-blind randomized controlled trial. *Stem Cells Transl Med*. 2016; 5 (1): 87–94, doi: 10.5966/sctm.2015-0004
19. *Lemoli RM, Catani L, Talarico S, Loggi E, Gramenzi A, Baccarani U et al.* Mobilization of bone marrow-derived hematopoietic and endothelial stem cells after orthotopic liver transplantation and liver resection. *Stem Cells*. 2007; 24: 2817–2825. doi: 10.1634/stemcells.2006-0333.
20. *Shoutko AN, Gerasimova OA, Ekimova LP, Zherebtsov FK, Mus VF, Matyurin KS et al.* Lymphocyte reproductive activity normalized to numbers of hematopoietic stem cells in blood and rate of death in fatal diseases. *Int J of Genetics and Genomics*. 2017; 5: 54–62. doi: 10.11648/j.ijgg.20170505.12.
21. *Heinig K, Sage F, Robin C. Sperandio M.* Development and trafficking function of haematopoietic stem cells and myeloid cells during fetal ontogeny. *Cardiovasc Res*. 2015; 107 (3): 352–363. doi: 10.1093/cvr/cvv146.
22. *Karamullin M, Baback A, Ekimova L, Phedorov V, Kireeva E, Sosukin A et al.* The blood stem cell's pool modulation in remote period improved health status of Chernobyl clean-up workers. *Radioprotection*. 2008; 43: 89. doi: 10.1051/radiopro:2008667.
23. *Baback A, Karamullin M, Ekimova L, Phedorov V, Kireeva E, Sosukin A et al.* Exercise performance vs. growth of haemopoietic stem cells amount in CUWs blood after nonivasive modulation. *Radioprotection*. 2008; 43: 161. doi: 10.1051/radiopro:2008724.
24. *Shutko AN, Fedorov VA.* Sposob obogashcheniya krovi stvolovymi krovetvornymi kletkami. Patent RF № 2166924, 20.07.2008. http://ru-patent.info/21/65-69/2166924.html.
25. *Eaker ShS, Hawley TS, Ramezani A, Hawley RG.* Detection and enrichment of hematopoietic stem cells by side population phenotype. *Hawley TS and Hawley RG, Eds., Methods in molecular biology: flow cytometry protocols*, 2nd Edition, Humana Press Inc., Totowa, 2008: 161–180. doi: 10.1385/1-59259-773-4:161.
26. *Sales-Pardo I, Avendaño A, Martinez-Muñoz V, García-Escarp M, Celis R, Whittle P et al.* Flow cytometry of the side population: tips and tricks. *Cellular Oncology*. 2006; 28: 37–53. https://www.ncbi.nlm.nih.gov/pubmed/16675880.
27. *Loveland JL.* Mathematical justification of introductory hypothesis tests and development of reference materials. All graduate plan B and other reports. Utah State University, Logan, 14. 2013.
28. *Oldenburg AL, Boppart SA.* Resonant acoustic spectroscopy of soft tissues using embedded magnetomotive nanotransducers and optical coherence tomography. *Physics in Medicine & Biology*. 2010; 55: 1189–1201. doi: 10.1088/0031-9155/55/4/019.
29. *Sharma A, Maurya AK.* Aggregate frequencies of body organs. *Int J of Electrical, Electronics and Data Communication*. 2017; 5: 94–98. http://iraj.in.
30. *Arredondo LT, Perez CA.* Spatially coincident vibrotactile noise improves subthreshold stimulus Detection. *PLoS One*. 2017; 12 (11): e0186932. doi: 10.1371/journal.pone.0186932.
31. *Milanese C, Cavedon V, Sandri M, Tam E, Piscitelli F, Boschi et al.* Metabolic effect of bodyweight whole-body vibration in a 20-min exercise session: a crossover study using verified vibration stimulus. *PLoS One*. 2018. 31; 13 (1): e0192046. doi: 10.1371/journal.pone.0192046.
32. *Richardson RB, Allan DS, Lea Y.* Greater organ involution in highly proliferative tissues associated with the early onset and acceleration of ageing in humans. *Experimental Gerontology*. 2014; 55: 80–91. doi: 10.1016/j.exger.2014.03.015.
33. *Agiasotelli D, Alexopoulou A, Vasilieva L, Kalpakou G, Papadaki S, Dourakis SP.* Evaluation of neutrophil/leukocyte ratio and organ failure score as predictors of reversibility and survival following an acute-on-chronic liver failure event. *Hepatology Research*. 2016; 46: 514–520. doi: 10.1111/hepr.12582.
34. *Ashman LK, Aylett GW.* Expression of CD31 epitopes on human lymphocytes: CD31 monoclonal antibodies differentiate between naïve (CD45RA+) and memory (CD-45RA–) CD4-positive T cells. *Tissue Antigens*. 1991; 38: 208–212. doi: 10.1111/j.1399-0039.1991.tb01899.x.
35. *Huch M, Dolle L.* The plastic cellular states of liver cells: are EpCAM and Lgr5 fit for purpose? *Hepatology*. 2016; 64: 652–662. doi: 10.1002/hep.28469.
36. *Teixeira JH, Silva AM, Almeida MI, Barbosa MA, Santos SG.* Circulating extracellular vesicles: their role in tissue repair and regeneration. *Transfus Apher Sci*. 2016; 55 (1): 53–61. doi: 10.1016/j.transci.2016.07.015.
37. *Rountree CB, Barsky L, Ge SH, Zhu J, Senadheera SH, Crooks GM.* A CD133-expressing murine liver oval cell population with bilineage potential. *Stem Cells*. 2007; 25: 2419–2429. doi: 10.1634/stemcells.2007-0176.
38. *Corbeila D, Fargeasa CA, Jászaib J.* CD133 might be a pan marker of epithelial cells with dedifferentiation capacity. *PNAS*. 2014; 111: E1451–E1452. doi: 10.1073/pnas.1400195111.
39. *Turner R, Lozoya O, Wang Y, Cardinale V, Gaudio E, Alpini G et al.* Human hepatic stem cell and maturation liver lineage biology. *Hepatology*. 2011; 53: 1035–1045. doi: 10.1002/hep.24157.
40. *Haruna Y, Saito K, Spaulding S, Nalesnik MA, Gerber MA.* Identification of bipotential progenitor cells in human liver development. *Hepatology*. 1996; 23: 476–481. doi: 10.1002/hep.510230312.
41. *Liang OD, Korff T, Eckhardt J, Rifaat J, Baal N, Herr FT et al.* Oncodevelopmental alphafetoprotein acts as a selective proangiogenic factor on endothelial cell from the fetomaternal unit. *J of Clin Endocrinology & Metabolism*. 2004; 89: 1415–1422. doi: 10.1210/jc.2003-031721.

The article was submitted to the journal on 23.04.2020

DOI: 10.15825/1995-1191-2020-4-52-57

TRANSCATHETER HEPATIC ARTERIAL CHEMOEMBOLIZATION IN CIRRHOTIC PATIENTS WITH HEPATOCELLULAR CARCINOMA BEFORE LIVER TRANSPLANTATION: THE PROGNOSTIC VALUE OF ALPHA-FETOPROTEIN CONCENTRATIONS

D.A. Granov[1], A.S. Polehin[2], P.G. Tarazov[1], I.O. Rutkin[1], I.I. Tileubergenov[1], V.V. Borovik[1]

[1] Granov Russian Scientific Center of Radiology and Surgical Technology, St. Petersburg, Russian Federation

[2] Leningrad Regional Clinical Oncological Dispensary, St. Petersburg, Russian Federation

Objective: to study liver transplantation (LT) outcomes in cirrhotic patients with hepatocellular carcinoma (HCC), who underwent transcatheter hepatic arterial chemoembolization (THACE). **Materials and methods.** From January 1998 to April 2020, we performed 245 orthotopic liver transplantation (OLTs) in 229 patients of which 25 (10.2%) had HCC in cirrhosis. In 9 (36%) patients, LT was performed without neoadjuvant therapy (Group 1). Group 2 consisted of 16 (66%) patients who underwent 49 THACE cycles before LT. 10 (62.5%) patients fell within the Milan criteria, while 6 (37.5%) were outside. According to the BCLC (Barcelona Clinic Liver Cancer) classification, 10 patients had A_1–A_4 stage, while 6 were in B stage. In 11 (68.5%) of 16 patients, increased serum alpha-fetoprotein (AFP) concentrations from 20 to 2463 (on average 493.8) ng/mL was revealed before treatment. In performing THACE, both the classical method (with lipiodol and hemostatic sponge) and the method with drug-eluting beads were performed 1 to 7 (on average 3) times. Doxorubicin was used in all cases. **Results.** Group 2 recorded a 100% technical success. There were no complications. We performed radiofrequency ablation (RFA) in three patients as an adjunct. In two patients, we performed laparoscopic RFA-assisted atypical liver resection, and in one – sequential resection and RFA. Under the m-Recist criteria, complete response was observed in 6 (37.5%), partial response in 7 (43.75%), and stabilization in 3 (18.75%) patients. Change in AFP concentrations were as follows: in 5 out of 11 patients with increased concentrations, we were able to reduce their AFP concentrations to the reference values, their long-term outcomes are comparable to those of Group 1. Four patients showed a 13–84% decrease; a directly proportional relationship between the degree of AFP decrease and the time to tumor progression was revealed. In 2 patients, there were 42% and 320% increase in AFP concentrations, the time to tumor progression was 3 and 1 month, both did not live up to 12 months. Among 9 (56%) of the living 16 patients, a maximum of 156 months and a minimum of 4 months (60.2 average) have elapsed since the surgery. Two of these nine have tumor progression (Cases 4 and 14). Seven (44%) patients died within 9 to 54 months. The 1, 3, 5-year actuarial survival rates were 93, 50, 32%, two patients lived more than 10 years. The average life expectancy was 28.0 ± 3.0 months. **Conclusion.** Serum AFP concentration is an important prognostic factor influencing the long-term outcomes of LT. Good biological response to THACE can be a positive predictor; LT outcomes in these patients are comparable to those in patients who meet the Milan criteria. A decrease in AFP concentrations by less than 50% after neoadjuvant THACE is an unfavorable factor, and its increase is extremely adverse.

Keywords: hepatocellular carcinoma, cirrhosis, hepatic arterial chemoembolization, neoadjuvant therapy, liver transplantation, alpha-fetoprotein.

INTRODUCTION

Liver transplantation (LT) is the only radical treatment for hepatocellular cancer (HCC) associated with liver cirrhosis (LC). However, in reaching a compromise between transplantation criteria and treatment guidelines for HCC, LT remains far from a routine operation and is feasible only in 10–15% of patients [1]. According to reports, over 55% of patients drop out of the waiting list within a year due to HCC progression [2, 3]. According to official statistical reports over the past 10 years, the peak incidence of HCC in the Russian Federation has not yet been passed [4–6]. Existing antiviral drugs against chronic hepatitis C virus (HCV) can significantly affect HCC statistics, as is the case in Western countries, but such drugs cannot yet be said to be widely available [7, 8].

Over 20 years have passed since the first transplant criteria was formulated. Being the basis and guarantor of

Corresponding author: Aleksey Polehin. Address: 37–39, Liteyny Prospekt, St. Petersburg, 191014, Russian Federation. Phone/fax: (812) 335- 23- 80. E-mail: polehin_aleksey@mail.ru

achieving the best survival rates (4-year survival rate is 83%), the Milan criteria are quite strict [9]. And during this time, various countries have come up with alternative LT guidelines for HCC against the background of LC. In addition to the number and size of foci, recent guidelines take into account biological tumor markers, the degree of differentiation, and tumor response to treatment. Presently, more than 20 extended LT criteria have been formulated. All of them are aimed at increasing the number of operations, with achievement of acceptable long-term outcomes, which directly depend on HCC progression in this group of patients [10, 11]. In order to keep the patient on the LT waiting list, methods of local anticancer treatment are increasingly being used, which, in addition to curbing the tumor process, can reduce the HCC stage, creating more favorable conditions for LT [12, 13]. The most commonly used is transcatheter hepatic arterial chemoembolization (THACE).

Objective of the study: to investigate our own LT outcomes in HCC patients on the background of LC, who underwent THACE.

MATERIALS AND METHODS

From 1998 to 2020, 229 patients underwent 245 orthotopic LTs with a graft from a deceased donor, of which 25 for HCC against the background of LC. In 22 patients, cirrhosis formed due to chronic hepatitis (B, C and D) virus, in two patients due to autoimmune hepatitis; one patient had primary biliary cirrhosis. Two patients (8%) were Child-Pugh class A, 18 (72%) were Child-Pugh class B, while 5 (20%) were Child-Pugh class C [14].

HCC diagnosis in 9 (36%) patients was established only by histological examination of the removed organs, and no THACE was performed in them. All of them retrospectively fell under the Milan criteria: maximum nodule diameter did not exceed 2 cm, no more than three foci in each organ, and stage "0" according to the BCLC classification (Barcelona Clinic Liver Cancer classification) [15]. These patients constituted Group 1.

In 16 (64%) patients of Group 2, 49 THACE cycles in various modifications were performed as neoadjuvant therapy (Table).

Of these, for 10 patients who met the Milan criteria, the goal of THACE was to prevent tumor progression in order to keep them on the waiting list. In 6 patients, THACE goal was to reduce the tumor volume to the Milan criteria and decrease its biological activity. At the start of treatment, 10 (62.5%) patients were BCLC A_1–A_4, while 6 (37.5%) patients were BCLC B [15]. Elevated serum alpha-fetoprotein (AFP) level from 20 to 2463 (mean 493.8) ng/mL was detected in 11 (68.5%) of 16 patients before treatment.

THACE was performed according to the standard technique using 10–50 mg of doxorubicin mixed with 5–10 mL of super-liquid Lipiodol, finely chopped hemostatic sponge, or doxorubicin-saturable spheres (Hepasphere, Biosphere Medical; DC Beads, Life Pearls, Terumo). Given the presence of severe manifestations of liver failure in patients, only superselective THACE was used, if necessary using 2.4–2.9 F microcatheters (Progreat, Terumo; Neuro Renegate, Boston).

Table

Group 2 characteristics

No./age	AFP before THACE	AFP after THACE	BCLC	MC after THACE (+/–)	Waiting time (months)	Time to tumor progression (months)	Outcome (month)	
							Alive	Died
1. K., 28	N	N	B	–	7	12		26
2. B., 58	N	N	B	+	15	–	62	–
3. R., 45	20	N	A	+	2	–	77	–
4. Z., 54	1300	1122 (<14%)	A	+	6	19	76	–
5. E., 49	183	30 (<84%)	B	+	6	24	–	36
6. K., 52	346	111 (<68%)	A	+	26	–	–	54
7. K.A., 53	113	N	B	+	10	–	–	19
8. K.B., 43	N	N	A	+	12	12	–	33
9 K., 53	59	N	A	+	7	–	138	–
10. S., 61	30	51 (>42%)	A	–	5	3	–	9
11. T., 45	2463	8666 (>320%)	A	+	16	1	–	20
12. U., 48	N	N	B	+	12	–	168	–
13. N., 55	31	N	B	+	23	–	62	–
14. P., 52	343	300 (<13%)	A	+	15	2	21	–
15. S., 47	N	N	A	+	12	–	30	–
16. Sh., 64	544	N	A	+	30	–	34	–

Note. BCLC – Barcelona Clinic Liver Cancer classification [14]; THACE – transcatheter hepatic arterial chemoembolization; MC – Milan Criteria [8]; AFP – alpha-fetoprotein.

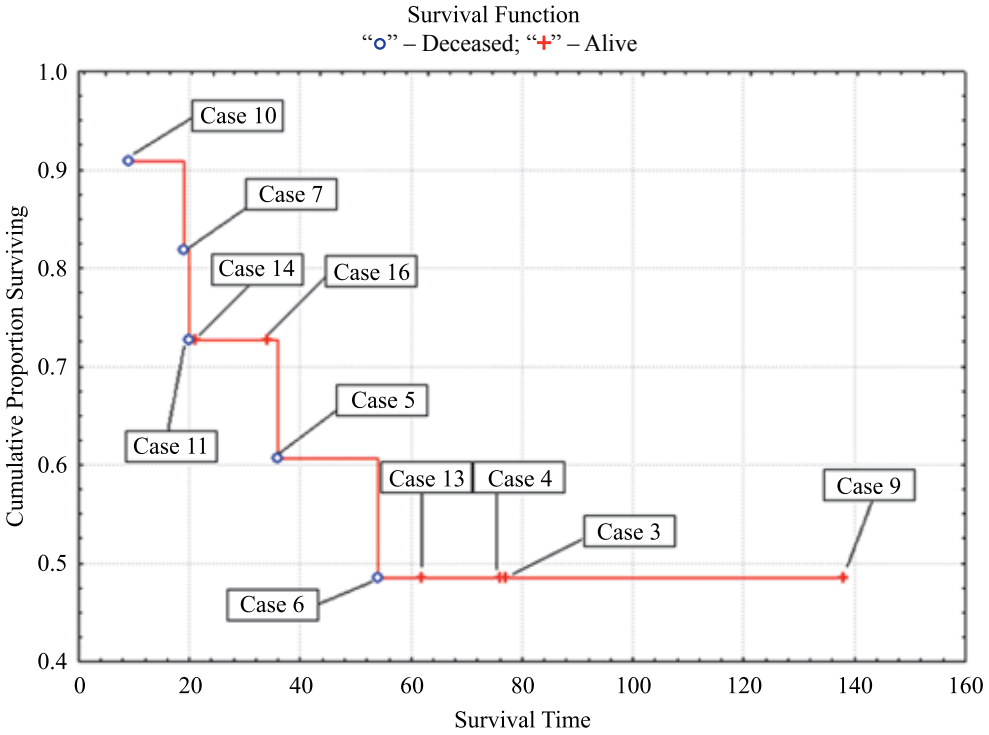

Fig. Calculation (by the Kaplan–Meier method) of survival in patients with increased AFP concentrations: "+" – alive; "o" – deceased

Treatment outcomes were assessed at week 3–5 based on data from multispiral computed tomography (MSCT) or magnetic resonance imaging (MRI) using the mRECIST criteria; AFP concentration dynamics were evaluated [16]. THACE was performed 1 to 7 times, and was repeated only with proven progression at worth 1–8 (mean 3.7).

After THACE, when partial response was achieved and tumor size decreased, radiofrequency ablation (RFA) was performed as an adjunct in three patients (Cases 7, 8, and 9), laparoscopic (LS) RFA-assisted atypical liver resection in two patients (Cases 14 and 16), successive resection and RFA in one patient with bilobar lesion (Case 2).

RESULTS

To date, 7 (78%) of 9 patients in Group 1 are alive at month 24 to 134 (mean 69.8), all without signs of HCC progression. The 1-3-5-year actuarial survival rates were 78–45–44%, with one patient alive for over 10 years. Two died within 1 (sepsis) and 7 months (HCC recurrence and graft rejection).

In Group 2, THACE's technical success was 100%. There were no complications. According to the mRECIST criteria, a complete response was observed in 6, partial in 7, stabilization in 3 patients. By the time of LT, 14 patients were BCLC A_1–A_4, 2 were BCLC B (Cases 1 and 10). In 4 out of 6 patients, we managed to achieve tumor response to treatment and return them to the Milan criteria (Cases 2, 5, 12 and 13). AFP dynamics was as follows: 5 of 11 patients with elevated levels were able to achieve reference values, 4 had a 13–84% decrease, 2 had 42% and 320% increases (Table).

At present, 9 (56%) of 16 patients are alive at month 4 to 156 (mean 60.2), of whom 2 had tumor progression (Cases 4, 14). Seven (44%) patients died between month 9 to 54: 5 due to HCC progression that occurred at month 1–24 (mean 11) (relapse in the graft, metastatic lung disease, dissemination), two from intercurrent disease (acute cerebral circulation disorder, cholangiogenic sepsis). The 1-3-5-year actuarial survival rates were 93–50–32%, two patients survived for more than 10 years. Average life expectancy was 28.0 ± 3.0 months.

In 5 out of 11 patients who managed to achieve reduction in AFP levels to reference values (according to mRECIST), complete response to treatment and total tumor necrosis based on histological studies were observed. In Cases 7 and 13, the patients were outside the Milan criteria before treatment. Currently, 4 out of 5 (Cases 16, 13, 3 and 9) are alive at month 34, 62, 77, and 138, with no signs of HCC progression. One patient (Case 7) died at month 19 from a cause unrelated to tumor progression. These results are comparable to those of Group 1.

Patients with decreased AFP levels according to mRECIST recorded a partial response. In Cases 5 and 6, AFP decreased by 84 and 68%, while in Case 6 there was no HCC progression, and in Case 5 it occurred after 24 months. Both patients died at month 36 and 54. The patient with a smaller decrease in AFP and from intercurrent disease lived for the longest period (Case 6). In

Cases 4 and 14, AFP decreased by 14% and 13%, the time to progression was 19 and 2 months, respectively.

Two patients with stable HCC showed a 42% and 320% increase in AFP, the time to progression was 3 and 1 month, both did not survive for 12 months.

DISCUSSION

The "stumbling block" in the formation of a waiting list for HCC patients with LC is the frequent inconsistency of stages of the tumor process and liver cirrhosis. So, if the reference Milan criteria are met, LT is indicated in the presence of one or three tumor nodes no larger than 3 cm in size. At the same time, following another rule, LT is indicated for subcompensated LC. Indeed, recently, with the development of surgical technologies, there is increasing evidence of sparing liver resections, and various methods of interventional radiology, which quite safely and effectively allow to control the tumor process even at late stages [17, 18]. So, the main indication for LT remains LC with irreversible liver dysfunction.

Let us imagine a common situation: a patient with single HCC up to 3 cm in diameter and Child-Pugh class B cirrhosis. According to the main choice of treatment tactics, BCLC classification, LT is indicated for him. Two months have passed since the moment of being placed on the waiting list, the focus has increased to 4 cm, and the AFP level has risen from 80 to 380 ng/mL. Is it worth doing nothing in such a situation? In our opinion, if nothing is done, then after another two months, only treatment with protein kinase inhibitors will be possible according to BCLC. Given the impossibility of guaranteeing even an approximate LT timeframe, we believe that all such patients should be treated with antitumor therapy. We consider THACE to be the most accessible and safest [19].

Over half of the available LT criteria take into account biological tumor markers, the most accessible of which is determination of AFP concentration. The criticality of its value, according to different authors, varies from 20 to 1000 ng/mL [10, 11]. According to the EASL and RUSSCO guidelines, a combination of clinical, radiological and laboratory data (LIRADS 2 or more + LC + tenfold increase in AFP concentration) is sufficient to diagnose HCC [15, 20, 21] without biopsy, associated with a high risk of bleeding after liver puncture against the background of hypocoagulation. Accordingly, evaluation of tumor differentiation degree is often performed only after LT. Both AFP and morphological picture, along with the number and size of tumor nodules, became the basis for formulation of prognostic scales of LT outcomes in HCC [11].

In our study, in Group 2, 11 (68.5%) of 16 patients had elevated AFP levels. After THACE, 5 out of 11 patients managed to achieve AFP reduction to reference values (Cases 3, 7, 9, 13, 16). As a result, such indicators as time to progression and survival in these patients were comparable to those of Group 1. In another 4 patients, THACE was able to achieve decreased AFP concentrations. In Cases 5 and 6, the decrease in AFP was 84% and 68%; HCC progression occurred only in Case 5 at month 24. In Cases 4 and 14, AFP decreased by 14% and 13%; the time to progression was 19 and 2 months, respectively. In two patients with an increase in AFP concentration (Cases 10, 11), time to progression was very short: 3 and 1 month, despite the fact that LT was performed in Case 11 according to the Milan criteria.

So, the dynamics of serum AFP levels was an important prognostic factor influencing long-term LT outcomes. A good biological response to THACE can serve as a positive prognosis factor; LT outcomes in these patients are comparable to those in patients who meet the Milan criteria. A less-than-50% decrease in AFP levels after neoadjuvant THACE was an unfavorable factor, and its increase was extremely unfavorable.

The authors declare no conflict of interest.

REFERENCES

1. *Gautier SV, Moysyuk YG, Poptsov VN et al*. Long-term outcomes of deceaded donor liver transplantation. *Russian Journal of Transplantology and Artificial Organs*. 2014; 16 (3): 45–53. (In Russ.).
2. *Salvalaggio PR, Felga G, Axelrod DA et al*. List and liver transplant survival according to waiting time in patients with hepatocellular carcinoma. *American J Transplant*. 2015; 15 (3): 668–677.
3. *Benmassaoud A, Tsochatzis EA*. Loco-regional treatments on the liver transplant waiting list: unmasking hepatocellular carcinoma (HCC) biology. *Hepatobiliary Surg Nutr*. 2018; 7 (3): 199–201.
4. *Bray F, Ferlay J, Soerjomataram I et al*. Global cancer statistics 2018: GLOBOCAN estimates of incidence and mortality worldwide for 36 cancers in 185 countries. *CA Cancer J Clin*. 2018; 68 (6): 394–424.
5. *Balakhnin PV, Shachinov EG, Shmelev AS*. The role of surgical technologies in the treatment of virus-associated tumors on the example of hepatocellular carcinoma. *Practical oncology*. 2018; 19 (4): 348–377. (In Russ.).
6. *Kaprin AD, Starinskij VV, Petrova GV*. Zlokachestvennye obrazovanija v Rossii v 2017 godu (zabolevaemost' i smertnost'). M.: RIIS FIAN, 2018. 250. (In Russ.).
7. *Crespo G, Trota N, Londono M-C et al*. The afficacy of direct anti-HCV drugs improves early post-liver transplant survival and induces significant changes in waiting list composition. *Journal of Hepatology*. 2018; 69 (1): 11–17.
8. EASL recommendation on treatment of hepatitis C 2018. *Journal of Hepatology*. 2018; 69 (2): 461–511.
9. *Mazzaferro V, Regalia E, Doci R et al.* Liver transplantation for the treatment of small hepatocellular carcinomas in patients with cirrhosis. *N Engl J Med*. 1996. (334): 693–699.
10. *Schielke A, Meurisse N, Lamproye A et al*. Selection criteria for liver transplantation in patients with hepa-

tocellular carcinoma. Eastern and western experiences, and perspectives for the future. *Acta Gastroenterol Belg*. 2019; 82 (2): 314–318.
11. *Maltseva AP, Syutkin VE, Kolyshev IYu et al*. Transplantation in oncology: the future of a multidisciplinary approach. *Transplantologiya. The Russian Journal of Transplantation*. 2019; 11 (3): 218–233. (In Russ.).
12. *Pompili M, Francica G, Romana Ponziani F et al*. Bridging and downstaging treatments for hepatocellular carcinoma in patients on the waiting list for liver transplantation. *World J Gastroenterol*. 2013; 19 (43): 7515–7530.
13. *Kulik L, Heimbach JK, Zaiem F et al*. Therapies for patients with hepatocellular carcinoma awaiting liver transplantation: A systematic review and meta-analysis. *Hepatology*. 2018. 67 (1): 381–400.
14. *Child CG, Turcotte JG*. Surgery and portal hypertension. *The liver and portal hypertension*. Philadelphia: W.B. Saunders Co., 1964: 50.
15. European Association for the Study of the Liver. EASL Clinical Practice Guidelines: Management of hepatocellular carcinoma. *J Hepatol*. 2018; 69 (1): 182–236.
16. *Lencioni R, Llovet JM*. Modified RECIST (mRECIST) assessment for hepatocellular carcinoma. *Semin Liver Dis*. 2010; (30): 52–60.
17. *Patjutko JuI, Kudashkin NE*. Hirurgicheskoe lechenie bol'nyh gepatocelljuljarnym rakom BCLC B. *Malignant Tumor*. 2016; 4, specvypusk 1: 46–47.
18. *Bhandare MS, Patkar S, Shetty N et al*. Liver Resection for HCC Outside the BCLC Criteria. *Langenbecks Arch Surg*. 2018; 403 (1): 37–44.
19. *Polekhin A.S., Tarazov PG, Polikarpov AA, Granov DA*. Transcatheter arterial chemoembolization in the treatment of patients with hepatocellular carcinoma on advanced liver cirrhosis. *Grekov's Bulletin of Surgery*. 2019; 178 (6): 29–35.
20. *Breder VV, Balahnin PV, Virshke ER et al*. Prakticheskie rekomendacii po lekarstvennomu lecheniyu gepatocellyulyarnogo raka. *Zlokachestvennye opuholi: Prakticheskie rekomendacii RUSSCO*. 2019; 9 (2): 420–438. (In Russ.).
21. American College of Radiology. Quality and safety resources: Liver Imaging – Reporting and Data System. Available at: http://www.acr.org/QualityB Safety/Resources/LIRADS. Accessed April 22, 2012.

The article was submitted to the journal on 20.08.2020

DOI: 10.15825/1995-1191-2020-4-58-64

MANAGEMENT OF VARICEAL BLEEDING IN THE LIVER TRANSPLANT WAITING LIST

V.L. Korobka[1, 2], M.Yu. Kostrykin[1], A.M. Shapovalov[1]

[1] Rostov Regional Clinical Hospital, Rostov-on-Don, Russian Federation
[2] Rostov State Medical University, Rostov-on-Don, Russian Federation

Objective: to study the outcomes of main surgical methods for stopping and preventing variceal hemorrhage in waitlisted cirrhotic patients. **Material and methods.** In our prospective case-control study, the "case" cohort included 132 patients with cirrhosis complicated by recurrent varicose bleeding, while the "control" group consisted of 92 patients with one episode of bleeding esophageal varices. Treatment included conservative therapy, endoscopic ligation, transjugular intrahepatic portosystemic shunt, and the original azygoportal disconnection technique. **Results.** High MELD scores, severe hepatic encephalopathy, portal vein thrombosis, high degree of varices, and recurrent bleeding significantly affect the mortality of cirrhotic patients. Irrational use of nonselective beta-blocker monotherapy has a negative impact on treatment outcomes. Combined use of drug therapy and surgical methods of stopping and preventing varicose bleeding, reduces the number of relapses, prolongs patients' life to two years or more, which allows to move on to the next stage of cirrhosis treatment – liver transplantation. **Conclusion.** The likelihood of recurrent variceal hemorrhage increases in patients who undergo passive surgical tactics. Azygoportal disconnection should be considered as the operation of choice if the patient has more than one episode of variceal bleeding. Timely and adequate treatment measures, clinical and diagnostic monitoring reduce waitlist mortality.

Keywords: variceal bleeding, liver transplantation, waiting list.

INTRODUCTION

Esophageal varices (EV) are a common clinical manifestation of liver cirrhosis (LC). The incidence of varices in the upper gastrointestinal tract in compensated cirrhosis ranges from 30% to 40%, and in decompensated cirrhosis reaches 60% [1, 2]. In case of variceal rupture, bleeding occurs, the first episode of which is fatal for 20–80% of patients with cirrhosis, and 50–70% of patients have a high risk of recurrence. From the moment of the first episode of variceal bleeding, slightly more than 40% of patients survive for two years [3, 4].

The prognosis of LC depends not only and not so much on age and concomitant disease as by the functional reserve of the liver, the degree and localization of varices, and severity of variceal bleeding [5].

To date, both drugs and various invasive techniques are used to stop bleeding EV and prevent its recurrence [6, 7–9]. However, the ineffectiveness of the former and the lack of radicalism of the others, often forces us to change tactics and resort to open methods of surgical treatment for this category of patients [10, 11]. Shunting, portal blood flow decoupling and resection operations, proposed at different times, improve the quality and prolong the life of patients with cirrhosis to some extent. However, none of these approaches can return portal blood flow to a normal state.

Currently, liver transplantation (LT) remains the only pathogenetically justified method providing long-term positive treatment for LC patients. However, its use is limited by a number of factors, particularly, donor organ shortage [12, 13]. The method often determines the actual waiting time for transplantation, often stretching for several years for 63% of patients [14]. This leads to increased deaths among liver transplant waitlisted patients due to bleeding esophageal varices.

In view of the above, the aim of the study was to study the outcomes of the main surgical methods for stopping and preventing bleeding esophageal varices in patients with liver cirrhosis who are on the waiting list.

MATERIAL AND METHODS

The study was prospective, conducted at Rostov Regional Clinical Hospital, lasting from 2015 to 2020. The data of 224 patients from the LT waitlist, for whom variceal bleeding from the upper gastrointestinal tract became a complication of LC, were analyzed.

Inclusion criteria: esophageal vein dilation (confirmed via imaging); anamnestic evidence of variceal bleeding episodes; evidence of surgical interventions or other actions aimed at stopping or preventing variceal bleeding. There were no specific exclusion criteria. All patients were examined in accordance with the diagnostic protocol for LC patients.

Corresponding author: Michael Kostrykin. Address: 170, Blagodatnaya str., Rostov-on-Don, 344015, Russian Federation. Phone: (918) 554-16-28. E-mail: michael_cs@mail.ru

The study was conducted in two "case-control" groups of patients. The main group "case" included 132 LC patients with recurrent variceal bleeding. The "control" group consisted of 92 patients who had no more than one bleeding EV.

All demographic, clinical and laboratory data for statistical analysis were obtained from a continuously updated electronic database of the Center for Surgery and Donation Coordination of the previously designated institution.

Methods for preventing and stopping bleeding EV included conservative measures, endoscopic variceal ligation, transjugular intrahepatic portosystemic shunt (TIPS) and the original azygoportal disconnection (APD) technique. The essence was resection of the abdominal esophagus and cardiac stomach, followed by formation of esophagogastroanastomosis and creation of anti-reflux cardia [15].

Statistical data analysis was conducted using the IBM SPSS Statistics 23 software. The statistical significance of the differences between compared parameters in normal distribution was assessed by the Student's t-test. In the absence of normal distribution, nonparametric tests were used: Wilcoxon for pairwise comparisons of dependent variables, Mann–Whitney U test, Pearson's chi-square for comparison of independent variables. Differences between compared parameters were considered statistically significant if the error probability was less than 0.05 ($p < 0.05$).

RESULTS

Characteristics of the "case" group

The group of patients with recurrent variceal bleeding consisted of 82 men (62.1%) and 50 women (37.9%). The average age of the patients was within 51 years (49.52 ± 10.92). The waitlist time was 17.14 ± 15.04 months.

Viral hepatitis was the cause of LC in 68 patients (51.5%), alcohol-related liver disease in 31 cases (23.5%), and 17 patients (12.9%) were diagnosed with cryptogenic cirrhosis. Autoimmune diseases and other causes resulted in cirrhosis in 16 patients (12.1%).

During examination, it was established that in 50 patients (37.9%), MELD score did not exceed 20; 64 patients (48.4%) had a MELD score from 20 to 30; in 18 (13.6%) patients, the score exceeded 30 points. In accordance with the Child-Turcotte-Pugh classification for cirrhosis, 126 (95.5%) patients in the group had class C cirrhosis, the rest were class B.

Endoscopic examination of the upper digestive tract showed that 28 patients (21.3%) had esophageal varices grade 1–2, 67 (50.8%) patients had grade 3, while 37 (28.0%) patients had grade 4.

The following were aggravating factors of the underlying disease in patients: overt hepatic encephalopathy – out of 124 (93.9%) patients that had this complication, 57 (43.1%) had grade 3–4; resistant ascites – 57 (43.2%) patients; hepatorenal syndrome – 71 (53.8%) cases; portopulmonary hypertension – 16 (12.1%) patients; thrombosis of the portal vein and its main branches – 27 (20.5%) patients.

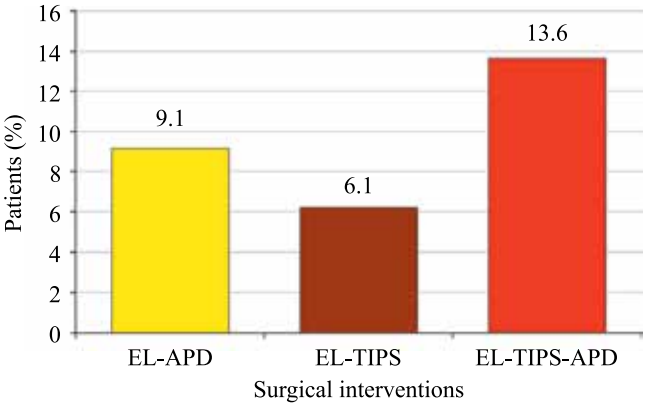

Fig. 1. Distribution of patients by types of surgical interventions: EL – endoscopic ligation; TIPS – transjugular intrahepatic portosystemic shunt; APD – azygoportal dissociation

As noted earlier, all patients in this group were characterized by recurrent bleeding from the esophageal varices. When taking anamnesis, it was found that 101 patients (76.5%) had two to three episodes of bleeding, up to five episodes were recorded in 27 (20.5%) patients, more than five bleeding episodes occurred in 4 (3.1%) patients, with one of them with documented 14 episodes.

With regards to treatment of patients in this group, it should be said that 126 patients (95.5%) received conservative therapy, including non-selective β-blockers. Besides, 77 patients (58.3%) underwent various surgical interventions aimed at stopping bleeding from the EV and preventing its recurrence.

Endoscopic EV ligation was the main type of surgical intervention in 31 patients (23.5%), TIPS in 7 patients (5.3%), 1 patient underwent an original disconnecting surgery. Frequent relapses of bleeding due to failure of endoscopic ligation or portosystemic shunt obstruction made us either resort to the already used techniques repeatedly or perform an open disconnecting surgery (Fig. 1). So, on average, 2.55 ± 1.55 interventions were required per patient in the group.

Despite comprehensive measures taken for the treatment and prevention of variceal bleeding, which were carried out in 76 (57.6%) patients, it still recurred in 38 (28.8%) patients.

Characteristics of the "control" group

Male patients predominated in the control group, as in the main group. There were fewer women – 51 (55.4%) men and 41 (44.6%) women. The average age of the

patients was 53 years (50.48 ± 10.38). Time on the LT waitlist was 15.99 ± 11.87 months.

The main cause of LC in 41 patients (44.6%) in this group was viral hepatitis; LC was a result of alcohol-related liver disease in 20 (21.7%) patients, and in 14 (15.2%) patients, it was autoimmune diseases. Cryptogenic cirrhosis was diagnosed in 14 more patients, congenital and metabolic diseases was the cause of LC in 3 (3.3%) patients.

Laboratory examination established that 49 (53.3%) patients had a MELD score <20; 29 (31.5%) patients had a MELD score within 20 to 30, while 14 (15.2%) patients had a MELD score >30. In accordance with the Child-Turcotte-Pugh LC severity classification, 5 (5.5%) and 87 (94.6%) cases were of classes B and C, respectively.

Endoscopic examination revealed esophageal varices grade 1 and 2 in 55 (59.8%) patients, grade 3 in 31 (33.7%) patients, and grade 4 in 6 (6.5%) patients.

Hepatic encephalopathy with its obvious clinical manifestations was the aggravating factor for 11 (12.0%) patients. Besides, 37 (40.2%) patients had resistant ascites and hepatorenal syndrome, 10 (10.9%) patients had portopulmonary hypertension, 4 (4.3%) cases showed portal vein thrombosis on Doppler ultrasonography.

As noted earlier, patients had one episode of EV bleeding, which characterized the treatment tactics. The main method of treatment was therapy with nonselective β-blockers; 78 (84.8%) patients received the drugs.

Table 1

Main indicators in case and control cohorts (comparative characteristics)

Indicator	Study groups		p
	Case (n = 132)	Control (n = 92)	
Male	82 (62.1%)	51 (55.4%)	0.316
Age (years)	49.52 ± 10.92	50.48 ± 10.38	0.504
MELD score	22.78 ± 6.32	21.41 ± 7.16	0.010
Hepatic encephalopathy (score)	2.47 ± 0.76	2.20 ± 0.75	0.008
Ascites (score)	2.16 ± 0.83	2.12 ± 0.82	0.725
Viral cirrhosis	68 (51.5%)	41 (44.6%)	0.307
Alcoholic cirrhosis	31 (23.5%)	20 (21.7%)	0.760
Child-Pugh class C	126 (95.5%)	87 (94.6%)	0.762
Portal vein thrombosis	27 (20.5%)	4 (4.3%)	0.001
Varicose vein	3.06 ± 0.72	2.40 ± 0.71	<0.001
VB frequency	2.84 ± 1.49	1.00 ± 0.00	<0.001
Waitlist mortality from VB	32 (24.2%)	2 (2.2%)	<0.001
Listing* (months)	17.14 ± 15.04	15.99 ± 11.87	0.524

Note. * length of stay on the liver transplant waiting list. VB – variceal bleeding.

Surgical methods, of which only endoscopic ligation was used, were resorted to in this group only in 6 (6.5%) cases. No other measures aimed at preventing bleeding recurrence or stopping it were taken. This approach resulted in recurrent variceal hemorrhage in 33 (35.9%) patients.

Comparison of indicators in the main and control groups

A comparison of the basic data of patients in both groups showed that a number of indicators had statistically significant differences ($p < 0.05$) (Table 1). This was an evidence of our assumption that patients with recurrent variceal bleeding are in a more severe initial condition. MELD score, severity of hepatic encephalopathy, presence of portal vein thrombosis, degree of EV, and the very fact of variceal bleeding relapse had a significant impact on waitlist mortality rate.

Comparison of the effectiveness of surgical techniques for stopping and preventing variceal bleeding

In the course of the work, we were particularly interested in assessing the effectiveness of each surgical technique used with regard to prevention of recurrent variceal bleeding and reduction of LT waitlist mortality.

Endoscopic EV ligation procedure, which was performed in 75 patients, had a lasting effect in 23 (30.7%) patients only; in 52 patients, varices had to be ligated repeatedly or the surgical tactics had to be changed. So, 6 (8.0%) patients underwent TIPS after several ineffective EV ligation procedures (1.83 ± 0.57) during the first year (6.13 ± 3.26 months); in 7 (9.3%) cases of sequential ligation and TIPS, we eventually had to perform APD, with 2 (2.7%) patients having APD as operation of choice after the second-third bleeding episode.

Of the 33 patients who underwent TIPS, the technique was effective in 28 (84.8%) patients within the first year (6.11 ± 3.08 months). Shunt thrombosis in 5 (15.2%) patients was the reason for a single re-TIPS procedure and one APD operation.

As can be seen, the APD surgery in a series of surgical manipulations performed to stop variceal bleeding becomes the final intervention, giving the patient a chance to avoid recurrent bleeding, stay alive and wait for LT. APD was primarily performed as an independent operation to stop bleeding in only one case, while in 30 (96.8%) cases, it was performed after failures in endoscopic ligation and TIPS.

During the entire follow-up period for patients who underwent APD, which averaged 28 months (0.5–140.8), recurrent variceal bleeding was noted in 3 (9.7%) cases from 0.2 to 63.2 months of follow-up. In spite of another bleeding episode in the life of the patients, they remained

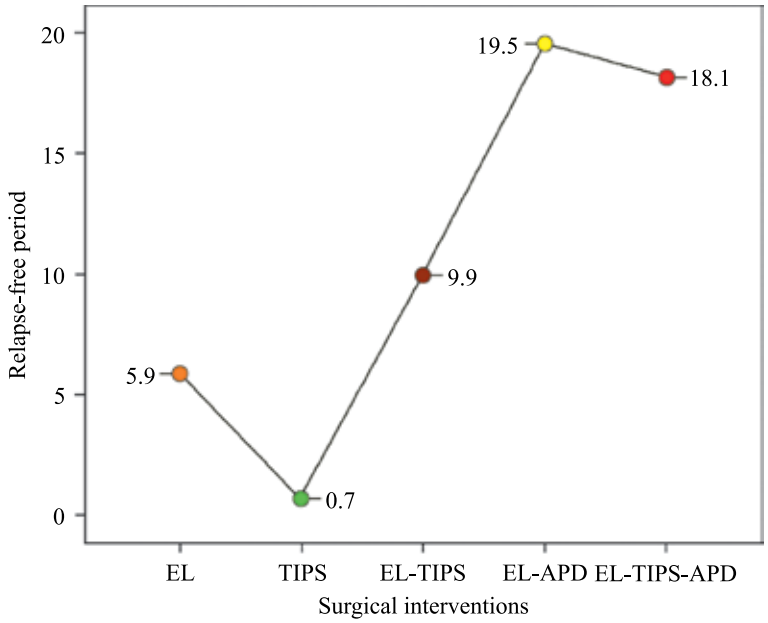

Fig. 2. Average time of variceal bleeding recurrence. One-way analysis of variance. Twenty-four months follow-up. Welch's t-test: value – 8.764; p = 0.001. EL – endoscopic ligation; TIPS – transjugular intrahepatic portosystemic shunt; APD – azygoportal dissociation

alive, including due to liver transplantation performed as soon as possible.

Considering that bleeding from EV can recur, the time of its recurrence with one or another type of surgical intervention was studied (Fig. 2). The analysis showed that the APD surgery allows to postpone the time of recurrence, thereby increasing the patient's time on the LT waiting list.

Analysis of the two-year mortality rate of patients showed that the largest number of patients die when portosystemic shunt is used as a method of stopping and preventing variceal bleeding, while the use of APD, both alone and in combination with other surgical interventions, significantly reduces mortality (Table 2).

The Kaplan–Meier estimator was used to assess patient survival. The two-year LT waitlist survival function in the created model was identified with the development of recurrent variceal bleeding, followed by death (Fig. 3). The significance of the differences between the survival times in the compared groups using different criteria is shown in Table 3.

The average predicted survival time of patients with variceal bleeding when endoscopic ligation and TIPS are used is 15.2 months and 14.3 months, respectively. When endoscopic ligation is used in the first stage of stopping bleeding, followed by TIPS or APD, the average survival time reaches 20.6 months and 20.7 months, respectively. When all the surgical methods we have considered are used, the average survival time will be 19.9 months.

Thus, the use of surgical techniques to arrest and prevent recurrent variceal bleeding certainly increases the patient's LT waitlist survival: 19.9 months with surgical treatment versus 12.9 months without surgery (Log Rank (Mantel-Cox): Chi-square – 9.399; p = 0.002). A significant proportion of patients will not die from bleeding in the next two years, which will give them a chance to move on to the next stage of treatment (liver transplantation) for the underlying disease.

DISCUSSION

The severity of the patient's condition, and, as a consequence, the urgency of a transplant surgery, undoubtedly determines the MELD score. However, in order to

Table 2

2-Year mortality in different methods of surgical treatment of bleeding varicose veins

Surgical intervention	Abs.	%
Endoscopic ligation	8	21.6
TIPS	3	42.9
Azygoportal disconnection	0	0.0
Endoscopic ligation-TIPS	3	37.5
Endoscopic ligation-APD	2	16.7
Endoscopic ligation-TIPS-APD	0	0.0

Table 3

Estimation of survival time differences

Criterion	Chi-square	Degrees of freedom	Significance
Log Rank (Mantel-Cox)	11.270	5	0.046
Breslow (Generalized Wilcoxon)	10.449	5	0.063
Tarone-Ware	11.617	5	0.040

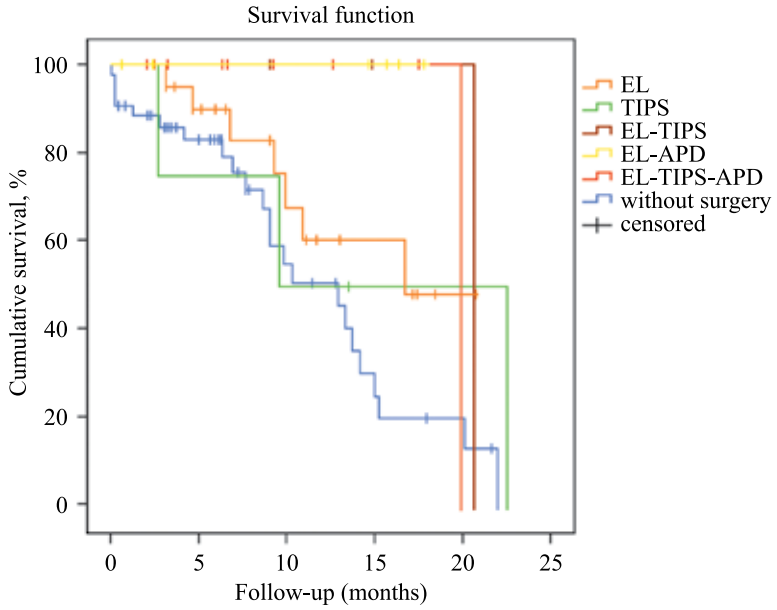

Fig. 3. Survival curves for various surgical methods of stopping and preventing bleeding varicose veins using the log-rank criterion. EL – endoscopic ligation of VRV; TIPS – transjugular portosystemic shunting; APD – azygoportal dissociation

achieve greater patient selection objectivity, especially in the background of recurrent variceal bleeding, each clinical case, in our opinion, should be evaluated separately и.

In addition to MELD, in order to objectively assess the severity of the patient's condition, it is necessary to take into account the degree of EV, number of bleeding episodes, severity of hepatic encephalopathy, and presence of portal vein thrombosis. In turn, the concept of therapeutic prophylaxis requires development of clear criteria for prescribing non-selective β-blockers, since their irrational use can have a negative impact on treatment outcomes in patients.

Syndromic therapy and also timely prevention and treatment of variceal bleeding are the guarantee for long-term management of patients on the liver transplant waitlist. In terms of surgical stopping of variceal bleeding and its prevention, patients with the original APD performed have an advantage. In 12 cases (38.7%), patients achieved stable remission, 7 patients (22.6%) were taken off the waiting list due to positive dynamics in the disease course.

CONCLUSION

Analysis and evaluation of the results of using the main methods for stopping and preventing bleeding from EV in patients with cirrhosis waitlisted for liver transplantation showed that recurrent bleeding occurs primarily in those patients for whom passive surgical tactics are followed. If a patient with EV is on the LT waitlist for a long time and has at least one episode of EV bleeding, APD should be considered as the surgery of choice. A prerequisite for reducing LT waitlist mortality is the timeliness and adequacy of treatment measures and systematic clinical and diagnostic monitoring.

The authors declare no conflict of interest.

REFERENCES

1. *Karatzas A, Konstantakis C, Aggeletopoulou I, Kalogeropoulou C, Thomopoulos K, Triantos C.* Non-invasive screening for esophageal varices in patients with liver cirrhosis. *Ann Gastroenterol*. 2018; 31 (3): 305–314. https://doi.org/10.20524/aog.2018.0241.
2. Korean Association for the Study of the Liver (KASL). KASL clinical practice guidelines for liver cirrhosis: Varices, hepatic encephalopathy, and related complications. *Clin Mol Hepatol*. 2020; 26 (2): 83–127. https://doi.org/10.3350/cmh.2019.0010n.
3. *Biecker E.* Gastrointestinal bleeding in cirrhotic patients with portal hypertension. *ISRN Hepatol*. 2013; 2013: 541836. Published 2013 Jul 22. https://doi.org/10.1155/2013/541836.
4. *Mallet M, Rudler M, Thabut D.* Variceal bleeding in cirrhotic patients. *Gastroenterol Rep* (Oxf). 2017; 5 (3): 185–192. doi: 10.1093/gastro/gox024.
5. *Malomuzh OI, Kpel' PE, Gautier SV, Tsipul'nikova OM et al.* Prognosis for patients with chronic diseases of the liver in formulating indications to orthotopic liver transplantation. *Terapevticheskii arkhiv*. 2009; 81 (2): 45–49. (In Russ.).
6. *Seo YS.* Prevention and management of gastroesophageal varices. *Clin Mol Hepatol*. 2018; 24 (1): 20–42. https://doi.org/10.3350/cmh.2017.0064.
7. *Boregowda U, Umapathy C, Halim N et al.* Update on the management of gastrointestinal varices. *World J Gastrointest Pharmacol Ther*. 2019; 10 (1): 1–21. https://doi.org/10.4292/wjgpt.v10.i1.1.

8. *Onnitsev IE, Bugaev SA, Ivanusa SYa et al.* Prevention of recurrent bleeding from varicose veins of the esophagus and stomach among patients with decompensated liver cirrhosis. *Kazan medical journal*. 2019; 100 (2): 333–339. (In Russ.). https://doi.org/10.17816/KMJ2019-333.
9. *Zanetto A, Garcia-Tsao G.* Management of acute variceal hemorrhage. *F1000Res*. 2019; 8: F1000 Faculty Rev-966. Published 2019 Jun 25. https://doi.org/10.12688/f1000research.18807.1.
10. *Yang L, Yuan LJ, Dong R et al.* Two surgical procedures for esophagogastric variceal bleeding in patients with portal hypertension. *World J Gastroenterol*. 2013; 19 (48): 9418–9424. https://doi.org/10.3748/wjg.v19.i48.9418.
11. *Coelho FF, Perini MV, Kruger JA et al.* Management of variceal hemorrhage: current concepts. *Arq Bras Cir Dig*. 2014; 27 (2): 138–144. https://doi.org/10.1590/s0102-67202014000200011.
12. EASL Clinical Practice Guidelines: Liver transplantation. *J Hepatol*. 2016 Feb; 64 (2): 433–485. https://doi.org/10.1016/j.jhep.2015.10.006.
13. *Toniutto P, Zanetto A, Ferrarese A et al.* Current challenges and future directions for liver transplantation. *Liver Int*. 2017; 37 (3): 317–327. https://doi.org/10.1111/liv.13255.
14. *Samuel D, Coilly A.* Management of patients with liver diseases on the waiting list for transplantation: a major impact to the success of liver transplantation. *BMC Med*. 2018; 16 (1): 113. Published 2018 Aug 1. https://doi.org/10.1186/s12916-018-1110-y.
15. *Korobka VL, Shapovalov AM, Danil'chuk OYa, Korobka RV*. Sposob khirurgicheskogo lecheniya i profilaktiki retsidiva krovotecheniy pri varikoznom rasshirenii ven pishchevoda i kardial'nogo otdela zheludka. Patent na izobretenie RU 2412657 C1, 27.02.2011. Zayavka № 2009128518/14 ot 23.07.2009.

The article was submitted to the journal on 31.08.2020

DOI: 10.15825/1995-1191-2020-4-65-68

CLINICAL AND FUNCTIONAL FEATURES OF PENETRATING KERATOPLASTY IN THE KINGDOM OF JORDAN. A SINGLE-CENTER EXPERIENCE

M.A. Tanash[1], M.A. Frolov[1], P.A. Gonchar[1], G.N. Dushina[1], L.T. Ababneh[2]

[1] Peoples' Friendship University of Russia, Moscow, Russian Federation

[2] Jordan University of Science and Technology, King Abdullah University Hospital, Irbid, Jordan

Objective: to determine the indications for penetrating keratoplasty (PK) in the Kingdom of Jordan and evaluate its clinical and functional outcomes. **Materials and methods.** 213 patients underwent PK at the ophthalmology department of King Abdullah University Hospital (KAUH) in Jordan from January 1, 2010 to December 31, 2018. While 196 (92.2%) patients were operated on in one eye, 17 (8.8%) underwent PK in both eyes. For all patients, the best corrected visual acuity (BCVA) was checked using the Snellen table and compared with the BCVA before surgery; biomicroscopy of the anterior segment of the eye, as well as applanation tonometry, were carried out. **Results.** Keratoconus was found to be the most common indication for PK – 154 patients (73.2%). For all patients, the BCVA improved from 0.08 before surgery to 0.25 after surgery. **Conclusion.** Keratoconus is the most common indication for PK in both men (97, 71.3%, $p < 0.05$) and women (57, 74%, $p < 0.05$) in the Kingdom of Jordan. PK is an effective method for treating various corneal disorders.

Keywords: corneal transplantation, indications, penetrating keratoplasty, keratoconus.

INTRODUCTION

Eye diseases are one of the most important economic and social problems in the world. According to the World Health Organization (WHO), corneal opacities affected 1.9 million people (5.1% of the total number of blind people) [1].

It is estimated that about 23 million people worldwide suffer from unilateral corneal blindness [2]. Common pathologies leading to vision loss include keratoconus, trachoma, onchocerciasis, neonatal conjunctivitis, and keratomalacia as a result of vitamin A deficiency [1].

Penetrating keratoplasty (PK) is the main intervention for restoring corneal structure and improving vision in these patients. This surgical procedure involves replacing the pathological cornea with a donor one [3].

Eduard Konrad Zirm performed the first successful PK in 1905. It was a solid organ transplant in a human. This solved one of the major problems of ophthalmology at the time – helping patients with bilateral corneal leukoma. "It was a ray of light that cut through the gloom of despondency," prominent Soviet ophthalmologist and surgeon Vladimir Filatov noted later [4].

Having learned about the success of PK, many researchers all over the world began to identify more and more new indications for such an intervention [5–9]. These conditions include keratoconus, pseudophakic bullous keratopathy, scars, corneal perforations, consequences of keratitis, and trachomatous keratopathy being a major problem in certain regions [1, 10].

Graft rejection was one of the most serious complications. This problem was later resolved through repeated PK with preoperative HLA typing of donor and recipient histocompatibility [11].

All the above conditions have a global prevalence and similar clinical symptoms – total corneal opacity requiring corneal replacement.

The number of PK surgeries performed in some regions that are endemic for certain diseases is quite high. For example, in the Kingdom of Jordan, 10,548 operations have been performed over the past 10 years.

The purpose of this study is to determine the indications for PK in the Kingdom of Jordan and to evaluate its clinical and functional outcomes.

MATERIALS AND METHODS

Data from patients at the ophthalmology department of King Abdullah University Hospital (KAUH) in Jordan who underwent PK from January 1, 2010 to December 31, 2018 were retrospectively analyzed. Approval from the KAUH Institutional Review Board (IRB) was obtained prior to the study (reference 13/3/122). The study enrolled 213 patients (136 males and 77 females), their ages ranging from 14 to 97 years (46.6 ± 19.6). The data were obtained from the annual statistical report of the Jordan Eye Bank of the University of Jordan.

The quality of the donor material is the key to the success of PK. According to annual reports, the number of cornea donors has increased significantly over the past

Corresponding author: Mohammed Tanash. Address: 21/3, Miklukho-Maklaya str., Moscow, 117198, Russian Federation. Phone: (985) 199-69-24. E-mail: dr.mohammedtanash@gmail.com

decade due to programs aimed at raising public awareness. These programs are regularly published freely on the Internet.

The following socio-demographic characteristics were taken into account: gender, age, marital status, educational level, nature of activity (presence of harmful factors affecting the eye), as well as existing concomitant diseases, including hereditary ones, and genetic defects aggravating the course of eye disease.

Further examination for all patients included checking the best corrected visual acuity (BCVA) using the Snellen table and comparing it with the BCVA before surgery, biomicroscopy of the anterior segment of the eye, applanation tonometry (in the absence of contraindications) and corneal topography on Pentacam system (OCULUS Optikgeräte GmbH). SPSS software (SPSS, Inc., Chicago, Illinois, USA) was used for data analysis. A p-value less than 0.05 was considered statistically significant.

RESULTS

Characteristics of the clinical material (213 patients); 196 (92.2%) of them underwent PK on one eye and 17 (8.8%) on both eyes.

The study included 136 males (63.8%) and 77 females (36.2%). It was found that keratoconus was the leading indication for PK both in men (71.3%, $p < 0.05$) and in women (74%, $p < 0.05$). This was followed by corneal opacities due to viral infection and dystrophies. Further, in descending order, were eye injuries and burns of various degrees of severity and previous graft rejection. Stevens-Johnson syndrome was the least among the indications for PK (Table).

Before PK was performed, patients had different visual acuity in correlation with age: from correct light projection to 0.5 (mean value 0.08). These results are shown in Fig. 1.

Table

Indications for penetrating keratoplasty by gender

Indications	Men	Women	Total	
			n	%
Keratoconus	97	57	154	72.3
Herpes keratitis	9	6	15	7
Graft rejection	11	4	15	7
Injury	10	4	14	6.7
Corneal dystrophy	8	2	10	4.7
Fungal keratitis	1	3	4	1.8
Stevens-Johnson syndrome	0	1	1	0.5
Total	136	77	213	100

Visual acuity improved after PK. The mean postoperative BCVA in correlation with age in these patients ranged from 0.05 to 1.0 (mean 0.25). The results are shown in Fig. 2.

DISCUSSION

Penetrating keratoplasty is currently the only possible way out for many corneal diseases. One of such conditions is keratoconus at advanced stages with changes in all corneal layers (Amsler-Krumeich classification 1998). Others include such urgent conditions as corneal ulcers with perforation [12].

It was established that PK makes it possible to obtain transparent engraftment in 93% with 60% stability.

Annual reports from the Jordan Eye Bank show that in Jordan, a country that is endemic for keratoconus, the number of PK operations has increased. This is due to an increased number of corneal donors, which has shortened the queue for this medical care [13].

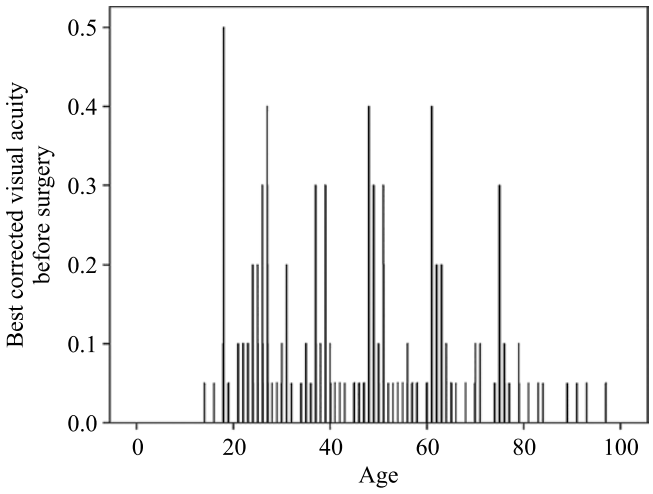

Fig. 1. Comparative characteristics of the best corrected visual acuity before penetrating keratoplasty in different age groups

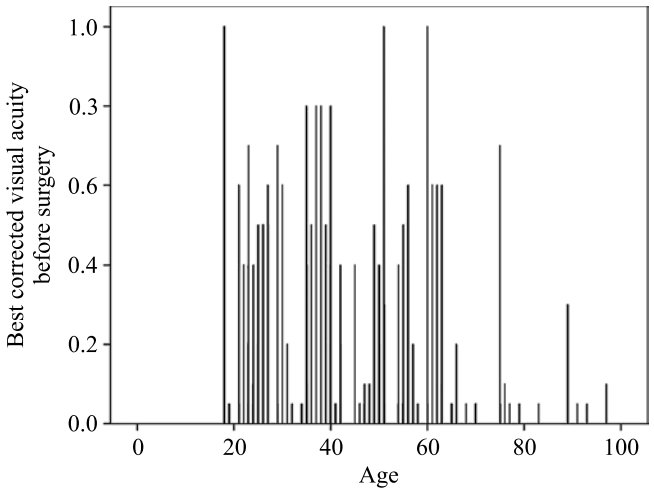

Fig. 2. Comparative characteristics of the best corrected visual acuity after penetrating keratoplasty in different age groups

Moreover, in two parallel independent studies by Gharaibeh et al. and Altay et al., it was noted that the most common indication for corneal transplantation was keratoconus, which is fully consistent with our study – 72.3% [14, 9]. According to Yorston et al., PK can also be a method for treating keratoconus and various corneal dystrophies in Africa [15].

Our data showed that PK is a highly efficient method in various corneal conditions. This has been justified by the significant improvement in visual acuity by 3 times from 0.08 to 0.25. These data quite correlate with the results obtained by Viera et al. from the University Hospital, São Paulo, Brazil, showing that PK is the gold standard for surgical treatment of keratoconus [16].

CONCLUSION

Keratoconus is the most common indication for PK in Jordan, accounting for 72.3%. PK is an effective method for treating various corneal diseases, improving visual acuity significantly. Eye care practice in Jordan provides a high percentage of corneal transplants, due to availability of donor material and qualified specialists.

The authors declare no conflict of interest.

REFERENCES

1. *Burton M.* Corneal Blindness; Prevention, treatment, and rehabilitation. *Comm Eye Health*. 2009; 22: 33–35. Retrieved from http://www.cehjournal.org/wpcontent/uploads/corneal-blindness.pdf.
2. *Oliva MS, Schottman T, Gulati M.* Turning the tide of corneal blindness. *Indian J Ophthalmol*. 2012 Sep-Oct; 60: 423–427. doi: 10.4103/0301-4738.100540.
3. *Koplin RS, Wu EI, Ritterband DC, Seedor JA.* Corneal Transplantation: Penetrating Keratoplasty. In The Scrub's Bible. New York, NY: Springer, 2013. doi: https://doi.org/10.1007/978-1-4614-5644-5_26.
4. *Zirm EK.* Eine erfolgreiche totale keratoplastik (A successful total keratoplasty). *Refract Corneal Surg.* 1906; 5 (4): 258–261.
5. *Zare M, Javadi MA, Einollahi B, Karimian F, Rafie AR, Feizi S, Azimzadeh A.* Changing indications and surgical techniques for corneal transplantation between 2004 and 2009 at a tertiary referral center. *Middle East Afr J Ophthalmol*. 2012; 19: 323–329. doi: 10.4103/0974-9233.97941.
6. *Tan DT, Janardhanan P, Zhou H, Chan YH, Htoon HM, Ang LP, Lim LS.* Penetrating keratoplasty in Asian eyes: the Singapore Corneal Transplant Study. *Ophthalmology*. 2008; 115: 975–982. doi: 10.1016/j.ophtha.2007.08.049.
7. *Zhang C, Xu J.* Indications for penetrating keratoplasty in East China, 1994–2003. *Graefes Arch Clin Exp Ophthalmol*. 2005; 243: 1005–1009. doi: 10.1007/s00417-005-1167-0.
8. *Majander A, Kivelä TT, Krootila K.* Indications and outcomes of keratoplasties in children during a 40-year period. *Acta Ophthalmol*. 2016; 94: 618–624. doi: 10.1111/aos.13040.
9. *Altay Y, Burcu A, Aksoy G, Ozdemir ES, Ornek F.* Changing indications and techniques for corneal transplantations at a tertiary referral center in Turkey, from 1995 to 2014. *Clin Ophthalmol*. 2016; 10: 1007–1013. doi: 10.2147/OPTH.S102315.
10. *Flores VG, Dias HL, de Castro RS.* Penetrating keratoplasty indications in "Hospital das Clínicas-UNICAMP". *Arq Bras Oftalmol*. 2007; 70: 505–508. doi: 10.1590/s0004-27492007000300020.
11. *Trufanov SV, Subbot AM, Malozhen SA, Krakhmaleva DA, Salovarova EP*. Corneal Graft Rejection after Keratoplasty. *Ophthalmology in Russia*. 2017; 14 (3): 180–187. [In Russ, English abstract]. doi: 10.18008/1816-5095-2017-3-180-187.
12. *Krumeich JH, Daniel J, Knulle A*. Live-epikeratophakia for keratoconus. *J Cataract Refract Surg*. 1998; 24: 456–463. doi: 10.1016/s0886-3350(98)80284-8.
13. www.eyebank.com.jo [Internet]. Jordan, Amman: Jordan Eye Bank, [cited 2019 Oct 9]. Available from: http://www.eyebank.com.jo/.
14. *Gharaibeh A, Atasi M, Alfoqahaa M, AbuKhader I*. Visual outcome of allogenic penetrating keratoplasty. *Jordan Med J*. 2017; 51 (4): 147–157. https://journals.ju.edu.jo/JMJ/article/view/100898.
15. *Yorston D, Wood M, Foster A*. Penetrating keratoplasty in Africa: graft survival and visual outcome. *Br J Ophthalmol*. 1996; 80: 890–894. doi: 10.1136/bjo.80.10.890.
16. *Vieira Silva J, Júlio de Faria e Sousa S, Mafalda Ferrante A.* Corneal transplantation in a developing country: problems associated with technology transfer from rich to poor societies. *Acta Ophthalmol Scand*. 2006; 84: 396–400. doi: 10.1111/j.1600-0420.2006.00663.x.

The article was submitted to the journal on 26.12.2019

DOI: 10.15825/1995-1191-2020-4-69-74

CLINICAL COURSE AND APPROACHES TO THERAPY IN KIDNEY TRANSPLANT RECIPIENTS WITH THE NOVEL COVID-19 DISEASE

O.N. Kotenko[1], L.Yu. Artyukhina[1], N.F. Frolova[1], E.S. Stolyarevich[1–3]

[1] Moscow City Hospital 52, Moscow, Russian Federation
[2] Evdokimov Moscow State University of Medicine and Dentistry, Moscow, Russian Federation
[3] Shumakov National Medical Research Center of Transplantology and Artificial Organs, Moscow, Russian Federation

The COVID-19 pandemic has had global consequences due to the wide spread of the infection in the world, lack of currently proven effective therapy, resistance to treatment in a significant proportion of those affected and, as a result, high mortality, especially among high-risk groups. Kidney transplant recipients with coronavirus-induced pneumonia are among the most problematic categories of patients. This patient cohort experiences a severe form of the disease, taking into account a combination of risk factors, such as long-term immunosuppression, comorbid background of patients, and consequences of chronic kidney disease. Difficulties in the management of recipients with COVID-19 are also down to the limitation of the use of drugs due to adverse drug-drug interactions. **Objective:** to analyze the course of COVID-19 disease in organ recipients, to assess the factors influencing the prognosis of the disease, and to optimize approaches to treatment of these patients. **Materials and methods.** During the period from April 15, 2020 to June 15, 2020, 68 people (38 men and 30 women) were hospitalized at our clinic. Their average age was 49.7 ± 9.2 years (22 to 70 years). COVID-19 diagnosis was verified by PCR. Multispiral computed tomography (MSCT) scans showed that in all cases, there were characteristic lung lesions of varying degrees of severity. **Results.** Out of the 68 people treated, 61 (89.8%) were discharged with recovery, 7 patients died. So, the mortality rate was 10.2%. This indicator did not depend on age and gender. First of all, mortality depended on the severity of lung lesions: at CT4 it was 43% (3/7), at CT3 – 11.1% (4/36), there were no deaths in patients with CT2. There was a 100% mortality among patients who received mechanical ventilation. Severity of graft dysfunction was also an important prognostic factor: with moderate dysfunction, this indicator was 8% (5/63), while with severe dysfunction it was 40% (2 out of 5). Besides, a more severe prognosis was observed in patients in the early post-transplant period: 5 patients out of the 7 who died of COVID-19 (71%) lived for less than a year after kidney allotransplantation (ATP). Mortality in this category of patients was 24%, while in the period from 1 to 5 years, this indicator was 13.6%; no deaths were recorded among patients with a period of over 5 years after ATP. All patients received antibacterial (levofloxacin or azithromycin) and antiviral (hydroxychloroquine) therapy. In all cases, the baseline immunosuppressive therapy (IST) was changed, including withdrawal of mycophenolic acid preparations, minimization of the calcineurin inhibitor dose (target concentration 1.5–3 ng/mL for tacrolimus and 30–50 ng/mL for cyclosporine), and increase in prednisolone dose by 5 mg relative to the current one. About 78% of cases received pathogenetic therapy with anti-interleukin monoclonal antibodies (mainly tocilizumab). These patients also received intravenous immunoglobulin at 10 g average dose. In severe COVID-19 accompanied in by clinical and laboratory signs of thrombotic microangiopathy 22% of cases, plasma exchange sessions and/or infusion of fresh frozen plasma and dose adjustment of low molecular weight heparins were performed. **Conclusion.** COVID-19-induced pneumonia in kidney transplant recipients is characterized by a high risk of progressive lung damage and respiratory failure. Mortality in COVID-19 is independent of gender and age, but correlates with post-transplantation period, severity of pneumonia, and severity of graft dysfunction. The need for mechanical ventilation is associated with an extremely unfavorable prognosis of the disease.

Keywords: COVID-19, pneumonia, kidney allotransplantation, kidney graft.

INTRODUCTION

The new coronavirus infection of 2019 COVID-19 (SARS-CoV-2) has been declared a pandemic [2] and has had global consequences due to the widespread infection worldwide, lack of currently proven effective therapy, and resistance to treatment among a large proportion of the patients and, as a result, high mortality rate worldwide. The most serious threat from COVID-19 is in the high-risk patients. One of the most problematic categories of patients is renal transplant recipients with

Corresponding author: Lyudmila Artyukhina. Address: 3, Pekhotnaya str., Moscow, 123182, Russian Federation. Phone: (916) 882-42-21. E-mail: arlyu-1404@yandex.ru

coronavirus pneumonia. It is assumed that immunosuppression worsens the course of the disease, exacerbating the severity of the process, and it is characterized by rapid progression of viral infection to pneumonia in organ transplant recipients. Optimal therapeutic approaches have not yet been developed. This remains a pressing issue and the subject of discussions by various specialists. The severity of prognosis of the disease in this patient cohort also depends on pronounced comorbid background (diabetes mellitus, arterial hypertension, cardiovascular disease, consequences of chronic kidney disease and pathogenetic therapy) in the vast majority of kidney transplant recipients. Difficulties in the management of transplant recipients with COVID-19 are also due to the limitation of the use of drugs as a result of adverse drug-drug interactions.

Currently, large-scale studies on the follow-up for this group of patients are lacking and are limited to registration of a series of cases at various clinics. According to the largest series reported to date in Europe and the United States, mortality ranged from 23% to 28% [1, 5–8], versus 5% mortality in the general population of patients infected with COVID-19 [5], and higher than the COVID-19 mortality among hospitalized severe non-transplant patients, which is 21% [9]. Interestingly, none of the series reported acute rejection and graft loss as a result of reduced immunosuppression [1, 5–8]. Various immunosuppressive therapy management strategies, based on stepwise reduction of immunosuppression depending on the severity of the disease, have been presented in reports.

The main pathogenetic mechanism of severe lung injury and development of a "cytokine storm" is attributed to a maladaptive immune response, which is particularly important in immunocompromised transplant patients. Treatment for COVID-19 is based on antiviral drugs that inhibit SARS-CoV-2 proliferation and on immunomodulatory drugs that inhibit the "cytokine storm" causing acute respiratory distress syndrome (ARDS) and life-threatening respiratory failure [3, 4]. Tocilizumab is currently the most popular treatment used to counteract hyperinflationary syndrome causing respiratory compromise [1, 10]. Also, vascular endothelial cell injury, which may be the cause of thrombotic microangiopathies (TMA), has recently received increasing attention in pathogenesis. In this regard, there are more and more publications on the use of plasma exchange, plasma infusions and eculizumab in the treatment of severe cases of COVID-19 complicated by TMA [11–14].

Our study was aimed at studying the characteristics of inpatient management of kidney transplant recipients with pneumonia caused by SARS-CoV-2. In this study, we included hospitalized renal transplant recipients with verified new coronavirus infection, pneumonia (PCR, MSCT). The aim of the study was to analyze the course of COVID-19 in organ transplant recipients, to assess the factors affecting the prognosis of the disease, and to optimize treatment approaches for these patients.

MATERIALS AND METHODS

From April 15, 2020 to June 15, 2020, 68 people (38 men and 30 women) were treated in our hospital. The mean age was 49.7 ± 9.2 years (22 to 70 years).

The post-kidney ATP period varied widely (from 1.5 months to 24 years) and averaged 62.6 ± 72.7 months. In 21 people (30.9%), the post-kidney ATP period did not exceed 1 year (13 of them had just a 3-month period). It ranged from 1 to 5 years, 5 to 10 years and over 10 years for 22 patients (32%), 14 patients (20.5%) and 11 patients (16%) respectively.

The majority of patients, 63 of 68 (92.6%), had moderate graft dysfunction not exceeding 200 μmol/L at the time of hospitalization. Dysfunction was severe (more than 400 μmol/L) in 5 (7.4%) cases and required renal replacement therapy. Plasma creatinine levels averaged 168.6 ± 92.7 μmol/L.

Immunosuppressive therapy (IST) at the time of hospitalization included prednisolone, mycophenolic acid preparations and calcineurin inhibitors (tacrolimus 91%, cyclosporine 9%). COVID-19 diagnosis was verified by PCR. MSCT revealed characteristic lung lesions of varying severity in all cases: CT grade 2 was diagnosed in 25 patients (37%); CT grade 3 in 36 patients (53%), and CT grade 4 in 7 patients (10%). Patients with CT grades 3 and 4 had progressive respiratory insufficiency and needed oxygen support.

The duration of hospitalization varied from 8 to 31 days, averaging 14.1 ± 5.9 days.

RESULTS

Of the 68 people, 61 (89.8%) recovered and were discharged, 7 patients died. The mortality rate was 10.2%. This indicator did not depend on age and sex. First of all, mortality depended on the severity of pulmonary involvement: 43% (3/7) CT4 and 11.1% (4/36) CT3 patients died. There were no deaths among CT2 patients (Fig. 1). Among the patients on mechanical ventilation, the mortality rate was 100%.

Severity of graft dysfunction was also an important prognostic factor: 8% (5/63) in moderate dysfunction against 40% (2/5) in severe dysfunction. During hospitalization, 20 patients with moderate dysfunction developed acute renal injury, followed by restoration of graft function to baseline in 15 cases out of 20, while 5 cases of progressive dysfunction within the framework of multiple organ failure ended in death. The average creatinine level at the time of hospitalization was 222.3 ± 118.4 μmol/L (median 185 μmol/L), which turned out to be significantly higher than in those who recovered (401.3 ± 291.8 μmol/L (median 322 μmol/L) (Fig. 2)

In addition, a more severe prognosis was observed in patients in the early post-kidney ATP period: in 5 out

of 7 patients who died from COVID-19 (71%), the post-kidney ATP period was less than a year. So, the mortality rate in patients in the early stages after kidney ATP (less than 12 months) was 24% (of the total number of treated patients). In the period from 1 to 5 years, mortality was 13.6%. There were no deaths among patients whose post-kidney ATP period was more than 5 years (Fig. 3). However, for more than 10 years, there were more often severe bacterial complications after COVID-19, which is probably due to long-term immunosuppression.

Based on the experience of our center, we developed an internal protocol for the treatment of kidney transplant recipients with COVID-19.

In all cases, the baseline immunosuppressive therapy (IST) was changed, including withdrawal of mycophenolic acid preparations, minimization of the dose of calcineurin inhibitors (target concentration of 1.5–3 ng/mL for tacrolimus and 30–50 ng/mL for cyclosporine), and increasing prednisolone dose by 5 mg relative to the current dosage.

During hospitalization, it was noteworthy that 30% of patients showed high tacrolimus levels against a background of usual dosages of the drug. At the same time, only half of them had diarrhea. In the remaining 15%, increased tacrolimus levels did not correlate with diarrheal syndrome. In 12% of patients, temporary withdrawal of calcineurin inhibitors was required (for 2–3 days).

All patients were prescribed antibiotic therapy: initial therapy with levofloxacin or azithromycin, with subsequent adjustment depending on the effectiveness of therapy and data from microbiological studies.

In all cases, antiviral therapy was also given: hydroxychloroquine in doses adjusted for renal function. In patients with a cardiac history and existing cardiac arrhythmias, hydroxychloroquine was administered without a loading dose.

We did not use ritonavir/lopinavir in renal transplant recipients due to adverse drug interactions with the main IST drugs (tacrolimus, cyclosporine).

Pathogenetic therapy with anti-interleukin monoclonal antibodies was administered in 53 patients (78%). Of these, 38 patients (72%) received tocilizumab, 8 (15%) received sarilumab, 5 (9%) were administered with canakinumab, while 2 (4%) got netakimab. At the same time, the tocilizumab dose was reduced taking into account the ongoing baseline immunosuppressive therapy. In most cases (79.5%), the dose did not exceed 200 mg. In 14 patients (20.5%), the dose ranged from 240 to 600 mg. The choice of a drug, dose and additional administration was determined based on the severity of the clinical, laboratory and X-ray picture.

Also, intravenous immunoglobulin (average dose 10 g) was administered in all patients in order to correct their immunological status.

In a number of patients (22%), mostly with severe COVID-19, there were clinical and laboratory signs of

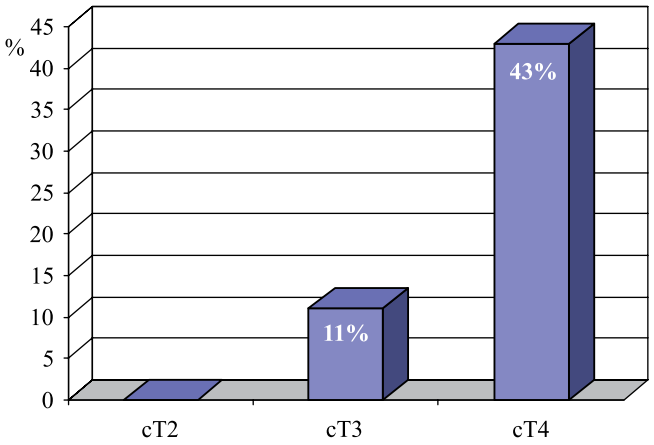

Fig. 1. Mortality depending on the severity of pulmonary involvement

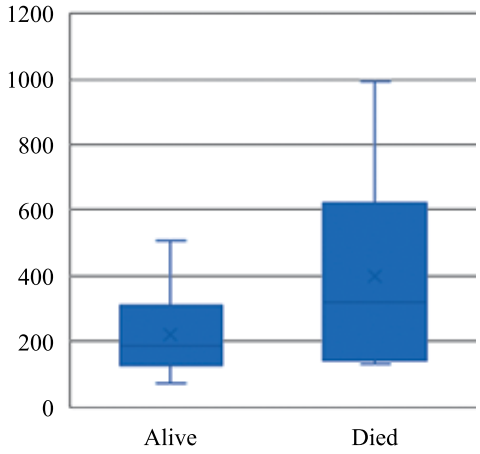

Fig. 2. Creatinine levels in surviving and deceased COVID-19 patients

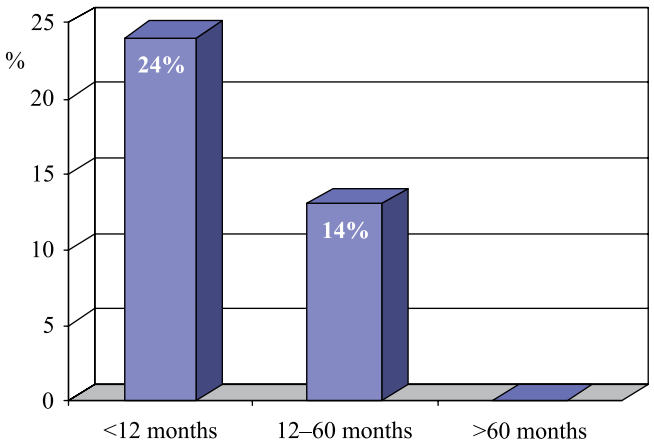

Fig. 3 Mortality depending on the post-kidney ATP period

thrombotic microangiopathy (anemia, thrombocytopenia, increased lactate dehydrogenase (LDH), D-dimer, organ ischemic disorders). Therefore, sessions of plasma exchange and/or FFP infusion were carried out as a pathogenetic therapy. The dose of low molecular weight heparin (LMWHs) was also adjusted. Against this back-

ground, regression of secondary TMA manifestations was observed in the majority of patients.

CONCLUSION

COVID-19-induced pneumonia is characterized by a high risk of progressive lung injury and respiratory failure. Mortality in COVID-19 does not depend on sex and age. However, it correlates with the post-transplant period, severity of pneumonia and severity of graft dysfunction. Transfer to mechanical ventilation is associated with an extremely unfavorable prognosis of the disease. The following categories of patients presented the greatest difficulty for management: patients in the early period after kidney ATP and patients with severe graft dysfunction due to a high risk of death, as well as patients with a post-transplantation period of more than 10 years due to a high risk of complications on the background of prolonged immunosuppressive therapy and severe comorbidity.

According to our experience in managing this patient cohort, COVID-19 therapy includes mandatory minimization of IST, and in moderate to severe course – administration of anti-interleukin drugs and immunoglobulin. If signs of secondary TMA appear, the use of plasma exchange and/or FFP infusion becomes effective. As in the general population, the use of LMWHs is recommended in renal transplant recipients. Thus, COVID-19 in renal transplant recipients is characterized by a greater severity of the infectious and inflammatory process against the background of immunosuppressive therapy compared to the general population of patients, frequent renal transplant dysfunction, and unstable levels of baseline immunosuppressants. Taking this into account, it is not advisable to use drugs that have pronounced interaction with baseline immunosuppressants (calcineurin inhibitors).

At present, the question on approaches to COVID-19 treatment in renal transplant recipients remains open and requires further study.

The authors declare no conflict of interest.

REFERENCES

1. How should I manage immunosuppression in a kidney transplant patient with COVID-19? An ERA-EDTA DESCARTES expert opinion. *Nephrol Dial Transplant*. 2020; 35: 899–904. doi: 10.1093/ndt/gfaa130 Advance Access publication 22 May 2020.
2. *Cucinotta D, Vanelli M*. WHO declares COVID-19 a pandemic. *Acta Biomed*. 2020; 91: 157–160.
3. *Barlow A, Landolf KM, Barlow B et al.* Review of emerging pharmacotherapy for the treatment of coronavirus disease 2019. *Pharmacotherapy*. 2020. doi: 10.1002/phar.2398.
4. *Sanders JM, Monogue ML, Jodlowski TZ et al.* Pharmacologic treatments for coronavirus disease 2019 (COVID-19): a review. *JAMA*. 2020. doi: 10.1001/jama.2020.6019.
5. *Akalin E, Azzi Y, Bartash R et al.* Covid-19 and kidney transplantation. *N Engl J Med*. 2020. doi: 10.1056/NEJMc2011117.
6. *Pereira MR, Mohan S, Cohen DJ et al.* COVID-19 in-solid organ transplant recipients: initial report from the US epicenter. *Am J Transplant*. 2020. doi: 10.1111/ajt.15941.
7. *Fernandez-Ruiz M, Andres A, Loinaz C et al.* COVID-19 in solid organ transplant recipients: a single-center case series from Spain. *Am J Transplant*. 2020. doi: 10.1111/ajt.15929.
8. *Alberici FD, Delbarba E, Manenti C et al.* A single center observational study of the clinical characteristics and short-term outcome of 20 kidneytransplant patients admitted for SARS-CoV2 pneumonia. *Kidney Int*. 2020. doi: 10.1016/j.kint.2020.04.002.
9. *Richardson S, Hirsch JS, Narasimhan M et al.* Presenting characteristics, comorbidities, and outcomes among 5700 patients hospitalized with COVID-19 in the New York City area. *JAMA*. 2020. doi: 10.1001/jama.2020.6775.
10. *Zhang C, Wu Z, Li JW et al.* The cytokine release syndrome (CRS) of severe COVID-19 and Interleukin-6 receptor (IL-6R) antagonist tocilizumab may be the key to reduce the mortality. *Int J Antimicrob Agents*. 2020. doi: 10.1016/j.ijantimicag.2020.105954.
11. Application of plasma exchange in association with higher dose CVVH in Cytokine Storm Complicating COVID-19. *Journal of the Formosan Medical Association.* 2020; 119: 1116e1118.
12. *Risitano AM, Mastellos DC, Huber-Lang M, Yancopoulou D, Garlanda C, Ciceri F, Lambris JD.* Complement as a target in COVID-19? *Nat Rev Immunol*. 2020 Jun; 20 (6): 343–344.
13. *Diurno F, Numis FG, Porta G*. Eculizumab treatment in patients with COVID-19: preliminary results from real life ASL Napoli 2 Nord experience. *European Review for Medical and Pharmacological Sciences*. 2020; 24: 4040–4047.
14. *Keith P, Day M, Perkins L, Moyer L, Hewitt K, Wells A.* A novel treatment approach to the novel coronavirus: an argument for the use of therapeutic plasma exchange for fulminant COVID-19. *Critical Care*. 2020; 24: 128. https://doi.org/10.1186/s13054-020-2836-4.

The article was submitted to the journal on 27.10.2020

DOI: 10.15825/1995-1191-2020-4-75-82

J-SHAPED STERNOTOMY IN AORTIC VALVE REPAIR AND ASCENDING AORTA REPLACEMENT. SHORT-TERM RESULTS

G.A. Akopov, A.S. Ivanov, T.N. Govorova, D.V. Moskalev

Shumakov National Medical Research Center of Transplantology and Artificial Organs, Moscow, Russian Federation

Objective: to evaluate the short-term outcomes of surgical treatment of aortic valve and ascending aorta defects performed through mini-sternotomy using normothermic cardiopulmonary bypass and hyperkalemic cardioplegia via Calafiori technique from May 8, 2019 to May 14, 2020. **Materials and methods.** The study enrolled 80 patients with isolated aortic valve disease and combined pathology of the aortic root and ascending aorta. It lasted from May 8, 2019 to May 14, 2020. The patients were divided into two groups: Group 1 included 30 patients in whom the upper median J-shaped sternotomy was applied as an access, while Group 2 consisted of 50 patients in whom standard median sternotomy was used as an access. The patients consisted of 43 (53.7%) males and 37 (46.3%) females; the average age was 55.1 ± 11.6 years. All patients were examined before surgery. There were no statistically significant differences between the two groups. **Results.** Group 2 had a 30-day mortality of 2% (n = 1) due to the development of acute heart failure against the background of heart rhythm disturbances. One patient in this group had a late mortality due to acute cerebrovascular accident occurring a month after discharge, which corresponded to 2% (n = 1). There were no deaths in Group 1. In Group 1, there were two conversions (6.7%) to longitudinal median sternotomy. In the first case, it was not possible to restore heart rhythm through repeated defibrillator discharges from mini-sternotomy access due to the presence of an adhesive process in the pericardial cavity. In the second case, ligation of the right internal thoracic artery was required after sternal wire sutures. Artificial ventilation (AV) lasted for 170.9 ± 70.2 minutes in Group 1 and 358.2 ± 169.5 minutes in Group 2. Cardiac activity was independently restored in 23 patients (77%) in Group 1, and in 12 (24%) in Group 2 ($p < 0.001$). Intraoperative blood loss was 400 ± 150 mL and 850 ± 150 mL ($p < 0.05$) in Group 1 and Group 2, respectively. In the early postoperative period, it was 200 ± 150 mL in Group 1 and 350 ± 150 mL in Group 2. The length of stay at the intensive care unit and the duration of intensive therapy did not exceed 1 day in both groups. In the early postoperative period, 4 patients in Group 1 (13%) and 27 patients in Group 2 (54%) needed inotropic support ($p < 0.001$). The need for painkillers and non-steroidal anti-inflammatory drugs was within 3–4 days in Group 1 and 8–10 days in Group 2. In-hospital postoperative period varied from 10 to 16 days in both groups, depending on the severity of the initial condition, presence of concomitant diseases and the need to select an adequate anticoagulant dose. The patients were discharged in satisfactory condition under the supervision of a cardiologist at their homes. There were no inflammatory complications in the access area in both groups during their in-hospital stay. Among the complications in the mid-term postoperative period, two months after discharge, mediastinitis was observed in Group 2. The patient was re-hospitalized, after a course of antibiotic therapy which resolved the mediastinitis; sternal osteosynthesis was performed. **Conclusion.** Based on the study, it has been shown that this technique reduces the duration of mechanical ventilation, ensures early extubation, decreases blood loss, and, accordingly, ensures the use of replacement therapy, chest stability and a better cosmetic effect. It should be noted that there was no mortality and sternal complications in the patient group with a minimally invasive approach.

Keywords: minimally invasive surgery, aortic surgery, aortic valve, mini-sternotomy.

Despite the first successful minimally invasive aortic valve replacement surgery performed in Cleveland in 1996 by Cosgrove and Sabik [1], longitudinal median sternotomy remains the main standard approach among cardiac surgical access techniques. In May 1997, at the 1st World Congress on Minimally Invasive Cardiac Surgery in Paris, it was decided that the main goal of minimally invasive surgery is to reduce the number of predicted complications and accelerate patient recovery, provided that the effectiveness of surgical treatment and the duration of therapeutic effect are maintained. In Russia, the first aortic valve replacement through the upper mininotomy was performed in October 1997 by L.A. Bockeria [2].

Some of the main advantages of minimally invasive techniques after surgery over the conventional access include reduced traumatic nature of surgical intervention, superior cosmetic results, reduced pain in the postope-

Corresponding author: Tuiaara Govorova. Address: 1, Shchukinskaya str., Moscow, 123182, Russian Federation. Phone: (985) 852-30-17. E-mail: tuyagov@inbox.ru

rative period, and possibility of early patient activation due to thoracic stability, which leads to shorter hospital stay [3].

Studies have shown that the minimally invasive technique provides reduced pain, lower number of sternal complications, respiratory disorders due to thoracic stability and preservation of the integrity of the diaphragmatic attachment to the chest wall, reduced blood loss and transfusions, and shorter hospital stay. There was also a decrease in the incidence of atrial fibrillation, myocardial infarction and strokes in the postoperative period [3–22]. In 2017, German colleagues reported on their experience, which showed that upper sternotomy during aortic arch surgery does not increase the risk of complications and mortality [3]. The Swiss Cardiac Surgery Guidelines, published in February 2020, reported that, when compared with the conventional access, minimally invasive aortic valve surgery reduces postoperative mortality and complications [23].

Most revealing is the data provided by T.A. Rayner et al. In January 2020, the results of a comparative meta-analysis based on online databases Medline, EMBASE, Cochrane Library and Web of Science, were published. The meta-analysis included 1101 patients with minimally invasive aortic surgery and 1405 patients with standard median sternotomy from thirteen published studies. The confidence level in all previously reported results remains very low. Mortality and incidence of stroke were similar between the 2 cohorts. Meta-analysis demonstrated increased length of cardiopulmonary bypass (CPB) time, more time in hospital and intensive care among patients undergoing standard median sternotomy compared with minimally invasive surgery of the aortic root and ascending aorta. This group also had higher risks of bleeding and renal impairment [24].

To reduce the risk of surgery, patients with concomitant coronary artery disease can be offered two-stage operations using endovascular surgery [8]. The success of minimally invasive surgery also depends on individual selection of patients. The patient's specific anatomical and pathophysiological characteristics, as well as the experience of the surgical team in provision of adequate access and working in minimally invasive conditions should be taken into account.

This technique has its disadvantages: the need (in some cases) for the use of peripheral cannulation for CPB, internal thoracic artery injury, as well as cases of conversion to complete longitudinal median sternotomy [5].

Objective: to evaluate the short-term outcomes of surgical treatment of aortic valve and ascending aorta defects performed through mini-sternotomy using normothermic cardiopulmonary bypass and hyperkalemic cardioplegia via Calafiori technique from May 8, 2019 to May 14, 2020.

MATERIALS AND METHODS

The study enrolled 80 patients with isolated aortic valve disease and combined pathology of the aortic root and ascending aorta. It lasted from May 8, 2019 to May 14, 2020. The patients were divided into two groups: group 1 included 30 patients in whom the upper median J-shaped sternotomy was applied as an access – aortic valve prosthetics (15), aortic valve and ascending aortic prosthetics with a valve-containing conduit according to the Bentall-De Bono technique (1) and the Kouchoukos modifications (4), valve-preserving operations according to the David I (3) and the Florida Sleeve (1) techniques, supracoronary ascending aortic replacements (4), ascending aorta prosthetics with annuloplasty of the aortic annulus fibrosus (2). Group 2 consisted of 50 patients in whom standard median sternotomy was used as an access: aortic valve replacement (17), aortic valve and ascending aorta valve replacement with valve-containing conduit according to the Bentall-De Bono technique (4) and the Kouchoukos modifications (1), valve-preserving operations according to the David I (18) and Florida Sleeve (5) techniques, aortic valve leaflet repair (5).

There were 43 (53.7%) males and 37 (46.3%) females that underwent surgery. Their mean age was 55.1 ± 11.6 years.

Before surgery, all patients underwent standard examinations, including collection of complaints, medical history, physical examination, laboratory and imaging investigations (electrocardiography, echocardiography (EchoCG)), chest X-ray in direct projection, direct X-ray contrast-enhanced spiral CT). Preoperative evaluation revealed no statistically significant differences between the two groups.

Chest X-ray in direct projection and chest X-ray contrast-enhanced spiral CT help to determine the level of the aortic root location and its projection onto the sternum and intercostal space, which is the determining factor for choosing the level of the intercostal space when conducting a median J-shaped mini-sternotomy for planning the access length and predicting visualization of the aortic root and ascending aorta (Fig. 1, 2).

The skin incision was made longitudinally for 7–9 cm, departing from the sternum handle by 2–3 cm. The median J-shaped mininotomy, depending on the projection of the aortic root onto the sternum, was performed along the 3rd and 4th intercostal spaces in 13 (43%) and 17 (57%) patients, respectively (Fig. 3, 4).

After opening the pericardium, standard direct aortic cannulation and venous cannulation of the right atrial appendage were performed using a two-level cannula. The left heart was drained through the right superior pulmonary vein (Fig. 5).

Surgical interventions were performed under cardiopulmonary bypass in conditions of moderate hypothermia or normothermia at 34.1–36.2 °C temperature with

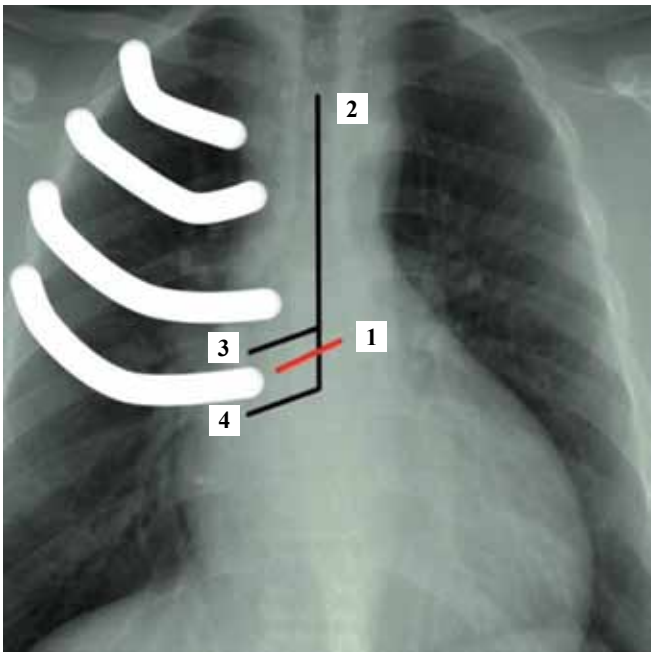

Fig. 1. Chest X-ray in a direct projection: (1) aortic root projection, (2) sternotomy line, (3) intersection of the sternum through the 3rd intercostal space, (4) intersection of the sternum through the 4th intercostal space. The white areas indicate the position of the ribs

selective introduction of blood hyperkalemic cardioplegia via Calafiori technique. A standard set of instruments, a small wound retractor and a defibrillator with small internal paddles were used.

All patients underwent surgical interventions under transesophageal echocardiography to assess myocardial contractility, fill the cardiac cavities, assess the adequacy of air embolism prevention and surgical treatment outcome.

When using a minimally invasive technique, ultrasound control is necessary to assess the location of the venous cannula in order to prevent impaired blood outflow in the CPB device, as well as to evaluate the correction performed (prosthetics or heart valve repair). Also, at the end of CPB, ultrasound assessment of the deaeration process and heart function is necessary, since direct visual monitoring of cardiac activity is impossible. Fig. 6 shows the final view after skin suturing. Fig. 7 shows X-ray contrast-enhanced spiral computed tomography with reconstruction of the aortic root and ascending aorta (a – before surgery, b – after reconstruction of the aortic root and ascending aorta according to the David I technique).

The peculiarity of using the mini-access is to effect drainage into the pericardial cavity and suture the electrode to the right ventricle for temporary stimulation before removing the clamp from the aorta, with an unfilled heart.

Air embolism was prevented by active drainage of the left heart and intraoperative injection of carbon dioxide into the pericardial cavity at 2 L/min. To prevent aeroembolism, the ascending aorta was additionally punctured.

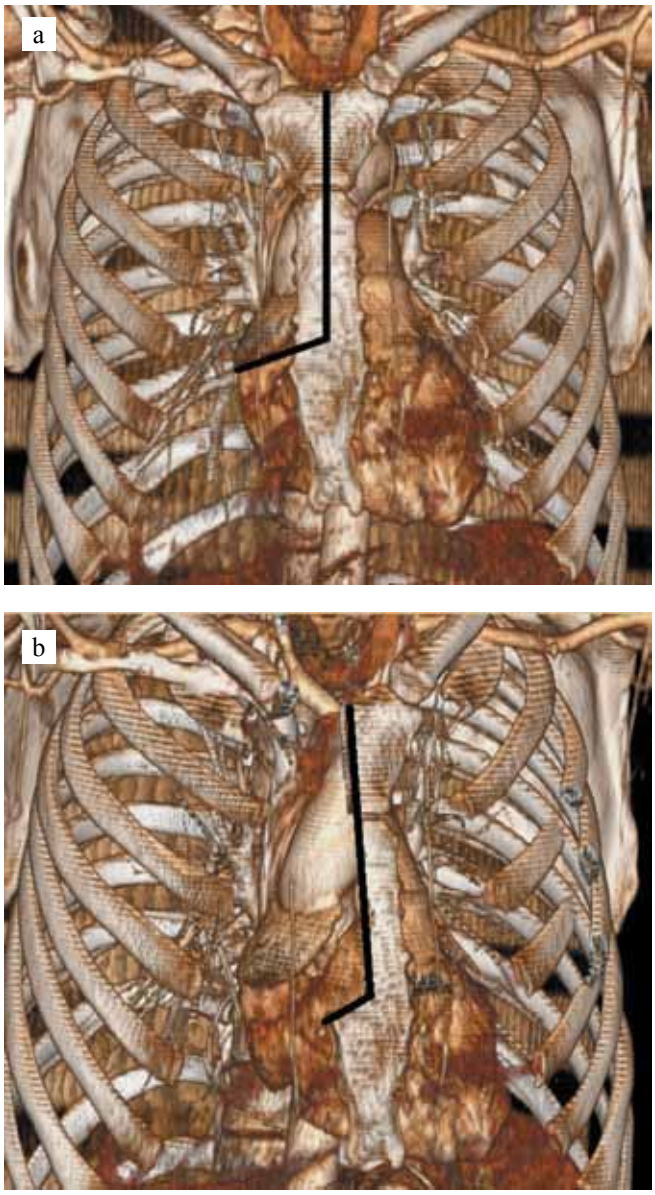

Fig. 2. X-ray contrast-enhanced spiral CT scan of the chest with a J-shaped access line. (a) the sternum is preserved, (b) a section of the sternum was removed along the cutting line, for the purpose of approximately visualizing the aortic root and ascending aorta

RESULTS

Thirty-day mortality in group 2 was 2% (n = 1) due to the development of acute heart failure amidst heart rhythm disturbances. Late mortality was also observed in group 2 in one patient due to stroke one month after discharge, corresponding to 2% (n = 1). There were no deaths in group 1.

In group 1, two patients underwent conversion to median longitudinal sternotomy – 6.7%. In the first case, it was not possible to restore rhythm with multiple defibrillator discharges from the ministerial access due to

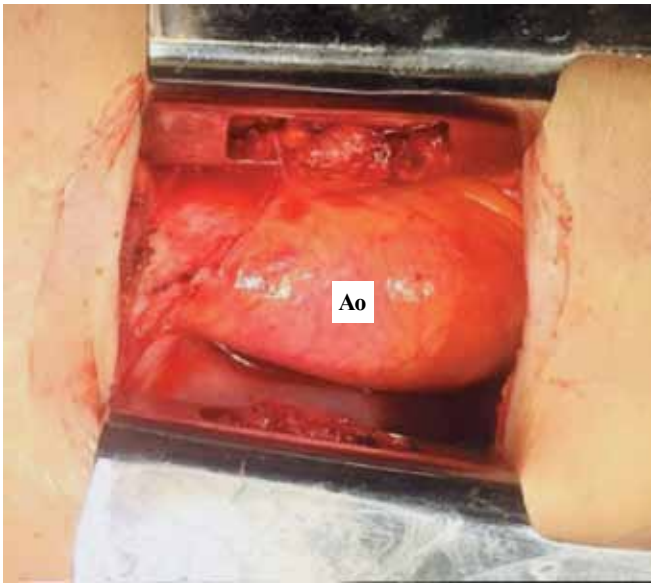

Fig. 3. Median J-shaped mini-sternotomy through the 3rd intercostal space. Optimal visualization of the aortic root and ascending aorta

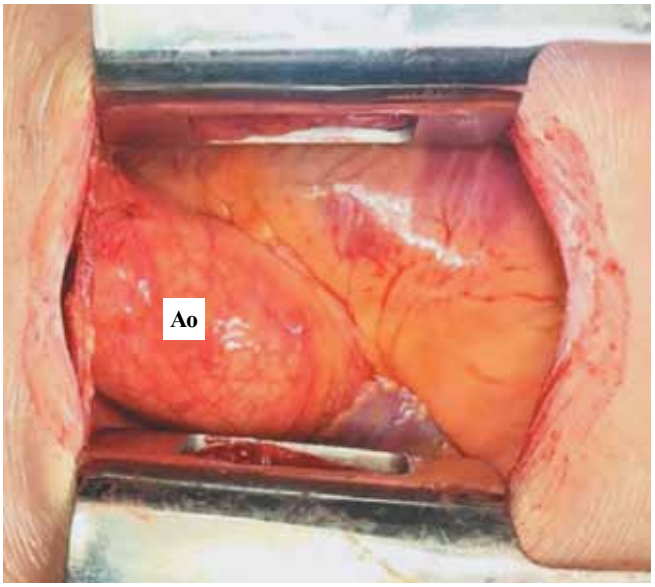

Fig. 4. Median J-shaped mini-sternotomy through the 4th intercostal space

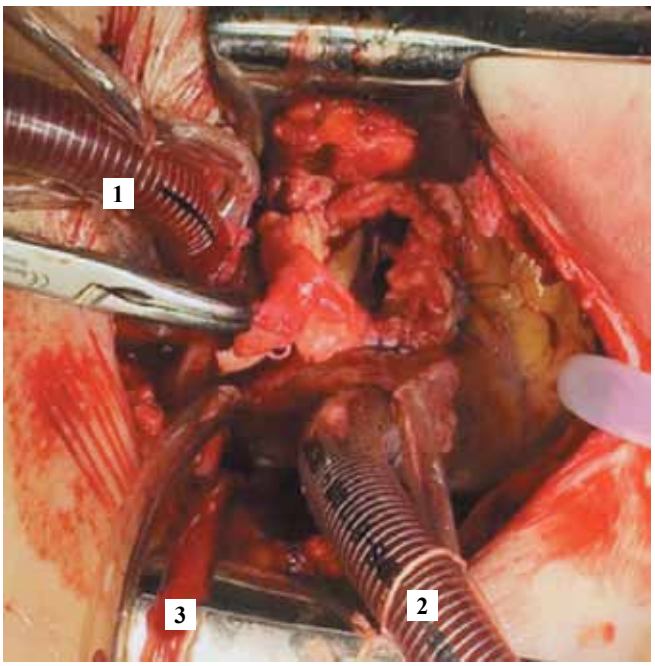

Fig. 5. (1) Central cannulation of the ascending aorta (2) and the right atrium (3) with the left cannula laid through the right superior pulmonary vein

Fig. 6. A 8.5-cm skin incision

adhesions in the pericardium. The second required ligation of the right internal thoracic artery after sternum stitching with wire sutures.

Artificial ventilation in group 1 and in group 2 lasted for 170.9 ± 70.2 minutes and 358.2 ± 169.5 minutes, respectively.

There was independent restoration of cardiac activity in 23 patients (77%) in group 1, and in 12 (24%) in group 2 ($p < 0.001$).

Intraoperative blood loss in group 1 and group 2 was 400 ± 150 mL and 850 ± 150 mL ($p < 0.05$), respectively. In the early postoperative period – 200 ± 150 mL and 350 ± 150 mL, respectively.

Length of intensive care among all patients in both groups did not exceed 1 day.

In the early postoperative period, 4 patients (13%) needed inotropic support in group 1, and 27 patients (54%) in group 2 ($p < 0.001$). The need for painkillers and non-steroidal anti-inflammatory drugs in group 1 and group 2 was within 3–4 days and 8–10 days, respectively.

In group 2, two patients (4%) required a second intervention due to sternal diastasis; sternal osteosynthesis was performed in the early postoperative period.

In-hospital postoperative period in both groups varied from 10 to 16 days, depending on severity of the initial

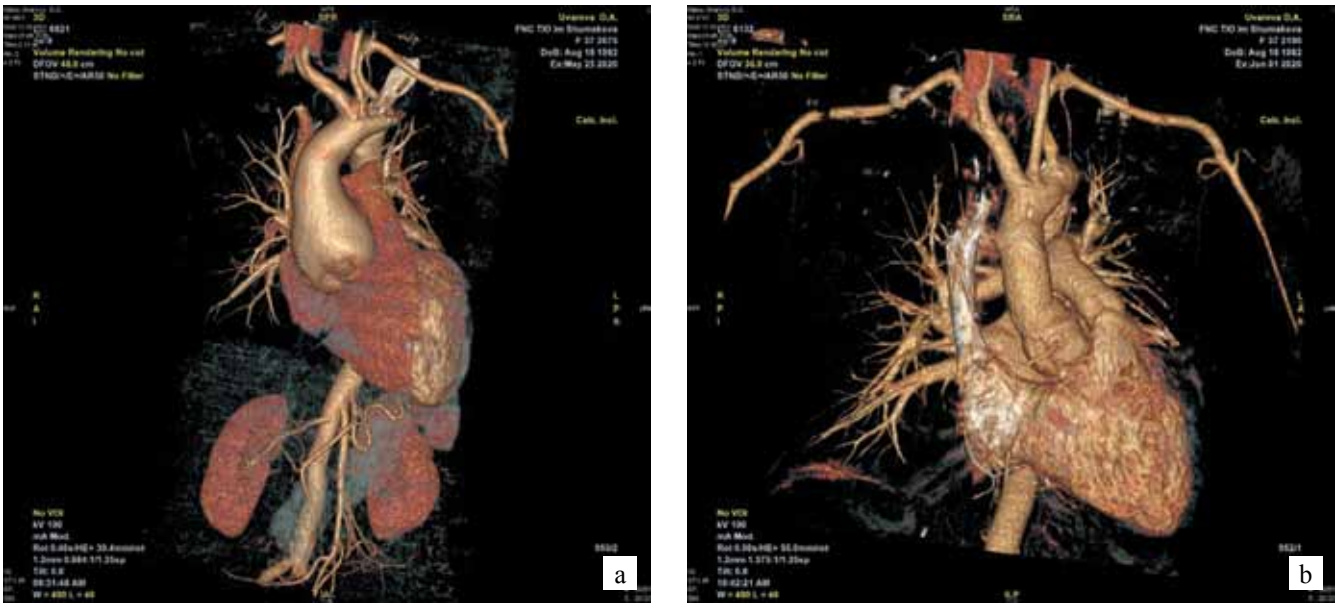

Fig. 7. X-ray contrast-enhanced spiral CT scan with reconstruction of the aortic root and ascending aorta: (a) before surgery, (b) after reconstruction of the aortic root and ascending aorta by the David I method

condition and presence of concomitant diseases and the need to select an adequate anticoagulant dose. The patients were discharged in satisfactory condition under the supervision of a cardiologist at their place of residence.

There were no inflammatory complications in the access area in both groups during the hospital period. Among the complications in the mid-term postoperative period, two months after discharge, mediastinitis was observed in group 2. The patient was re-hospitalized, after a course of antibiotic therapy with resolution of mediastinitis, sternal osteosynthesis was performed.

FINDINGS:

1. Median J-shaped mini-sternotomy is a safe and feasible approach to perform a full range of interventions on the aortic valve and ascending aorta, which provides adequate visualization to the aortic root and ascending aorta and partially to the right heart, while maintaining the integrity of the thoracic cage.
2. Mini-sternotomy, in contrast to the standard median sternotomy, showed reduced blood loss, earlier extubation, reduced need for inotropic support, absence of wound, infectious and other sternal complications, and absence of in-hospital mortality.
3. In planning the length of access and predicting adequate visualization of the aortic root and ascending aorta, chest X-ray contrast-enhanced spiral computed tomography should be performed.
4. Blood hyperkalemic cardioplegia by Calafiori technique is the preferred method of myocardial protection in surgical correction of aortic defect. Our experience shows that independent restoration of the rhythm was recorded in 77% of cases when this myocardial protection method was carried out.
5. Repeated interventions and pronounced adhesions can complicate heart rhythm restoration, increasing the likelihood of conversion to median sternotomy.

CONCLUSION

The technique reduces the duration of mechanical ventilation, ensures early extubation, reduced blood loss (and, accordingly, reduced use of replacement therapy), and provides thoracic stability and superior cosmetic results. Note that there was no mortality and sternal complications in the group of patients with a minimally invasive approach.

A better thoracic stability makes minimally invasive surgical access the first choice both in comorbid patients and in patients with high body mass index, and in high-risk patients in general.

A properly performed surgery shortens the operation time. This in turn reduces the cardiopulmonary bypass, myocardial ischemia, anesthesia and blood loss during operation.

We also agree with our colleagues about the need for a prospective randomized study in order to avoid possible erroneous conclusions from retrospective data.

The authors declare no conflict of interest.

REFERENCES

1. *Cosgrove DM 3rd, Sabik JF*. Minimally invasive approach for aortic valve operations. *Ann Thorac Surg*. 1996; 62: 596–597.
2. *Bokerija LA, Skopin II, Narsija BE, Sedov IN*. Minimal'no invazivnaja hirurgija priobretennyh poro-

kov serdca. *Grudnaja i serdechno-sosudistaja hirurgija*. 1999; 3: 4–7.
3. *Goebel N, Bonte D, Salehi-Gilani S, Nagib R, Ursulescu A, Franke UFW*. Minimally Invasive Access Aortic Arch Surgery. *Innovations (Phila)*. 2017 Sep/Oct; 12 (5): 351–355. doi: 10.1097/IM000000000000390.
4. *Fenton JR, Doty JR*. Minimally invasive aortic valve replacement surgery through lower half sternotomy. *J Thorac Dis*. 2013 Nov; 5 (Suppl 6): S658–S661. doi: 10.3978/j.iss072-1439.2013.09.22. PMCID: PMC3831833. PMID: 24251024.
5. *Klein P, Klop IDG, Kloppenburg GLT, van Putte BP*. Planning for minimally invasive aortic valve replacement: key steps for patient assessment. *Eur J Cardiothorac Surg*. 2018; 53: ii3–ii8. doi: 10.1093/ejcts/ezy086.
6. *Young CP, Sinha S, Vohra HA*. Outcomes of minimally invasive aortic valve replacement surgery. *Eur J Cardiothorac Surg*. 2018; 53: ii19–ii23. doi: 10.1093/ejcts/ezy186.
7. *Boix-Garibo R, Uzzaman MM, Bapat VN*. Review of Minimally Invasive Aortic Valve Surgery. *Interventional cardiology (London, England)*. 2015; 10 (3): 144–148. https://doi.org/10.15420/IC015.10.03.144.
8. *Paredes FA, Cánovas SJ, Gil O, García-Fuster R, Hornero F, Vázquez A et al*. Minimally Invasive Aortic Valve Surgery. A Safe and Useful Technique Beyond the Cosmetic Benefits. *Revista Española de Cardiología (English Edition)*. 2013; 66 (9): 695–699. doi: 10.1016/j.re013.02.013.
9. *Brown JM, O'Brien SM, Wu C et al*. Isolated aortic valve replacement in North America comprising 108,687 patients in 10 years: changes in risks, valve types, and outcomes in the Society of Thoracic Surgeons National Database. *J Thorac Cardiovasc Surg*. 2009; 137: 82–90.
10. *Gilmanov D, Bevilacqua S, Murzi M, Cerillo AG, Gasbarri T, Kallushi E et al*. Minimally invasive and conventional aortic valve replacement: a propensity score analysis. *Ann Thorac Surg*. 2013; 96 (3): 837–843.
11. *Yamada T, Ochiai R, Takeda J, Shin H, Yozu R*. Comparison of early postoperative quality of life in minimally invasive versus conventional valve surgery. *J Anaesth*. 2003; 17 (3): 171–176.
12. *Mihaljevic T, Cohn LH, Unic D, Aranki SF, Couper GS, Byrne JG*. One thousand minimally invasive valve operations: early and late results. *Ann Surg*. 2004; 240 (3): 529–534.
13. *Gilmanov D, Bevilacqua S, Murzi M, Cerillo AG, Gasbarri T, Kallushi E et al*. Minimally invasive and conventional aortic valve replacement: a propensity score analysis. *Ann Thorac Surg*. 2013; 96 (3): 837–843.
14. *Cheng DC, Martin J, Lal A, Diegeler A, Folliguet TA, Nifong LW et al*. Minimally invasive versus conventional open mitral valve surgery. A metaanalysis and systematic review. *Innovations (Phila)*. 2011; 6 (2): 84–103.
15. *Tabata M, Khalpey Z, Aranki SF et al*. Minimal access surgery of ascending and proximal arch of the aorta: a 9-year experience. *Ann Thorac Surg*. 2007; 84: 67–72.
16. *Brown ML, McKellar SH, Sundt TM et al*. Ministernotomy versus conventional sternotomy for aortic valve replacement: a systematic review and meta-analysis. *J Thorac Cardiovasc Surg*. 2009; 137: 670–679.e5.
17. *Gilmanov D, Solinas M, Farneti PA et al*. Minimally invasive aortic valve replacement: 12-year single center experience. *Ann Cardiothorac Surg*. 2015; 4: 160–169.
18. *Shehada SE, Öztürk Ö, Wottke M et al*. Propensity score analysis of outcomes following minimal access versus conventional aortic valve replacement. *Eur J Cardiothorac Surg*. 2016; 49 (2): 464–469; discussion 469–470.
19. *Charchyan ER, Breshenkov DG, Belov YuV*. Minimally invasive approach in thoracic aortic surgery: a single center experience. *Russ Jour of Card and Cardiovasc Surg. = Kard i serd-sosud khir*. 2019; 12 (6): 522–535. (In Russ.). https://doi.org/10.17116/kardio201912061522.
20. *Bakir I, Casselman FP, Wellens F, Jeanmart H, De Geest R, Degrieck I et al*. Minimally invasive versus standard approach aortic valve replacement: a study in 506 patients. *Ann Thorac Surg*. 2006; 81 (5): 1599–1604.
21. *Belov JuV, Stepanenko AB, Gens AP, Babaljan GV*. Protezirovanie aortal'nogo klapana iz mini-dostupa. *Vestnik hirurgii im. I.I. Grekova*. M., 1998; 157 (3): 47–49.
22. *Charchyan ER, Skvortsov AA, Panfilov VA, Belov YuV*. J-shaped mini-sternotomy for frozen elephant trunk procedure. *Kardiologija i serdechno-sosudistaja hirurgija*. 2017; 10 (1): 42–46. doi: 10.17116/kardio201710142-46.
23. *Glauber M, Miceli A*. Minimally Invasive Aortic Valve Surgery. *S. Raja (eds). Cardiac Surgery*. Springer, Cham. 2020 Feb; 12: 421–428. https://doi.org/10.1007/978-3-030-24174-2_46.
24. *Rayner TA, Harrison S, Rival P, Mahoney DE, Caputo M, Angelini GD et al*. Minimally invasive versus conventional surgery of the ascending aorta and root: a systematic review and meta-analysis. *European Journal of Cardio-Thoracic Surgery*. 2020 Jan; 57 (Issue 1): 8–17. https://doi.org/10.1093/ejcts/ezz177.

The article was submitted to the journal on 9.07.2020

DOI: 10.15825/1995-1191-2020-4-83-88

THE PROBLEM OF BIOCOMPATIBILITY AND THROMBOGENICITY IN MECHANICAL CIRCULATORY ASSIST DEVICES

M.O. Zhulkov, D.A. Sirota, A.V. Fomichev, A.S. Grenaderov, A.M. Chernyavsky
Meshalkin National Medical Research Center, Novosibirsk, Russian Federation

Patients suffering from end-stage congestive heart failure are in the severe category of cardiac patients. For many decades, there has been active development of circulatory assist devices. However, despite significant progress made in this area, the use of such devices is associated with several dangerous complications, one of which is thrombosis. The problem of creating biocompatible materials still remains unresolved. Analyzing the mechanism and risk of this complication allows to determine the ways of solving this problem.

Keywords: heart failure, heart transplantation, circulatory support, thrombosis, mechanical circulatory support devices.

Over 50 years have passed since the first heart transplant surgery was performed by Christian Barnard and his team at Groote Schuur Hospital [1].

Unfortunately, acute shortage of donor organs was and still remains the "Achilles' heel" of this treatment method. For instance, due to organ shortage, the number of heart transplants performed in the United Kingdom (UK) and in many Western countries has dropped sharply over the past decades. Moreover, the waiting list continues to increase [2]. In the UK, of the estimated 750,000 heart transplant candidates, only around 0.02% undergo transplantation. Consequent to this mismatch between supply and demand, almost 10% of patients on the heart transplant waiting list continue to die every year [3]. According to the Canadian Institute for Health Information, over the past 10 years, the annual mortality rate of patients awaiting heart transplantation was 16% [4]. In the United States of America, despite 35,000–64,000 patients requiring heart transplants, only 2,200–2300 operations are performed per year [5]. In the Russian Federation, data for 2018 shows that there were 823 patients on the waiting list, but only 282 heart transplants were performed during the year [6].

To solve this problem, many mechanical devices capable of effectively and safely providing circulatory support have been developed over the past few decades [7].

In the vast majority of cases, existing devices do not actually replace the heart, but function as a ventricular assist device (LVAD), providing the proper minute volume of blood circulation. Perhaps the main purpose of using LVAD today is to serve as a "bridge to transplantation". The use of circulatory support devices in patients with extremely poor prognosis of life expectancy can significantly improve the quality of life and increase survival to heart transplantation. According to the REMATCH randomized trial published in 2001, the annual survival rate of patients who received first-generation LVADs was 52% versus 25% in the medical drug therapy group. At 24 months, the trend continued, with 23% survival in the LVAD group and 8% in the medical therapy group. Currently, second- and third-generation LVADS provide similar 1-year survival (approximately 90%) compared to cardiac transplantation [8].

According to other studies, almost 70% of patients receiving LVAD support survive the waiting period for the donor organ, and in the case of implantation of the latest generations of devices, this figure reaches 79% [9, 10].

Since organ shortage was the main problem that prompted the development of circulatory assist devices, the predicted period of operation was rather short. However, subsequent development of technologies and production of biocompatible materials has significantly improved the safety of device models. Over time, there appeared a separate group of patients in whom regression of clinical signs of circulatory insufficiency and, as a consequence, absence of indications for heart transplantation, was observed against the background of previously implanted LVAD. This fact contributed to the consideration of mechanical circulatory support as a means of "destination therapy". In addition, the emergence of new LVAD models has achieved long-term circulatory support. This has led to restoration of full pumping function of the heart with the possibility of subsequent explantation of the device. According to some researchers, this "bridge to recovery" strategy has been successfully implemented in 5–10% of adult patients [11, 12].

The key problems preventing LVAD from becoming a complete alternative to heart transplant procedure are the development of biocompatible materials and a reliable pumping unit mechanism.

Corresponding author: Maxim Zhulkov. Address: 15, Rechkunovskaya str., 630055 Novosibirsk, Russian Federation.
Phone: (906) 909-05-05. E-mail: maks.zhulkov.92@mail.ru

The idea of prosthetics for the pumping function of the heart naturally guided engineers towards simulating pulsatile blood flow, synchronized with the heart's own rhythm. So, in 1975 the first generation of the HeartMate system (Thratec Corporation) was created.

In principle, this pump was an elastic chamber that changed its volume through a special installation using the force of an injected gas, liquid, or an electromechanical method. At the inlet and outlet of this chamber, valves were installed to ensure unidirectional blood flow. Like a living heart, during the filling phase, blood entered the elastic chamber of the pump, after which, during the ejection phase, it was released into the patient's arterial system. The first devices were rather bulky, required synchronization with the heart's own rhythm, and were difficult to operate. However, in spite of the fact that the pulsating nature of blood movement is physiological, in subsequent years in the clinical practice of using LVAD in adult patients, on-pulsating devices (more than 94%) became the most widespread devices [13].

Rotary blood pumps have several important advantages, one of them being that they do not require a large chamber volume to generate a working ejection comparable to the native heart ventricle. In subsequent pump generations, the flow was generated by rotating the impeller either as an axial (straight) or centrifugal (from the center to the tangential edge) flow. Rotary pumps consume significantly less energy, have fewer moving parts, and have no valves or cyclic drives. In second-generation designs, the main places of wear are bearings. For instance, it is known that the estimated service life of devices implemented by a rotor-supported bearing system is 1–2 years, at 9000–15000 rpm, and despite numerous attempts to adapt the operation of this part of the pump in specific blood conditions, most of the problems (thrombosis, breakage, exhaustion of the strength resource) have not been resolved [14].

In the third-generation devices, mechanical wear has been reduced by magnetic suspension of the rotor. This innovative design has greatly improved overall reliability and durability. Lower total weights and volumes of implantable devices make the third-generation systems applicable to patients with a small body surface area (small women and children). Without valves, a pump bag compression and bearing source, the third-generation rotary pumps are much quieter than their predecessors.

While rotary pumps are free of some of the disadvantages of pulsatile LVADs, they come with a number of unique biocompatibility issues. The high rotor speeds (~5000–10000 rpm), required to generate a flow rate of ~5 liters per minute, expose the blood cells to high peak shear stresses. And although these stresses are of a very short duration, they can lead to hemolysis and platelet activation. That is why, from this point of view, centrifugal disc-type pumps, allowing to develop the design capacity at minimum (less than 3000 rpm) rotor revolutions, minimizing the risk of blood hemolysis, are better [15, 16].

Besides hemolysis, one of the main problems limiting the long-term use of any LVAD model is thromboembolic complications. The difficulty in analyzing thromboembolic complications is due to differences in the understanding of assessment criteria. Thromboembolic complications range from focal tissue necrosis, detected only on histological studies, to persistent neurologic symptoms (stroke). Data published in 2009 by INTERMACS described 199 neurological, 14 arterial, and 33 venous thrombotic complications in 483 LVAD patients over a two-year period. In this report, central nervous system events were the leading cause of death (11%), which further emphasizes the difficulty of addressing the biocompatibility problem and its present urgency [17].

One of the ways to combat major complications was to reduce the area of the inner surface of the pump in order to reduce the blood-contacting surface area. Thus, the surface area of the latest generations of pumps was significantly reduced (for HeartMate I, the blood-contacting surface area varied from 400 to 500 cm^2). However, despite this, the problem of thromboembolism still remains unsolved. Another way of tackling this problem was to accelerate endothelialization of the inner surface of the pump, for example, despite the large blood-contacting surface area, a textured surface was successfully used in the HeartMate XVE model. The blood- and tissue-contacting surfaces of titanium cannulas were covered with sintered titanium microspheres 50–75 μm in diameter (Fig.), and 25 mm xenopericardial valves (Medtronic) were installed at the pump inlet and outlet. The diameter of the fibrils of the fully textured polyurethane surface of a flexible diaphragm was approximately 18 μm.

Despite the fact that the idea of using a textured surface seemed risky at first, this concept turned out to be an original solution to the biocompatibility problem. The clots of heterogeneous composition, rapidly forming and tightly fixed on the inner surface, containing platelets, monocytes, macrophages, lymphocytes and multipotent circulating cells created optimal conditions for early (about 7 days) formation of pseudo-intima, significantly reducing the risk of thromboembolism [18].

In this case, formation of the neointima, apparently, occurred due to the natural drift of pluripotent cells by the blood stream. At the same time, it was shown that the forming neointima does not exceed 150 μm in thickness within a year after implantation [19].

The resulting pseudointima does not have antithrombotic properties. However, Spanier et al. suggested that such a surface could work by creating a stable prothrombotic and potentially pro-inflammatory environment that induces continued coagulation through the tissue factor pathway. An enhanced fibrinolytic response by the body, which has been described many times in literature, serves as a natural autoanticoagulation to prevent the develop-

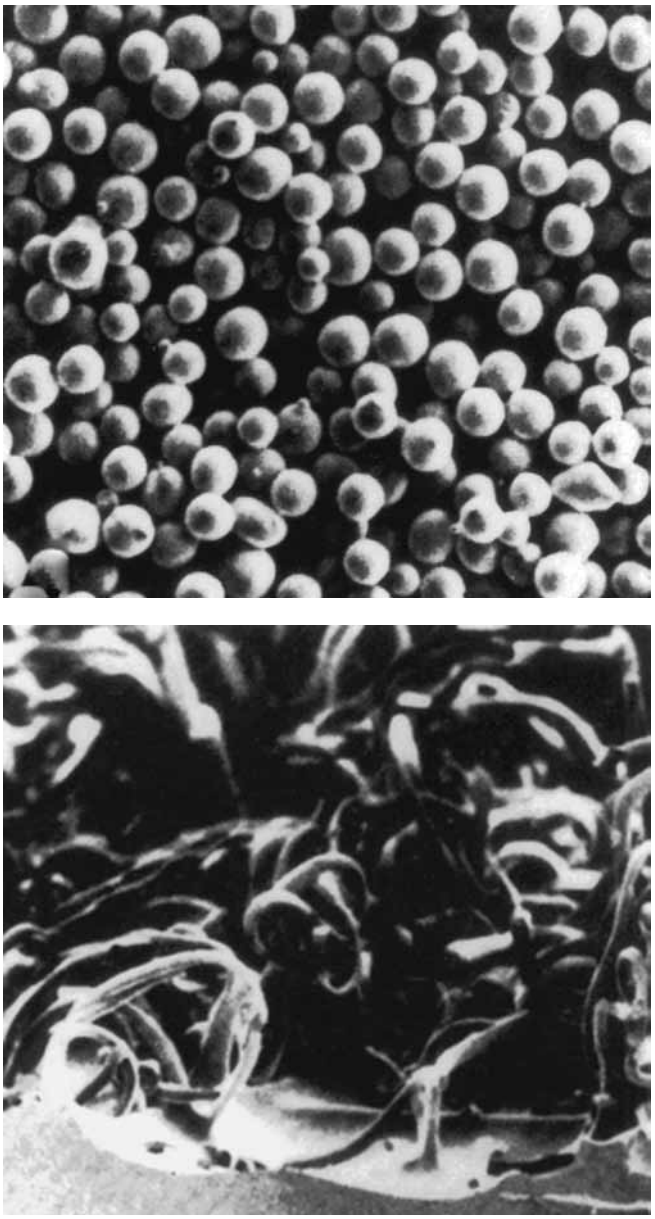

Fig. Textured surface of the HeartMate XVE

ment of thromboembolic syndrome. In addition, impressive clinical results recorded by the first generation of the pump is due to the fact that the formed thrombi are much less likely to migrate due to the stronger adhesion to the extracellular matrix present on the surface.

Unfortunately, this concept of natural surface modification cannot be implemented in smaller continuous flow pumps, and it is likely that the smaller blood-contacting surfaces of these pumps could offset any potential increased risk.

The HeartMate II has the highest efficacy and safety record of any LVAD implanted. It has been implanted in over 10,000 patients in about 300 different clinics around the world. In patients under 70 years of age without cardiogenic shock, diabetes, and renal failure, the HeartMate II circulatory support showed a 1-year and 2-year survival of 80% and 70%, respectively, which is comparable to heart transplantation outcomes. Moreover, the PREVENT study showed a 4.8% risk of thrombosis for this device in the first 6 months after implantation. According to Kreuziger et al., HeartMate II thrombosis occurs in 10% of patients after implantation [20–22].

The main cause of thrombosis in these cases is the heat generated in the inflow part of the bearing unit. This is where thrombotic masses were found most often; apparently, this was associated with the heat released during rotor rotation, protein denaturation and fibrin deposition. Histological analysis of the thrombi found around the inlet bearing in HeartMate II showed high levels of fibrin, which supports the coagulation theory of thrombosis. Administration of warfarin therapy by reducing the concentration of clotting factors II, VII, IX and X helped to reduce the likelihood of thrombosis [23, 24].

However, artificial surfaces can directly activate proteins of the internal pathway – factors XI and XII, on which warfarin has no effect, whereas the activity of the internal pathway was significantly affected by the nature of the flow generated by LVAD. An absolute 40–50% decrease in clotting factors XI and XII after pulsatile LVAD implantation has been proven [25].

The latest-generation HeartMate III (Abbott, Chicago, IL) with a fully magnetic rotor suspension has software that allows for generation of a pulsatile flow. The first large study conducted in 10 centers (Europe, Kazakhstan, Canada, Australia) showed excellent outcomes: no hemolysis, no thrombosis or failure within 12 months, not a single case of stroke was recorded [26, 27]. According to Krabatsch et al., there was a 92% 6-month survival and an 81% 12-month survival [28].

However, according to a study published in 2018 by Konstantin et al., comparing three different LVADs – HeartMate II, HeartMate III, and HeartWare, the overall 30-day survival rate was 70.4%, annual survival 51.9% and 5-year survival 38% with no significant difference in complication rates between these three LVAD models. Despite the significant advantages of latter pump generations, the probability of death from pump thrombosis and subsequent embolic stroke was 24% within 3 months after implantation [29, 30].

Since the risk of thrombus formation mainly determines the hemodynamic flow profile in pump cavities, the available theoretical evidence and previously performed experimental studies create obvious prerequisites for considering Tesla-turbine disc pumps (viscous friction pumps) as circulatory assist devices [31].

In such devices, centrifugal force creates a uniform hydraulic velocity profile and ensures pumping of a liquid medium without pulsations and vibrations with formation of a boundary layer. The boundary layer not only transfers kinetic energy to the fluid between the discs, but also acts as a molecular buffer between the disc surface and blood. An element-free blood plasma layer is formed

around the surfaces of the rotating discs, minimizing the contact of blood cells with the disc surface [32, 33].

Despite encouraging results of the first trials of the new disc pump model showing minimal blood cell injury, largely due to modification of the a-C:H:SiO_x film surface, an understating of the risk of thrombus formation and the incidence of other complications remain unclear [34, 35].

CONCLUSION

At present, none of the existing LVAD models can ensure complete absence of thromboembolic complications and hemolysis. Analysis of literature data and recent experiments on adaptation of implantable materials show that the problem is still a highly urgent one.

The authors declare no conflict of interest.

REFERENCES

1. *Barnard CN*. Human cardiac transplant: An interim report of a successful operation performed at Groote Schuur Hospital, Cape Town. *South African Medical Journal*. 1967; 41 (48): 1271–1274.
2. Blood N.H.S. Transplant. Organ Donation and Transplantation activity figures for the UK as at 12 April 2013. 2014.
3. *Messer S, Ardehali A, Tsui S*. Normothermic donor heart perfusion: current clinical experience and the future. *Transplant International*. 2015; 28 (6): 634–642.
4. Canadian Institute for Health Information. Canadian Organ Replacement Register Annual Report: Treatment of End-Stage Organ Failure in Canada, 2004 to 2013. Ottawa, ON: Canadian Institute for Health Information; (2015).
5. National Center for Health Statistics (US et al. Health, United States, 2018. 2019.
6. *Gauthier SV, Khomyakov SM*. Organ donation and transplantation in the Russian Federation in 2018. XI message of the register of the Russian transplant society. *Bulletin of transplantology and artificial organs*. 2019; 21 (3): 7–32.
7. *Ammar KA, Jacobsen SJ, Mahoney DW, Kors JA, Redfield MM, Burnett Jr JC, Rodeheffer RJ*. Clinical perspective. *Circulation*. 2007; 115 (12): 1563–1570.
8. *Englert JAR, Davis JA, Krim SR*. Mechanical circulatory support for the failing heart: Continuous-flow left ventricular assist devices. *Ochsner Journal*. 2016; 16 (3): 263–269.
9. *Mehta PA, Dubrey SW, McIntyre HF, Walker DM, Hardman SM, Sutton GC, Cowie MR*. Improving survival in the 6 months after diagnosis of heart failure in the past decade: population-based data from the UK. *Heart*. 2009; 95 (22): 1851–1856.
10. *Rogers JG, Pagani FD, Tatooles AJ, Bhat G, Slaughter MS, Birks EJ, Gregoric ID*. Intrapericardial left ventricular assist device for advanced heart failure. *New England Journal of Medicine*. 2017; 376 (5): 451–460.
11. *Massad MG, McCarthy PM, Smedira NG, Cook DJ, Ratliff NB, Goormastic M, Stewart RW*. Does successful bridging with the implantable left ventricular assist device affect cardiac transplantation outcome? *The Journal of thoracic and cardiovascular surgery*. 1996; 112 (5): 1275–1283.
12. *Simon MA, Kormos RL, Murali S, Nair P, Heffernan M, Gorcsan J, McNamara DM*. Myocardial recovery using ventricular assist devices: prevalence, clinical characteristics, and outcomes. *Circulation*. 2005; 112 (9_supplement): I-32–I-36.
13. *Kirklin JK et al*. The fourth INTERMACS annual report: 4,000 implants and counting. *The Journal of Heart and Lung Transplantation*. 2012; 31 (2): 117–126.
14. *Parashin VB, Itkin GP, Shchukin SI*. Biomechanics of blood circulation. M.: Publishing house of MSTU, 2005.
15. *Zhulkov MO, Golovin AM, Golovina EO, Grenaderov AS, Fomichev AV, Alsov SA, Chernyavsky AM*. Investigation of the hemolytic properties of a disk-type pump. *Blood circulation pathology and cardiac surgery*. 2020. T. 24. No. 1. S. 87–93.
16. *Medvedev AE, Fomin VM, Chernyavskiy AM, Prikhodko YM, Zhulkov MO, Golovin AM*. Implanted system of mechanical support of the disk-based heart pump viscous friction. AIP Conference Proceedings. AIP Publishing LLC, 2018; 2027 (1): 030149.
17. *Holman WL, Pae WE, Teutenberg JJ, Acker MA, Naftel DC, Sun BC, Kirklin JK*. INTERMACS: interval analysis of registry data. *Journal of the American College of Surgeons*. 2009; 208 (5): 755–761.
18. *Rafii S, Oz MC, Seldomridge JA, Ferris B, Asch AS, Nachman RL, Levin HR*. Characterization of hematopoietic cells arising on the textured surface of left ventricular assist devices. *The Annals of thoracic surgery*. 1995; 60 (6): 1627–1632.
19. *Menconi MJ, Pockwinse S, Owen TA, Dasse KA, Stein GS, Lian JB*. Properties of blood-contacting surfaces of clinically implanted cardiac assist devices: Gene expression, matrix composition, and ultrastructural characterization of cellular linings. *Journal of cellular biochemistry*. 1995; 57 (3): 557–573.
20. *Kirklin JK, Naftel DC, Pagani FD, Kormos RL, Stevenson L, Miller M, Young JB*. Long-term mechanical circulatory support (destination therapy): on track to compete with heart transplantation? *The Journal of thoracic and cardiovascular surgery*. 2012; 144 (3): 584–603.
21. *Maltais S, Kilic A, Nathan S, Keebler M, Emani S, Ransom J, Entwistle III JW*. PREVENtion of HeartMate II pump thrombosis through clinical management: the PREVENT multi-center study. *The Journal of Heart and Lung Transplantation*. 2017; 36 (1): 1–12.
22. *Kreuziger LB, Slaughter MS, Sundareswaran K, Mast AE*. Clinical relevance of histopathologic analysis of HeartMate II thrombi. *ASAIO journal (American Society for Artificial Internal Organs: 1992)*. 2018; 64 (6): 754.
23. *Maltais S, Kilic A, Nathan S, Keebler M, Emani S, Ransom J, Entwistle III JW*. PREVENtion of HeartMate II pump thrombosis through clinical management: the

PREVENT multi-center study. *The Journal of Heart and Lung Transplantation*. 2017; 36 (1): 1–12.
24. *Hamaguchi S, Hirose T, Akeda Y, Matsumoto N, Irisawa T, Seki M, Tomono K*. Identification of neutrophil extracellular traps in the blood of patients with systemic inflammatory response syndrome. *Journal of international medical research*. 2013; 41 (1): 162–168.
25. *Büller HR, Bethune C, Bhanot S, Gailani D, Monia BP, Raskob GE, Weitz JI*. Factor XI antisense oligonucleotide for prevention of venous thrombosis. *New England Journal of Medicine*. 2015; 372 (3): 232–240.
26. *Zimpfer D, Netuka I, Schmitto JD, Pya Y, Garbade J, Morshuis M, Sood P*. Multicentre clinical trial experience with the HeartMate 3 left ventricular assist device: 30-day outcomes. *European Journal of Cardio-Thoracic Surgery*. 2016; 50 (3): 548–554.
27. *Netuka I, Sood P, Pya Y, Zimpfer D, Krabatsch T, Garbade J, Damme L*. Fully magnetically levitated left ventricular assist system for treating advanced HF: a multicenter study. *Journal of the American College of Cardiology*. 2015; 66 (23): 2579–2589.
28. *Krabatsch T, Netuka I, Schmitto JD, Zimpfer D, Garbade J, Rao V, Pya Y*. Heartmate 3 fully magnetically levitated left ventricular assist device for the treatment of advanced heart failure – 1 year results from the Ce mark trial. *Journal of cardiothoracic surgery*. 2017; 12 (1): 23.
29. *Zhigalov K, Mashhour A, Szczechowicz M, Mkalaluh S, Karagezian S, Gogia I, Eichstaedt HC*. Clinical Outcome and Comparison of three different left ventricular assist devices in a high-risk cohort. *Artificial organs*. 2018; 42 (11): 1035–1042.
30. *Smedira NG, Blackstone EH, Ehrlinger J, Thuita L, Pierce CD, Moazami N, Starling RC*. Current risks of HeartMate II pump thrombosis: non-parametric analysis of Interagency Registry for Mechanically Assisted Circulatory Support data. *The Journal of Heart and Lung Transplantation*. 2015; 34 (12): 1527–1534.
31. *Medvedev AE, Fomin VM, Samsonov VI*. Mathematical modeling of the blood flow in blood vessels. Circulatory System and Arterial Hypertension: Experimental Investigation, Mathematical and Computer Simulation. 2012: 55–114.
32. *Medvedev AE*. Two-phase model of blood flow. Russian journal of biomechanics. 2013; 4.
33. *Izraelev V et al*. A passively-suspended Tesla pump left ventricular assist device. *ASAIO journal (American Society for Artificial Internal Organs: 1992)*. 2009; 55 (6): 556.
34. *Grenadyorov AS, Solovyev AA, Oskomov KV, Onischenko SA, Chernyavskiy AM, Zhulkov MO, Kaichev VV*. Modifying the surface of a titanium alloy with an electron beam and aC: H: SiOx coating deposition to reduce hemolysis in cardiac assist devices. *Surface and Coatings Technology*. 2020; 381: 125113.
35. *Zhulkov MO, Golovin AM, Golovina EO, Grenaderov AS, Fomichev AV, Alsov SA, Chernyavsky AM*. Investigation of the hemolytic properties of a disk-type pump. *Blood circulation pathology and cardiac surgery*. 2020; 24 (1): 87–93.

The article was submitted to the journal on 2.06.2020

DOI: 10.15825/1995-1191-2020-4-89-97

FUNCTIONAL EFFICIENCY OF CELL-ENGINEERED LIVER CONSTRUCTS BASED ON TISSUE-SPECIFIC MATRIX (EXPERIMENTAL MODEL OF CHRONIC LIVER FAILURE)

M.Yu. Shagidulin[1, 2], N.A. Onishchenko[1], Yu.B. Basok[1], A.M. Grigoriev[1], A.D. Kirillova[1], E.A. Nemets[1], E.A. Volkova[1], I.M. Iljinsky[1], N.P. Mozheiko[1], V.I. Sevastianov[1], S.V. Gautier[1, 2]

[1] Shumakov National Medical Research Center of Transplantology and Artificial Organs, Moscow, Russian Federation

[2] Sechenov University, Moscow, Russian Federation

Objective: to investigate the functional efficiency of a cell-engineered construct (CEC) of the liver based on tissue-specific matrix consisting of decellularized rat liver fragments, allogeneic liver cells and multipotent mesenchymal stromal cells (MSCs) isolated from the bone marrow on an experimental model of chronic liver failure (CLF). **Materials and methods.** In creating liver CECs, the liver for decellularization and liver cells were obtained from male Wistar rats. MSCs were isolated from rat bone marrow. The functional efficacy of CEC was investigated on an experimental CLF model obtained by priming rats with CCl_4 solution. At different periods after implantation, the outcomes were assessed based on the biochemical parameters of cytolysis. Morphological changes in the liver were analyzed by histochemical methods in the control (administration of saline solution into the liver parenchyma) and experimental (administration of liver CEC into the liver parenchyma) groups. **Results.** It was shown that implantation of the proposed CEC normalizes blood biochemical parameters and structural disorders of the damaged rat liver faster (by day 30 after introduction of CEC instead of day 180 in the control). The CEC was also shown to have reduced animal mortality from 50 to 0%, which is due to early activation of proliferation of viable liver cells and faster formation of new blood vessels. These effects are down to either stimulation of the internal regenerative potential of the damaged liver during CEC implantation or long-term functioning of the transplanted cells as part of the CEC based on the decellularized liver matrix. **Conclusion.** The liver CEC, implanted into the liver parenchyma in laboratory animals with a CLF model, has a functional activity.

Keywords: liver, liver failure, regeneration, cell-engineered constructs, bioartificial organs, matrixes.

INTRODUCTION

Liver transplantation is the gold standard treatment for end-stage liver disease. However, donor organ shortage limits the widespread use of this only radical method for treatment of decompensated cirrhosis. The number of patients requiring liver transplantation significantly exceeding the number of emerging organs suitable for transplantation indicates the need to develop alternative treatment options, among which the use of regenerative medicine and tissue engineering methods seems to be the most promising [1, 2].

Most of the technical approaches in the field of liver tissue engineering are based on isolation of primary hepatocytes or obtaining of hepatocyte-like cells from stem cells and 3D cultivation subsequently [3]. Note that it is advisable to use mesenchymal stromal cells in the composition of cell-engineered constructs (CECs) in the treatment of a number of liver diseases to stimulate organ regeneration [4]. Biocompatible and bioresorbable matrices are used to provide the CEC cells with favorable conditions for their vital activity.

In our opinion, decellularized carriers/scaffolds belonging to the class of biomimetics of the extracellular matrix (ECM) and obtained by removing cells and their fragments from tissue with maximum preservation of the structure and composition of natural ECM commands the greatest interest [5, 6].

A lot of work is devoted to whole organ decellularization by perfusion with surfactants and enzyme solutions [7]. A similar approach has been described for the heart, kidney, pancreas, and uterus [8–11]. Note that whole liver decellularization comes with several disadvantages: low efficiency in cell detritus removal and difficulty in penetration of cells, nutrients, and gases into the organ volume due to microcirculatory disorders. In previous works, we obtained a tissue-specific matrix from fragments of decellularized rat liver with intact structure and no cells and cell fragments [12]. The next logical step is to create liver CECs, consisting of a tissue-specific matrix, liver cells (LCs), and bone marrow-derived multipotent mesenchymal stromal cells (BM-MSCs) with subsequent proof of its functional efficiency in

Corresponding author: Murat Shagidulin. Address: 1, Shchukinskaya str., Moscow, 123182, Russian Federation. Phone: (499) 196-87-90. E-mail: dr.shagidulin@mail.ru

an experimental model of chronic liver failure (CLF), which was the purpose of this work.

MATERIALS AND METHODS

To solve the set tasks, experimental studies were carried out on 60 male Wistar rats weighing 150–250 grams. The animals were kept in a vivarium at 18–20 °C temperature on a mixed diet with free access to water. Experiments on the animals were carried out from 9 to 19 hours at room temperature (t = 22–24 °C). All manipulations with the rats were carried out in accordance with the rules adopted by the European Convention for the Protection of Vertebrate Animals Used for Experimental and Other Scientific Purposes (ETS No. 123) Strasbourg, 1986).

The experiments were carried out on 60 male Wistar rats weighing 250 grams. Of these, 10 rats were used as LC donors and 10 rats as liver donors for decellularization. The experiment lasted for 180 days.

Rat liver fragments (n = 10) no larger than 2 × 2 × 2 mm in size were obtained using a scalpel and scissors. Decellularization of rat liver fragments was carried out in three changes of phosphate-buffered saline (PBS) (138 mM NaCl, 2.67 mM KCl, 1.47 mM KH_2PO_4, 8.1 mM Na_2HPO_4, pH = 7.4) containing 0.1% sodium dodecyl sulfate and increasing Triton X-100 concentration: 1%, 2% and 3% [12]. The total decellularization time was 72 hours – 24 hours for each change of surfactants solution with magnetic stirrer. To obtain microparticles, decellularized liver fragments were placed in the CryoMill RETSCH cryomill (Retsch GmbH, Germany) and milled in a mode that included 3 milling cycles for 3 minutes at 25 Hz frequency. The fraction of 100–250 μm particles was separated using sieves of appropriate sizes.

Washing against surfactants included exposing the matrix to PBS containing an antibiotic (ampicillin, 20 μg/mL) and an antimycotic (amphotericin B, 2.0 μg/mL) for 96 hours. The washed samples were sterilized by γ-irradiation at 1.5 Mrad dose.

LCs and BM-MSCs were isolated and cultured in accordance with the general principles of carrying out culture studies on 10 male Wistar rats weighing 150 g.

To populate the decellularized liver matrix with cellular components according to a known technique [15], we used the previously established optimal cell ratio: LCs : BM-MSCs = 5 : 1 [17]. Prior to implantation, LCs and BM-MSCs were co-cultivated in the same 5 : 1 ratio for 3 days.

It should be noted that the introduction of BM-MSCs into the cellular component of CECs is due to their ability to induce cell proliferation processes, including through their own transdifferentiation [17].

The functional efficacy of the resulting liver CECs was evaluated in the CLF model.

CLF was modeled on male Wistar rats weighing 250 g (n = 40) by inoculating rats with CCl_4 solution according to our modified scheme [16]. Control of the adequacy of the created CLF model was assessed by the level of mortality and survival of the animals, the state of blood biochemical parameters, and morphological characteristics of the liver state. At the CLF modeling stage, 9 rats (22.5%) died.

As a result, after CLF modeling, the surviving rats with the experimental CLF model were divided into 2 groups: control group 1 (16 animals) – saline was injected into the parenchyma of the damaged liver, and experimental group 2 (15 animals) – liver CECs were injected into the parenchyma of the damaged liver 7 days after CCl_4 injection. Immunosuppression was not used.

The rats from the control and experimental groups were taken out of the experiment on days 28–30, day 90 and day 180 by intraperitoneal administration of sodium thiopental in a dosage causing respiratory arrest. At the aforementioned periods, before complete respiratory arrest, venous blood was taken for biochemical studies. Liver function (ALT, ASAT, bilirubin, gamma-glutamyl transpeptidase (GGT), alkaline phosphatase levels) was studied using clinical chemistry analyser Reflotron™ (Roche, Switzerland) with special Reflotron™ test strips (measurement accuracy: ±0.5%; reproducibility: ≤0.2%; linearity: ±0.05%).

After complete respiratory arrest, the liver was explanted for morphological studies. We performed biopsies of healthy and damaged liver: liver failure without treatment – control; liver failure with treatment, studies were carried out in the CECs implantation areas and outside at days 28–30, day 90, and day 180 of the experiment. Data from light microscopy with staining of sections (H&E stain, Van Gieson and Mallory stains) were evaluated. We used a Leica DM 6000 B microscope and a Leica LTDCH 9435 camera (Germany).

Morphometric analysis was performed using the ImageScopeM software (Systems for Microscopy and Analysis, Russia) using a Leica DM 1000 microscope and a Leica LTDCH 9435 DFC 295 camera (Leica Camera AG, Germany). The presence of cirrhosis was determined morphometrically (counting the number of false lobules); specific area of connective tissue (%ratio to the total area of the liver section) [18, 19].

The viability of LCs in liver CECs was assessed using immunohistochemical staining with hepatocyte specific antigens (OCH1E5).

The results were statistically processed using statistical analysis software package BioStat. The significance of differences was assessed by Student's t-test, with the Bonferroni correction taken into account.

RESULTS AND DISCUSSION

After inoculation, the clinical condition of the surviving animals was characterized by decreased body weight, adynamia and partial baldness. After inoculation, during the entire experiment (180 days), 50% (n = 8) more rats in the control group died against the background of CLF at different times. In the experimental

group, the survival rate by the same period was 100%. In this regard, assessment of functional and morphological changes in the liver of the experimental rats after CLF modeling was studied in 8 and 15 rats in the control and experimental groups, respectively. Absence of mortality in the experimental group allowed us to conclude that the implanted CECs had a positive effect on the survival rate of the CLF model rats. Fig. 1 shows a macropreparation of rat liver after the end of inoculation, i.e. day 42 from the start of CCl_4 inoculation. The liver was dense and enlarged. The surface was shallowly, finely grained, with rounded edges.

Microscopically, within the first month after the end of inoculation, a typical picture of cirrhotic transformation of the liver architectonics with progressive disorder in its structure at later follow-up periods (especially at days 60 and 90) due to connective tissue proliferation and emerging fibrosis was revealed (Fig. 2).

After decellularization [12], liver fragments were washed completely of LCs (Fig. 3), followed by colonization of the resulting tissue-specific matrix with cellular components of LCs and BM-MSCs.

The histological data presented in Fig. 4 demonstrate the presence of adherent hepatocytes on the decellularized matrix of rat liver.

At day 90 and 180 after implantation of CECs, representing finely dispersed particles of decellularized liver tissue with LCs and BM-MSCs seeded on it in a 5 : 1 ratio, viable and functioning hepatocytes were detected (Fig. 5).

At day 90, donor liver cells co-cultured with BM-MSCs formed associates of viable and functionally active cells within CECs. There were no pronounced inflammatory reactions and signs of rejection. Similar data were obtained at day 180 of CECs implantation.

To quantify the changes occurring in the liver structure of the CLF model rats in both groups, a morphometric study of the state of non-parenchymal structures (determination of the specific area of connective tissue and the number of false lobules in the liver) was carried out at different times for 180 days. It was found that in group 2, 60–90 days after administration of CECs, restoration of both parenchyma and non-parenchymal

Fig. 1. Rat liver after injection, 42 days

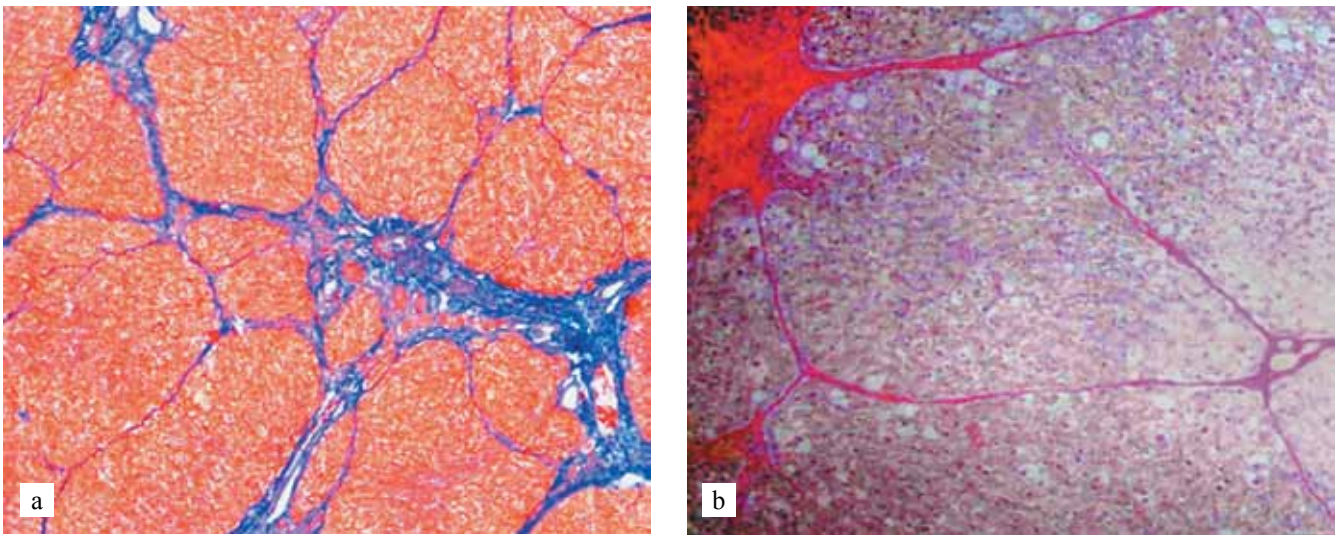

Fig. 2. Rat liver tissue after CLF modeling (CCl_4 injection = 42 days). a) 90 days, false lobules. Mallory staining for connective tissue. Microscope magnification 100×. b) 180 days, formed false lobules, sclerosis and cirrhosis. Van Gieson's stain. 100×

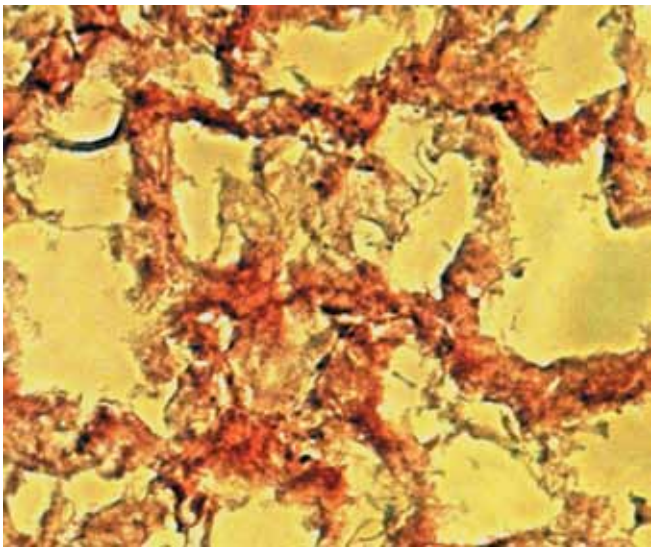

Fig. 3. Fragment of decellularized rat liver. H&E stain. 200×

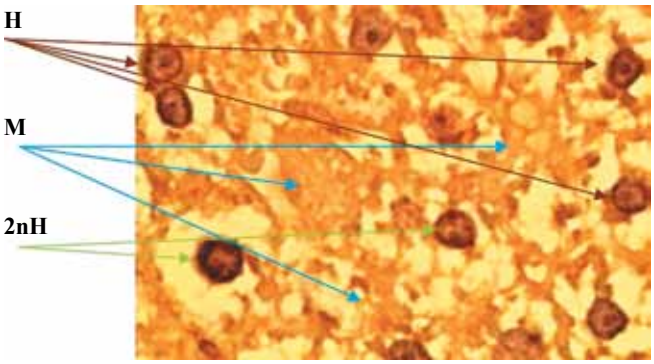

Fig. 4. Hepatocytes adhered to the tissue-specific liver matrix: M – decellularized liver matrix; H – adhered hepatocytes; 2nH – binuclear hepatocytes. H&E stain. 400×

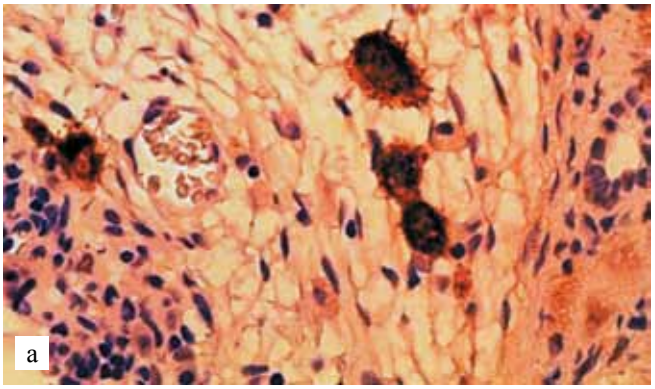

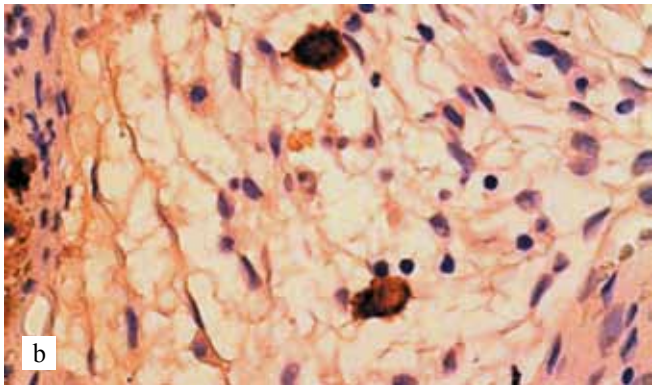

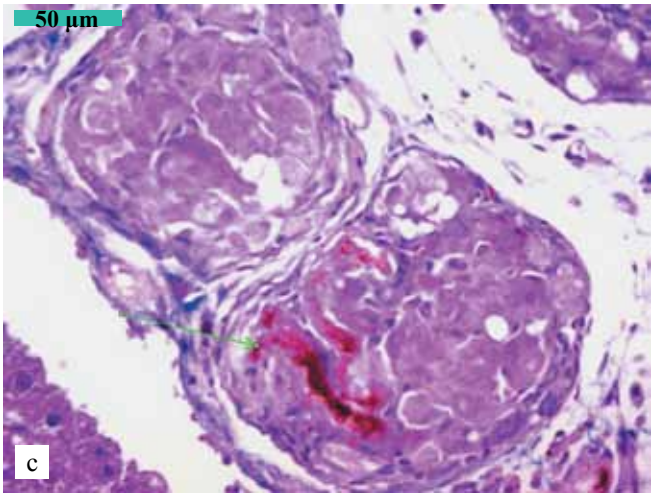

Fig. 5. Histological liver preparations in the CEC transplanted area (LC : MMSC BM = 5 : 1) in the parenchyma of the damaged liver: viable hepatocytes at 90 (a) and 180 (b) days. Immunohistochemical study with hepatocyte-specific antigens (OCH1E5) – positive granular cytoplasmic staining; c – Bile production (green arrow) by transplanted hepatocytes. H&E stain, 400×

structures occurred. This is confirmed by a dynamic morphometric study of the decrease in the specific area of the liver connective tissue and the number of false lobules in it (Fig. 6).

Liver function was assessed over time by measuring the serum biochemical parameters. Determination of the level of cytolysis enzymes (ALT, ASAT, ALP) in the blood serum of the rats (Fig. 7) made it possible to establish a sharp increase in the level of these enzymes during the first 2 weeks of inoculation. After the end of the inoculation, 7 days later, ALT and AST levels increased by more than 4.5 and 3 times, respectively, while ALP levels increased by almost 5 times. 28–30 days after the end of the inoculation, the levels of cytolysis enzymes decreased, but continued to remain at a significantly ($p < 0.05$) higher level for a long time (Fig. 7) for 180 days compared with normal values in intact animals. In the experimental group, cytolytic processes were also

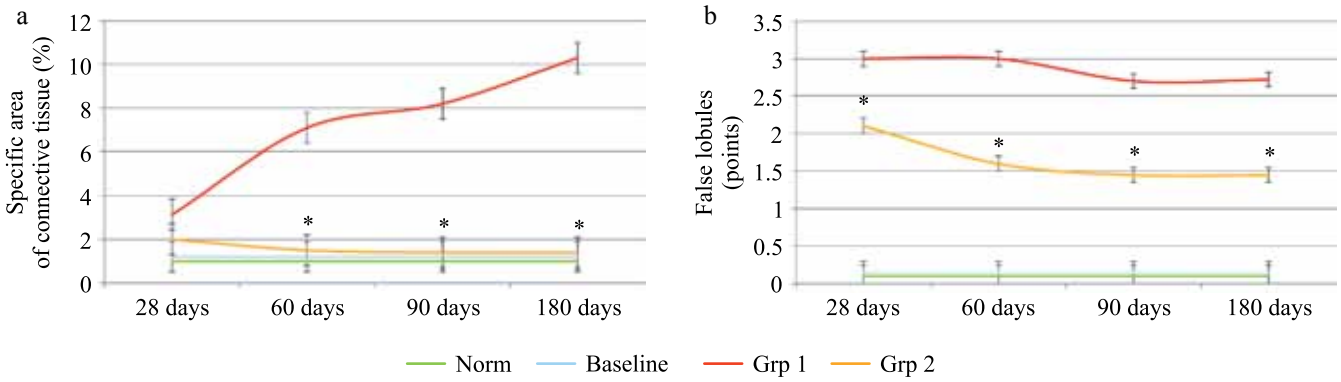

Fig. 6. Dynamic morphometric assessment of the state of non-parenchymal structures of the rat liver during CLF modeling and CEC implantation. a – change in the specific area of connective tissue; b – counting the number of false lobules in the liver: group 1 – control (saline); group 2 – liver CEC. * The difference is significant compared to the level of the indicator in the rat liver in the control group, $p < 0.05$

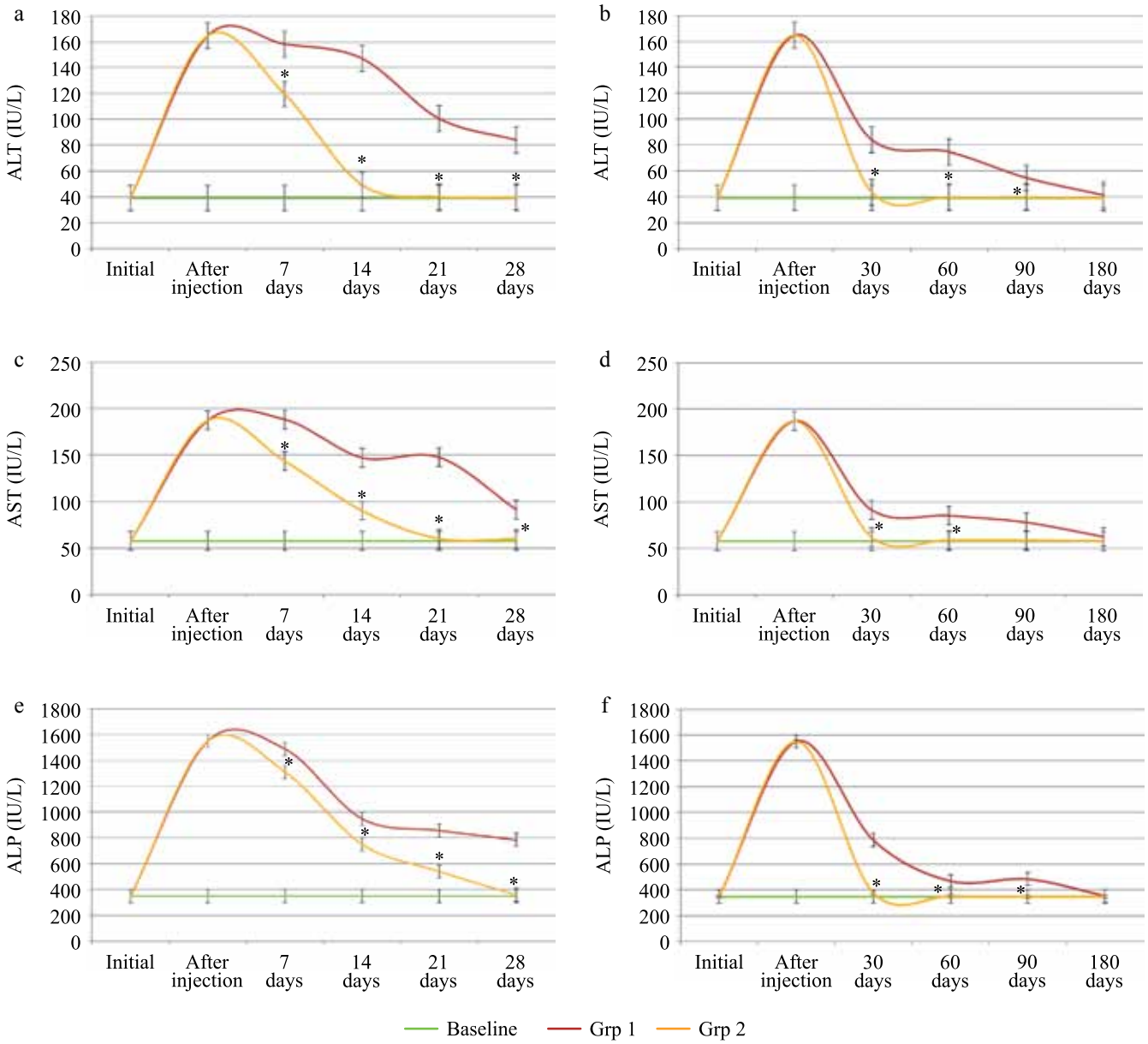

Fig. 7. Dynamics of normalization of the cytolysis enzymes level (ALT, AST, ALP) in the blood serum of rats after CLF modeling and CEC implantation. Level for healthy rats: ALT up to 40 IU/L; AST – up to 60 IU/L; ALP – up to 350 IU/L. a, b, e – observation period 28 days; b, d, f – observation period 180 days. * The difference is significant compared to the level of enzymes in the control (group 1); $p < 0.05$

observed in the liver parenchymal cells, but which were significantly less intense than in the control group. The corresponding indicators reached normal values by 30 days after CECs implantation, while for the control, the AST, ALT, and ALP levels normalized only at day 180 of the experiment (Fig. 7).

The serum gamma-glutamyl transpeptidase (γ-GTP) and bilirubin levels in the experimental animals remained within the normal range at all follow-up periods.

The observed effects could be due to stimulation of the intrinsic regenerative potential of the damaged liver during CECs implantation, or by the active functioning of the transplanted cells within CECs based on the decellularized liver matrix.

CONCLUSION

Implantation of the proposed CECs provides a more rapid normalization of biochemical blood parameters and structural disorders in the damaged rat liver (at day 30 after introduction of CECs instead of day 180 as was obtained in the control) and reduced animal mortality from 50% to 0% due to earlier activation of viable LCs proliferation processes and faster formation of new blood vessels.

Thus, the outcomes obtained prove that liver CECs implanted into the liver parenchyma of laboratory CLF model animals have a functional activity.

The authors declare no conflict of interest.

REFERENCES

1. *Salim MS, Issa AM, Farrag ARH, Gabr H.* Decellularized liver bioscaffold: a histological and immunohistochemical comparison between normal, fibrotic and hepatocellular carcinoma. *Clin Exp Hepatol.* 2019; 5 (1): 35–47. doi: 10.5114/ceh.2019.83155.
2. *Acun A, Oganesyan R, Uygun BE.* Liver bioengineering: promise, pitfalls, and hurdles to overcome. *Curr Transplant Rep.* 2019; 6 (2): 119–126. doi: 10.1007/s40472-019-00236-3.
3. *Mazza G, Al-Akkad W, Rombouts K, Pinzani M.* Liver tissue engineering: from implantable tissue to whole organ engineering. *Hepatol Commun.* 2017; 2 (2): 131–141. doi: 10.1002/hep4.1136.
4. *Elchaninov A, Fatkhudinov T, Usman N, Arutyunyan I, Makarov A, Lokhonina A et al.* Multipotent stromal cells stimulate liver regeneration by influencing the macrophage polarization in rat. *World J Hepatol.* 2018; 10 (2): 287–296. doi: 10.4254/wjh.v10.i2.287.
5. *Crapo PM, Gilbert TW, Badylak SF.* An overview of tissue and whole organ decellularization processes. *Biomaterials.* 2011; 32 (12): 3233–3243. doi: 10.1016/j.biomaterials.2011.01.057.
6. *Uygun BE, Yarmush ML, Uygun K.* Application of whole-organ tissue engineering in hepatology. *Nature Reviews Gastroenterology & Hepatology.* 2012; 9 (12): 738–744. doi: 10.1038/nrgastro.2012.140.
7. *Rossi EA, Quintanilha LF, Nonaka CKV, Souza BSF.* Advances in hepatic tissue bioengineering with decellularized liver bioscaffold. *Stem Cells Int.* 2019; 2019: 2693189. doi: 10.1155/2019/2693189.
8. *Ferng AS, Connell AM, Marsh KM, Qu N, Medina AO, Bajaj N et al.* Acellular porcine heart matrices: whole organ decellularization with 3D-bioscaffold & vascular preservation. *J Clin Transl Res.* 2017; 3 (2): 260–270.
9. *Figliuzzi M, Bonandrini B, Remuzzi A.* Decellularized kidney matrix as functional material for whole organ tissue engineering. *J Appl Biomater Funct Mater.* 2017; 15 (4): e326–e333. doi: 10.5301/jabfm.5000393.
10. *Kuna VK, Kvarnström N, Elebring E, Holgersson SS.* Isolation and decellularization of a whole porcine pancreas. *J Vis Exp.* 2018; (140): 58302. doi: 10.3791/58302. PMID: 30371658.
11. *Daryabari SS, Kajbafzadeh AM, Fendereski K, Ghorbani F, Dehnavi M, Rostami M et al.* Development of an efficient perfusion-based protocol for whole-organ decellularization of the ovine uterus as a human-sized model and in vivo application of the bioscaffolds. *J Assist Reprod Genet.* 2019; 36 (6): 1211–1223. doi: 10.1007/s10815-019-01463-4.
12. *Gautier SV, Sevastyanov VI, Shagidulin MYu, Nemets EA, Basok YuB*. Tkanespetsificheskiy matriks dlya tkanevoy inzhenerii parenkhimatoznogo organa i sposob ego polucheniya. Patent na izobretenie RU 2693432 C2, 02.07.2019.
13. *Shumakov VI, Onishhenko NA.* Biologicheskie rezervy kletok kostnogo mozga i korrekcija organnyh disfunkcij: [monografija]. M.: Lavr, 2009. 307.
14. *Gautier SV, Shagidulin MYu, Onishhenko NA, Krasheninnikov ME, Nikol'skaja AO, Bashkina LV, Sevast'janov VI.* Sposob lechenija pechenochnoj nedostatochnosti. Patent na izobretenie RU 2586952 C1, 10.06.2016.
15. *Shagidulin MYu, Onishchenko NA, Krasheninnikov ME, Iljinsky IM, Mogeiko NP, Shmerko NP et al.* Survival of liver cells, immobilized on 3d-matrixes, in liver failure model. *Russian Journal of Transplantology and Artificial Organs.* 2011; 13 (3): 59–66. [In Russ, English abstract]. doi: 10.15825/1995-1191-2011-3-59-66.
16. *Nikol'skaja AO, Gonikova ZZ, Kirsanova LA, Shagidulin MJu, Onishhenko NA, Sevast'janov VI.* Sposob modelirovanija tjazhjologo spontanno neobratimogo povrezhdenija pecheni. Patent na izobretenie RU 2633296 C, 11.10.2017.
17. *Shagidulin MYu, Onishchenko NA, Krasheninnikov ME, Nikol'skaja AO, Volkova EA, Il'inskij IM et al.* The influence of the ratio of liver cells and bone marrow in the implantable cell-engineering structures of the liver on the recovery efficiency of functional and morphological parameters in chronic liver failure. *Russian Journal of Transplantology and Artificial Organs.* 2019; 21 (1): 122–134. [In Russ, English abstract]. doi: 10.15825/1995-1191-2019-1-122-134.
18. *Avtandilov GG.* Medicinskaja morfometrija. Rukovodstvo. M.: Medicina, 1990. 384.
19. *Ishak K., Baptista A, Bianchi L, Callea F, Grootes J et al.* Gistologicheskaya ocenka stadii i stepeni hronicheskogo gepatita. *Klinicheskaya gepatologiya*. 2010; 2: 8–11.

The article was submitted to the journal on 14.10.2020

DOI: 10.15825/1995-1191-2020-4-98-104

NATURAL SILK FIBER MICROCARRIERS FOR CELL CULTURE

M.M. Bobrova, L.A. Safonova, A.E. Efimov, O.I. Agapova, I.I. Agapov

Shumakov National Medical Research Center of Transplantology and Artificial Organs, Moscow, Russian Federation

The development of effective and versatile microcarriers is a pressing issue in tissue engineering and regenerative medicine. The **objective** of this work is to create biocompatible fiber microparticles from the cocoons of the *Bombyx mori* silkworm, and to study their structure and biological properties. **Materials and methods.** In obtaining microparticles, the *Bombyx mori* cocoons washed from sericin were cryo-milled in liquid nitrogen. The structure of the resulting microparticles was analyzed via scanning electron microscopy. The cytotoxicity of the obtained fibers was assessed using MTT-cell culture assay of 3T3 mouse fibroblasts. Cell adhesion analysis was performed using the Hep-G_2 human hepatocarcinoma cell line. Cell visualization was performed by staining the nuclei with DAPI fluorescent dye. **Results.** Natural silk microparticles were obtained in the form of cylindrical fibers with 200–400 μm average length and 15 μm diameter. It was shown that the surface of the resulting microparticles has a rough relief; no pores were found. The microparticles are non-toxic for 3T3 mouse fibroblasts, they maintain a high level of adhesion by human hepatocellular carcinoma $HepG_2$ cells. **Conclusion.** The method developed by us for fabrication of biocompatible silk fibroin microparticles in the form of fibers without using toxic reagents and significant time costs is promising for cell cultivation and delivery to the damaged area for tissue and organ regeneration.

Keywords: microcarriers, silk fibroin, fibers.

INTRODUCTION

The traditionally used two-dimensional cell culturing distorts to some extent cell behavior and its biological functions in comparison to cells in native tissue [1, 2]. For example, 2D *in vitro* cultivation of tumor cells showed slower tumor growth and lower drug resistance compared to tumors in vivo, which leads to lower efficiency of screening and drug testing [3, 4]. Therapeutic use of cell culture is also ineffective because of the low level of cell viability and, as a consequence, minimal efficiency of regeneration of damaged tissue [5–7]. This is mainly due to the fact that in a 2D *in vitro* culture, cells are unable to recreate effective and multidirectional cell-cell and cell-extracellular matrix interactions present in the native microenvironment, which causes changes in cell morphology and gene expression. To obtain cells with normal morphology, metabolism, and functions, 3D culturing of cells on different microcarriers is used [8, 9].

In regenerative medicine, microcarriers are widely used both as a substrate for culturing various cell types and as a means of cell delivery to the damaged tissue or organ area [10]. When microcarriers are used as a delivery system, cells remain viable for a longer period of time [11], which allows them to secrete growth factors and actively participate in the formation of the intercellular matrix, promoting tissue regeneration [12]. Both natural and synthetic biopolymers are used to obtain microcarriers of various types and for regeneration of various tissues [13–16].

One of the promising materials for creating biocompatible microcarriers for tissue engineering and regenerative medicine is silk fibroin from the cocoons of the *Bombyx mori* silkworm [17]. The structure of silk fibroin provides unique properties that allow it to be used as a material for tissue engineering. The main advantage of silk over other biocompatible materials lies in its mechanical properties. The advantages of fibroin as a material used in regenerative medicine include the fact that fibroin-based constructs are biodegradable and biocompatible, they can be obtained under mild conditions and their production does not require special chemical treatment. Silk fibroin promotes cell adhesion, proliferation and differentiation, including with regard to mesenchymal stem cells [18–20]. For instance, silk fibroin-based microparticles are used for bone tissue [21] and nervous tissue [22] regeneration, as well as stem cell delivery [23]. Thus, fibroin has unique properties that makes it possible to form from it 2D and 3D constructs, including microcarriers, and widely use it as a biocompatible material in various areas of tissue engineering.

In this study, biocompatible microcarriers were developed from *Bombyx mori* silkworm cocoons in the form of fibers, their structure was studied, and the possibility of their application in tissue engineering was shown.

Corresponding author: Igor Agapov. Address: 1, Shchukinskaya str., 123182, Moscow, Russian Federation.
Phone: (499) 190-66-19. E-mail: igor_agapov@mail.ru

MATERIALS AND METHODS

Obtaining microcarriers

Cocoons from mulberry silkworm *Bombyx mori*, provided by Bogoslovsky V.V. (Zheleznovodsk, Stavropol Krai), director of the Republican Research Station for Silkworm Breeding, were used as a source of silk fibroin fibers. At the first stage, the cocoons were purified of sericin according to the following procedure. 1 g of silk from cocoons was boiled in 500 mL of double-distilled water water with 1260 mg of soda for 40 min in a water bath, then washed with 3.6 L of distilled water. Next, it was boiled in 500 mL of double-distilled water water for 30 minutes and washed with 3.6 L of distilled water. The last procedure was repeated 3 times. The purified silk fibroin was air-dried at room temperature. Then silk fibroin weighing 80 mg was placed in a 3% aqueous solution of glycerin, incubated for 120 minutes and frozen in liquid nitrogen, after which the fibroin was crushed for 5 minutes using a mortar and pestle to an average fiber size of 200–400 μm. The resulting fibers were transferred into 5 mL of 70% ethanol for 30 minutes, and then the ethanol was changed [24].

Analysis of microcarrier structure by scanning electron microscopy

The fiber samples under study were fixed in a 2.5% glutaraldehyde solution in phosphate-buffered saline with pH = 7.4 for 2 hours in the dark at 4 °C, the samples were washed of the fixing solution with phosphate-buffered saline (pH = 7.4) 5 times for 5 minutes each. Then the samples were dehydrated with increasing ethanol concentrations. Ethanol concentrations used were 10%, 20%, 50%, 70% and 96%, the samples were incubated for 1 hour in ethanol of each concentration. Samples were then transferred to acetone for 30 minutes, and then the acetone was changed.

The samples were dried by critical point transition ($T_{cr.CO_2}$ = 31 °C, $p_{cr.CO_2}$ = 72.8 kg/cm^2)) using a K850 unit (Quorum Technologies, UK). The dried samples were coated with a 10 nm thick gold layer in argon atmosphere at 20 mA ion current and 1 mbar pressure using the Q150R ES vacuum sputtering machine (Quorum Technologies, Great Britain). The obtained samples were analyzed using a Tescan Vega3 SBU scanning electron microscope (Tescan, Czech Republic) at 15 kV operating voltage. Images were obtained and analyzed using the VegaTC software (Tescan, Czech Republic).

Analysis of microcarrier cytotoxicity

The mouse 3T3 fibroblast cell line was used in the experiments. Cells were cultured in plastic vials in DMEM low glucose medium containing 10% fetal bovine serum, 0.324 mg/mL glutamine and 10 mg/mL gentamicin at 37 °C, 5% CO_2. The culture medium was changed every 48 hours. Cell monolayer was disaggregated using a trypsin-Versene solution. Cells were counted in the Goryaev chamber and seeded in a 1 : 3 ratio.

Cytotoxicity of all obtained samples was analyzed in accordance with the GOST ISO 10993-5-2011 standard [25] using the MTT test [26] in the mouse 3T3 fibroblast cell line model.

For this purpose, mouse 3T3 fibroblasts were cultured in 300 μL of culture medium in a 96-well plate in a thermostat at 37 °C and 5% CO_2 for 3 days. Then, the culture medium was changed and 50 μL of fiber suspension was added to the wells of the plate. The culture plate was used as a control. The plates were incubated in an incubator at 37 °C, 5% CO_2. Cytotoxicity was assessed on days 3, 5 and 7 of the experiment. For this purpose, 60 μL of MTT solution with 5 mg/mL concentration was added to each well of the plate. It was incubated in a thermostat at 37 °C and 5% CO_2 for 4 hours until dark blue crystals of formazan precipitated out. Fibers were then removed from the wells, and the plate was centrifuged for 5 minutes at 885 g. The supernatant was removed, the formazan precipitate was dissolved in 300 μL dimethyl sulfoxide for 20 minutes, and the optical density of the solution was measured at 540 nm wavelength on a Picon device (Picon incorporated company, Uniplan, Russia).

Analysis of cell adhesion on microcarriers

Human liver cancer cell line Hep-G2 was used in the experiments. The cells were incubated in plastic culture vials in a 1 : 1 mixture in DMEM high glucose medium and in Ham's F-12 medium containing 10% fetal bovine serum, 0.324 mg/mL glutamine and 10 mg/mL gentamicin at 37 °C, 5% CO_2.

The experiment was performed in a 96-well plate. For the experiment, a 150 μL fiber suspension was transferred to the wells of the plate. The culture plate was used as a control. Sterile phosphate-salt buffer solution (pH = 7.4) was then added to the wells of the plate and incubated for 15 minutes, after which the phosphate-buffered saline was changed. This procedure was repeated three times. Next, 300 μL of incubation medium was added to the plate wells for 30 minutes.

Cell suspension in the incubation medium was transferred to 96-well plates at 1000 cells per well. The plates were incubated in a thermostat at 37 °C and 5% CO_2 for 7 days.

Cell adhesion was assessed visually using a Carl Zeiss Axio Vert.A1 microscope (Zeiss, Germany). For this purpose, samples were stained with DAPI fluorescent dye, which binds to cell DNA. Before staining, samples were washed twice of the incubation medium and non-adherent cells with phosphate-buffered saline (pH = 7.4). Afterwards, an aqueous dye solution with 3 μg/mL concentration was added at a rate of 300 μL per well and incubated in the incubation chamber at 37 °C and 5% CO_2 for 5 minutes. Samples were then washed twice with phosphate-buffered saline (pH = 7.4) to remove unbound dye. The obtained samples were analyzed on a

Fig. 1. Fabrication of fiber microcarriers. a) *Bombyx mori* silkworm cocoons; b) sericin-free silk fibroin; c) fiber microcarriers. Scale bar 100 μm

fluorescence microscope using a filter with 360–370 nm excitation range, and 420–470 nm emission range.

Cell images were obtained using an Axiocam 305 color camera (Carl Zeiss, Germany). The images were processed using the Zen 2.3 Blue Edition software (Carl Zeiss, Germany).

Statistical processing of results

The data were processed by analysis of variance. Statistical significance of the results was assessed using the Mann–Whitney U test. The statistical significance level α was taken to be 0.05.

RESULTS AND DISCUSSION

In this study, a suspension of microparticles from the cocoons of the *Bombyx mori* silkworm was obtained using cryogenic grinding (Fig. 1). The microparticles are cylindrical fragments of silkworm cocoon fibers, 200–400 μm in average length and 15 μm in diameter. This microparticle shape has a high surface area to volume ratio and, therefore, a larger surface area available for cell adhesion and for formation of more cell contacts compared to spherical particles. Silk fibroin is one of the promising materials for tissue engineering due to a unique combination of mechanical properties and a high level of biocompatibility and can be used in many areas of tissue engineering, both as an independent material for creating constructs and as a carrier for cell delivery or targeted drug delivery [27]. The advantage of the proposed technology for the manufacture of microcarriers in the form of fibers is to obtain biocompatible carriers for cells of controlled size and shape without the use of toxic reagents and significant time costs. The size and shape of the microcarriers can be regulated by varying the cryogenic grinding time and the volume of the washed silk fibroin. Also, the shape of microcarriers in the form of fiber allows for easier positioning of the cells during targeted delivery and facilitates cell orientation.

The structure of the resulting microcarriers was studied by scanning electron microscopy. The surface of the fibers has micro- and nanorelief in the form of roughness (Fig. 2). This method did not reveal any pores in the microcarrier structure. The surface structure of the construct is known to influence cell adhesion [28, 29]. This is because the presence of roughness on the substrate surface increases the surface area available for cell adhesion. At the same time, there is an optimal level of substrate roughness for each cell culture [30].

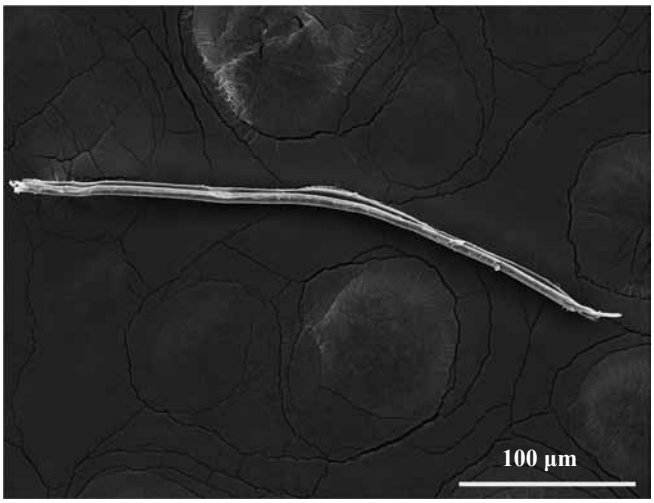

Fig. 2. Image of a microcarrier obtained using scanning electron microscopy. Scale bar 100 μm

The resulting microcarriers were tested for cytotoxicity by MTT. During the study, the effect of samples on the number of cells cultured on the plate was evaluated. The culture plate was used as a control. No cytotoxic effect of the obtained fibers was detected during the experiment; the number of cells did not differ in the experimental and control samples.

The analysis of cell adhesion on the obtained microcarriers in the form of fibers was performed visually using a fluorescent microscope; the cells were pre-stained with the DAPI fluorescent dye to visualize the nuclei. Fibers were positioned in the wells of culture plates; the culture plate was used as a control. The studies were carried out using human liver cancer cell line Hep-G2. The experimental results are shown in Fig. 3.

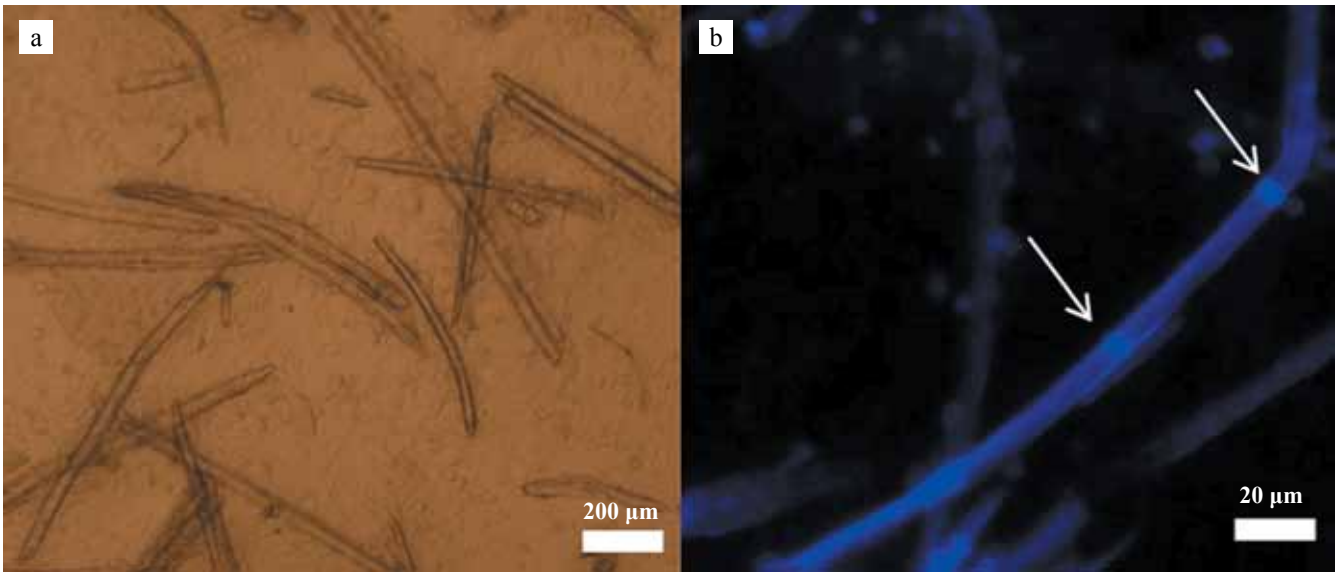

Fig. 3. Adhesion of Hep-G_2 cells on the obtained microcarriers. a) optical image, scale bar 200 μm; b) fluorescent image, nuclei of dapi-stained adherent cells are indicated by arrows, scale bar 20 μm

Cell morphology was assessed using a light microscope; cells formed filopodia and adhered tightly to the substrate, while cell adhesion occurring irregularly. It was found that the obtained microcarriers were biocompatible and maintained a high level of cell adhesion, which can be attributed to the optimal level of fiber roughness and biocompatible properties of silk fibroin [31, 32]. Thus, the resulting silk fibroin microcarriers in the form of fibers are biocompatible and can be further used in regenerative medicine as universal carriers for cells obtained without the use of toxic reagents and significant time costs.

CONCLUSION

As part of the presented work, microparticles were obtained from the cocoons of the *Bombyx mori* silkworm in the form of fibers with 200–400 μm average length and 15 μm diameter. It was shown that the surface of the obtained microparticles has a rough relief; no pores were detected. The microparticles are non-toxic for the culture of mouse 3T3 fibroblast cells, they maintain a high level of cell adhesion of human liver cancer cell line Hep-G2. The technique developed by us for creating biocompatible microcarriers from *Bombyx mori* silkworm cocoons in the form of fibers is promising for cell culture and cell delivery to the damaged area for tissue and organ regeneration.

The authors declare no conflict of interest.

REFERENCES

1. *Asghar W, El Assal R, Shafiee H, Pitteri S, Paulmurugan R, Demirci U*. Engineering cancer microenvironments for *in vitro* 3-D tumor models. *Mater Today (Kidlington)*. 2015; 18 (10): 539–553. doi: 10.1016/j.mattod.2015.05.002. PMID: 28458612.
2. *In JG, Foulke-Abel J, Estes MK, Zachos NC, Kovbasnjuk O, Donowitz M*. Human mini-guts: new insights into intestinal physiology and host-pathogen interactions. *Nat Rev Gastroenterol Hepatol*. 2016; 13 (11): 633–642. doi: 10.1038/nrgastro.2016.142. PMID: 27677718.
3. *Edmondson R, Broglie JJ, Adcock AF, Yang L*. Three-dimensional cell culture systems and their applications in drug discovery and cell-based biosensors. *Assay Drug Dev Technol*. 2014; 12 (4): 207–218. doi: 10.1089/adt.2014.573. PMID: 24831787.
4. *Skardal A, Devarasetty M, Rodman C, Atala A, Soker S*. Liver-Tumor Hybrid Organoids for Modeling Tumor Growth and Drug Response *In Vitro*. *Ann Biomed Eng*. 2015; 43 (10): 2361–2373. doi: 10.1007/s10439-015-1298-3. PMID: 25777294.
5. *Bao J, Shi Y, Sun H, Yin X, Yang R, Li L et al.* Construction of a portal implantable functional tissue-engineered liver using perfusion-decellularized matrix and hepatocytes in rats. *Cell Transplant.* 2011; 20 (5): 753–766. doi: 10.3727/096368910X536572.
6. *Soto-Gutierrez A, Zhang L, Medberry C, Fukumitsu K, Faulk D, Jiang H et al*. A whole-organ regenerative medicine approach for liver replacement. *Tissue Eng Part C Methods*. 2011; 17 (6): 677–686. doi: 10.1089/ten.TEC.2010.0698. PMID: 21375407.
7. *Zhou P, Lessa N, Estrada DC, Severson EB, Lingala S, Zern MA et al*. Decellularized liver matrix as a carrier for the transplantation of human fetal and primary hepatocytes in mice. *Liver Transpl*. 2011; 17 (4): 418–427. doi: 10.1002/lt.22270. PMID: 21445925.
8. *Pampaloni F, Reynaud EG, Stelzer EH*. The third dimension bridges the gap between cell culture and live tissue. *Nat Rev Mol Cell Biol.* 2007; 8 (10): 839–845. doi: 10.1038/nrm2236. PMID: 17684528.
9. *Achilli TM, Meyer J, Morgan JR*. Advances in the formation, use and understanding of multi-cellular spheroids. *Expert Opin Biol Ther*. 2012; 12 (10): 1347–1360. doi: 10.1517/14712598.2012.707181. PMID: 22784238.

10. *Chen AK, Reuveny S, Oh SK*. Application of human mesenchymal and pluripotent stem cell microcarrier cultures in cellular therapy: achievements and future direction. *Biotechnol Adv*. 2013; 31 (7): 1032–1046. doi: 10.1016/j.biotechadv.2013.03.006. PMID: 23531528.
11. *Quittet MS, Touzani O, Sindji L, Cayon J, Fillesoye F, Toutain J et al.* Effects of mesenchymal stem cell therapy, in association with pharmacologically active microcarriers releasing VEGF, in an ischaemic stroke model in the rat. *Acta Biomater*. 2015; 15: 77–88. doi: 10.1016/j.actbio.2014.12.017. PMID: 25556361.
12. *Georgi N, van Blitterswijk C, Karperien M.* Mesenchymal stromal/stem cell-or chondrocyte-seeded microcarriers as building blocks for cartilage tissue engineering. *Tissue Eng Part A*. 2014; 20 (17–18): 2513–2523. doi: 10.1089/ten.TEA.2013.0681. PMID: 24621188.
13. *Yang Y, Rossi FM, Putnins EE*. *Ex vivo* expansion of rat bone marrow mesenchymal stromal cells on microcarrier beads in spin culture. *Biomaterials*. 2007; 28 (20): 3110–3120. doi: 10.1016/j.biomaterials.2007.03.015. PMID: 17433434.
14. *Chen M, Wang X, Ye Z, Zhang Y, Zhou Y, Tan WS*. A modular approach to the engineering of a centimeter-sized bone tissue construct with human amniotic mesenchymal stem cells-laden microcarriers. *Biomaterials*. 2011; 32 (30): 7532–7542. doi: 10.1016/j.biomaterials.2011.06.054. PMID: 21774980.
15. *Zhou Y, Yan Z, Zhang H, Lu W, Liu S, Huang X et al*. Expansion and delivery of adipose-derived mesenchymal stem cells on three microcarriers for soft tissue regeneration. *Tissue Eng Part A*. 2011; 17 (23–24): 2981–2997. doi: 10.1089/ten.tea.2010.0707. PMID: 21875329.
16. *Sun LY, Hsieh DK, Syu WS, Li YS, Chiu HT, Chiou TW.* Cell proliferation of human bone marrow mesenchymal stem cells on biodegradable microcarriers enhances *in vitro* differentiation potential. *Cell Prolif*. 2010; 43 (5): 445–456. doi: 10.1111/j.1365-2184.2010.00694.x. PMID: 20887551.
17. *Agapov II, Moisenovich MM, Vasilyeva TV, Pustovalova OL, Kon'kov AS, Arkhipova AY et al*. Biodegradable matrices from regenerated silk of *Bombix mori*. *Dokl Biochem Biophys*. 2010; 433: 201–204. doi: 10.1134/S1607672910040149.
18. *Uebersax L, Merkle HP, Meinel L*. Insulin-like growth factor I releasing silk fibroin scaffolds induce chondrogenic differentiation of human mesenchymal stem cells. *J Control Release*. 2008; 127 (1): 12–21. doi: 10.1016/j.jconrel.2007.11.006. PMID: 18280603.
19. *Altman AM, Gupta V, Ríos CN, Alt EU, Mathur AB*. Adhesion, migration and mechanics of human adipose-tissue-derived stem cells on silk fibroin-chitosan matrix. *Acta Biomater*. 2010; 6 (4): 1388–1397. doi: 10.1016/j.actbio.2009.10.034. PMID: 19861180.
20. *Kotliarova MS, Zhuikov VA, Chudinova YV Khaidapova DD, Moisenovich AM, Kon'kov AS et al.* Induction of osteogenic differentiation of osteoblast-like cells MG-63 during cultivation on fibroin microcarriers. *Moscow Univ Biol Sci Bull.* 2016; 71: 212–217. doi: 10.3103/S0096392516040052.
21. *Luetchford KA, Chaudhuri JB, De Bank PA.* Silk fibroin/gelatin microcarriers as scaffolds for bone tissue engineering. *Mater Sci Eng C Mater Biol Appl*. 2020; 106: 110116. doi: 10.1016/j.msec.2019.110116. PMID: 31753329.
22. *Moisenovich MM, Plotnikov EY, Moysenovich AM, Silachev DN, Danilina TI, Savchenko ES et al*. Effect of Silk Fibroin on Neuroregeneration After Traumatic Brain Injury. *Neurochem Res*. 2019; 44 (10): 2261–2272. doi: 10.1007/s11064-018-2691-8. PMID: 30519983.
23. *Perteghella S, Martella E, de Girolamo L, Perucca Orfei C, Pierini M, Fumagalli V et al.* Fabrication of Innovative Silk/Alginate Microcarriers for Mesenchymal Stem Cell Delivery and Tissue Regeneration. *Int J Mol Sci*. 2017; 18 (9): 1829. doi: 10.3390/ijms18091829. PMID: 28832547.
24. *Agapov II, Agapova OI, Bobrova MM, Safonova LA, Efimov AE*. Mikronositel' dlya kletok na osnove natural'nogo shelka i sposob ego polucheniya. Patent na izobretenie RU2732598 S1, 21.09.2020.
25. GOST ISO 10993-1-2011 "Izdeliya meditsinskie. Otsenka biologicheskogo deystviya meditsinskikh izdeliy. Chast' 5. Issledovanie na tsitotoksichnost': metody *in vitro*". M.: Standartinform, 2014.
26. *Mosmann T*. Rapid colorimetric assay for cellular growth and survival: application to proliferation and cytotoxicity assays. *J Immunol Methods*. 1983; 65 (1–2): 55–63. doi: 10.1016/0022-1759(83)90303-4. PMID: 6606682.
27. *Kundu B, Rajkhowa R, Kundu SC, Wang X*. Silk fibroin biomaterials for tissue regenerations. *Adv Drug Deliv Rev*. 2013; 65 (4): 457–470. doi: 10.1016/j.addr.2012.09.043. PMID: 23137786.
28. *Zhang Q, Zhao Y, Yan S, Yang Y, Zhao H, Li M et al*. Preparation of uniaxial multichannel silk fibroin scaffolds for guiding primary neurons. *Acta Biomater*. 2012; 8 (7): 2628–2638. doi: 10.1016/j.actbio.2012.03.033. PMID: 22465574.
29. *Safonova LA, Bobrova MM, Agapova OI, Kotliarova MS, Arkhipova AYu, Moisenovich MM, Agapov II*. Biological Properties of Regenerated Silk Fibroin Films. *Sovremennye tehnologii v medicine*. 2015; 7 (3): 6–13. [In English]. doi: 10.17691/stm2015.7.3.01.
30. *Surguchenko VA, Ponomareva AS, Efimov AE, Nemets EA, Agapov II, Sevastianov VI.* Characteristics of adhesion and proliferation of mouse nih/3t3 fibroblasts on the poly(3-hydroxybutyrate-co-3-hydroxyvalerate) films with different surface roughness values. *Russian Journal of Transplantology and Artificial Organs*. 2012; 14 (1): 72–77. [In Russ. English abstract]. doi: 10.15825/1995-1191-2012-1-72-77.
31. *Servoli E, Maniglio D, Motta A, Predazzer R, Migliaresi C*. Surface properties of silk fibroin films and their interaction with fibroblasts. *Macromol Biosci*. 2005; 5 (12): 1175–1183. doi: 10.1002/mabi.200500137. PMID: 16315185.
32. *Sokolova AI, Bobrova MM, Safonova LA, Agapova OI, Moisenovich MM, Agapov II.* The Relation of Biological Properties of the Silk Fibroin/Gelatin Scaffolds with the Composition and Fabrication Technology. *Sovremennye tehnologii v medicine*. 2016; 8 (3): 6–15. [In English]. doi: 10.17691/stm2016.8.3.01.

The article was submitted to the journal on 16.10.2020

DOI: 10.15825/1995-1191-2020-4-105-114

BIODEGRADABLE MATERIALS BASED ON NATURAL SILK FABRIC AS PROMISING SCAFFOLDS FOR TISSUE ENGINEERING AND REGENERATIVE MEDICINE

L.A. Safonova, M.M. Bobrova, A.E. Efimov, O.I. Agapova, I.I. Agapov

Shumakov National Medical Research Center of Transplantology and Artificial Organs, Moscow, Russian Federation

Objective: to develop a method for obtaining scaffolds based on natural silk fabric and to study their biocompatibility *in vitro*. **Materials and methods.** To obtain biodegradable scaffolds based on natural silk fabric, we propose treating natural silk fabric with a water-ethanol solution of calcium chloride. Differences in the structure of the resulting scaffolds were identified via scanning electron microscopy. **Conclusion.** The resulting scaffolds are non-toxic to cells and support cell adhesion and proliferation. Our studies make it possible to consider the resulting biodegradable scaffolds as promising constructs for tissue engineering and regenerative medicine.

Keywords: silk, natural silk fabric, biodegradable scaffolds, biodegradation rate.

INTRODUCTION

Development of biodegradable constructs (scaffolds) for regeneration of damaged organs and tissues is one of the most important and urgent problems in tissue engineering and regenerative medicine. Such constructs should be biocompatible, have high mechanical properties for surgical manipulations, and their biodegradation rate should be the same with the rate of regeneration of damaged tissue.

One of the most promising natural polymers for creating such constructs is silk fibroin produced by the Bombyx mori silkworm. Various groups of researchers have shown the successful application of silk fibroin-based constructs in many areas of tissue engineering, such as cultivation of cells of various species, regeneration of bone and cartilage tissue, regeneration of the skin, cornea, nervous tissue, etc [1–4].

The source of silk fibroin can be both silkworm cocoons and commercial products made from natural silk – sutures and woven materials. The use of suture and woven materials does not require multistage silk processing and production of regenerated silk fibroin solutions. This can be an advantage for solving a number of problems in tissue engineering and regenerative medicine.

The unique combination of high mechanical characteristics (such as strength and elasticity) with biocompatibility makes silk fibroin very suitable for reinforcing structures based on brittle and fragile materials with higher biological activity.

Silk fibroin-based constructs are positioned in tissue engineering and regenerative medicine as biodegradable. However, in some cases, the degradation period of these constructs can reach 1 year [5]. Many factors, such as the secondary structure of the polymer, polymer processing technology during production of the structure, source of silk, etc., can influence the value of the biodegradation rate of the resulting construct. The structure of silk fibroin provides the ability to control the rate of degradation of silk fibroin-based constructs, which can significantly expand the scope of application of silk fibroin in tissue engineering and regenerative medicine [6–8]. Therefore, development of methods for monitoring and regulating the degradation rate of silk fibroin-based constructs to increase the efficiency and expand the scope of their application is an urgent task.

One of the strategies for working in this direction is to use free chemical groups present in the structure of silk fibroin molecule. These groups can be linked by various crosslinking agents, such as glutaraldehyde and 1-Ethyl-3-(3-dimethylaminopropyl)carbodiimide (EDC) [9, 10]. By adjusting the silk fibroin crosslinking degree, the degradation rate of the resulting material can be changed. However, crosslinking agents can reduce the biocompatibility of a scaffold due to its toxicity. Moreover, the use of amino acid sequences does not in all cases have a significant effect on the rate of its biodegradation. At the same time, both methods can only reduce the degradation rate of silk fibroin-based constructs. However, in tissue engineering and regenerative medicine, rapid biodegradation of the material is often required for more efficient cell proliferation.

Another strategy is to create silk fibroin-based composite materials. Silk fibroin solutions are mixed with solutions of synthetic and natural materials used in tissue engineering and regenerative medicine, such as alginates, hyaluronic acid, gelatin, collagen, chitosan, polylactides,

Corresponding author: Igor Agapov. Address: 1, Schukinskaya str., Moscow, 123182, Russian Federation. Phone: (985) 231-60-42. E-mail: igor_agapov@mail.ru

polycaprolactone, etc. [11–16]. This makes it possible to create composite materials and composite constructs, whose degradation rate depends on the quantitative ratio of various substances that make up the construct. In this case, it becomes possible to both increase and decrease the biodegradation rate of the construct. However, introduction of composite additives is accompanied by a change in the structure of the construct and its mechanical properties, which limits the scope of application of such constructs in tissue engineering [17]. In addition, the degradation of some substances (for example, polylactides) introduced into the construct is accompanied by formation of products that cannot be incorporated into cell metabolism and create unfavorable conditions for their proliferation, which reduces the biocompatibility of the constructs [18].

We have previously proposed a method for regulating the biodegradation rate of natural silk tissues to obtain natural silk biodegradable scaffolds [19]. Within the framework of this study, various approaches to the use of natural silk fabrics for production of biodegradable scaffolds are shown, their structure and biocompatibility *in vitro* are studied.

MATERIALS AND METHODS

Obtaining biodegradable scaffolds

Natural silk fabrics were used to obtain biodegradable scaffolds. In this study, two types of fabrics of different densities were used: gas-chiffon (15 g/m^2 density) and double-sided satin (155 g/m^2 density). Fabric samples for research were obtained according to the method previously described by the authors [19].

The fabrics were preliminarily washed from impurities according to the following procedure. Fabric flaps were boiled in a water bath in a sodium bicarbonate solution prepared at 500 mL of double-distilled water, 1260 mg of sodium bicarbonate per 1 g of tissue for 40 minutes, then washed with 3.6 L of distilled water. Then it was boiled in 500 mL of double-distilled water for 30 minutes and washed with 3.6 L of distilled water. The last procedure was repeated 3 times. The fabric flaps were dried in air at room temperature. The obtained flaps were cut into 5 cm × 5 cm fragments. Group 1 and 4 samples were obtained in this manner (Table).

Next, the fabric fragments were processed according to the following procedure. At the first stage, the fabrics were incubated in a water-alcohol solution of calcium chloride containing 389 mg of $CaCl_2$, 388 μL of C_2H_5OH, and 544 μL of H_2O per 1 mL of solution for 45 minutes at 37 °C temperature. Then 16 washes were carried out with double-distilled water, 30 minutes each, and air-dried at room temperature. Group 2 and 5 samples were obtained in this manner (Table).

The fabric fragments were then incubated in type A gelatin solution with 20 mg/mL concentration for 1 hour and air-dried on the surface of polished Teflon at room temperature. The dried fabric fragments, treated with gelatin solution, were additionally put in a solution containing 30 mM EDC, 8 mM N-hydroxysuccinimide (NHS), 50 mM sodium dihydrogen phosphate, and 100 mM sodium chloride (pH = 6) for 2 hours at room temperature. Then 16 washes were carried out with double-distilled water, 30 minutes each, and air-dried at room temperature. Group 3 and 6 samples were obtained in this manner (Table).

Analysis of the surface structure of biodegradable scaffolds by scanning electron microscopy (SEM)

Samples of 8 mm × 8 mm biodegradable scaffolds were fixed with 2.5% glutaraldehyde solution in phosphate-buffered saline with pH = 7.4 for 2 hours in the dark at 4 °C, after which the samples were washed five times from the fixing solution with phosphate-buffered saline with pH = 7.4 for 10 minutes. Then the samples were dehydrated with increasing ethanol concentrations. Ethanol concentrations of 10%, 20%, 50%, 70% and 96% were used, incubating the samples for 1 hour in ethanol of each concentration. Samples were then transferred to acetone for 30 minutes, and then the acetone was changed.

The prepared samples were dried by critical point transition ($T_{cr.CO_2}$ = 31 °C, $p_{cr.CO_2}$ = 72.8 kg/cm^2) using a K850 unit (Quorum Technologies, UK). The dried samples were coated with a 10 nm thick gold layer in argon atmosphere at 20 mA ion current and 1 mbar pressure using the Q150R ES vacuum sputtering machine (Quorum Technologies, Great Britain). The obtained samples were analyzed using a Tescan Vega3 SBU scanning electron microscope (Tescan, Czech Republic) at 15 kV operating voltage. Images were obtained and analyzed using the VegaTC software (Tescan, Czech Republic).

Analysis of cytotoxicity of the obtained constructs

Mouse 3T3 fibroblast cell line was used in the experiments. Cells were cultured in plastic vials in DMEM low glucose medium containing 10% fetal bovine serum, 0.324 mg/mL glutamine and 10 mg/mL gentamicin at 37 °C, 5% CO_2. The culture medium was changed every 48 hours. Cell monolayer was disaggregated using a trypsin-Versene solution. Cells were counted in the Goryaev chamber and seeded in a 1 : 3 ratio.

Cytotoxicity of all obtained samples was analyzed in accordance with the GOST ISO 10993-5-2011 standard "Medical devices. Assessment of the biological effect of medical devices. Part 5. Cytotoxicity studies: *in vitro* methods" using the MTT test [20] in the mouse 3T3 fibroblast cell line model.

For this purpose, mouse 3T3 fibroblasts were cultured in 300 μL of culture medium in a 96-well plate in a thermostat at 37 °C and 5% CO_2 for 3 days. Samples of 3 mm × 3 mm biodegradable scaffolds were sterilized in an MLS-3020U autoclave (Sanyo, Japan) at 121 °C for 15 minutes. Before the test, the culture medium was changed, and sterile samples of biodegradable scaffolds were introduced into the plate wells. The culture plate was used as a control. The plates were incubated in a thermostat at 37 °C, 5% CO_2. Cytotoxicity was assessed on days 3, 5 and 7 of the experiment. For this purpose, 60 μL of MTT solution with 5 mg/mL concentration was added to each well of the plate. It was incubated in a thermostat at 37 °C and 5% CO_2 for 4 hours until dark blue crystals of formazan precipitated out. The biodegradable scaffold samples were then removed from the wells, and the plate was centrifuged for 5 minutes at 885 g. The supernatant was removed, the formazan precipitate was dissolved in 300 μL of dimethyl sulfoxide for 20 minutes, and the optical density of the solution was measured at 540 nm wavelength.

Analysis of cell adhesion and proliferative activity on the obtained constructs

Human liver cancer cell line Hep-G2 was used in the experiments. The cells were cultured in plastic vials in a 1 : 1 mixture in DMEM high glucose medium and in Ham's F-12 medium containing 10% fetal bovine serum, 0.324 mg/mL glutamine and 10 mg/mL gentamicin at 37 °C, 5% CO_2. The culture medium was changed every 48 hours. Cell monolayer was disaggregated using a trypsin-Versene solution. Cells were counted in a Goryaev chamber and seeded in a 1 : 3 ratio.

Samples of 4 mm × 4 mm biodegradable scaffolds were sterilized in an MLS-3020U autoclave (Sanyo, Japan) at 121 °C for 15 minutes. Sterile 4 mm × 4 mm biodegradable scaffold samples were positioned in the wells of sterile 96-well culture plates. The culture plate was used as a control. Sterile phosphate-salt buffer solution was added to the wells of the plate and incubated for 15 minutes, after which the phosphate-buffered saline was changed. This procedure was repeated three times. Next, 300 μL of incubation medium was added to the plate wells for 30 minutes.

Cell suspension in the incubation medium was transferred to 96-well plates at 1000 cells per well in 300 μL of the incubation medium. The plates were incubated in a thermostat at 37 °C and 5% CO_2.

Cell adhesion was assessed visually using a Carl Zeiss Axio Vert.A1 microscope (Zeiss, Germany). Cell proliferative activity was assessed on days 3, 5 and 7 of the experiment using MTT [20]. To this end, 50 μL of a 3-(4,5-Dimethylthiazol-2-yl)-2,5-diphenyltetrazolium bromide (MTT) solution with a 200 μg/mL concentration was added to each well of the plate. The plates were incubated in a thermostat at 37 °C and 5% CO_2 for 4 hours until dark blue formazan crystals precipitated, and then centrifuged for 5 minutes at 885 g. The supernatant was removed, the formazan precipitate was dissolved in dimethyl sulfoxide at 300 μL of dimethyl sulfoxide per well. The optical density of the solution was measured at 540 nm wavelength.

Statistical data processing

The statistical significance of the results was assessed using the Mann–Whitney U test. The statistical significance level α was taken to be 0.05.

RESULTS

In this study, 6 groups of scaffold samples were obtained on the basis of two varieties of natural silk fabrics with different densities (Fig. 1). The composition of the samples of each group is described in Table.

Table

Samples of natural silk fabric-reinforced scaffolds obtained during the study

Group	Natural silk fabric used as the base for scaffold	Natural silk fabric processing method
1	Gas-chiffon (density 15 g/m^2)	1) Washing the fabric of impurities
2	Gas-chiffon (density 15 g/m^2)	1) Washing the fabric of impurities 2) Treatment with a water-ethanol solution of calcium chloride
3	Gas-chiffon (density 15 g/m^2)	1) Washing the fabric of impurities 2) Treatment with a water-ethanol solution of calcium chloride 3) Treatment with gelatin solution, covalent crosslinking with an EDC/NHS solution
4	Double-sided satin (density 155 g/m^2)	1) Washing the fabric of impurities
5	Double-sided satin (density 155 g/m^2)	1) Washing the fabric of impurities 2) Treatment with a water-ethanol solution of calcium chloride
6	Double-sided satin (density 155 g/m^2)	1) Washing the fabric of impurities 2) Treatment with a water-ethanol solution of calcium chloride 3) Treatment with gelatin solution, covalent crosslinking with an EDC/NHS solution

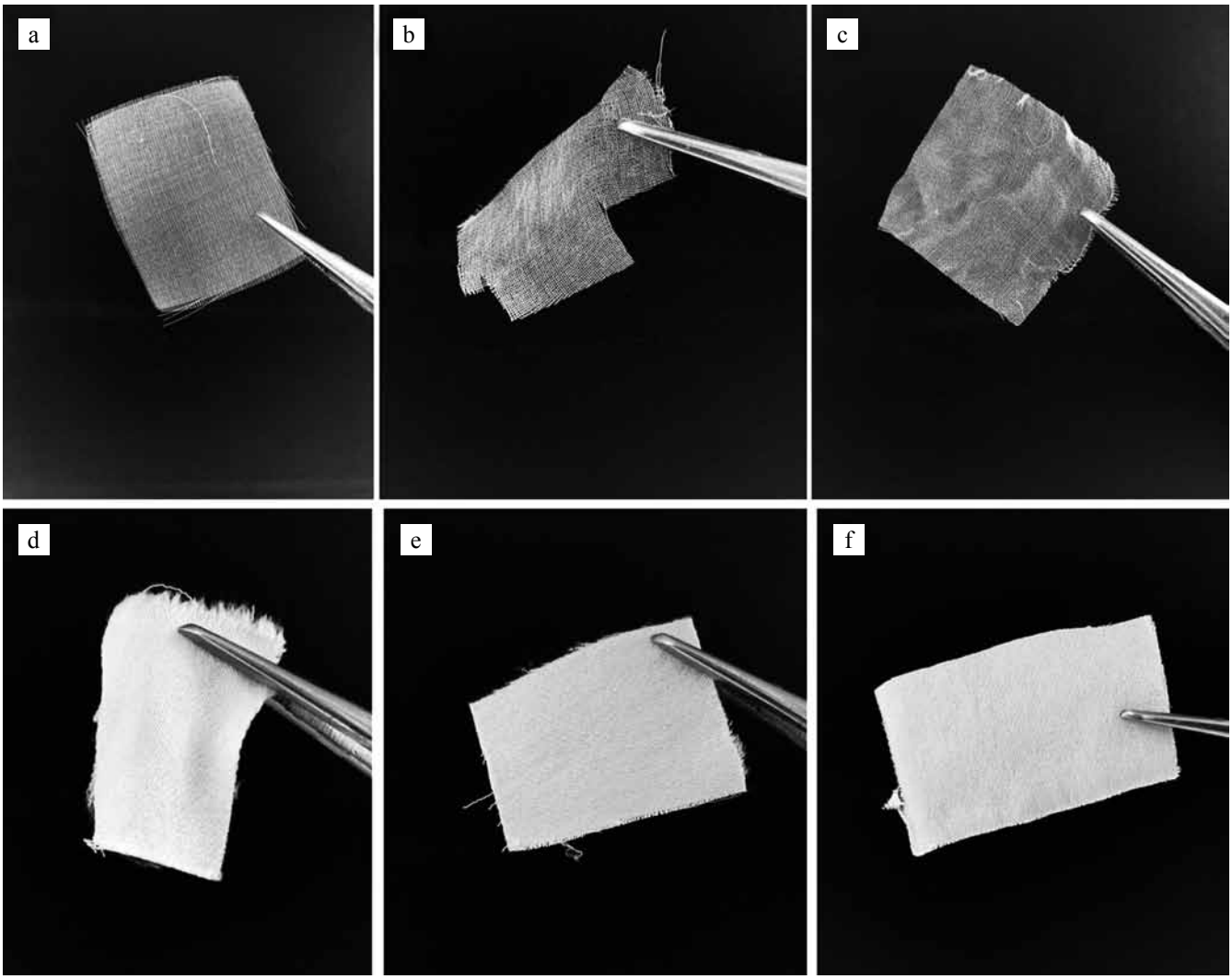

Fig. 1. Samples of natural silk fabric-reinforced scaffolds obtained during the study: a) Group 1, b) Group 2, c) Group 3, d) Group 4, e) Group 5, f) Group 6

The structure of the resulting scaffolds was studied by SEM (Fig. 2, 3). According to SEM data, samples of scaffolds based on textiles with a lower density (groups 1–3) were characterized by regular arrangement of fabric fibers (Fig. 2). Group 1 and 2 scaffolds were a mesh with an approximate mesh size of 300 μm × 300 μm, consisting of a single layer of fabric fibers with 100–150 μm average thickness. According to SEM data, no differences in surface microstructure were found between the samples of groups 1 and 2 (Fig. 2a, 2b).

Group 3 scaffolds were fiber-reinforced gelatin films. In this case, the gelatin in the scaffold composition evenly covers the fabric fibers, which leads to alignment of the microrelief of the fibers of the fabric.

Samples of scaffolds based on natural silk fabric with a higher density (groups 4–6) were characterized by dense arrangement of fabric fibers with 150–200 μm thickness. Group 5 scaffolds had a more pronounced surface microrelief compared to group 4 scaffolds. Gelatin forms a uniform coating on the surface of group 3 scaffolds, which, as in the case of textile-based scaffolds with a lower density, led to alignment of textile microrelief.

The samples of all the resulting scaffolds were then examined for cytotoxicity (Fig. 4a, 5a), which revealed that the obtained samples had no toxic effect on cells, which made it possible to conduct further studies on the biocompatibility of the resulting scaffolds.

Cell adhesion on the obtained scaffolds was assessed on day 1 of the experiment. Cell adhesion was detected on all scaffold samples; the morphology of adhered cells on different samples did not differ.

The proliferative activity of cells on the obtained scaffolds was assessed on days 3, 5 and 7 of the experiment (Fig. 4b, 5b).

The proliferative activity of cells on scaffold samples based on textiles with a lower density (groups 1–3, Fig. 4b) steadily increased during the experiment. At the same time, there were no differences in the proliferative activity of cells in the samples of the different groups.

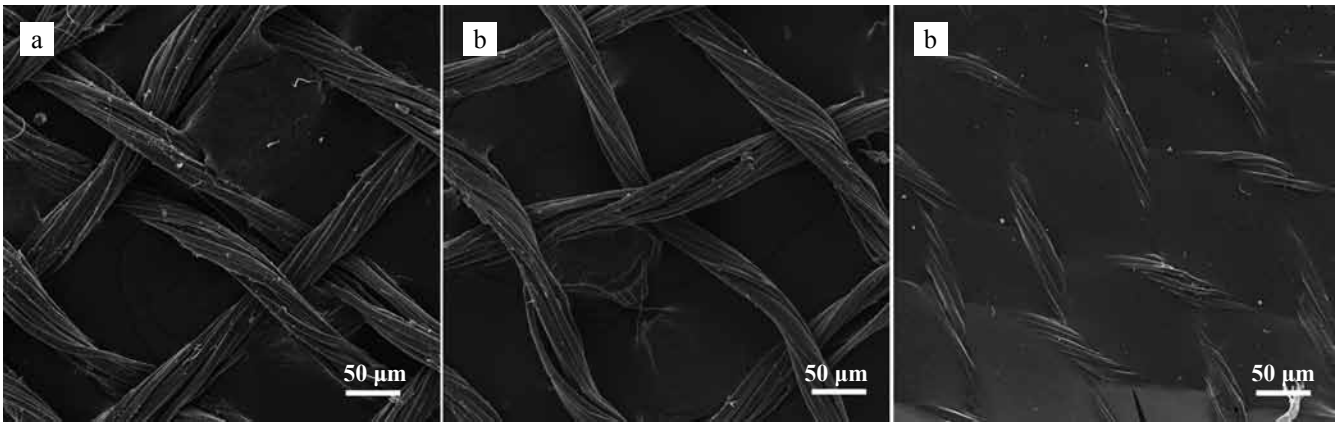

Fig. 2. Images of scaffold samples based on natural silk fabric with 15 g/m^2 density (gas-chiffon): a) Group 1, b) Group 2, c) Group 3. 50 μm

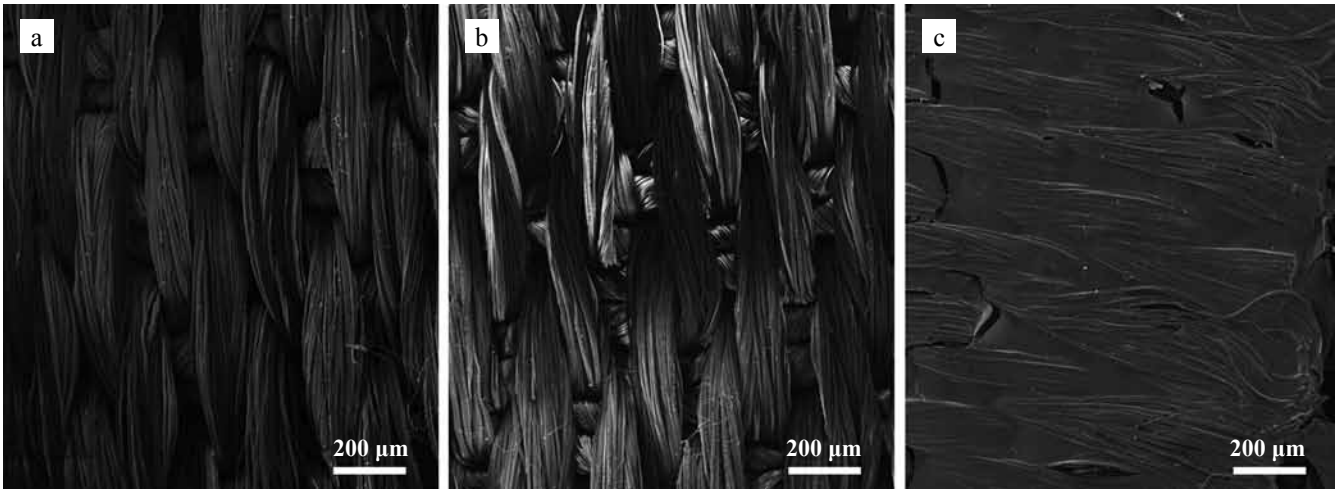

Fig. 3. Images of scaffold samples based on natural silk fabric with 155 g/m^2 density (double-sided satin): a) Group 4, b) Group 5, c) Group 6. 200 μm

Similar results were obtained for samples of scaffolds based on tissue with a higher density. However, from days 5 to 7 of the experiment, the proliferative activity of cells on the scaffold samples did not change and remained at a high level.

DISCUSSION

Six groups of natural silk fabric-reinforced scaffold samples were obtained for the study (Fig. 1). We developed a technique for regulating the rate of biodegradation of silk fabric-reinforced scaffold. The technique involves treating the natural silk fabric with an aqueous-alcoholic solution of calcium chloride [19]. In this study, the fabrics were treated with the solution for 45 minutes at 37 °C. Treatment with an aqueous-alcoholic solution of calcium chloride in a water bath is used by various scientific groups as one of the stages of obtaining an aqueous solution of silk fibroin for transition of silk fibroin molecules to an α-conformation state, which promotes protein dissolution [13, 21, 22]. It is also known that the rate of degradation of silk fibroin-reinforced constructs depends on conformation of protein molecules within the constructs. It was shown that the degradation rate of silk fibroin-based constructs increases when the proportion of molecules in the α-helix state increases [23]. Thus, the development considered in the study is based on implementation of the phase transition of silk fibroin without its dissolution due to the mild conditions in which the treatment is carried out.

Changes in the surface microstructure of the obtained scaffold samples as a result of treatment were shown by SEM. The study revealed an increase in the roughness of a scaffold based on a denser fabric after treatment. A similar effect after treatment of lower-density fabric was not detected by this method; so, it is necessary to study the structure of these samples with high resolution to reveal the features of micro- and nanostructure using methods that provide higher resolution, for example, scanning probe nanotomography [24].

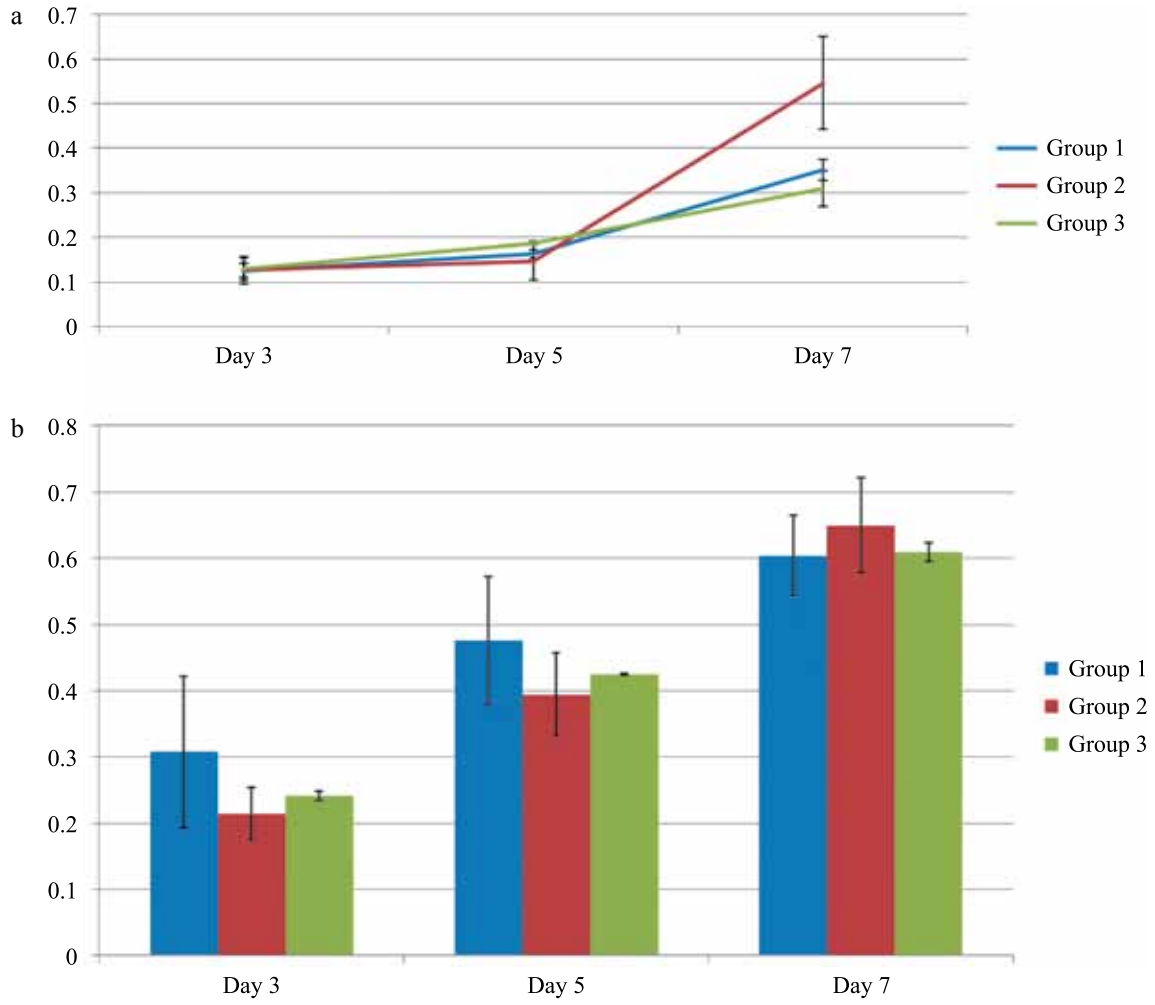

Fig. 4. Results of biocompatibility studies of scaffold samples based on natural silk fabric with 15 g/m^2 density (gas-chiffon, Groups 1–3): a) cytotoxicity, b) proliferative activity of Hep-G2 cells. Standard deviation values are shown for 5 independent measurements

The protocol of treatment with an aqueous-alcoholic solution of calcium chloride used in this study does not lead to fabric destruction and significant changes in its organoleptic properties. This allows for further manipulations with the treated fabric.

In this study, samples of biodegradable natural silk fabric-based scaffolds were treated with a gelatin type A solution. Gelatin type A is widely used in the field of cell technologies and tissue engineering to improve the biocompatible properties of constructs made of other polymers, as well as to ensure hemocompatibility [25, 26]. Treatment of biodegradable natural silk fabric-reinforced scaffolds with gelatin illustrates several possible ways of using such a construct.

Today, a wide range of naturally occurring polymers such as chitosan, alginate, gelatin, collagen, etc. are used for various tasks of tissue engineering and regenerative medicine. The main drawback is that they have low mechanical characteristics, such as strength and elasticity, which leads to fragility of the constructs obtained on their basis [27]. The use of natural silk fabrics as a reinforcing component of such constructs can provide the necessary mechanical characteristics and expand the scope of these polymers. Thus, a fabric with a lower density within the framework of this study can be considered as a reinforcing component of a gelatin film.

Another promising area of application of natural silk fabrics is their use as carriers for targeted drug delivery for gradual drug release. Thus, it is possible to obtain a scaffold with a predetermined degradation period, containing various bioactive substances or drugs that will be released from the scaffold as it degrades and provides effective organ and tissue regeneration.

Samples of the obtained biodegradable scaffolds do not exhibit a cytotoxic effect and are biocompatible, maintaining a high level of cell proliferative activity. The experiments did not reveal any differences in cell proliferative activity between the scaffolds of different groups. This is due to the fact that gelatin reduces the roughness of the scaffold surface, thereby hindering cell adhesion, which affects proliferative activity. At the same time, gelatin dissolution in the scaffold does not occur

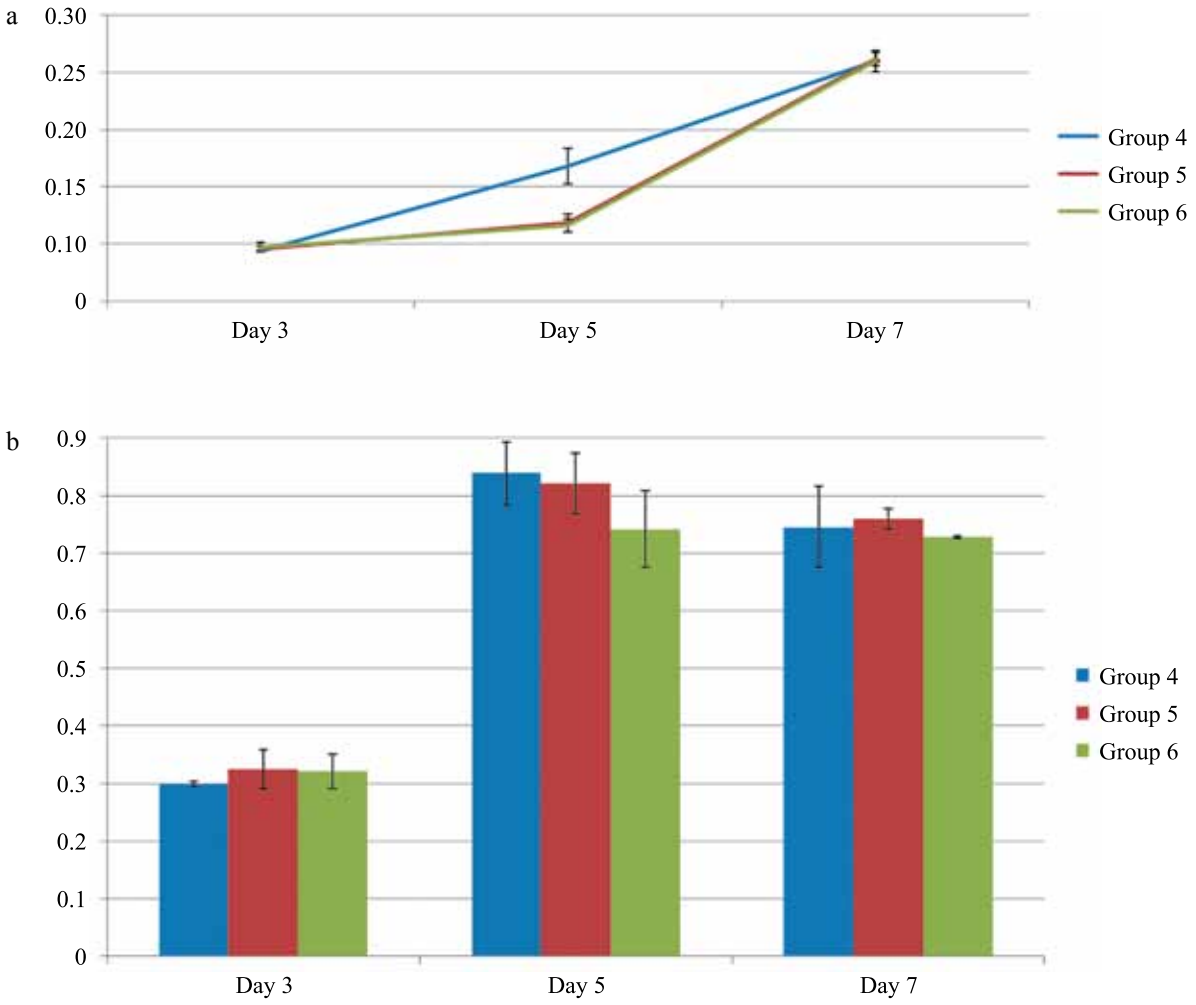

Fig. 5. Results of biocompatibility studies of scaffold samples based on natural silk fabric with 155 g/m^2 density (double-sided satin, groups 4–6): a) cytotoxicity, b) proliferative activity of Hep-G2 cells. Standard deviation values are shown for 5 independent measurements

due to treatment with crosslinking agents – EDC and NHS, which reduce the rate of degradation of the gelatin coating.

Thus, the approach to the use of natural silk fabrics used in the study makes it possible to obtain biocompatible silk fabric-reinforced scaffolds. The use of natural silk fabrics is a promising technological solution for obtaining biocompatible biodegradable scaffolds and their use in various fields of tissue engineering and regenerative medicine.

CONCLUSION

The developed technique facilitates production of silk fibroin-based scaffolds. The scaffolds obtained are biocompatible, which opens up the possibility of them being used in various fields of tissue engineering and regenerative medicine. The structure of the obtained scaffolds, as well as the dynamics of degradation *in vitro* and *in vivo*, require further detailed analysis.

The authors declare no conflict of interest.

REFERENCES

1. *Koh L-D, Cheng Y, Teng C-P, Khin Y-W, Loh X-J, Tee S-Y et al.* Structures, mechanical properties and applications of silk fibroin materials. *Progress in Polymer Science*. 2015; 46: 86–110. doi: 10.1016/j.progpolymsci.2015.02.001.
2. *Ding Z, Han H, Fan Z, Lu H, Sang Y, Yao Y et al.* Nanoscale Silk–Hydroxyapatite Hydrogels for Injectable Bone Biomaterials. *ACS applied materials & interfaces.* 2017; 9: 16913–16921. doi: 10.1021/acsami.7b03932. PMID: 28471165.
3. *Kim DK, Sim BR, Khang G.* Nature-derived aloe vera gel blended silk fibroin film scaffolds for cornea endothelial cell regeneration and transplantation. *ACS applied materials & interfaces.* 2016; 8: 15160–15168. doi: 10.1021/acsami.6b04901. PMID: 27243449.
4. *Dinis T, Elia R, Vidal G, Dermigny Q, Denoeud C, Kaplan D et al.* 3D multi-channel bi-functionalized silk electrospun conduits for peripheral nerve regeneration. *Journal of the mechanical behavior of biomedical materials.* 2015; 41: 43–55. doi: 10.1016/j.jmbbm.2014.09.029. PMID: 25460402.

5. *Wang Y, Rudym DD, Walsh A, Abrahamsen L, Kim H-J, Kim HS et al. In vivo* degradation of three-dimensional silk fibroin scaffolds. *Biomaterials*. 2008; 29: 3415–3428. doi: 10.1016/j.biomaterials.2008.05.002. PMID: 18502501.
6. *Gupta P, Lorentz KL, Haskett DG, Cunnane EM, Ramaswamy AK, Weinbaum JS et al.* Bioresorbable silk grafts for small diameter vascular tissue engineering applications: *In vitro* and *in vivo* functional analysis. *Acta Biomater*. 2020; 15 (105): 146–158. doi: 10.1016/j.actbio.2020.01.020. PMID: 31958596.
7. *Hasturk O, Jordan KE, Choi J, Kaplan DL*. Enzymatically crosslinked silk and silk-gelatin hydrogels with tunable gelation kinetics, mechanical properties and bioactivity for cell culture and encapsulation. *Biomaterials*. 2019; 232: 119720. doi: 10.1016/j.biomaterials.2019.119720. PMID: 31896515.
8. *Wang Y, Fan S, Li Y, Niu C, Li X, Guo Y et al.* Silk fibroin/sodium alginate composite porous materials with controllable degradation. *Int J Biol Macromol.* 2019; 1 (150): 1314–1322. doi: 10.1016/j.ijbiomac.2019.10.141. PMID: 31747567.
9. *Ratanavaraporn J, Kanokpanont S, Damrongsakkul S.* The development of injectable gelatin/silk fibroin microspheres for the dual delivery of curcumin and piperine. *J Mater Sci Mater Med*. 2014; 25 (2): 401–410. doi: 10.1007/s10856-013-5082-3. PMID: 24186150.
10. *Yang W, Xu H, Lan Y, Zhu Q, Liu Y, Huang S et al.* Preparation and characterisation of a novel silk fibroin/hyaluronic acid/sodium alginate scaffold for skin repair. *Int J Biol Macromol.* 2019; 1 (130): 58–67. doi: 10.1016/j.ijbiomac.2019.02.120. PMID: 30797808.
11. *Marcolin C, Draghi L, Tanzi M, Faré S.* Electrospun silk fibroin-gelatin composite tubular matrices as scaffolds for small diameter blood vessel regeneration. *J Mater Sci Mater Med*. 2017; 28 (5): 80. doi: 10.1007/s10856-017-5884-9. PMID: 28397163.
12. *Safonova LA, Bobrova MM, Agapova OI, Arkhipova AYu, Goncharenko AV, Agapov II*. Fibroin Silk Based Films For Rat's Full-Thickness Skin Wound Regeneration. *Russian Journal of Transplantology and Artificial Organs***.** 2016; 18 (3): 74–84. [In Russ, English abstract]. doi: 10.15825/1995-1191-2016-3-74-84.
13. *Li T, Song X, Weng C, Wang X, Gu L, Gong X et al.* Silk fibroin/carboxymethyl chitosan hydrogel with tunable biomechanical properties has application potential as cartilage scaffold. *Int J Biol Macromol.* 2019; 137: 382–391. doi: 10.1016/j.ijbiomac.2019.06.245. PMID: 31271796.
14. *Wang F, Wu H, Venkataraman V, Hu X.* Silk fibroin-poly(lactic acid) biocomposites: Effect of protein-synthetic polymer interactions and miscibility on material properties and biological responses. *Mater Sci Eng C Mater Biol Appl.* 2019; 104: 109890. doi: 10.1016/j.msec.2019.109890. PMID: 31500018.
15. *Roy T, Maity PP, Rameshbabu AP, Das B, John A, Dutta A et al.* Core-Shell Nanofibrous Scaffold Based on Polycaprolactone-Silk Fibroin Emulsion Electrospinning for Tissue Engineering Applications. *Bioengineering (Basel)*. 2018; 5 (3): 68. doi: 10.3390/bioengineering5030068. PMID: 30134543.
16. *Zhou F, Zhang X, Cai D, Li J, Mu Q, Zhang W et al.* Silk fibroin-chondroitin sulfate scaffold with immuno-inhibition property for articular cartilage repair. *Acta Biomater.* 2017; 63: 64–75. doi: 10.1016/j.actbio.2017.09.005. PMID: 28890259.
17. *Shen Y, Tu T, Yi B, Wang X, Tang H, Liu W, Zhang Y.* Electrospun acid-neutralizing fibers for the amelioration of inflammatory response. *Acta Biomater.* 2019; 97: 200–215. doi: 10.1016/j.actbio.2019.08.014. PMID: 31400522.
18. *Agapov II, Agapova OI, Efimov AE, Sokolov DYu, Bobrova MM, Safonova LA*. Sposob polucheniya biodegradiruemykh skaffoldov na osnove tkaney iz natural'nogo shelka. Patent na izobretenie RU2653428 S1, 08.05.2018.
19. *Mosmann T.* Rapid Colorimetric Assay for Cellular Growth and Survival: Application to Proliferation and Cytotoxicity Assays. *J lmmunol Methods.* 1983; 65 (1–2): 55–63. doi: 10.1016/0022-1759(83)90303-4. PMID: 6606682.
20. *Shen T, Wang T, Cheng G, Huang L, Chen L, Wu D.* Dissolution behavior of silk fibroin in a low concentration $CaCl_2$-methanol solvent: From morphology to nanostructure. *Int J Biol Macromol*. 2018; 1 (113): 458–463. doi: 10.1016/j.ijbiomac.2018.02.022. PMID: 29421494.
21. *Hino T, Tanimoto M, Shimabayashi S.* Change in secondary structure of silk fibroin during preparation of its microspheres by spray-drying and exposure to humid atmosphere. *J Colloid Interface Sci.* 2003; 266 (1): 68–73. doi: 10.1016/s0021-9797(03)00584-8. PMID: 12957583.
22. *Hu Y, Zhang Q, You R, Wang L, Li M.* The Relationship between Secondary Structure and Biodegradation Behavior of Silk Fibroin Scaffolds. *Adv Mater Sci and Eng*. 2012; 2012: 21–25. https://doi.org/10.1155/2012/185905.
23. *Efimov AE, Agapova OI, Safonova LA, Bobrova MM, Agapov II.* Three-dimensional analysis of micro and nanostructure of biomaterials and cells by method of scanning probe nanotomography. *Russian Journal of Transplantology and Artificial Organs*. 2017; 19 (4): 78–87. doi: 10.15825/1995-1191-2017-4-78-87.
24. *Zhang F, Xu S, Wang Z.* Pre-treatment optimization and properties of gelatin from freshwater fish scales. *Food Bioprod Proc.* 2011; 89: 185–193. doi: 10.1016/j.fbp.2010.05.003.
25. *Su K., Wang C.* Recent advances in the use of gelatin in biomedical research. *Biotechnol Lett.* 2015; 37 (11): 2139–2145. doi: 10.1007/s10529-015-1907-0. PMID: 26160110.
26. *Abdulghani S, Mitchell GR.* Biomaterials for In Situ Tissue Regeneration: A Review. *Biomolecules.* 2019; 9 (11): 750. doi: 10.3390/biom9110750. PMID: 31752393; PMCID: PMC6920773.

The article was submitted to the journal on 16.10.2020

DOI: 10.15825/1995-1191-2020-4-115-122

INVESTIGATION OF THE MICRO- AND NANO-STRUCTURE OF LIVER CELLS CULTURED ON BIODEGRADABLE SILK FIBROIN-BASED SCAFFOLDS USING SCANNING PROBE OPTICAL NANOTOMOGRAPHY

O.I. Agapova, A.E. Efimov, L.A. Safonova, M.M. Bobrova, I.I. Agapov

Shumakov National Medical Research Center of Transplantology and Artificial Organs, Moscow, Russian Federation

Objective: to analyze the 3D micro- and nano-structure and quantitative morphological parameters of liver cells cultured on biodegradable silk fibroin-based film scaffolds. **Materials and methods.** Samples of biodegradable silk fibroin-based scaffolds with cultured Wistar rat liver cells were obtained for the study. The 3D structure of liver cells cultivated on the scaffolds was studied by scanning probe optical nanotomography using an experimental setup combining an ultramicrotome and a scanning probe microscope in correlation with fluorescence microscopy. **Results.** Nanoscale images and 3D nanotomographic reconstructions of rat liver cells cultured on scaffold were obtained. The morphological parameters of liver cells (average roughness, specific effective area) were determined. The average surface roughness of the liver cells R_a was found to be 124.8 ± 8.2 nm, while the effective surface area σ was 1.13 ± 0.02. Analysis of the volume distribution of lipid droplets showed that they occupy 28% of the cell volume. **Conclusion.** Scanning probe optical nanotomography can successfully analyze the nanostructure and quantify the nanomorphology of liver cells cultured on biodegradable scaffolds.

Keywords: liver cells, biodegradable scaffolds, silk fibroin, scanning probe microscopy, fluorescence microscopy, nanotomography.

INTRODUCTION

One of the tasks in modern transplantation include the search for new materials for creating scaffolds with improved adhesive properties for the development of constructs for tissue engineering and regenerative medicine. When solving these problems, it is necessary to use new technological approaches to analyze the micro- and nanostructural features of constructs and cells in them, as well as the parameters of interaction between the cells and the surface of the constructs at the micro- and nanolevel.

A combination of various microscopy techniques (electron microscopy, scanning probe microscopy, high-resolution optical micro-spectroscopy) makes it possible to carry out correlative studies of micro- and nanostructures with high resolution [1]. The information obtained during the analysis using various microscopic technologies makes it possible to comprehensively characterize the structure of biological objects and obtain new knowledge about their properties [2].

One of the most in-demand areas in this field is the development of methods and approaches for analyzing the three-dimensional micro- and nanostructure of biomaterials, biological objects, and tissue-engineered constructs, which would provide correlative information about both nanomorphology and the biological structure of the objects under study.

The unique technique of scanning probe optical nanotomography (SPONT) allows combining the functional capabilities of a scanning probe microscope (SPM) and an ultramicrotome in one device in correlation with optical fluorescence microscopy methods [3, 4]. SPONT makes it possible to study the 3D nanostructure of biomaterials, cells, tissues, and tissue-engineered constructs, in correlation with the study of fluorescent marker localization in the volume of measured samples. Analysis of the obtained 3D reconstructions of the structure of biological objects and materials allows one to quantitatively determine such important parameters of their nanomorphology as micro- and nanoporosity [5], effective surface area and surface roughness [6], and the surface area to volume ratio [7].

Silk fibroin-based biodegradable film scaffolds with cultured rat liver cells were chosen as objects of this study.

Silk fibroin, derived from Bombyx mori cocoons, is one of the promising materials for tissue engineering. This biopolymer not only meets all the requirements for

Corresponding author: Igor Agapov. Address: 1, Shchukinskaya str., 123182, Moscow, Russian Federation.
Phone: (499) 190-66-19. E-mail: igor_agapov@mail.ru

materials in regenerative medicine, but also has a number of advantages over other materials. Its biocompatibility, optimal mechanical properties, and biodegradability provide possible application in many areas of regenerative medicine, both as an independent material and as a component of various composites based on it [8]. All these properties make it possible to obtain from it two-dimensional and three-dimensional constructs for various purposes [9–11].

At present, many materials that can be effectively used to make scaffolds for culturing liver cells are being considered. There are known materials, whose coatings support hepatocyte adhesion, but formation of constructs from them is associated with difficulties. Such materials include, for example, chitosan, gelatin, collagen, etc. Silk fibroin has attracted the attention of researchers since it supports hepatocyte adhesion and proliferation, and also has suitable mechanical properties [12]. Fibroin can also be used in composite materials. For example, 3D porous scaffolds made of fibroin and chitosan that are mixed in different ratios support adhesion and proliferation of human hepatocellular carcinoma in vitro, and adhesion capacity of cells on scaffolds is much higher than on a control substrate [13]. Scaffolds of similar composition, made using electrospinning, were also used for culturing mouse hepatocytes [12].

In this work, the micro- and nanostructure of rat liver cells adhered to biodegradable silk fibroin-based film scaffolds were studied. A similar study for these cell types using SPONT has been performed for the first time.

MATERIALS AND METHODS

Production of film scaffolds for cells based on silkworm fibroin *Bombyx mori*

Fibroin for manufacturing film scaffolds for cells was isolated from silk filaments of the *Bombyx mori* silkworm. For this purpose, 1 g of silk filaments was weighed, and the filaments were cut into 0.5 cm fragments. The filaments were boiled in a water bath for 40 minutes in a solution with the addition of sodium bicarbonate to clean the filaments of sericin and other impurities. Then the filaments were washed with 3600 mL of distilled water. The filaments were boiled 3 times for 30 minutes each in double-distilled water, rinsing after each boiling with distilled water. After that, they were dried in a desiccator.

To obtain an aqueous fibroin solution, a sample of fibroin weighing 130 mg/ml was added to a solution prepared at the rate of 389 mg $CaCl_2$, 388 μl C_2H_5OH, and 544 μl H_2O per 1 ml of solution. The solution was heated in a water bath at 40 °C for 4 hours. Then the solution was dialyzed against double-distilled water. The optical density of the silk fibroin solution in the solution obtained after dialysis was measured spectrophotometrically at 280 nm wavelength, then the concentration was calculated using the formula D = ECL, where E is the extinction coefficient of silk fibroin equal to 1.07.

Next, an aqueous silk fibroin solution obtained by the technique described above was applied to the bottom of a Petri dish and dried at room temperature. The dried silk fibroin was dissolved in formic acid at 20 mg/mL by heating to 40 °C in a water bath for 30 minutes. The resulting solution was centrifuged for 5 minutes at 12,100 g.

Samples of biodegradable scaffolds in the form of silk fibroin films were obtained by irrigation. To make the films, 150 μL of a solution of a given composition was applied to the bottom wells of a 48-well culture plate and dried for two days at room temperature. The total protein concentration in the film was 20 mg/mL. After the fibroin solution had dried, 100 μL of 10 μg/mL fibronectin solution was applied to the wells of the plate and dried for two days at room temperature.

Before cell culturing, film scaffolds were sterilized: treated with 70% ethanol for 30 minutes, then irradiated with ultraviolet light for 30 minutes. After that, a sterile phosphate-salt buffer solution was introduced into the wells of the plate and incubated for 15 minutes, after which the phosphate-buffered saline was changed. This procedure was repeated three times. Then, 300 μL of incubation medium was added to the wells of the plate for 30 minutes.

Preparation of Wistar rat liver cell samples cultured on silk fibroin scaffolds for scanning probe optical nanotomography

Rat liver cells were isolated as follows. In the experiment, 1 year old male Wistar rats (weighing 250–350 g) were used. The rat was put to sleep using diethyl ether inhalation anesthesia. Then, the rat was placed belly-up on the operating table and the paws were straightened. Using tweezers, pulling aside the skin on the abdomen, a longitudinal skin incision was made with scissors in the midline of the abdominal side of the body from the genital opening to the sternum. The skin was turned away and secured. Then the abdominal cavity was opened, making a longitudinal incision along the midline; the muscle flaps were turned aside. The liver was harvested by cutting off the vena cava, portal vein, hepatic arteries, and veins. After sampling, the liver was placed in a sterile 0.9% sodium chloride solution and washed of blood. Next, the liver fragment was transferred into a second portion of sterile 0.9% sodium chloride solution and the liver was cut into 5×5 mm fragments using scissors. Then each liver fragment was washed with 0.9% sodium chloride solution using a syringe without a needle. After wa-

shing off blood, the liver fragment was transferred into a sterile dry Petri dish and injected with a collagenase type 2 solution with a 2 mg/mL concentration using an insulin syringe. Then the tissue was incubated for 20 minutes. Next, the liver was chopped with scissors and incubated for another 5 minutes, then transferred to ice. After that, 5 mL of 0.9% sodium chloride solution was added to the liver tissue. The resulting solution was transferred to a test tube, stirred, and centrifuged for 5 minutes at 1770 g and –5 °C. The supernatant was removed, the culture medium was added to the resulting precipitate, stirred and the cell suspension was transferred into previously prepared 48-well plates. The cells were incubated in a thermostat at 37 °C and 5% CO_2 for 2 days. Liver cells for further experiments using the SPONT method were visually localized using an optical microscope.

To examine cells on scaffolds by fluorescence SPONT, cells were pre-stained with fluorescent dyes FITC and DAPI. The wells were washed twice with sterile 0.9% sodium chloride solution, then a DAPI solution with 3 μg/mL concentration was added and incubated for 5 minutes at 37 °C. Two short washes were then performed with a sterile 0.9% sodium chloride solution, after which a 2.5% glutaraldehyde solution in phosphate-buffered saline (pH = 7.4) was added to the wells and incubated for 2 hours in the dark at +4 °C. Next, one short wash with a sterile 0.9% sodium chloride solution and one short wash with a carbonate-bicarbonate buffer solution (pH = 9.0) were performed. Then an FITC solution in dimethyl sulfoxide with a 1 mg/mL concentration was added to the wells and incubated for 40 minutes in the dark, followed by two short washes with a carbonate-bicarbonate buffer solution (pH = 9.0).

To prepare a preparation for SPONT, dehydration of scaffold samples with cultured liver cells was performed by conducting through alcohols with increasing concentration according to the following scheme:

a) 30% ethanol solution – 10 min;
b) 50% ethanol solution – 10 min;
c) 70% ethanol solution – 10 min;
d) 80% ethanol solution – 10 min;
e) 96% ethanol solution – 10 min.

The samples were washed three times with 100% ethyl alcohol for 10 minutes each, and then incubated in a mixture of 100% ethyl alcohol and epoxy resin in a 1 : 1 ratio for 30 minutes, after which the samples were transferred into a mixture of 100% ethyl alcohol and epoxy resin in a ratio of 1 : 2 and incubated for 30 minutes. Then the samples were embedded in epoxy resin, incubated in a thermostat at 45 °C for 12 hours, after which the incubation was continued for 72 hours at 60 °C. The scaffolds in epoxy resin were then separated from the bottom of the plates using a scalpel.

To embed the samples, we used an epoxy medium (Epoxy Embedding Medium) mixed with an equal weight of the embedding medium hardener (dodecenyl succinic anhydride DDSA) and 4% by weight of 2,4,6-Tris(dimethylaminomethyl)phenol (DMP-30).

Scanning probe optical nanotomography

An experimental unit Ntegra Tomo was used to study samples of rat liver cells by scanning probe nanotomography techniques. This unit allows for sequential SPM measurements of sample surface immediately after cutting into slices with an ultramicrotome. Consecutive 100 nm thick slices were made using a Diatome Ultra AFM 35 diamond knife (Diatome AG, Switzerland) with 2.0 mm cutting edge width.

SPM measurements were carried out in a semi-contact mode at 1.0 Hz scanning speed using NSG10 silicon cantilever probes (NT-MDT, Moscow) with 240 kHz resonance frequency and <10 nm tip curvature radius. Primary image processing was carried out using the Nova ImageAnalysis 1.0.26.1443 software (NT-MDT, Moscow); 3D tomographic reconstructions of the liver cell structure were obtained using the ImagePro Plus 6.0 software (Media Cybernetics, Inc, USA).

Correlative measurements of slices using optical fluorescence microscopy were performed using an AxioVert.A1 fluorescence inverted microscope (Carl Zeiss, Germany) equipped with an HBO 100 mercury lamp. Fluorescence images were obtained using oil-immersion lens Carl Zeiss EC Plan-Neofluar 100x/1.30 Oil Ph3. The Zen software package (Carl Zeiss, Germany) was used to analyze fluorescence images.

Analysis of surfaces reconstructed by the SPONT method using ImagePro Plus 6.0 software (Media Cybernetics, Inc, USA) makes it possible to determine and analyze the nanoscale parameters of these surfaces, such as average roughness Ra and effective surface area σ. The algorithms used for calculating these parameters are given in [6].

RESULTS AND DISCUSSION

Prepared samples of rat liver cells cultured on silk fibroin scaffolds were examined using SPONT technology. After separation of the scaffold samples embedded in epoxy medium from the plates, the cultured liver cells were localized in the scaffold plane using fluorescence microscopy. Based on analysis of the obtained images, scaffolds were selected for further SPONT analysis, then primary cutting of the sample into slices were performed with an ultramicrotome in a plane perpendicular to the scaffold plane. The distance from the plane of the primary slice to the liver cells being registered was measured using fluorescence microscopy. In accordance with the

measurements taken, subsequent slices of the scaffold with a controlled total thickness were made in order to obtain liver cell slices. Fig. 1 shows a fluorescence image of a sample of a silk fibroin-based film with liver cells adhered to it. The line marks the slice plane, the arrow indicates the cell localization area where SPONT analysis was performed.

Fig. 2 shows images obtained during analysis of liver cells adhered to silk fibroin-based film scaffolds. SPM analysis (Fig. 2a) revealed the presence of a nucleus, as well as inclusions in the form of a lipid droplet occupying a significant volume of the cell. Such inclusions are one of the characteristic features of liver cells. The findings were confirmed by correlative fluorescence images. The DAPI dye distribution confirms the presence of a nucleus in the cell (Fig. 2c); no dye fluorescence was observed in the lipid droplet area (Fig. 2b, c).

Further analysis of the structure of rat liver cells adhered to silk fibroin-based film scaffolds revealed the presence of a large number of inclusions. Analysis of the images presented in Fig. 3 revealed inclusions in the form of lipid droplets in the structure of liver cells, in the area of which no fluorescence was registered (Fig. 3b), and shaped granules, presumably glycogen (indicated by arrows in Fig. 3b).

Analysis of the structure of rat liver cells adhered to silk fibroin-based film scaffolds with high resolution revealed extensive areas of cytoplasm with a heterogeneous structure (Fig. 4), which may indicate a high level of cell metabolism due to developed endoplasmic reticulum system.

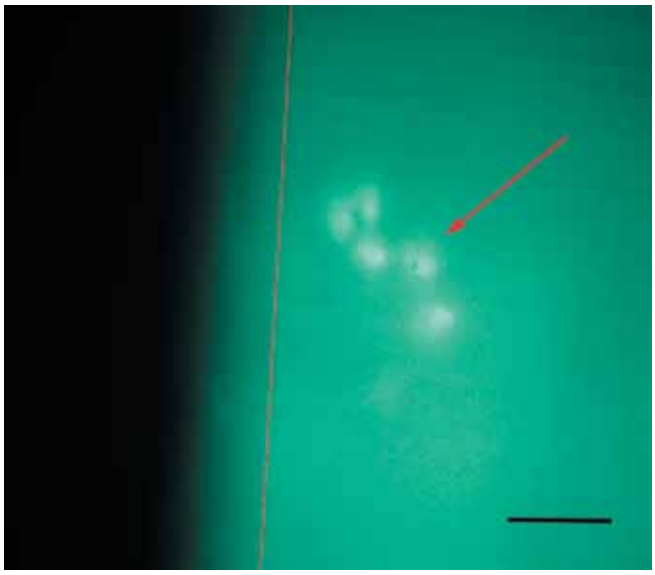

Fig. 1. Fluorescence image of a silk fibroin film sample with liver cells adhered to it; FITC stain, magnification 200×, 50 μm scale bar

To assess the 3D morphology of a liver cell adhered to the surface of a silk fibroin-based film scaffold, a 3D reconstruction of the cell fragment was performed using SPONT. For this purpose, 14 successive 200 nm thick slices of the sample were made, and 14 successive SPM images of the scaffold area measuring 32×16 μm

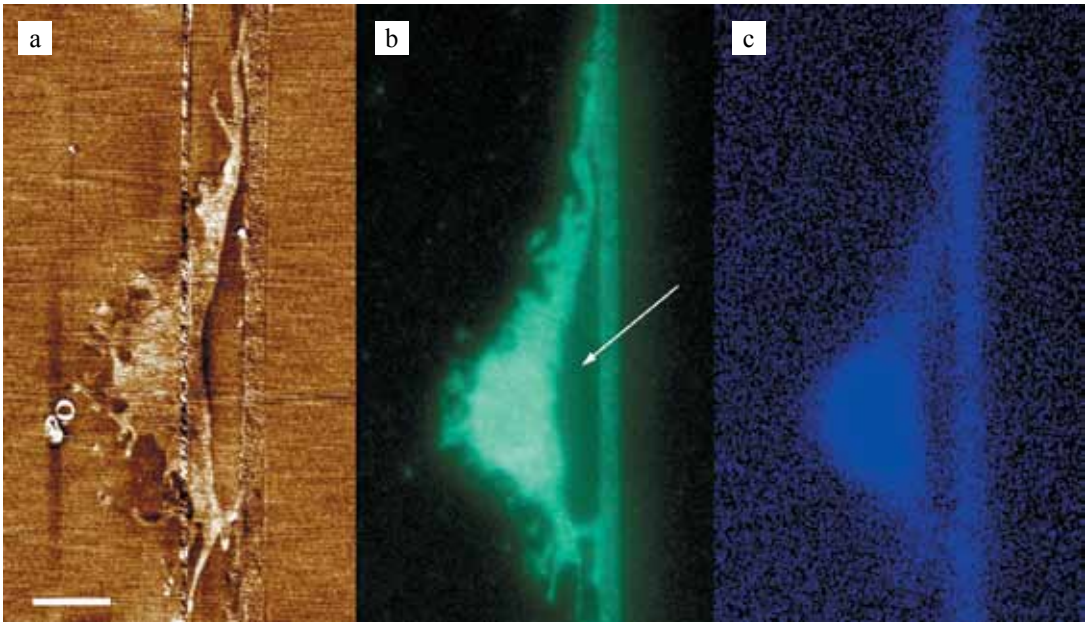

Fig. 2. Analysis of liver cell samples cultured on silk fibroin-based film scaffolds. a) SPM image of the surface topography of a cross-section of the silk fibroin-based film scaffold with adhered liver cell: scan size 25×12 μm, height variation range 11 nm, scale bar 3 μm. b) correlative fluorescence image of a cross-section of the silk fibroin-based film scaffolds with adhered liver cell, FITC stain, magnification 1000×, the arrow indicates a lipid droplet. c) correlative fluorescence image of a cross-section of the silk fibroin-based film scaffold with adhered liver cell, DAPI stain, magnification 1000×

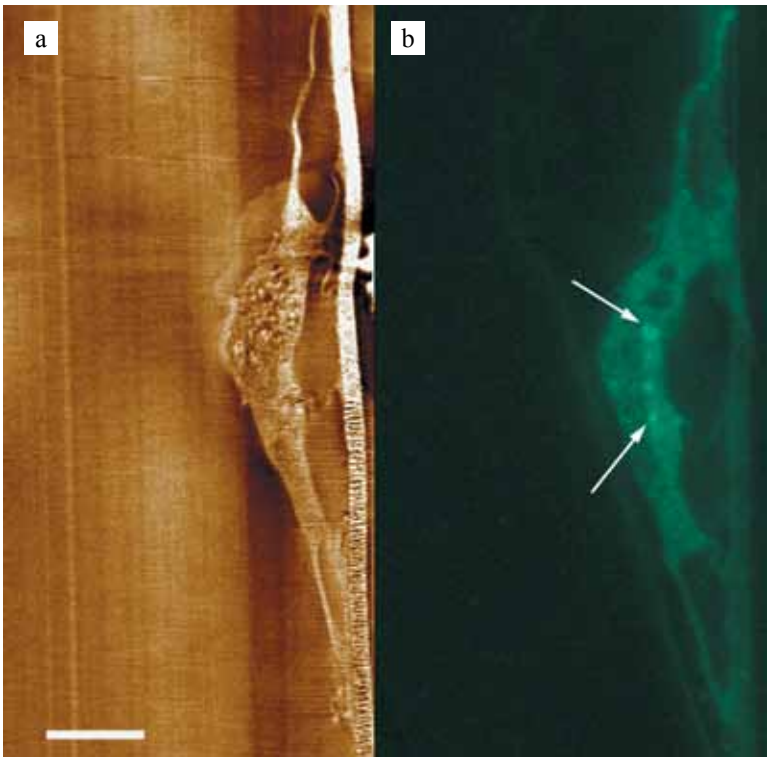

Fig. 3. Analysis of liver cell samples cultured on silk fibroin-based film scaffold. a) SPM image of the surface topography of a cross-section of the silk fibroin-based film scaffold with adhered liver cell: scan size 32×15 μm, height variation range 40 nm, scale bar 4 μm; b) correlative fluorescence image of a cross-section of the silk fibroin-based film scaffold with adhered liver cell, FITC stain, magnification 1000×, arrows indicate glycogen granules

Fig. 4. SPM image of the topography of a cross-section of the silk fibroin-based film scaffold with adhered liver cell: scan size 7.0×6.0 μm, height variation range 20 nm, scale bar 1 μm

in size were obtained. The resulting visualization of the 3D structure of the liver cell is shown in Fig. 5.

Analysis of the obtained 3D data made it possible to determine morphological parameters of the reconstructed 3D structure of the liver cell. So, the average cell surface roughness Ra is 124.8 ± 8.2 nm, while the effective surface area σ, calculated as the ratio of surface area to the area of its 2D projection onto the plane, is 1.13 ± 0.02. This dimensionless parameter determines the degree of surface development. Analysis of volumetric distribution of lipid droplets showed that they occupy 28% of the volume of the reconstructed cell fragment.

The technique developed by us for studying the nanoscale structures of rat liver cells that are adhered to biodegradable scaffolds using SPONT is applicable for studying the features of the 3D structure of cells of different types in micro- and nanoscale.

CONCLUSION

In this work, the nanoscale structures of rat liver cells adhered to the silk fibroin-based biodegradable film scaffolds were studied using the SPONT method. Three-dimensional reconstructions of a rat liver cell and its correlative fluorescence images were obtained; the parameters of three-dimensional cell nanomorphology were determined. The results obtained demonstrated that

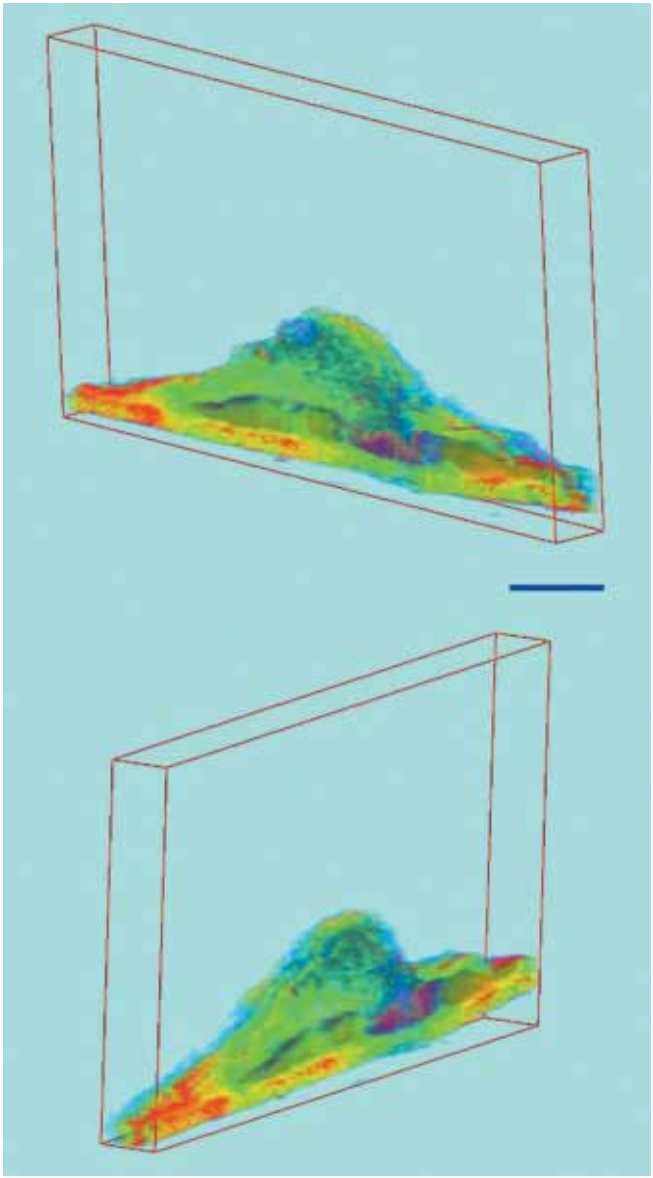

Fig. 5. SPONT 3D-reconstruction of the liver cell adhered to the silk fibroin-based film scaffold, 32.0×15.0×2.8 μm, slice thickness 200 nm, scale bar 5 μm

the developed method of fluorescence scanning probe optical nanotomography can be effectively used for correlation analysis of the structure of biodegradable silk fibroin-reinforced scaffolds with cells cultured on them.

The authors declare no conflict of interest.

REFERENCES

1. *Caplan J, Niethammer M, Taylor RMII, Czymmek KJ.* The Power of Correlative Microscopy: Multi-modal, Multi-scale, Multi-dimensional. *Curr Opin Struct Biol.* 2011; 21 (5): 686–693. doi: 10.1016/j.sbi.2011.06.010.
2. *Balashov V, Efimov A, Agapova O, Pogorelov A, Agapov I, Agladze K.* High resolution 3D microscopy study of cardiomyocytes on polymer scaffold nanofibers reveals formation of unusual sheathed structure. *Acta Biomaterialia.* 2018; 68 (1): 214–222. doi: 10.1016/j.actbio.2017.12.031.
3. *Efimov AE, Agapov II, Agapova OI, Oleinikov VA, Mezin AV, Molinari M et al.* A novel design of a scanning probe microscope integrated with an ultramicrotome for serial block-face nanotomography. *Review of Scientific Instruments.* 2017; 88 (2): 023701. doi: 10.1063/1.4975202.
4. *Mochalov KE, Chistyakov AA, Solovyeva DO, Mezin AV, Oleinikov VA, Molinari M et al.* An instrumental approach to combining confocal microspectroscopy and 3D scanning probe nanotomography. *Ultramicroscopy.* 2017; 182: 118–123. doi: 10.1016/j.ultramic.2017.06.022.
5. *Efimov AE, Moisenovich MM, Bogush VG, Agapov II.* 3D nanostructural analysis of silk fibroin and recombinant spidroin 1 scaffolds by scanning probe nanotomography. *RSC Adv.* 2014; 4: 60943–60947. doi: 10.1039/c4ra08341e.
6. *Efimov AE, Agapova OI, Safonova LA, Bobrova MM, Agapov II.* 3D analysis of the micro- and nanostructure of lung tissue by scanning probe nanotomography. *Russian Journal of Transplantology and Artificial Organs*. 2020; 22 (3): 143–148. [In Russ, English abstract]. doi: 10.15825/1995-1191-2020-3-143-148.
7. *Efimov AE, Agapova OI, Safonova LA, Bobrova MM, Parfenov VA, Koudan EV et al.* 3D scanning probe nanotomography of tissue spheroid fibroblasts interacting with electrospun polyurethane scaffold. *Express Polymer Letters.* 2019; 13 (7): 632–641. doi: 10.3144/expresspolymlett.2019.53.
8. *Kim HH, Park JB, Kang MJ, Park YH.* Surface-modified silk hydrogel containing hydroxyapatite nanoparticle with hyaluronic acid–dopamine conjugate. *Int J Biol Macromol.* 2014; 70: 516–522. doi: 10.1016/j.ijbiomac.2014.06.052.
9. *Gil ES, Panilaitis B, Bellas E, Kaplan DL.* Functionalized Silk Biomaterials for Wound Healing. *Adv Healthc Mater.* 2013; 2: 206–217. doi: 10.1002/adhm.201200192.
10. *Zhua M, Wanga K, Meia J, Lib C, Zhanga J, Zhenga W et al.* Fabrication of highly interconnected porous silk fibroin scaffolds for potential use as vascular grafts. *Acta Biomater.* 2014; 10 (5): 2014–2023. doi: 10.1016/j.actbio.2014.01.022.
11. *Gu Y, Zhu J, Xue C, Li Z, Ding F, Yang Y, Gu X.* Chitosan/silk fibroin-based, Schwann cell-derived extracellular matrix modified scaffolds for bridging rat sciatic nerve gaps. *Biomaterials.* 2014; 35 (7): 2253–2263. doi: 10.1016/j.biomaterials.2013.11.087.
12. *Kasoju N, Bora U.* Silk fibroin based biomimetic artificial extracellular matrix for hepatic tissue engineering applications. *Biomed Mater.* 2012; 7 (4): 1–12. doi: 10.1088/1748-6041/7/4/045004.
13. *She Z, Jin C, Huang Z, Zhang B, Feng Q, Xu Y.* Silk fibroin/chitosan scaffold: preparation, characterization, and culture with HepG2 cell. *J Mater Sci: Mater Med.* 2008; 19: 3545–3553. doi: 10.1007/s10856-008-3526-y.

The article was submitted to the journal on 19.10.2020

DOI: 10.15825/1995-1191-2020-4-123-132

CHARACTERISTICS OF MECHANISMS OF THE DISTANT STIMULATING EFFECT OF SKIN FLAP AUTOGRAFT ON MICROVASCULAR PERFUSION IN LOCAL AND SYSTEMIC MICROCIRCULATION DISORDERS

A.N. Ivanov, D.D. Lagutina, T.V. Stepanova
Saratov State Medical University, Saratov, Russian Federation

Objective: to study the characteristics of mechanisms of the distant stimulating effect of full-thickness skin autograft (FTSG) on microvascular perfusion in local and systemic microcirculation disorders. **Materials and methods.** The experiment was carried out on 87 white male rats, divided into 5 groups: 1) control; 2) animals with local microcirculation disorders induced by sciatic nerve transection and neuroraphy; 3) animals with systemic microcirculation disorders caused by alloxan-induced diabetes; 4) animals that underwent FTSG after sciatic nerve transection and neurography; 5) animals that underwent FTSG in alloxan-induced diabetes. Laser Doppler flowmetry (LDF) was used to study microcirculation of the dorsal skin of the rear paw. Serum concentrations of vasoactive substances, including catecholamines (CA), histamine, and vasculoendothelial growth factor (VEGF) in the experimental animals were measured. A morphological study of the tissues of the autograft site was carried out on day 42 of the experiment. **Results.** On day 42 of the experiment, FTSG normalized perfusion in local and systemic microcirculation disorders. FTSG decreases CA level in nerve injury, and to a greater extent in alloxan-induced diabetes. Serum histamine increase under FTSG was more pronounced in rats with nerve injury. Serum VEGF in rats with nerve injury and FTSG increased, which was not observed in alloxan-induced diabetes. Histological assay of the autograft site revealed degenerative changes in the epidermis and dermis of the autotransplant in both experimental models of microcirculatory disorders. Eosinophilic infiltration of the autograft site was more pronounced in nerve injury than in alloxan-induced diabetes. **Conclusion.** FTSG has a distant stimulating effect on microcirculation, which manifests itself in the same degree in both local and systemic microcirculation disorders. The distant stimulating effect of FTSG on microcirculation is multicomponent in nature and includes a set of regulatory reactions, whose severity differs in local and systemic microcirculatory disorders.

Keywords: autograft, microcirculation, regeneration, skin flap.

INTRODUCTION

The physiological basis for maintaining homeostasis in tissues and organs of living organisms is transcapillary metabolism in the microcirculatory bloodstream, while the normal functioning of microcirculation is associated with the metabolic activity of cells [1]. In addition, microcirculatory disorders are the main link in the pathogenesis of various pathological processes. They also play an important role in sanogenesis, providing trophic support for reparative processes [2]. Systemic and local metabolic disorders affect the state of the microcirculatory bloodstream, which leads to an even greater aggravation of dysmetabolism in organs and tissues [3, 4]. Under normal and disease conditions, the body's own cells and tissues are able to influence the state of microcirculation through synthesis and release of bioactive substances that regulate microcirculation at the local and systemic levels [5].

The current level of scientific knowledge determines the process of regeneration of body tissues and organs as a complex of interconnected sequential local and general reactions of the body, which proceed with involvement of many regulatory systems with different levels of organization [6]. However, it should be noted that different body cells and tissues have different regenerative potential and intensity of production of bioactive substances stimulating reparative processes. So, some researchers have demonstrated the acceleration of regenerative processes under the influence of placenta-based drugs [7, 8]. Despite the effectiveness of allotissues, including tissues of the fetoplacental complex, in regenerative medicine, they are associated with the risk of infectious and immune complications. Therefore, a more promising method for stimulating regenerative processes is the use of autogenous tissue, particularly skin. It has been shown that the subcutaneous adipose tissue is rich in bioactive substances providing a high regenerative potential [9]. It was experimentally shown that autotransplantation of adipose tissue stimulates microcirculation, and also positively influences systemic changes in metabolic

Corresponding author: Alexey Ivanov. Address: 137/5, Bolshaya Sadovaya str., Saratov, 410054, Russian Federation. Phone: (927) 279-95-99. E-mail: lex558452@gmail.com

processes [10, 11]. In addition, skin cell populations include leukocyte cells that produce various bioactive substances [12].

It has been previously demonstrated that autologous transplantation of a full-thickness skin autograft (FTSG) into the interscapular region has a distant stimulating effect on microcirculation in the dorsal skin of the rear paw in intact white rats, in animals with sciatic nerve injury, and also under conditions of experimental alloxan-induced diabetes [13, 14]. It has been shown that FTSG's mechanism of action is multicomponent in nature and includes a complex of changes in the histology of the autotransplantation zone, concentrations of vasoactive substances in the blood, and mechanisms of microcirculatory modulation [13, 14]. At the same time, previous studies did not take into account the dependence of FTSG's biostimulating effect on prevalence of microcirculatory bloodstream lesions. For instance, differences in the degree of the effect in local and systemic vascular bed lesions were not established, which is critically important for determining the limitations of this method in systemic microcirculatory disorders. Besides, there are currently no data on the influence of the etiology of vascular lesions on this effect, which may contribute to identifying additional restrictions for practical application of the method, since in some cases, changes in metabolic processes that cause microcirculation dysfunction can quantitatively and qualitatively change the nature of regulatory reactions in FTSG, including modulation of inflammatory response, vasomotor activity, and others. As indicated above, the mechanism of the distant stimulating effect of FTSG is complex and includes many regulatory reactions, whose interactions and hierarchy remain unclear. For instance, available data is not enough to unequivocally determine which regulatory reactions have a trigger value and which are secondary. It is not clear which of them are universal, and which are strictly specific for a certain method of modeling microcirculatory disorders. In this regard, it is of scientific and practical importance to identify the dependence of the complex of regulatory reactions during biostimulation by the body's own tissues on the nature and extent of damage to the microcirculatory system, which determined the direction of this study, the purpose of which was to study the features of FTSG's distant stimulating effect on perfusion of the skin microcirculation system in local and systemic microcirculatory disorders.

MATERIALS AND METHODS

The studies were performed on 87 white nonlinear rats. The experiment was carried out in accordance with the recommendations of the Ethics Committee of the Razumovsky Saratov State Medical University (Protocol No. 1 dated February 5th, 2019). All manipulations were carried out under general anesthesia by intramuscular injection of xylazine (Interchemie, Netherlands) at 1 mg/kg dose and zoletil (VirbacSanteAnimale, France) at 0.1 mL/kg dose. In the course of the experiment, 5 groups of animals were formed: 1) control, which included 10 intact rats; 2) comparative group, consisting of 27 rats with local microcirculatory disorders caused by sciatic nerve transection and neurorrhaphy; 3) comparative group of 20 rats with systemic microcirculatory disorders caused by alloxan-induced diabetes mellitus; 4) experimental group, which included 20 rats that received FTSG in the interscapular region simultaneously with sciatic nerve neurorrhaphy; 5) experimental group, consisting of 10 rats, which received FTSG on day 21 after alloxan injection.

As a model of local microcirculation dysfunction, denervation hypersensitivity, which occurs and develops during transection and delayed sciatic nerve neurorrhaphy and is accompanied by microvascular vasospasm and microcirculation deterioration, was used [15]. Sciatic nerve transection was performed at the level of the middle third of the thigh. Neurorrhaphy was performed 21 days after nerve transection by applying epineural suturing using atraumatic needles and 7/0 USP suture material.

Systemic microcirculation disorders were modeled by development of alloxan-induced diabetes in animals, which has a direct β-cytotoxic effect on the pancreatic islet and causes absolute insulin deficiency that is characteristic of type 1 diabetes [16]. Alloxan (100 mg/kg of animal weight) was injected subcutaneously once. Development of diabetes mellitus was verified by a statistically significant ($p < 0.05$) increase in glycated hemoglobin levels by 1.7 times to 9.3% (6.9; 12.1) compared to the intact animals.

FTSG in the experimental groups was performed on day 21 from the beginning of the experiment (sciatic nerve transection or alloxan administration, respectively). A full-layer skin flap, 0.1% of the animal's body surface area, was excised in the interscapular region, and treated alternately in 3% hydrogen peroxide, 70% ethyl alcohol and 0.9% saline solution. In the wound formed during the excision of the flap, a subcutaneous pocket was formed where the processed autograft was placed. The operating wound was tightly sutured [17].

Microcirculation in the dorsal skin of the posterior paw using LAKK-OP (NPP "Lazma", Russia) on day 42 of the experiment in the comparative and experimental groups. LDF-grams of intact animals were used as a control. Microcirculation state was assessed by the value of perfusion index in perfusion units.

Blood was collected from animals on day 42 of the experiment by puncture of the right heart sections using VACUETTE blood tubes (Greiner Bio-One, Austria) with a coagulation activator and a separating polyester gel to obtain serum, as well as with 3.2% sodium citrate for obtaining plasma and making smears.

The serum catecholamine (CA) level as the main vasoconstrictor substances was determined by microscopy using μ-Vizo 101 microvisor (LOMO, Russia) of smears stained with silver nitrate and eosin by Mardar and Kladienko cytochemical method (1986) with preliminary exposure in a potassium dichromate solution to obtain adrenochromes adsorbed on red blood cell. Serum CA levels were expressed in arbitrary units, defined as the amount of silver-impregnated adrenochrome granules adsorbed on 100 red blood cells of a smear.

Blood concentrations of vasodilator substances, including histamine and vascular endothelial growth factor (VEGF), were determined by enzyme immunoassay using semi-automated readers StatFax4200 (Awareness Technology, USA) and Epoch (BioTekInstruments, USA), as well as VEGF Rat reagents (RnDSystems, USA) and Histamine-ELISA (IBL International, Germany).

The animals were withdrawn from the experiment by an overdose of anesthesia drugs immediately after blood sampling. The tissues of the FTSG zone were harvested and fixed in 10% formalin for histology. Skin samples from intact animals were used as controls. 5μm-thick histological sections were stained with Mayer's hematoxylin (OOO Biovitrum, Russia) and eosin (Biovitrum, Russia). Microscopy of the FTSG zone preparations was performed using the AxioImager Z2 system (CarlZeiss, Germany). Quantitative calculation of cell populations of the autograft dermis was performed at a magnification of 40× objective lens.

Statistical processing was done using the Statistica 10.0 software package. Most of the data obtained did not conform to the law of normal distribution. So, they are presented as median and interquartile range. The groups were compared using the Mann–Whitney U test and the certainty index of the difference p, whose critical level was taken to be 0.05.

RESULTS

A study of microcirculation of the dorsal skin of the rear paw in the group of animals that underwent transection and deferred sciatic nerve neurorrhaphy showed a significant decrease in the perfusion index relative to the control values on day 42 of the experiment. The animals that underwent FTSG simultaneously with neurorrhaphy showed an improved microcirculation state on day 42 of the experiment, as evidenced by the significant increase in perfusion index by 44% compared to its value in animals in the corresponding comparison group. The perfusion index in this group did not differ from the values observed in the control group (Fig.).

It was shown that animals with experimental diabetes by day 42 after alloxan injection showed a statistically significant decrease in perfusion of the dorsal skin of the rear paw compared to the control group, indicating a reduction in microcirculation. In animals that underwent FTSG against the background of alloxan-induced diabetes, a statistically significant increase (by 43%) in this indicator was observed on day 42 of the experiment relative to the group of animals with impaired carbohydrate metabolism, indicating improved microcirculation. For the two experimental groups, it was found that the level of perfusion was statistically higher in animals that underwent FTSG against the background of systemic microcirculatory disorders (Fig.).

In studying the role of changes in the sympathetic regulation of vascular tone in realization of the distant stimulating effect of FTSG, it was found that in rats

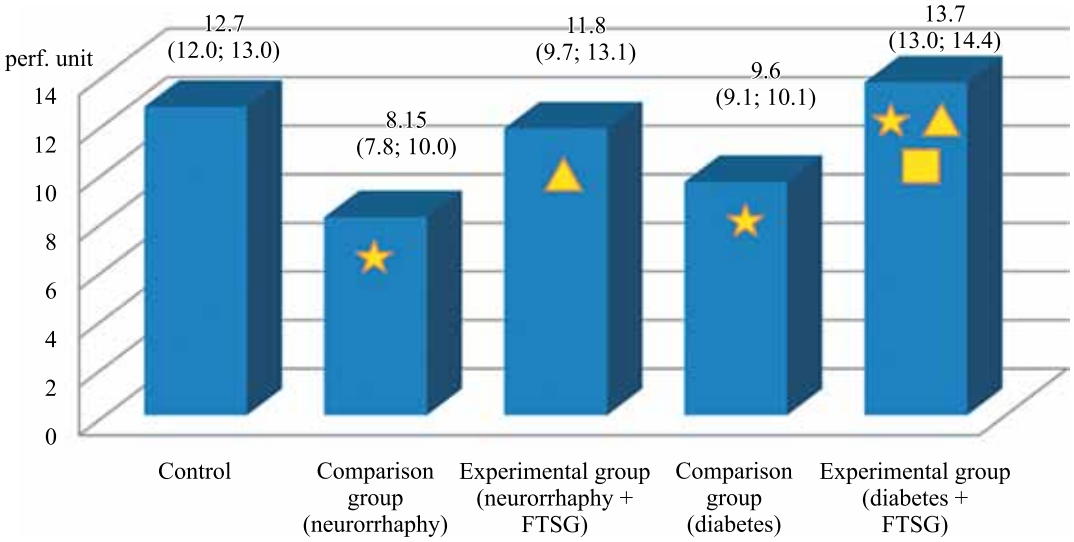

Fig. Changes in the perfusion index of the dorsal skin of the rear paw with FTSG autotransplantation in sciatic nerve injury and alloxan-induced diabetes. Statistically significant differences ($p < 0.05$) are indicated by: a star (relative to the control), a triangle (relative to the corresponding comparison group), and a square (comparison of the experimental groups between each other)

that underwent neurorrhaphy, there was a statistically significant increase in blood catecholamine levels on day 42 after surgery relative to the control. In this group, we found that FTSG reduced catecholamine levels by about 1.5 times as compared to the group of animals that did not receive FTSG against the background of neurorrhaphy (Table 1).

At the same time, animals with systemic microcirculatory disorders induced by alloxan-induced diabetes also showed a significant increase in serum catecholamine levels by day 42. FTSG in rats with alloxan-induced diabetes almost halved the serum catecholamine levels relative to the corresponding comparison group. Consequently, FTSG limits the activity of the sympathetic nervous system more pronounced in systemic microcirculatory disorders occurring against the background of impaired carbohydrate metabolism (Table 1).

The study of serum histamine levels revealed that transection and neurorrhaphy does not cause significant changes in histamine concentrations relative to the control. At the same time, in the experimental group, which underwent FTSG, plasma histamine levels on day 42 of the experiment exceeded both the control values and the values of the corresponding comparison group. It was found that FTSG, performed against the background of impaired carbohydrate metabolism, increases the blood histamine levels on day 42 of the experiment, which exceeds both the control values and the values of the comparison group by an average of 2.5 times (Table 1). This being said, blood histamine levels in animals that underwent FTSG against the background of alloxan-induced diabetes were significantly lower than in rats with FTSG against the background of sciatic nerve injury and neurorrhaphy.

It was found that FTSG, performed simultaneously with neurorrhaphy of the injured sciatic nerve, increases serum VEGF concentrations on day 42 of the experiment, which exceeds the control values by 1.8 times (Table 1). Alloxan was found to cause a significant increase in plasma VEGF levels in rats. Moreover, the FTSG animals also had increased VEGF levels relative to the control values, which did not differ significantly from that in the rats of the corresponding comparison group (Table 1).

Microscopy of tissue preparations from the autograft area revealed skin flap thinning accompanied by epidermis degradation. At the same time, there is a change in the composition of the cellular populations of the autograft dermis, manifested by increased number of fibroblasts, lymphocytes and macrophages. A distinctive feature of preparations in this group is the increased number of eosinophils, averaging up to 6 cells in the field of view (Table 2).

Morphological analysis of the preparations in animals with alloxan-induced diabetes revealed that by day 42 of the experiment, the autograft had thinned. The epidermis was absent in 20% of rats in this group. The thickness of the hypodermis was sharply reduced in all animals. Full-blooded arterial and venous vessels were observed in the dermis and hypodermis. Degenerating hair follicles were present in the dermis. The dermis of the autograft contained a large number of fibroblasts and was moderately infiltrated with leukocytes. Leukocyte infiltration was dominated by lymphocytes and macrophage cells. Animals with impaired carbohydrate metabolism had single eosinophils in the autograft dermis, but they were significantly less in number than in rats with sciatic nerve injury (Table 2).

DISCUSSION

The mechanism of local microcirculatory disorders in sciatic nerve injury is due to, on one hand, denerva-

Table 1

Changes in serum concentrations of vasoactive substances after FTSG autotransplantation in rats with sciatic nerve injury and alloxan-induced diabetes

Group / Indicator	Control	Comparison group (neurorrhaphy)	Experimental group (neurorrhaphy + FTSG)	Comparison group (diabetes)	Experimental group (diabetes + FTSG)
Serum catecholamine levels, units	22 (16; 25)	105 (95; 110) $p_1 = 0.000161$	65 (60; 70) $p_1 = 0.000176$ $p_2 = 0.021572$	56 (49; 60) $p_1 = 0.000001$	30 (26; 33) $p_1 = 0.001236$ $p_2 = 0.000001$ $p_3 = 0.000003$
Histamine, mg/L	1.7 (0.6; 2.1)	1.34 (1.19; 2.1) $p_1 = 0.885234$	3.16 (2.59; 3.69) $p_1 = 0.000939$ $p_2 = 0.001764$	1.1 (0.6; 2.2) $p_1 = 0.732678$	2.8 (2.2; 3.2) $p_1 = 0.025348$ $p_2 = 0.021828$ $p_3 = 0.023271$
VEGF, pg/mL	9.4 (7.3; 15.7)	8.6 (4.65; 9.96) $p_1 = 0.222082$	16.97 (9.96; 28.5) $p_1 = 0.004041$ $p_2 = 0.045501$	85.2 (79.6; 97.5) $p_1 = 0.000453$	83.3 (78.9; 86.3) $p_1 = 0.001033$ $p_2 = 0.286423$ $p_3 = 0.001033$

Note. p_1 – significance of differences relative to the control group; p_2 – significance of differences relative to the comparison group; p_3 – significance of differences when the two experimental groups are compared to each other.

Table 2

Dynamics of cell populations of the autograft dermis in sciatic nerve injury and alloxan-induced diabetes

Group / Indicator	Control	Comparison group (neurorrhaphy + FTSG)	Experimental group (alloxan-induced diabetes + FTSG)
Fibroblasts	42 (27; 52)	104 (60; 182) $p_1 = 0.000077$	119 (97; 165) $p_1 = 0.000028$ $p_2 = 0.394742$
Fibrocytes	18 (13; 23)	21 (14; 32) $p_1 = 0.558185$	27 (21; 44) $p_1 = 0.034962$ $p_2 = 0.183147$
Neutrophils	0 (0; 0)	1 (0; 4) $p_1 = 0.005414$	0 (0; 1) $p_1 = 0.291698$ $p_2 = 0.044686$
Eosinophils	0 (0; 0)	3 (2; 8) $p_1 = 0.000016$	1 (0; 2) $p_1 = 0.010519$ $p_2 = 0.000292$
Lymphocytes	0 (0; 2)	13 (5; 19) $p_1 = 0.000034$	20 (14; 27) $p_1 = 0.000017$ $p_2 = 0.077135$
Monocytes / histiocytes / macrophages	0 (0; 0)	1 (1; 3) $p_1 = 0.001393$	2 (0; 3) $p_1 = 0.047679$ $p_2 = 0.394742$

Note. p_1 – significance of differences relative to the control; p_2 – significance of differences relative to the comparison group.

tion hypersensitivity of the pre-capillary vessels of the microcirculatory bloodstream, characterized by increased expression of alpha-1 adrenergic receptors on the membrane of smooth muscle cells and their sensitivity to catecholamines [15]. On the other hand, traumatic injury to the nerve trunk is accompanied by activation of the sympathetic nervous system and, as evidenced by obtained data, by increased serum CA levels. Together, these two factors lead to increased tone of smooth muscle cells of the precapillary vessels and vasoconstriction of small arteries and arterioles, which is manifested by decreased perfusion of the dorsal skin of the rear paw of the operated limb. Recent studies indicate that alloxan administration in mice is also accompanied by increased expression of alpha-1 adrenergic receptors in the smooth muscle cells of the skin vessels during 2–4 weeks of development of alloxan-induced diabetes. Using laser speckle contrast imaging, it was shown that in these animals, norepinephrine reduces arterial and venous blood flow in the dorsal skin without subsequent recovery, which reflects a persistent vasospastic response caused by vascular hypersensitivity to catecholamines [18]. Results obtained in the course of this study indicate that the level of circulating catecholamines increases in alloxan-induced diabetic rats. Elevated blood catecholamine levels in alloxan-induced diabetes may be associated with the effect of hyperglycemia on the activity of enzymes providing synthesis and degradation of these biogenic amines. Thus, under experimental conditions, it was shown that hyperglycemia in diabetic mice increases the expression of tyrosine hydroxylase in renal mesangial cells, accompanied by increased consumption of tetrahydrobiopterin and increased production of catecholamines. Moreover, there was reduced activity of monoamine oxidase, which prevented the destruction of catecholamines [19]. Consequently, in diabetes and in nerve injury, microcirculatory disorders are caused, on one hand, by increased levels of circulating catecholamines, and, on the other hand, by increased expression of alpha-1 adrenergic receptors on the membrane of smooth muscle cells, causing development of vascular hypersensitivity to the action of circulating catecholamines. That is, the observed microcirculatory disorders in rats with traumatic sciatic nerve injury and animals with alloxan-induced diabetes are not only similar, but also have homologous developmental mechanisms. However, in the case of nerve injury, microcirculatory disorders are predominantly local, while in alloxan-induced diabetes, they are systemic.

FTSG in the interscapular region against the background of both nerve injury and alloxan-induced diabetes has a distant stimulating effect on the microcirculation of the dorsal skin of the rear paw in white rats. The perfusion index of the foot skin surface in experimental animals of the experimental groups increased on average by 43–44% relative to the corresponding comparison groups, indicating the same degree of severity of the distant stimulating effect of FTSG both in local and in systemic microcirculatory disorders. Earlier studies indicate that realization of the distant stimulating effect of FTSG on microcirculation in intact rats, under conditions of sciatic nerve injury and in carbohydrate metabolism disorders, is associated with decreased neurogenic vascular tone [14, 17]. The dynamics of serum catechola-

mine levels presented in this work is consistent with the previously obtained data and indicates that FTSG in the interscapular region, against the background of local and systemic microcirculatory disorders, limits the activity of the sympathoadrenal system. Limitation of the influence of the sympathetic system on the microcirculatory bloodstream vessels under the influence of autologous transplantation may explain the maintenance of adequate perfusion in the distal limb in rats of the experimental groups. The mechanism of limiting the activity of the sympathoadrenal system under FTSG influence may be due to the detected degenerative changes in the skin flap, which may be accompanied by formation of peptide fragments acting as cytomedines. As peptide regulators, cytomedines can exert distant effects, including on the nervous system [20]. A similar mechanism for limiting the effects of the sympathetic nervous system on the vascular bed has been described for peptide drug SEMAX, whose action was characterized by decreased expression of alpha-adrenergic receptors under experimental conditions in white rats [21]. The data obtained in the course of this work indicate that limitation of the influence of the sympathetic nervous system on microcirculation in FTSG is more pronounced in systemic microcirculatory disorders caused by absolute insulin deficiency.

It was noted earlier that FTSG performed against the background of sciatic nerve neurorrhaphy has an effect not only on the blood levels of circulating catecholamines, but also on the levels of other biogenic amines, including those with vasodilatory activity. For instance, it increases plasma histamine levels [13]. The results of this work demonstrate that FTSG exerts a similar effect on plasma histamine levels after alloxan injection. Meanwhile, the average value of the histamine levels in the group of animals that received FTSG after alloxan administration was 12% lower than the values in the experimental group that underwent autotransplantation against the background of sciatic nerve injury.

One of the possible mechanisms for realization of the distant stimulating effect of FTSG on microcirculation under normal carbohydrate metabolism with impaired innervation of the limb is the ability to prolong the production of growth factors, particularly VEGF and neurotrophin 3 [13, 22]. The sources of growth factors can be fibroblasts [23] and leukocyte infiltration cells of the autograft. For example, eosinophils [24], mast cells [25], and macrophages [26] secrete VEGF, which stimulates angiogenesis, causing vascular dilatation and an increase in their permeability. However, this study found that FTSG does not implement this mechanism of action in conditions of alloxan-induced diabetes in rats. The blood levels of this factor in the experimental group significantly exceeds the control values, but does not differ from the comparative group of rats with alloxan-induced diabetes. In systemic microcirculatory disorders caused by experimental diabetes, high plasma VEGF levels are associated with systemic endothelial alteration by hyperglycemia, which is a compensatory mechanism for vascular wall repair [27]. In this regard, the initially high level of VEGF in rats with alloxan-induced diabetes is likely to block its production by autograft cells through a negative feedback mechanism.

The above described biochemical mechanisms of realization of the distant stimulating effect of FTSG on microcirculation are closely interrelated with histomorphological restructuring of the autograft. Histomorphological changes in the autograft are stereotypic and include degradation of the epidermis, thinning of the dermis and hypodermis, and mild leukocyte infiltration. Minor differences between the experimental groups lie in the number of eosinophils in the composition of cell populations of the autograft dermis. Their presence in autograft tissues is associated with the release of histamine by mast cells, which is involved in distant vasodilating effect [28]. In animals, against the background of impaired carbohydrate metabolism, there was a lower number of eosinophils in the autograft region compared to animals with neurorrhaphy. These histological examination results are consistent with biochemical data reflecting a less pronounced increase in plasma histamine levels under FTSG influence in animals with alloxan-induced diabetes. The authors in [29] have shown that alloxan in rats significantly reduces the content of mast cells in the skin. Given the less pronounced increase in plasma histamine levels in FTSG under carbohydrate metabolism disorders, the small number of eosinophils in the autograft composition in rats with alloxan-induced diabetes is probably due to decreased intensity of mast cell degranulation.

CONCLUSION

FTSG has a distant stimulating effect on microcirculation, which manifests itself to the same extent under conditions of both local and systemic microcirculatory disorders, and does not have an obvious dependence on the etiological factor inducing them. The data obtained from comparative analysis of FTSG effects on two models of vascular alteration in white rats indicate that local structural and functional changes in the autograft are stereotypic. Therefore, they can be considered triggering, while biochemical changes in the concentrations of regulatory substances have an unequal degree of severity depending on the etiology and prevalence of microcirculatory disorders. Differences in the blood levels of bioactive substances allow to isolate universal and variable responses in the complex of FTSG regulatory mechanisms. Universal reactions include changes in the balance of biogenic amines in the blood, in particular, changes in the blood levels of catecholamines and histamine. It should also be noted that correction of vasoconstrictor activity using FTSG is more pronounced in systemic microcirculatory disorders induced by alloxan-induced

diabetes. In contrast, realization of the FTSG effect on production of vasodilator substances, in particular histamine, is more pronounced in local microcirculatory disorders in the denervated limb. Variable responses depend on the etiology of simulated microcirculatory disorders; in particular, changes in the production of growth factors, including VEGF, are specific for the microcirculatory effects of FTSG in limb denervation.

Thus, the relationship between structural and functional tissue changes in the field of autotransplantation and microcirculation regulation factors circulating in systemic blood flow determine a compensatory change in the balance of regulatory mechanisms, which provides a stable implementation of the distant stimulating effect of FTSG on microcirculation, regardless of the prevalence and etiology of its injury.

The authors declare no conflict of interest.

REFERENCES

1. *Mironov SP, Krupatkin AI, Golubev VG, Panov DE.* Diagnostika i vybor taktiki lecheniya pri povrezhdeniyah periphericheskih nervov. *Vestnik travmatologii i ortopedii im. N.N. Priorova*. 2005; 2: 33–39.
2. *Shchanicyn IN, Ivanov AN, Bazhanov SP, Ninel' VG, Puchin'yan DM, Norkin IA.* Stimulyaciya regeneracii periphericheskogo nerva: sovremennoe sostoyanie, problem i perspektivy. *Uspekhi fiziologicheskih nauk*. 2017; 48 (3): 92–112.
3. *Inanc M, Tekin K, Kiziltoprak H, Ozalkak S, Doguizi S, Aycan Z.* Changes in Retinal Microcirculation Precede the Clinical Onset of Diabetic Retinopathy in Children With Type 1 Diabetes Mellitus. *J Ophthalmol*. 2019; 207: 37–44. doi: 10.1016/j.ajo.2019.04.011.
4. *Stacenko ME, Turkina SV, Shilina NN, Kosivcova MA, LopushkovaYuE, Vinnikova AA i dr.* Osobennosti sostoyaniya mikrocirkulyacii u bol'nyh hronicheskoj serdechnoj nedostatochnost'yu i saharnym diabetom vtorogo tipa. *Volgogradskij nauchno-medicinskij zhurnal.* 2015; 1 (45): 35–39.
5. *Kuo L, Hein TW.* Vasomotor regulation of coronary microcirculation by oxidative stress: role of arginase. *Front Immunol.* 2013; 19 (4): 237.
6. *Mihajlusov RN.* Faktory rosta – perspektivnye tekhnologii vozdejstviya na ranevoj process. *Harkivs'ka hirurgichna shkola*. 2014; 5 (68): 90–98.
7. *Gromova OA, Torshin IYu, Volkov AYu*. Elementnyj sostav preparata Laennek i ego klyuchevaya rol' v farmakologicheskom vozdejstvii preparata. *Plasticheskaya hirurgiya i kosmetologiya*. 2010; 4: 1–7.
8. *Öhnstedt E, Lofton Tomenius H, Vågesjö E, Phillipson M.* The discovery and development of topical medicines for wound healing. *Expert Opinionon Drug Discovery*. 2019; 14: 485–497. doi: 10.1080/17460441.2019.1588879/.
9. *Nozdrin VI, Belousova TA, Al'banova VI, Lavrik OI.* Gistofarmakologicheskie issledovaniya kozhi (nash opyt). M., 2006. 376.
10. *Hocking SL, Stewart RL, Brandon AE*. Subcutaneous fat transplantation alleviates diet-induced glucose intolerance and inflammation in mice. *Diabetologia.* 2015; 58 (7): 1587–600.
11. *Foster MT, Shi H, Softic S et al.* Transplantation of non-visceral fat to the visceral cavity improves glucose tolerance in mice: investigation of hepatic lipids and insulin sensitivity. *Diabetologia*. 2011; 54 (11): 2890–2899.
12. *Hramcova YuS, Artashyan OS, Yushkov BG, Volkova YuL, Nezgovorova NYu.* Vliyanie tuchnyh kletok na reparativnuyu regeneraciyu tkanej s raznoj stepen'yu immunologicheskoj privilegirovannosti. *Citologiya*. 2016; 58 (5): 356–363.
13. *Ivanov AN, Lagutina DD, Gladkova EV, Matveeva OV, Mamonova IA, Shutrov IE i dr.* Mekhanizmy distantnogo stimuliruyushchego dejstviya autotransplantacii kozhnogo loskuta pri povrezhdenii periphericheskogo nerva. *Rossijskij fiziologicheskij zhurnal im. I.M. Sechenova*. 2018; 11: 1313–1324.
14. *Ivanov AN, Popyhova EB, Stepanova TV, Pronina EA, Lagutina DD*. Izmenenie pokazatelej mikrocirkulyacii pri autotransplantacii polnoslojnogo kozhnogo loskuta na fone eksperimental'nogo saharnogo diabeta u krys. *Regionarnoe krovoobrashchenie i mikrocirkulyaciya.* 2019; 4: 72–80.
15. *Ivanov AN, Norkin IA, Ninel' VG, Shchanicyn IN, Shutrov IE, Puchin'yan DM.* Osobennosti izmenenij mikrocirkulyacii pri regeneracii sedalishchnogo nerva v usloviyah eksperimenta. *Fundamental'nye issledovaniya*. 2014; 4 (2): 281–285.
16. *Dzhafarova RE*. Sravnitel'noe issledovanie razlichnyh modelej alloksan-inducirovannogo saharnogo diabeta. *Kazanskij medicinskij zhurnal*. 2013; 94 (6): 915–919.
17. *Ivanov AN, Shutrov IE, Norkin IA*. Autotransplantaciya polnoslojnogo kozhnogo loskuta kak sposob biostimulyacii mikrocirkulyacii v usloviyah normal'noj i narushennoj innervacii. *Regionarnoe krovoobrashchenie i mikrocirkulyaciya.* 2015; 3 (55): 59–65.
18. *Feng W, Shi R, Zhang C, Liu S, Yu T, Zhu D*. Visualization of skin microvascular dysfunction of type 1 diabetic mice using *in vivo* skin optical clearing method. *J Biomed Opt*. 2018; 24 (3): 1–9.
19. *Marco GS, Colucci JA, Fernandes FB, Vio CP, Schor N, Casarini DE*. Diabetes induces changes of catecholamines in primary mesangial cells. *Int J Biochem Cell Biol.* 2008; 40 (4): 747–754.
20. *Anohova LI, Pateyuk AV, Kuznik BI, Kohan ST*. Sravnitel'noe vliyanie polipeptidov endometriya i timalina na nekotorye pokazateli immuniteta i gemostaza v opytah *in vitro* i *in vivo*. *Byulleten' VSNC SO RAMN*. 2011; 6: 156–159.
21. *Gorbacheva AM, Berdalin AB, Stulova AN, Nikogosova AD, Lin MD, Buravkov SV i dr.* Izmenenie simpaticheskoj innervacii hvostovoj arterii krysy pri eksperimental'nom infarkte miokarda; vliyanie peptida "SEMAKS". *Byulleten' eksperimental'noj biologii i mediciny*. 2016; 4: 462–467.
22. *Ivanov AN, Shutrov IE, Ninel' VG, Korshunova GA, Gladkova EV, Matveeva OV i dr.* Vliyanie autotransplantacii kozhnogo loskuta i pryamoj elektrostimulyacii

sedalishchnogo nerva na regeneraciyu nervnyh volokon. *Citologiya.* 2017; 7: 489–497.

23. *Chakroborty D, Sarkar Ch, Lu K, Bhat M*. Activation of dopamine d1 receptors in dermal fibroblasts restores vascular endothelial growth factor-a production by these cells and subsequent angiogenesis in diabetic cutaneous wound tissues. *Am J Pathol*. 2016; 186 (9): 2262–2270. doi: 10.1016/j.ajpath.2016.05.008.
24. *Panagopoulos V, Zinonos I, Leach D, Evdokiou A*. Human peripheral blood eosinophils induce angiogenesis. *The International Journal of Biochemistry & Cell Biology*. 2005; 37 (3): 628–636. doi: 10.1016/j.biocel.2004.09.001.
25. *Lee AJ, Ro MJ, Park JI, Jang JH, Kim JH*. The synthesis of VEGF in allergen-stimulated mast cells is through a leukotriene B4 receptor-2-dependent signaling pathway. *J Immunol*. 2016; 1: 196.
26. *Monastyrskaya EA, Lyamina SV, Malyshev IYu.* M1 i M2 fenotipy aktivirovannyh makrofagov i ih rol' v immunnom otvete i patologii. *Patogenez*. 2008; 4: 31–39.
27. *Iskakova SS, Zharmahanova GM, Dvoracka M.* Mesto angiogeneza v razvitii saharnogo diabeta i ego oslozhnenij (obzor literatury). *Vestnik KazNMU*. 2014; 2 (2): 303–307.
28. *Swartzendruber JA, Byrne AJ, Bryce PJ.* Cutting edge: histamine is required for IL-4-driven eosinophilic allergic responses. *J Immunol*. 2012; 188 (2): 536–540.
29. *De F Carvalho V, Campos LV, Farias-Filho FA, Florim LT, Barreto EO, Pirmez C et al.* Suppression of allergic inflammatory response in the skin of alloxan-diabetic rats: relationship with reduced local mast cell numbers. *Int Arch Allergy Immunol.* 2008; 147 (3): 246–254.

The article was submitted to the journal on 6.03.2020

DOI: 10.15825/1995-1191-2020-4-133-139

AUTOLOGOUS REGENERATIVE STIMULANTS FOR BONE ALLOGRAFT IMPLANTATION

K.A. Vorobyov[1], T.O. Skipenko[1], N.V. Zagorodniy[1], D.V. Smolentsev[1], A.R. Zakirova[1], V.I. Sevastianov[2]

[1] Priorov National Medical Research Center for Traumatology and Orthopedics, Moscow, Russian Federation

[2] Shumakov National Medical Research Center of Transplantology and Artificial Organs, Moscow, Russian Federation

There are many different surgical techniques for bone reconstruction. However, biological reconstruction methods are being increasingly developed. The main purpose is not only to fill up defects, but to stimulate the processes of reconstruction and regeneration of bone as a complete organ. In this report, we describe the basic principles of orthobiology and the essential orthobiological materials. A clinical case is presented where a combination of allogeneic osteoplastic materials with autologous platelet-rich plasma is used to reconstruct a cavity defect in the tibia.

Keywords: orthobiology, bone regeneration, bone defect, bone graft, allogeneic bone graft material, bone marrow aspirate, platelet-rich plasma.

INTRODUCTION

Orthobiology is a conceptual concept, which includes a group of biological materials and substrates promoting bone regeneration. Such include bone grafts, osteoplastic materials, growth factors, regulatory protein, and cellular biomedical products [1, 2]. The role of orthobiology in bone healing lies in osteoconduction, osteoinduction and osteogenesis, which are part of the "diamond concept" proposed by Giannoudis et al. [3], where the authors identified four basic conditions for successful bone healing: potent osteogenic cell populations, osteoconductive matrix scaffolds, osteoinductive stimulus, and mechanical stability.

Bone transplantation

Bone transplantation in the classical concept is possible only if the bone tissue is preserved in its native form and is applicable only for two types of materials – autologous bone and allograft. Autografts have three functional properties (osteoconductivity, osteoinduction and osteogenicity) and demonstrate the highest ability for osseointegration and remodeling; therefore, they are rightfully considered the 'gold standard' for bone grafting. However, their use is limited because they can be used in a small volume and there is a need to form an additional access for collection of donor fragments [4]. Spongy bone autografts are the most commonly used type of materials because they contain a small number of osteoblasts and osteocytes, with a high content of living multipotent mesenchymal stromal cells (MSCs) and they create an osteogenic potential for neoosteogenesis from the graft. Moreover, proteins contained in the autograft allow maintaining the natural osteoinductive potential [2]. In the early post-autograft period, at the stage of hematoma and inflammation, the contained MSCs allow quick formation of granulation tissue; necrotic tissues are removed by macrophages, and graft neovascularization occurs [3].

Allogeneic bone materials

Unlike autografts, allografts are immunogenic and exhibit rejection reactions, which are caused by antigens of the major histocompatibility complex (MHC) [5]. The initial osseointegration phase is accompanied by severe inflammation due to immune response, causing necrosis of osteoprogenitor cells [6]. The necessary conditions for the use of allografts should be considered a decrease in immunogenicity and the conduct of donor/recipient compatibility studies, by analogy with organ transplantation [7]. Another problem is the risk of infection transmission, which has been resolved in most countries in the world thanks to the widespread development of a network of tissue banks and advanced processing technologies [4]. Due to immune response, purified decellularized and delipidized bone grafting materials (DDBGM) are very popular in clinical practice [8]. Purification of bone tissue of bone marrow cells and lipids and then of mineral-collagen matrix significantly reduces the degree of inflammatory response during DDBGM implantation, but does not prevent it. According to various literary sources, the probability of an immune response after implantation of such materials is about 10% [9]. Demineralized

Corresponding author: Konstantin Vorobyov. Adress: 10, Priorova str., Moscow, 127299, Russian Federation. Phone: (905) 222-10-00. E-mail: vorobyov_doc@mail.ru

bone matrix (DBM) is a highly purified, allogeneic bone derivative, a material devoid (by more than 40%) of the mineral component, while preserving collagenous and non-collagenous inducer proteins [10] that determine osteoinductivity. Having plasticity and high degree of biodegradation, the process of osseointegration and remodeling of the implanted DBM is more intensive than with non-demineralized bone materials [4].

The clinical outcome of a reconstructive-restorative surgery depends on the patient's health status, the tissues surrounding the recipient bed, and the quality and functional characteristics of the implanted materials. To improve the functional properties of bone grafting materials, they are used in combination with autologous bone marrow aspirate and/or autologous platelet-rich plasma [2, 11, 12]. The use of such combinations is a simple, affordable and effective way to reduce the risk of immune reactions after implantation, increase the osteoinductive potential and impart osteogenic properties to materials.

Autologous bone marrow aspirate

Autologous bone marrow aspirate (ABMA) contains 2 types of adult stem cells: hematopoietic stem cells (HSCs) and MSCs. The main mechanism of ABMA as a stimulator of bone regeneration, is realized due to MSCs content, which differentiate into osteoblasts in the presence of specific growth factors and cytokines. The mediated mechanism of action of ABMA is the effect of cytokines derived from MSCs on endothelial cells, which promote angiogenesis.

Autologous platelet-rich plasma

The use of autologous platelet-rich plasma (aPRP) as a biogenic stimulator of regeneration is a fairly popular and widespread method in orthopedics. Regenerative potential is achieved through a cascade of reactions and release of growth factors contained in platelet-rich plasma [13]. Besides, plasma platelets are able to release over 300 molecules that are responsible for complex intercellular and extracellular interactions [14]. Unlike soft tissue, bone regeneration is a long process. In this regard, many researchers suggest the use of thrombin-activated aPRP in the form of a dense fibrin clot to create conditions for slow release of the factors contained in it [16].

The main orthobiological materials and their comparative characteristics are presented in Table.

CASE

Patient M., born in 1979, medical record card No. H2019-10342, was treated at the 12th department of the Priorova National Medical Research Center of Traumatology and Orthopedics from December 18, 2019 to December 24, 2019 for post-traumatic deformity of the proximal third of the right tibia. Posttraumatic type II medial right-sided gonarthrosis. Cyst of the upper third of the central-medial right tibia. Old damage to the body and anterior horn of the medial meniscus, partial damage to the anterior cruciate ligament of the right knee joint. Moderate right knee synovitis. The patient complained of swelling and pain in his right knee during physical exercise, impaired lower limb function. Examination revealed a deformity of the proximal metaphysis of the right tibia along the anterior surface and a varus deformity of the tibia. The right knee contours were unchanged, and edema was moderate. The right thigh muscles were satisfactorily developed. On palpation, the internal articular cavity was painful. Positive Baykov's symptoms. Capsular ligament apparatus: anterior drawer test (–/+), Lachman test (–), posterior drawer test (–), Varus stress test (–), Valgus stress test (–). Joint movement was full, painful when flexing mainly along the inner surface. Patella movements were painless. No vascular or neurological disorders in the limb were revealed at the time of examination. The patient underwent X-ray and multispiral computed tomography (MRI), which diagnosed a cyst of the proximal central-medial metaphysis of the right tibia (Fig. 1).

Punch trephine biopsy of the cyst was performed; cytological examination revealed no atypical cells. Given the clinical and diagnostic data, a decision was taken to surgically reconstruct the abnormal focus – combined

Table

Comparative biological properties of bone grafts and autologous regenerative stimulants

Autologous and allogenic orthobiological materials				
Material type/functional properties	Osteoconduction	Osteoinduction	Osteogenicity	Osseointegration
Cortical autograft	+	+	+	+
Spongy autograft	+++	+++	+++	+++
Cortical allo-implant	+	+/–	–	+
Spongy allo-implant	+	+/–	–	++
Demineralized bone matrix	+	++	–	++
Autologous bone marrow aspirate	–	++	+++	+++1
Autologous platelet-rich plasma	–	+++	+	++2

Note. [1] – effect on the osseointegration process is achieved due to the content bone marrow-derived multipotent mesenchymal stromal cells; [2] – effect on the osseointegration process is achieved due to the content of growth factors.

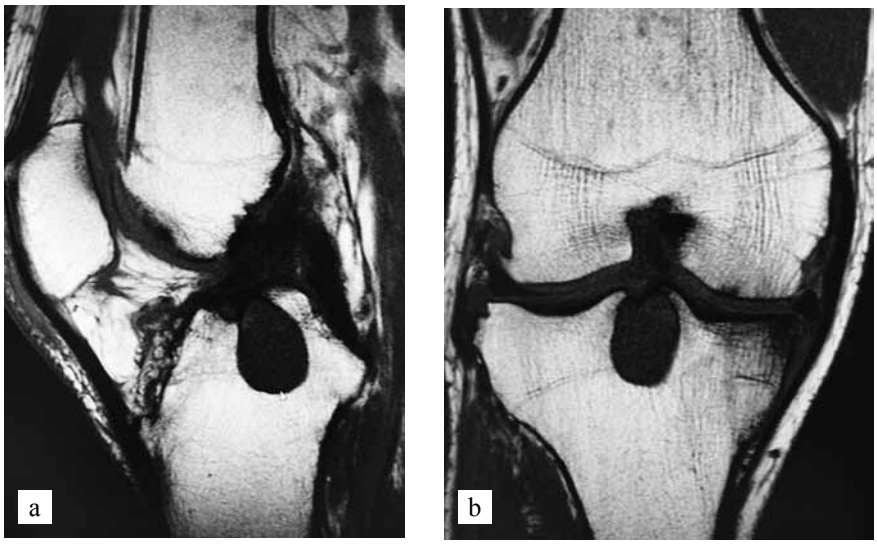

Fig. 1. Magnetic resonance imaging (MRI) of the knee. Tibial cyst. a) sagittal plane. b) frontal plane

bone grafting with allogeneic cancellous implants impregnated with aPRP. Allogeneic cancellous chips and Perfoost blocks from the Tkanevoy Bank of the Priorova National Medical Research Center of Traumatology and Orthopedics (RU # FSR 2009/05682 dated December 17, 2018) and a sets for preparation of aPRP and activation platelet-rich plasma Regen BCT-SP (R-BCT-SP) and Regen ATS-SP (R-ATS-SP) produced by Regen Lab SA, Switzerland were used to perform the surgical procedure.

The permission of the ethics committee was not required for the surgical intervention since the materials used have registration certificates. Blood sampling and preparation of autologous plasma were done prior to surgery, according to the manufacturer's instructions.

***Surgery process.** The operation was performed under spinal anesthesia, with the patient in the supine position, with reoperative antibiotic prophylaxis. The right lower limb was fixed in a knee brace in the middle third of the thigh. After treating the operating site three times with antiseptic solutions, a blood-squeezing tourniquet was applied from the lower third of the leg to the lower third of the thigh, then a pneumatic tourniquet was inflated in the upper third of the thigh. Under the control of an electronic optical transducer, below and lateral to the superficial goose foot, a 5 cm longitudinal skin incision was made, skin-subcutaneous flaps were mobilized, and access to the bone was made. An osteotomy was performed along the needle inserted into the cyst cavity of the central-medial metaphysis of the right tibia, then a canal was formed using a drill. The defect cavity was repeatedly washed with aseptic solutions, and the walls were treated. Bone-grafting materials were fragmented to the required size, then autologous plasma was added to them and plasma activation using thrombin was performed.*

The resulting combined bone-grafting material was placed in the defect cavity, and it was impacted for uniform distribution in the cavity. For the purpose of intraoperative control, a picture was taken with an electronic optical converter. Wound suturing was performed in layers.

CT multiscan was performed the next day after surgery. According to visual data obtained in three planes – axial, frontal, sagittal (Fig. 2) – there was a uniform filling of the defect with bone-grafting material.

Fig. 2. Multispiral computed tomography (MSCT) of the knee joint. Tibial cyst after bone grafting. a) axial projection; b) frontal projection; c) sagittal projection

DISCUSSION

Analyzing the literature on this topic [1–3, 12, 15, 17], we should note the tendency that reconstructive and grafting interventions on bone tissues are aimed not only at addressing pain, restoring function, filling a defect or eliminating deformity, but also at stimulating regenerative processes. This explains the development of such a conceptual approach in orthopedics as orthobiology, since orthobiological products and their combinations can create the necessary conditions for achieving this goal.

Transplantation of frozen massive bone-cartilaginous allografts for bone tumors was performed by M.V. Volkov in 1960–70s [18]. The author described 145 cases, of which half of the results were unsatisfactory, which was due to insufficient understanding, at that time, of the mechanisms of transplant immunology. One of the first studies on the histocompatibility of cartilage tissue was carried out by Langer and Gross [19], where it was shown that intact articular cartilage does not cause humoral immune responses. This is due to the fact that antibodies are unable to penetrate through the dense cartilage matrix and reach the chondrocytes. This peculiarity of cartilage tissue allows transplantation without the necessary HLA compatibility studies [20], making the cartilage an "immune-privileged" tissue. Bone tissue, on the contrary, has enough immunogen; its transplantation in its native form requires the necessary compatibility studies to reduce the rejection risks and degree of immune response [20, 21]. Modern possibilities of laboratory screening and understanding of the mechanisms of transplant immunology and immunosuppression create the necessary conditions for the development of tissue transplantation, which is confirmed by literature data. For example, C. Krettek et al. [17] describes positive clinical results after transplantation of allogeneic osteochondral blocks and massive grafts. The use of allogeneic grafts from femoral heads from living donors is very popular among many orthopedic surgeons in the USA and European countries [22, 23]. In Russia, due to gaps and conflicts in legal regulations on tissue donation and transplantation, the lack of a network of regional tissue banks and the complexity of interaction of specialists in the sequence from donor to recipient patient, bone tissue transplantation remains a difficult surgical procedure to access [24].

Allogeneic bone grafting materials are the most popular and often used method in reconstructive surgery. The ability to process bone tissue to a mineral-collagen or demineralized matrix reduces immunogenicity and minimizes the likelihood of complications associated with it. In Russia, the production of materials is not subject to uniform standards on which the tissue processing and sterilization technology is based [8, 25]. As a result, bone grafting materials differ in their properties. This complicates the repeatability and predictability of clinical outcomes, and sometimes leads to post-implantation complications [9].

The efficiency of autologous bone marrow aspirate use to improve bone regeneration processes, both alone and in combination with osteoplastic materials, has been confirmed by many studies. Gianakos et al. [26] described the results of 35 animal studies in which BMA was used in long bone defects. Healing occurred in 100% of cases, and 90% reported significant improvement in earlier bone healing on histologic/histomorphometric assessment. Hernigou et al. [27] described the use of concentrated BMA concentrate after centrifugation in the pseudarthrosis of the tibia in 60 patients, of whom fusion was achieved in 53. Desai et al. [28] described the positive results of the use of BMA in combination with osteoplastic materials in false tibial joints. Schotter and Warner [29] published data indicating a positive effect when using BMA in combination with allogeneic bone grafting materials.

Sanchez [30] and Gallasso [31] published clinical cases of the use of aPRP to accelerate fracture healing. A positive effect was achieved in all cases. Kesyan G.A. et al. [11] described a number of clinical cases, which also noted the positive effect of the use of aPRP in combination with osteoplastic materials for the treatment of pseudoarthrosis. Despite the widespread use of aPRP to stimulate bone regeneration, the data on the effectiveness of its use remain controversial. Peerbooms et al. [32] reported that there is no beneficial effect of using aPRP to stimulate bone regeneration. Chahla et al. [15] published an analytical review of the literature, which reflected the analysis of 105 studies, of which 16% fully describe the characteristics of the cellular composition and the content of growth factors, and only 10% describe in detail the protocol for preparing aPRP. The need to standardize aPRP preparation protocols and guidelines for its use is described by many authors [15, 16]. Relying on recommendations from the same publications, it should be noted that to stimulate bone regeneration, thrombin-activated plasma in the form of a dense fibrin clot, which is able to form and maintain the required shape and slowly release the growth factors contained in it, is necessary. For this reason, we used the Regen BCT-SP (R-BCT-SP) and Regen ATS-SP (R-ATS-SP) kits, described in our clinical case.

CONCLUSION

The use of bone grafts and bone grafting materials in combination with bone marrow aspirate or platelet-rich plasma reduces the degree of immune response, promotes osseointegration and remodeling processes, which expands the possibilities of using surgical methods for biological reconstruction of bone tissues. To stimulate bone regeneration, it is recommended to use thrombin-activated platelet-rich plasma in the form of a dense fibrin clot. Only in this case can one create and

maintain the necessary shape of the material and ensure slow release of growth factors.

The authors declare no conflict of interest.

REFERENCES

1. *Raghuram A, Singh A, Chang DK, Nunez M, Reece EM.* Bone Grafts, Bone Substitutes, and Orthobiologics: Applications in Plastic Surgery. *Semin Plast Surg*. 2019 Aug; 33 (3): 190–199.
2. *Calcei JG, Rodeo SA.* Orthobiologics for Bone Healing. *Clin Sports Med*. 2019 Jan; 38 (1): 79–95.
3. *Giannoudis PV, Einhorn TA, Marsh D.* Fracture healing: the diamond concept. *Injury*. 2007; 38 (4): 3–6.
4. *Khan SN, Cammisa FP, Sandhu HS, Diwan AD, Girardi FP, Lane JM.* The biology of bone grafting. *J Am Acad Orthop Surg*. 2005; 13 (1): 77–86.
5. *Stevenson S, Horowitz M.* The response to bone allografts. *J Bone Joint Surg Am*. 1992 Jul; 74 (6): 939–950.
6. *Stevenson S, Li XQ, Martin B.* The fate of cancellous and cortical bone after transplantation of fresh and frozen tissue-antigen-matched and mismatched osteochondral allografts in dogs. *J Bone Joint Surg Am*. 1991 Sep; 73 (8): 1143–1156.
7. *Gautier SV.* Transplantologiya i iscusstvenniye organy. M.: Laboratoriya znaniy, 2018. 319.
8. *Vorobyov KA, Bozhkova SA, Tikhilov RM, Cherny AZh.* Current methods of processing and sterilization of bone allografts. *Traumatology and orthopedics of Russia*. 2017; 23 (3): 134–147. [In Russ, English abstract].
9. *Volkov AV.* On the safety of osteoplastic materials. *N.N. Priorov journal of Traumatology and Orthopedics*. 2015; 1: 46–51. [In Russ, English abstract].
10. *Bal Z, Kushioka J, Kodama J, Kaito T, Yoshikawa H, Korkusuz P, Korkusuz F.* BMP and TGFβ Use and Release in Bone Regeneration. *Turk J Med Sci.* 2020 Apr 27.
11. *Kesyan GA, Berchenko GN, Urazgildeev RZ, Mikelaishvili DS, Shulashov BN.* Combined application of platelet-rich plasma and biocomposite material collapan in complex treatment of patient with non-united fractures and pseudarthrosis of extremity long bones. *N.N. Priorov journal of Traumatology and Orthopedics*. 2011; 2: 26–32. [In Russ, English abstract].
12. *Bray CC, Walker CM, Spence DD.* Orthobiologics in Pediatric Sports Medicine. *Orthop Clin North Am*. 2017 Jul; 48 (3): 333–342.
13. *Lenza M, Ferraz SB, Viola DCM et al.* Platelet-rich plasma for long bone healing. *Einstein (Sao Paulo)*. Jan–Mar 2013; 11 (1): 122–127.
14. *El Backly RM, Zaky SH, Muraglia A, Tonachini L, Brun F, Canciani B et al*. A platelet-rich plasma-based membrane as a periosteal substitute with enhanced osteogenic and angiogenic properties: a new concept for bone repair. *Tissue Eng Part A*. 2013 Jan; 19 (1–2): 152–165.
15. *Chahla J, Cinque ME, Piuzzi NS, Mannava S, Geeslin AG, Murray IR et al*. A Call for Standardization in Platelet-Rich Plasma Preparation Protocols and Composition Reporting: A Systematic Review of the Clinical Orthopaedic Literature. *J Bone Joint Surg Am*. 2017 Oct 18; 99 (20): 1769–1779.
16. *Navani A, Li G, Chrystal J.* Platelet Rich Plasma in Musculoskeletal Pathology: A Necessary Rescue or a Lost Cause? *Pain Physician*. 2017 Mar; 20 (3): E345–E356.
17. *Krettek C, Clausen J-D, N Bruns, Neunaber C*. Partial and complete joint transplantation with fresh osteochondral allografts – the FLOCSAT concept. [Article in German]. *Unfallchirurg*. 2017 Nov; 120 (11): 932–949.
18. *Volkov M.* Allotransplantation of joints. *J Bone Joint Surg Br*. 1970 Feb; 52 (1): 49–53.
19. *Langer F, Gross AE*. Immunogenicity of allograft articular cartilage. *J Bone Joint Surg Am*. 1974 Mar; 56 (2): 297–304.
20. *Kandel RA, Gross AE, Ganel A, McDermott AG, Langer F, Pritzker KP.* Histopathology of failed osteoarticular shell allografts. *Clin Orthop Relat Res*. Jul-Aug 1985; (197): 103–110.
21. *Stevenson S, Shaffer JW, Goldberg VM.* The humoral response to vascular and nonvascular allografts of bone. *Clin Orthop Relat Res*. 1996 May; (326): 86–95.
22. *Hernigou P.* Bone transplantation and tissue engineering, part III: allografts, bone grafting and bone banking in the twentieth century. *Int Orthop*. 2015 Mar; 39 (3): 577–587.
23. *Hovanyecz P, Lorenti A, Lucero JMJ, Gorla A, Castiglioni AE.* Living donor bone banking: processing and discarding – from procurement to therapeutic use. *Cell Tissue Bank*. 2015 Dec; 16 (4): 593–603.
24. *Gautier SV, Khomyakov SM.* Legal and organizational basis of organ donation and transplantation in the Russian Federation. *Hospital Medicine: Science and Practice*. 2018; 1 (S): 61–74. [In Russ, English abstract].
25. *Shangina OR, Khasanov RA*. The role of a multidisciplinary tissue bank in development and clinical implementation of regenerative surgery technologies. *Practical medicine*. 2019; 17 (1): 17–19. [In Russ, English abstract].
26. *Gianakos A, Ni A, Zambrana L, Kennedy JG, Lane JM*. Bone Marrow Aspirate Concentrate in Animal Long Bone Healing: An Analysis of Basic Science Evidence. *J Orthop Trauma*. 2016 Jan; 30 (1): 1–9.
27. *Hernigou P, Mathieu G, Poignard A, Manicom O, Beaujean F, Rouard H.* Percutaneous autologous bone-marrow grafting for nonunions. Surgical technique. *J Bone Joint Surg Am*. 2006 Sep; 88 Suppl 1 Pt 2: 322–327.
28. *Desai P, Hasan SM, Zambrana L, Hegde V, Saleh A, Cohn MR, Lane JM.* Bone Mesenchymal Stem Cells with Growth Factors Successfully Treat Nonunions and Delayed Unions. *HSS J*. 2015 Jul; 11 (2): 104–111.
29. *Schottel PC, Warner SJ.* Role of Bone Marrow Aspirate in Orthopedic Trauma. *Orthop Clin North Am*. 2017 Jul; 48 (3): 311–321.
30. *Sanchez M, Anitua E, Cugat R, Azofra J, Guadilla J, Seijas R, Andia I.* Nonunions treated with autologous preparation rich in growth factors. *J Orthop Trauma*. 2009 Jan; 23 (1): 52–59.
31. *Galasso O, Mariconda M, Romano G, Capuano N, Romano L, Iannò B, Milano C.* Expandable intramedullary nailing and platelet rich plasma to treat long bone nonunions. *J Orthop Traumatol*. 2008 Sep; 9 (3): 129–134.
32. *Peerbooms JC, Colaris JC, Hakkert AA et al.* No positive bone healing after using platelet rich plasma in a skeletal defect. An observational prospective cohort study. *Int Orthop*. 2012 Oct; 36 (10): 2113–2119.

The article was submitted to the journal on 21.09.2020

DOI: 10.15825/1995-1191-2020-4-140-148

THE ROLE OF ENDOVASCULAR AND ENDOBILIARY METHODS IN THE TREATMENT OF POST-LIVER TRANSPLANT COMPLICATIONS

S.V. Gautier[1, 2], M.A. Voskanov[1], A.R. Monakhov[1, 2], K.O. Semash[1]

[1] Shumakov National Medical Research Center of Transplantology and Artificial Organs, Moscow, Russian Federation

[2] Sechenov University, Moscow, Russian Federation

Liver transplantation is the treatment of choice for patients with end-stage liver disease or acute liver failure. However, vascular complications, such as hepatic artery stenosis and/or thrombosis, graft portal vein stenosis and biliodigestive strictures following liver transplantation are still common despite improvements and innovations in surgical techniques. These complications can lead to graft damage or even death, and they are caused by many factors. Although minimally invasive interventional radiology is an optional treatment for such post-liver transplant complications, there is little research on this method of treatment.

Keywords: liver transplantation, endovascular treatment, endobiliary treatment, hepatic artery stenosis, hepatic artery thrombosis, portal vein stenosis, biliodigestive strictures.

INTRODUCTION

The American Association for the Study of Liver Diseases and the American Society of Transplantation suggest that screening and detection of post-liver transplant surgical complications be performed regularly and routinely [1].

Surgical complications such as hepatic artery stenosis and thrombosis, portal vein stenosis and biliary strictures are optimally diagnosed and treated at the transplant center. However, there is no consensus on the monitoring of these complications and their treatment tactics.

HISTORICAL ASPECTS OF THE DEVELOPMENT OF MINIMALLY INVASIVE TREATMENT METHODS

The development of catheter technology dates back to ancient times. The ancient Egyptians, 3,000 BC, were the first in the world to perform bladder catheterization using special tubes. Erasistratus was the first to use the word "καθετηρ" (catheter) around 300 BC. to describe this instrument. Classic S-shaped catheters date from this period, and some of them were discovered during excavations of the house of a surgeon in Pompeii, who was buried by a volcanic eruption in 79 AD [2].

In 1711, Dutch physiologist Stephen Hales performed the first catheterization of the heart chambers in a horse using brass and glass tubes [3].

A very important discovery for further development of medicine was made by Wilhelm Roentgen, who in 1895, discovered radiation, which he called X-rays [4]. By 1896, Vladimir Bekhterev had predicted the discovery of angiography: "...*Since it became known that some solutions do not transmit X-rays, brain vessels can be filled with them and photographed in situ*" [5].

The year of emergence of interventional radiology can be considered 1929. Werner Forssmann, a 25-year-old resident surgeon at Auguste Viktoria Home Red Cross Hospital in Eberswalde, Germany, in an experiment, for the first time in the world, proved the safety of inserting catheters into the human heart when he performed a catheter through the ulnar vein into the right atrial cavity [6].

In 1953, Swedish doctor, Sven Seldinger, was the first to use a technique for obtaining puncture access to the Seldinger's artery, which laid the foundations of modern interventional radiology [7].

In 1958, Mason Sones, a pediatric cardiologist at the Cleveland Clinic (USA), was the first to record X-ray contrast images of coronary arteries on film during aortography [8]. The first selective coronary angiography in the USSR was performed in 1971 by Yu.S. Petrosyan and L.S. Zingerman at Bakulev Institute of Cardiovascular Surgery under the USSR Academy of Medical Sciences [9].

In 1977, Andreas Gruentzig and Richard Myler at St. Mary's in San Francisco (USA) performed the first coronary balloon angioplasty in humans [10]. The first coronary balloon angioplasty procedure in the USSR was performed by Rabkin and Abugov at the All-Union Scientific Center of Surgery in 1982 [11].

The end of the 20th century was the heyday of endovascular surgery, whose methods have been applied in other fields of medicine.

Corresponding author: Mikhail Voskanov. Address: 1, Shchukinskaya str., Moscow, 123182, Russian Federation. Phone: (915) 230-76-10. E-mail: voskanov.mikhail@mail.ru

Bjerkvik *et al.* [12] in 1989 described a case of percutaneous graft revascularization by transcatheter fibrinolysis in one patient with hepatic artery thrombosis (HAT). However, balloon angioplasty (BA) was required in this case. The role of fibrinolysis in the treatment of early HAT remains a subject of dispute. Hidalgo *et al.* [13] in 1995 achieved good outcomes using urokinase for local fibrinolysis in two patients with early HAT; however, after fibrinolysis, both patients also required additional BA.

Angioplasty and portal vein stenting were described for the first time in 1990 by Olcott *et al.* [14] at the University of California, San Francisco, USA. Raby *et al.* [15] was the first to propose portal angioplasty in children. In subsequent years, this technique has become the treatment of choice for post-transplant portal stenosis with good outcomes and low rate of postoperative complications.

In 2001, Schwarzenberg et al. from the University of Minnesota, USA, reported positive outcomes in the relief of biliary stricture [16]. Balloon dilatation of the anastomotic stenosis and installation of external-internal drainage were performed in 6 patients after developing biliary strictures.

HEPATIC ARTERY STENOSIS AND/OR THROMBOSIS AFTER LIVER TRANSPLANTATION

Arterial blood flow disorders include hepatic artery thrombosis (HAT), hepatic artery stenosis (HAS), kinked or tortuous hepatic artery, and hepatic graft arterial steal syndrome.

Depending on the time interval between liver transplantation and HAT, early HAT (up to 4 weeks) and late HAT (over 4 weeks after transplantation) can be distinguished).

Bekker *et al.* [17] conducted a systematic literature review, which showed that the incidence of early HAT in children and adults after liver transplantation is 8.3% and 2.9%, respectively. Timely diagnosis and treatment of HAT can prevent injury to the biliary tract and liver transplant parenchyma.

RISK FACTORS FOR HEPATIC ARTERY GRAFT STENOSIS AND/OR THROMBOSIS

Donor risk factors

Atypical liver arterial anatomy on the donor side is a risk factor, especially in cases of "caliber" mismatch during formation of liver graft arterial anastomosis [18].

As for the graft-to-recipient weight ratio (GRWR), data obtained from various studies are still debatable. Sanada *et al.* [19] reported that grafts with GRWR <1.1% are a risk factor for hepatic artery thrombosis.

According to a study by Li *et al.* [20], grafts with GRWR ≥4% are significantly associated with development of HAT in related liver transplantation in children. However, Uchida *et al.* [21] showed that grafts with a GRWR ≥4% can be used safely in pediatric transplantation.

Besides, defects in surgical technique during graft retrieval are an important risk factor for HAS and/or HAT [22].

Recipient risk factors

Uchida *et al.* [21] also analyzed the risk factors for liver graft arterial blood flow disorders. It was established that gender (female), body weight (lower), and GRWR (higher) were associated with the risk of developing HAT.

A subject of disagreement is the recipient's low weight as a risk factor for thrombosis. Several studies have reported that the recipient's body weight is not a risk factor for HAT [19, 23]. Meanwhile, Desai *et al.* [24] found that the risk of developing HAT is higher in patients weighing less than 10 kg.

Atypical arterial anatomy of the recipient is also a risk factor for developing HAS and/or HAT [25].

Preoperative factors

According to Uchida *et al.*, long cold ischemia time and long warm ischemia time were factors leading to HAT [21].

However, according to the Organ Transplantation Center in Tianjin, China, there was no association found between high risk of HAT and prolonged cold ischemia time [26].

Intraoperative factors

With regard to transfusion risk factors, Uchida *et al.* [21] reported that over 6 doses of red blood cell suspension and/or transfusion of over 15 doses of fresh frozen plasma during surgery are risk factors for HAT.

According to some authors, the priority in using a microscope rather than conventional surgical optics during formation of hepatic artery anastomosis does not change HAT incidence [27, 28].

Backes *et al.* [29] reported that the use of a vascular insert in hepatic artery anastomosis is a useful option for pediatric liver transplantation. In contrast, however, Duffy *et al.* [30] reported that the use of a vascular insert is a significant independent risk factor for HAT.

According to Julka *et al.* [31] and Uchida *et al.* [21], multiple hepatic artery anastomoses had no effect on development of HAS and/or HAT. Nonetheless, Seda-Neto *et al.* [32] found a protective effect against development of thrombosis during formation of two arterial anastomoses.

Secondary edema of the liver graft resulting from ischemic reperfusion "stroke" is also a risk factor for HAT [33].

Postoperative factors

A group of authors believes that the presence of HAS and hepatic artery kinking (HAK) in the recipient after transplantation are initiating factors for development of HAT [34].

Early administration of aspirin has also been shown to be effective in preventing HAT [35].

DIAGNOSIS OF HEPATIC ARTERY STENOSIS AND/OR THROMBOSIS AFTER LIVER TRANSPLANTATION

Typically, the clinical presentation of HAS and/or HAT includes moderate increase in serum transaminase and bilirubin levels (75%), biliary complications (15%), fever and sepsis (6%), dysfunction or liver failure (4%) [36]. HAT can present as an isolated elevation in markers of cytolysis enzymes or as sepsis resulting from severe graft dysfunction.

HAS and/or HAT are most often detected by Doppler ultrasound followed by CT angiogram. According to some studies, Doppler ultrasound showed a 92–100% sensitivity and a 99.5% specificity [37].

The Doppler ultrasonic signs of HAS and/or HAT include peak hepatic artery systolic velocity <20.0 cm/s or resistance index <0.6 distal to the anastomosis region [38].

However, a vast majority of researchers believe that angiography is the gold standard for HAS and/or HAT diagnostics.

TECHNIQUES FOR MINIMALLY INVASIVE CORRECTION OF HEPATIC ARTERY STENOSIS AND/OR THROMBOSIS

A study by Chen *et al.* [18], as well as studies by Yanaga *et al.* [39] demonstrated that urgent revascularization in cases of early HAT after liver transplantation can significantly reduce graft loss and eliminate the need for retransplantation. The above studies showed that early revascularization achieved 55% graft recovery, whereas late revascularization was unsuccessful in 100% of cases.

Sanada *et al.* presented an extensive retrospective study in 2018 [40]. From May 2001 to September 2016, 279 related liver transplants were performed in 271 children.

Posttransplant hepatic artery complications were found in 15 cases (5.4%), which includes HAT and HAS in 14 (5.0%) cases and occlusion due to compression by fluid accumulation in one case (0.36%). Minimally invasive correction was the first-line treatment in seven cases (46.7%). The success rate in cases of minimally invasive techniques for HAS and/or HAT was 100%. Besides, graft survival rate in patients with vascular complications was 94.4% in the present study.

Techniques for performing endovascular correction of HAS and/or HAT have been widely used in adult patients after liver transplantation for many years; however, as for pediatric practice, these minimally invasive methods of treating complications are poorly transposed.

LIVER

Arterial hypoperfusion of a liver graft in the absence of hepatic artery occlusion was first described by Langer *et al.* in 1990 [41]. This complication occurs in the early postoperative period in more than 80% of diagnosed cases [54–74].

Angiography is the gold standard for diagnosing splenic steal syndrome. The diagnosis is determined by reduced blood flow through the hepatic artery in the absence of significant arterial anatomical defects, such as HAS, HAT or HAK [39, 42]

Thorough assessment of celiac trunk angiography to identify underlying vascular defects (HAS, HAT or HAK) is the first step [43]. Splenic artery embolization is considered to be the method of choice for shifting the hemodynamic balance in favor of the liver graft, as well as decreasing hyperdynamic portal blood flow [44].

POST-LIVER TRANSPLANT PORTAL VEIN STENOSIS

Interventional radiology is now widely used, and is considered a safe and effective treatment for portal vein stenosis (PVS) of hepatic graft [45]. Funaki *et al.* [46] reported that portal vein balloon angioplasty for treatment of PVS had a 50% recurrence rate on average at 6.3 months, while stenting showed 100% portal vein patency at 47 months of follow-up.

Portal inflow disorders after liver transplantation can be classified as early (detected within 3 months after liver transplantation) or late (detected more than 3 months after liver transplantation) [68]. As for portal vein thrombosis, endovascular methods have not been shown to be as effective as they should be [47]. In cases of early portal thrombosis, open thromboextraction is the appropriate treatment, and in cases of late portal thrombosis, formation of a mesenteric-portal bypass (Meso-Rex) shunt [48].

In cases of orthotopic whole liver transplantation, incidence of PVS is quite low in adult patients.

The most common indication for liver transplantation in children is biliary atresia [49]; in this disease, portal vein hypoplasia is quite common in patients. This factor provokes the development of PVS, and also complicates the formation of portal anastomosis due to the discrepancy between the "calibers" of the donor portal vein and the recipient's portal vein [50].

RISK FACTORS FOR PORTAL VEIN STENOSIS

The risk factors for portal vein complications include technical difficulties in anastomosis formation, young age, body weight <6 kg, recipient portal vein diameter <3.5 mm [51], graft rotation, simultaneous thrombectomy of preexisting portal vein thrombosis, and use of vascular conduits for portal reconstruction [50].

Several surgical techniques can play an important role in preventing PVS, especially in related liver transplantation or split liver transplantation. To overcome the discrepancy between the calibers of the donor and recipient portal veins, the use of "growth factor" in the vascular suture has proven to be an effective method.

Another method is to ensure adequate blood flow – ligation of the small portal branches on the recipient side. The use of large grafts can cause compromised blood flow during abdominal closure, which can lead to vascular thrombosis. In this case, delayed closure of the anterior abdominal wall is used to prevent a sharp increase in intra-abdominal pressure.

DIAGNOSIS AND TREATMENT OF PORTAL VEIN STENOSIS AFTER LIVER TRANSPLANTATION

The clinical manifestations of PVS range from asymptomatic to severe symptoms, including massive ascites, anemia, persistent splenomegaly with or without thrombocytopenia, and gastrointestinal bleeding [52]. Platelet counts may be below normal due to hypersplenism in patients with portal vein stenosis [53]. Portal vein stenosis is usually detected on routine Doppler ultrasound, CT scan, or MRI.

Currently, two types of endovascular approaches are widely used. The antegrade method – access to PVS is secured through the mesenteric vein system, from a mini-access. The second, less invasive approach is considered to be the retrograde method – access to the portal vein branches is secured by percutaneous transhepatic puncture of these branches under ultrasound control [54].

Among researchers of this complication, there is also an "opposition" to the methods of direct correction of stenosis, wondering whether balloon angioplasty or stenting is a necessary option for PVS treatment.

Sakamoto *et al.* [55] and Bertram *et al.* [56] demonstrated that balloon angioplasty is an effective and relatively safe method of treating PVS; however, 28–50% of patients develop PVS recurrence after the procedure. These studies suggest stenting and/or repeated balloon angioplasty to address this issue. Cheng *et al.* [47] also reported the efficacy of stenting for PVS in adults and children. Stent patency rate was 90.9% over a mean follow-up period of 12 months.

In contrast, other studies have raised concerns about the side effects of stenting [57, 58]. These side effects include intimal hyperplasia, size mismatch during retransplantation, and possibility of stent migration.

In 2019, Katano *et al.* [59] presented an extensive retrospective study at the Jichi Medical University, Japan. A related liver transplant was performed in 282 children. Portal vein complications occurred in 40 (14.2%) cases. In 36 cases, balloon angioplasty was performed. In 4 patients, portal vein stenting was carried out. Recurrence occurred in 27.5% of the patients after the initial treatment. Stent patency rate was 100%.

In 2017, a major collaborative study was conducted by Incheon St. Mary's Hospital, Korea and Asan Medical Center, Seoul, Korea [60]. Of the 296 patients, 55 (18.6%) developed PVS.

12 patients underwent balloon angioplasty, and 41 patients underwent stenting. There was 89% success with balloon angioplasty. Relapses occurred in 3 (25%) patients. Stenting was performed if, after angioplasty, the deployed balloon demonstrated waist deformation >50% or portal pressure gradient was >5 mm Hg. Satisfactory portal blood flow was observed in all patients who underwent stenting. The 1-, 5-, and 10-year primary stent patency rates were 90% (±7%), 90% (±7%), and 85% (±8%), respectively.

POST-LIVER TRANSPLANT BILIARY STRICTURES

Biliary strictures and biliary fistulas are the most common early post-transplant complications, with a 10–30% risk according to various sources [61, 62].

Biliary strictures are classified into anastomotic (AS) or non-anastomotic biliary strictures (NAS) [40].

RISK FACTORS FOR POST-LIVER TRANSPLANT BILIARY STRICTURES

The risk factors for biliary strictures (BS) are: cold ischemia time of the liver graft, impaired arterial blood supply to the graft, rejection, and cytomegalovirus (CMV) infection [63].

Several authors have provided studies proving that there is a relationship between BS occurrence and preexisting arterial complications. Thus, according to the data obtained by Darius *et al.* [64], HAT increased the risk of anastomotic BS in children ($p < 0.001$). In 2018, Fang-Min Liao *et al.* [38] demonstrated that children after liver transplantation with a hepatic artery resistance index according to Doppler ultrasound ≤0.57 had a higher risk of BS ($p = 0.001$). Feier *et al.* in 2016 reported that multiple arterial anastomoses can "protect" a child from developing biliary strictures [65].

DIAGNOSIS AND TREATMENT OF POST-LIVER TRANSPLANT BILIARY STRICTURES

Clinically, biliary strictures should be suspected in patients with signs of cholestasis or episodes of cholangitis. However, most patients have a nonspecific clinical picture, as well as discrete changes in liver enzyme levels. Ultrasound does not usually reveal significant

changes, while magnetic resonance cholangiography, an instrument superior to ultrasound, is a priority method in non-invasive imaging diagnosis of this complication [66].

Percutaneous transhepatic cholangiography plays a crucial role in the diagnosis of post-liver transplant biliary stricture, as it is considered the gold standard for detecting and quantifying stenosis [67].

Percutaneous transhepatic bilioplasty (PTB) is a minimally invasive method and has a success rate of 34% to 75%. Its outcomes are similar to those of surgical revision [61, 62]. The main disadvantage of PTB is the potential need for prolonged external biliary drainage and repeated procedures, with potential psychological consequences.

Belenky *et al.* [68] recommended that stent placement should be a priority treatment option in cases of late biliary strictures. This method provides long-term outcomes that are superior to those obtained with isolated dilation with balloon catheters.

There are no large cohort or randomized controlled trials to compare the short-term and long-term outcomes of PTB and surgery. In most published studies, only short-term or mid-term observations are available. In addition, different centers use different methods and/or therapeutic algorithms, making it difficult to compare outcomes and complications reported in the literature.

In 2008, Miraglia *et al.* reported PTB outcomes in 20 children who underwent liver transplantation between 2004 and 2007 [69]. Biliary anastomoses stricture was successfully completed in all patients, after which PTB was performed without major complications. The average number of balloon dilations performed was 4. Cholangiostomy drainage placement lasted for 5 months on average. Recurrent stenosis developed in 28%, which required a second series of PTB.

Normalization of liver enzymes and resolution of intrahepatic biliary dilatation are the endpoints used to measure technical success in the most recent series involving PTB or surgical reconstruction of biliary strictures [62, 63].

CONCLUSION

In cases of development of post-liver transplant complications in adult patients, endovascular and endobiliary methods for correcting these complications have become the first-line therapy, since they are less invasive and easier tolerated by recipients compared to volumetric reconstructive surgery. In recent years, with the development of minimally invasive technologies and techniques, the number of new cases of treatment of graft blood supply disorders and biliary strictures has increased. Although urgent retransplantation has long been considered the treatment of choice, minimally invasive interventional radiology is now being used as a first-line treatment for adult recipients in a number of leading centers.

However, in pediatric liver transplantation, endovascular technologies and techniques have not been as widely studied. Development of algorithms for minimally invasive interventional diagnosis and treatment of vascular complications and biliary strictures following a liver transplantation for pediatric practice is necessary to achieve long-term optimal outcomes and graft function.

The authors declare no conflict of interest.

REFERENCES

1. *Kelly DA, Bucuvalas JC, Alonso EM et al.* Long-term medical management of the pediatric patient after liver transplantation: 2013 practice guideline by the American Association for the Study of Liver Diseases and the American Society of Transplantation. *Liver Transpl*. 2013; 19 (8): 798–825. doi: 10.1002/lt.23697.
2. *Milne JS.* Surgical Instruments in Greek and Roman Times. Oxford: At the Clarendon Press, 1907. 179.
3. *Cournand A.* Cardiac catheterization; development of the technique, its contributions to experimental medicine, and its initial applications in man. *Acta Med Scand Suppl*. 1975; 579: 3–32.
4. *Fye WB.* Coronary arteriography – it took a long time! *Circulation*. 1984; 70 (5): 781–787. doi: 10.1161/01.cir.70.5.781.
5. *Rozhchenko LV, Ivanov AYu, Goroshchenko SA, Blagorazumova GP, Hristoforova MI.* Razvitie sosudistoj hirurgii v RNHI im. prof. A.L. Polenova (k 50-letnemu yubileyu otdeleniya hirurgii sosudov golovnogo mozga RNHI im. prof. A.L. Polenova). *Rossijskij nejrohirurgicheskij zhurnal imeni professora A.L. Polenova*. 2017; 9 (1): 5–10.
6. *Meyer JA*. Werner Forssmann and catheterization of the heart, 1929. *Ann Thorac Surg*. 1990; 49 (3): 497–499. doi: 10.1016/0003-4975(90)90272-8.
7. *Seldinger SI.* Catheter replacement of the needle in percutaneous arteriography. A new technique. *Acta Radiol Suppl (Stockholm)*. 2008; 434: 47–52. doi: 10.1080/02841850802133386.
8. *Sones FM, Shirey EK*. Cine coronary arteriography. *Modern concepts of cardiovascular disease*. 1962; 58: 1018–1019.
9. *Petrosyan YuS, Zingerman LS.* Koronarografiya. Medicina, 1974. 152.
10. *Barton M, Grüntzig J, Husmann M, Rösch J.* Balloon Angioplasty – The Legacy of Andreas Grüntzig, M.D. (1939–1985). *Front Cardiovasc Med*. 2014 Dec 29; 1: 15. doi: 10.3389/fcvm.2014.00015. PMID: 26664865; PMCID: PMC4671350.
11. *Sorokina TS.* Istoriya meditsiny. 8-e izd. ster. M.: Akademiya, 2008. 560 s. ISBN 978-5-7695-5781-1.
12. *Bjerkvik S, Vatne K, Mathisen O, Søreide O*. Percutaneous revascularization of postoperative hepatic artery thrombosis in a liver transplant. *Transplantation*.

1995; 59 (12): 1746–1748. doi: 10.1097/00007890-199506270-00021.
13. *Hidalgo EG, Abad J, Cantarero JM et al.* High-dose intra-arterial urokinase for the treatment of hepatic artery thrombosis in liver transplantation. *Hepatogastroenterology*. 1989; 36 (6): 529–532.
14. *Olcott EW, Ring EJ, Roberts JP, Ascher NL, Lake JR, Gordon RL.* Percutaneous transhepatic portal vein angioplasty and stent placement after liver transplantation: early experience. *J Vasc Interv Radiol*. 1990; 1 (1): 17–22. doi: 10.1016/s1051-0443(90)72496-7.
15. *Raby N, Karani J, Thomas S, O'Grady J, Williams R.* Stenoses of vascular anastomoses after hepatic transplantation: treatment with balloon angioplasty. *AJR Am J Roentgenol*. 1991; 157 (1): 167–171. doi: 10.2214/ajr.157.1.1828649.
16. *Schwarzenberg SJ, Sharp HL, Payne WD et al.* Biliary stricture in living-related donor liver transplantation: management with balloon dilation. *Pediatr Transplant*. 2002; 6 (2): 132–135. doi: 10.1034/j.1399-3046.2002.01053.x.
17. *Bekker J, Ploem S, de Jong KP.* Early hepatic artery thrombosis after liver transplantation: a systematic review of the incidence, outcome and risk factors. *Am J Transplant*. 2009; 9 (4): 746–757. doi: 10.1111/j.1600-6143.2008.02541.x.
18. *Chen J, Weinstein J, Black S, Spain J, Brady PS, Dowell JD.* Surgical and endovascular treatment of hepatic arterial complications following liver transplant. *Clin Transplant*. 2014; 28 (12): 1305–1312. doi: 10.1111/ctr.12431.
19. *Yamada N, Sanada Y, Hirata Y et al.* Selection of living donor liver grafts for patients weighing 6 kg or less. *Liver Transpl*. 2015; 21 (2): 233–238. doi: 10.1002/lt.24048.
20. *Li JJ, Zu CH, Li SP, Gao W, Shen ZY, Cai JZ.* Effect of graft size matching on pediatric living-donor liver transplantation at a single center. *Clin Transplant*. 2018; 32 (1): 10.1111/ctr.13160. doi: 10.1111/ctr.13160.
21. *Uchida Y, Sakamoto S, Egawa H et al.* The impact of meticulous management for hepatic artery thrombosis on long-term outcome after pediatric living donor liver transplantation. *Clin Transplant*. 2009; 23 (3): 392–399. doi: 10.1111/j.1399-0012.2008.00924.x.
22. *Oberkofler CE, Reese T, Raptis DA et al.* Hepatic artery occlusion in liver transplantation: What counts more, the type of reconstruction or the severity of the recipient's disease? *Liver Transpl*. 2018; 24 (6): 790–802. doi: 10.1002/lt.25044.
23. *Oh CK, Pelletier SJ, Sawyer RG et al.* Uni- and multivariate analysis of risk factors for early and late hepatic artery thrombosis after liver transplantation. *Transplantation*. 2001; 71 (6): 767–772. doi: 10.1097/00007890-200103270-00014.
24. *Desai CS, Sharma S, Gruessner A, Fishbein T, Kaufman S, Khan KM.* Effect of small donor weight and donor-recipient weight ratio on the outcome of liver transplantation in children. *Pediatr Transplant*. 2015; 19 (4): 366–370. doi: 10.1111/petr.12459.
25. *Gunsar F, Rolando N, Pastacaldi S et al.* Late hepatic artery thrombosis after orthotopic liver transplantation. *Liver Transpl*. 2003; 9 (6): 605–611. doi: 10.1053/jlts.2003.50057.
26. *Valente JF, Alonso MH, Weber FL, Hanto DW.* Late hepatic artery thrombosis in liver allograft recipients is associated with intrahepatic biliary necrosis. *Transplantation*. 1996; 61 (1): 61–65. doi: 10.1097/00007890-199601150-00013.
27. *Guarrera JV, Sinha P, Lobritto SJ, Brown RS Jr, Kinkhabwala M, Emond JC.* Microvascular hepatic artery anastomosis in pediatric segmental liver transplantation: microscope vs loupe. *Transpl Int*. 2004; 17 (10): 585–588. doi: 10.1007/s00147-004-0782-8.
28. *Carnevale FC, de Tarso Machado A, Moreira AM et al.* Long-term results of the percutaneous transhepatic venoplasty of portal vein stenoses after pediatric liver transplantation. *Pediatr Transplant*. 2011; 15 (5): 476–481. doi: 10.1111/j.1399-3046.2011.01481.x.
29. *Backes AN, Gibelli NE, Tannuri AC et al.* Hepatic artery graft in pediatric liver transplantation: single-center experience with 58 cases. *Transplant Proc*. 2011; 43 (1): 177–180. doi: 10.1016/j.transproceed.2010.11.006.
30. *Duffy JP, Hong JC, Farmer DG et al.* Vascular complications of orthotopic liver transplantation: experience in more than 4,200 patients. *J Am Coll Surg*. 2009; 208 (5): 896–905. doi: 10.1016/j.jamcollsurg.2008.12.032.
31. *Julka KD, Lin TS, Chen CL, Wang CC, Komorowski AL.* Reconstructing single hepatic artery with two arterial stumps: biliary complications in pediatric living donor liver transplantation. *Pediatr Surg Int*. 2014; 30 (1): 39–46. doi: 10.1007/s00383-013-3436-z.
32. *Seda-Neto J, Antunes da Fonseca E, Pugliese R et al.* Twenty Years of Experience in Pediatric Living Donor Liver Transplantation: Focus on Hepatic Artery Reconstruction, Complications, and Outcomes. *Transplantation*. 2016; 100 (5): 1066–1072. doi: 10.1097/TP.0000000000001135.
33. *Miraglia R, Maruzzelli L, Caruso S et al.* Minimally invasive endovascular and biliary treatments of children with acute hepatic artery thrombosis following liver transplantation. *Pediatr Radiol*. 2014; 44 (1): 94–102. doi: 10.1007/s00247-013-2772-4.
34. *Segel MC, Zajko AB, Bowen A et al.* Hepatic artery thrombosis after liver transplantation: radiologic evaluation. *AJR Am J Roentgenol*. 1986; 146 (1): 137–141. doi: 10.2214/ajr.146.1.137.
35. *Hashikura Y, Kawasaki S, Okumura N et al.* Prevention of hepatic artery thrombosis in pediatric liver transplantation. *Transplantation*. 1995; 60 (10): 1109–1112. doi: 10.1097/00007890-199511270-00009.
36. *Piardi T, Lhuaire M, Bruno O et al.* Vascular complications following liver transplantation: A literature review of advances in 2015. *World J Hepatol*. 2016; 8 (1): 36–57. doi: 10.4254/wjh.v8.i1.36.
37. *Uller W, Knoppke B, Schreyer AG et al.* Interventional radiological treatment of perihepatic vascular stenosis or occlusion in pediatric patients after liver transplantation.

Cardiovasc Intervent Radiol. 2013; 36 (6): 1562–1571. doi: 10.1007/s00270-013-0595-1.

38. *Liao FM, Chang MH, Ho MC et al.* Resistance index of hepatic artery can predict anastomotic biliary complications after liver transplantation in children. *J Formos Med Assoc*. 2019; 118 (1 Pt 2): 209–214. doi: 10.1016/j.jfma.2018.03.014.
39. *Yanaga K, Lebeau G, Marsh JW et al.* Hepatic artery reconstruction for hepatic artery thrombosis after orthotopic liver transplantation. *Arch Surg*. 1990; 125 (5): 628–631. doi: 10.1001/archsurg.1990.01410170076016.
40. *Sanada Y, Katano T, Hirata Y et al.* Interventional radiology treatment for vascular and biliary complications following pediatric living donor liver transplantation – a retrospective study. *Transpl Int*. 2018; 31 (11): 1216–1222. doi: 10.1111/tri.13285.
41. *Langer R, Langer M, Neuhaus P, Scholz A, Felix R.* Angiographische Diagnostik bei Lebertransplantation. Teil II: Angiographie nach Transplantation [Angiographic diagnosis in liver transplantation. II: Angiography after transplantation]. *Digitale Bilddiagn*. 1990; 10 (3–4): 92–96.
42. *Cheng YF, Ou HY, Tsang LL et al.* Vascular stents in the management of portal venous complications in living donor liver transplantation [published correction appears in Am J Transplant. 2011 Jan; 11 (1): 186]. *Am J Transplant*. 2010; 10 (5): 1276–1283. doi: 10.1111/j.1600-6143.2010.03076.x.
43. *Saad WE, Davies MG, Sahler L et al.* Hepatic artery stenosis in liver transplant recipients: primary treatment with percutaneous transluminal angioplasty. *J Vasc Interv Radiol*. 2005; 16 (6): 795–805. doi: 10.1097/01.RVI.0000156441.12230.13.
44. *Saad WE.* Management of nonocclusive hepatic artery complications after liver transplantation. *Tech Vasc Interv Radiol*. 2007; 10 (3): 221–232. doi: 10.1053/j.tvir.2007.09.016.
45. *Jurim O, Csete M, Gelabert HA et al.* Reduced-size grafts – the solution for hepatic artery thrombosis after pediatric liver transplantation? *J Pediatr Surg*. 1995; 30 (1): 53–55. doi: 10.1016/0022-3468(95)90609-6.
46. *Funaki B, Rosenblum JD, Leef JA et al.* Percutaneous treatment of portal venous stenosis in children and adolescents with segmental hepatic transplants: long-term results. *Radiology*. 2000; 215 (1): 147–151. doi: 10.1148/radiology.215.1.r00ap38147.
47. *Cheng YF, Ou HY, Tsang LL et al.* Vascular stents in the management of portal venous complications in living donor liver transplantation [published correction appears in Am J Transplant. 2011 Jan; 11 (1): 186]. *Am J Transplant*. 2010; 10 (5): 1276–1283. doi: 10.1111/j.1600-6143.2010.03076.x.
48. *de Ville de Goyet J, Lo Zupone C, Grimaldi C et al.* Meso-Rex bypass as an alternative technique for portal vein reconstruction at or after liver transplantation in children: review and perspectives. *Pediatr Transplant*. 2013; 17 (1): 19–26. doi: 10.1111/j.1399-3046.2012.01784.x.
49. *Rawal N, Yazigi N.* Pediatric Liver Transplantation. *Pediatr Clin North Am*. 2017; 64 (3): 677–684. doi: 10.1016/j.pcl.2017.02.003.
50. *Umehara M, Narumi S, Sugai M et al.* Hepatic venous outflow obstruction in living donor liver transplantation: balloon angioplasty or stent placement? *Transplant Proc*. 2012; 44 (3): 769–771. doi: 10.1016/j.transproceed.2012.01.048.
51. *Seu P, Shackleton CR, Shaked A et al.* Improved results of liver transplantation in patients with portal vein thrombosis. *Arch Surg*. 1996; 131 (8): 840–845. doi: 10.1001/archsurg.1996.01430200050009.
52. *Nosaka S, Isobe Y, Kasahara M et al.* Recanalization of post-transplant late-onset long segmental portal vein thrombosis with bidirectional transhepatic and transmesenteric approach. *Pediatr Transplant*. 2013; 17 (2): E71–E75. doi: 10.1111/petr.12050.
53. *Sanada Y, Kawano Y, Mizuta K et al.* Strategy to prevent recurrent portal vein stenosis following interventional radiology in pediatric liver transplantation. *Liver Transpl*. 2010; 16 (3): 332–339. doi: 10.1002/lt.21995.
54. *Baccarani U, Gasparini D, Risaliti A et al.* Percutaneous mechanical fragmentation and stent placement for the treatment of early posttransplantation portal vein thrombosis. *Transplantation*. 2001; 72 (9): 1572–1582. doi: 10.1097/00007890-200111150-00016.
55. *Sakamoto S, Nakazawa A, Shigeta T et al.* Devastating outflow obstruction after pediatric split liver transplantation. *Pediatr Transplant*. 2013; 17 (1): E25–E28. doi: 10.1111/j.1399-3046.2012.01761.x.
56. *Bertram H, Pfister ED, Becker T, Schoof S.* Transsplenic endovascular therapy of portal vein stenosis and subsequent complete portal vein thrombosis in a 2-year-old child. *J Vasc Interv Radiol*. 2010; 21 (11): 1760–1764. doi: 10.1016/j.jvir.2010.06.025.
57. *Shibata T, Itoh K, Kubo T et al.* Percutaneous transhepatic balloon dilation of portal venous stenosis in patients with living donor liver transplantation. *Radiology*. 2005; 235 (3): 1078–1083. doi: 10.1148/radiol.2353040489.
58. *Ko GY, Sung KB, Yoon HK et al.* Endovascular treatment of hepatic venous outflow obstruction after living-donor liver transplantation. *J Vasc Interv Radiol*. 2002; 13 (6): 591–599. doi: 10.1016/s1051-0443(07)61652-2.
59. *Katano T, Sanada Y, Hirata Y et al.* Endovascular stent placement for venous complications following pediatric liver transplantation: outcomes and indications. *Pediatr Surg Int*. 2019; 35 (11): 1185–1195. doi: 10.1007/s00383-019-04551-9.
60. *Shim DJ, Ko GY, Sung KB, Gwon DI, Ko HK.* Long-Term Outcome of Portal Vein Stent Placement in Pediatric Liver Transplant Recipients: A Comparison with Balloon Angioplasty. *J Vasc Interv Radiol*. 2018; 29 (6): 800–808. doi: 10.1016/j.jvir.2017.11.019.
61. *Anderson CD, Turmelle YP, Darcy M et al.* Biliary strictures in pediatric liver transplant recipients – early diagnosis and treatment results in excellent graft outcomes. *Pediatr Transplant*. 2010; 14 (3): 358–363. doi: 10.1111/j.1399-3046.2009.01246.x.

62. *Feier FH, Chapchap P, Pugliese R et al.* Diagnosis and management of biliary complications in pediatric living donor liver transplant recipients. *Liver Transpl*. 2014; 20 (8): 882–892. doi: 10.1002/lt.23896.
63. *Sunku B, Salvalaggio PR, Donaldson JS et al.* Outcomes and risk factors for failure of radiologic treatment of biliary strictures in pediatric liver transplantation recipients. *Liver Transpl*. 2006; 12 (5): 821–826. doi: 10.1002/lt.20712.
64. *Darius T, Rivera J, Fusaro F et al.* Risk factors and surgical management of anastomotic biliary complications after pediatric liver transplantation. *Liver Transpl*. 2014; 20 (8): 893–903. doi: 10.1002/lt.23910.
65. *Feier FH, Seda-Neto J, da Fonseca EA et al.* Analysis of factors Associated with biliary complications in children after liver transplantation. *Transplantation*. 2016; 100 (9): 1944–1954. doi: 10.1097/TP.0000000000001298.
66. *Kinner S, Dechêne A, Paul A et al.* Detection of biliary stenoses in patients after liver transplantation: is there a different diagnostic accuracy of MRCP depending on the type of biliary anastomosis? *Eur J Radiol*. 2011; 80 (2): e20–e28. doi: 10.1016/j.ejrad.2010.06.003.
67. *Seehofer D, Eurich D, Veltzke-Schlieker W, Neuhaus P.* Biliary complications after liver transplantation: old problems and new challenges. *Am J Transplant*. 2013; 13 (2): 253–265. doi: 10.1111/ajt.12034.
68. *Belenky A, Mor E, Bartal G et al.* Transhepatic balloon dilatation of early biliary strictures in pediatric liver transplantation: successful initial and mid-term outcome. *Cardiovasc Intervent Radiol*. 2004; 27 (5): 491–494. doi: 10.1007/s00270-003-2675-0.
69. *Miraglia R, Maruzzelli L, Tuzzolino F, Indovina PL, Luca A.* Radiation exposure in biliary procedures performed to manage anastomotic strictures in pediatric liver transplant recipients: comparison between radiation exposure levels using an image intensifier and a flat-panel detector-based system. Cardiovasc Interv Radiol. 2013; 36 (6): 1670–1676.

The article was submitted to the journal on 21.08.2020

DOI: 10.15825/1995-1191-2020-4-149-153

REVIEW OF SURGICAL TECHNIQUES FOR PERFORMING LAPAROSCOPIC DONOR HEPATECTOMY

K.O. Semash[1], S.V. Gautier[1, 2]

[1] Shumakov National Medical Research Center of Transplantology and Artificial Organs, Moscow, Russian Federation

[2] Sechenov University, Moscow, Russian Federation

Living related liver transplantation has proved to be an effective, safe and radical method for treating end-stage liver diseases. In the last decade, a laparoscopic approach to donor hepatectomy has been gradually introduced into clinical practice. According to world literature, there are presently no uniform standards for performing laparoscopic liver resections in living donors. This literature review considers almost all methods for performing this surgery in living donors. These methods are described in transplant centers around the world.

Keywords: liver transplantation, living donation, laparoscopic liver resection.

INTRODUCTION

Laparoscopic hepatectomy in living donors typically consists of several basic stages: trocar placement, liver mobilization, dissection of hepatoduodenal ligament structures, formation of a resection plane, and parenchymal dissection and graft removal.

POSITION OF THE PATIENT ON THE TABLE

The patient was positioned on the operating table in Fowler's position (Reverse Trendelenburg position). According to various literary sources, the angle of the table in relation to the floor ranges from 30° to 45°. The patient's legs are spread apart (French position) [1–3]. Interestingly enough, when performing laparoscopic right hemihepatectomy, the position of the patient on the operating table is slightly different from that for resection of the left lateral segment or left lobe of liver in a related donor. The patient is also placed in the French position in Fowler's position. However, a 10–15 cm diameter roll is placed under the patient's right at the costal arch level [4]. At some transplant centers, the patient is placed on the left side [5].

TROCAR PLACEMENT

All clinics have their own trocar placement approaches. For example, during the first laparoscopic removal of the left lateral section from a living donor [6], the following trocar port placement scheme was described: a 10-mm-diameter optical trocar was placed paraumbilically 2 cm above the navel, two 12-mm-diameter trocars were placed 7–9 cm to the left and to the right, then, a 10-mm-diameter trocar was placed 5 cm proximally to them along the midclavicular line under the costal arch. In most French transplant centers, and at the Shumakov National Medical Research Center of Transplantology and Artificial Organs, when performing laparoscopic left lateral (LL) resection, trocars are placed as follows: an optical 10–12-mm trocar is placed paraumbilically 2–3 cm to the right of the navel, then 10-mm trocar is placed at a 15° angle to the right and 10 cm to the back, and another 12-mm trocar at a 15° angle to the left from the bottom. One 5-mm trocar is placed in the epigastric region, and, if necessary, one more is placed along the anterior axillary line in the right hypochondrium [3, 7–9].

In South Korea, the placement pattern is similar for laparoscopic left lateral sectionectomy, but 12-mm trocars are mostly used [1]. For a more rational port placement, some transplant centers performed ultrasound imaging of the liver [7, 10].

When resecting the left lobe in a living donor, trocar placement is the same as when performing LL resection, except that the main working ports are placed equidistantly upward at an angle of 30° from the paraumbilical optical access [11]. Some transplant centers have a modified version of trocar port placement using 6 trocars [12].

Trocar placement in right-sided hemihepatectomy is shown in Figure 4. Standardized approaches to port placement have been developed using a three-dimensional laparoscope for laparoscopic resection of the right lobe of the liver in living donors [13].

LIVER MOBILIZATION AND HEPATODUODENAL LIGAMENT DISSECTION

Carboxyperitoneum is achieved to target values of 8–13 mm Hg when performing left lateral sectionectomy or left lobar resection [1, 3, 6, 8, 9, 11, 12]. For right-sided hemihepatectomy, the reference intra-abdominal pressure value, according to various literary sources, is 12–15 mm Hg [14, 15]. A 30° optical transducer is mostly used for imaging, although a laparoscope with an

Corresponding author: Konstantin Semash. Address: 1, Shchukinskaya str., Moscow, 123182, Russian Federation. Phone: (999) 986-76-19. E-mail: mail@doctorsemash.com

adjustable viewing angle has been increasingly reported of recent [16, 17].

When resecting the left lateral segment or the left lobe, after revision of the abdominal cavity, the liver is mobilized by intersecting the round, sickle, coronary and left triangular ligaments using a harmonic scalpel and monopolar scissors [3, 6–8]. When mobilizing the left lobe of the liver, namely the gastrohepatic ligament, it is worth noting a possible aberrant artery branching to the left lobe from the left gastric artery.

It should be noted that preliminary circular mobilization of the left hepatic vein during LL resection is not routinely performed in most transplant centers, although there have been recent reports on this maneuver [18].

Next, the hepatoduodenal ligament structures are isolated: the left hepatic artery is mobilized along the length and circularly bypassed with a webbing or its alternatives. After that, the short portal branches are ligated to segment 1, the left branch of the portal vein is also circularly bypassed. Then, using a harmonic scalpel or bipolar coagulation, the venous branches draining segment 4 (Sinus Rexi) are transected.

It should be noted that mobilization of the hepatoduodenal ligament structures is performed using the caudal approach, while, for better visualization, traction is performed for the transected round ligament of the liver [7]. However, in some cases, the left lateral segment is rotated counterclockwise to facilitate its mobilization and isolation of afferent vessels [9].

In the case of hemihepatectomy, it is necessary to take into account the anatomical border of separation into the left and right lobes of the liver, namely, the line running from the bottom of the gallbladder to the suprahepatic part of the inferior vena cava [19]. Cholecystectomy is performed based on the Critical View of Safety principle, a control system based on assessment and registration of three key elements:

– Dissection of the Calot's triangle (cystic duct – hepatic duct – liver);
– Visualization of only two tubular structures leading to the gallbladder;
– Mobilization of the lower part of the gallbladder and visualization of the lower 1/3 of the gallbladder bed before intersecting any tubular structures [20].

As for right-sided hemihepatectomy, some authors believe that cholecystectomy should be performed before mobilizing the hepatoduodenal ligament to achieve more detailed visualization of the arterial blood supply to the right lobe of the liver [4, 14]. In some Asian clinics, for example, in South Korea, the operation begins with mobilization of the right lobe of the liver, and then proceeds to dissection of afferent vessels and cholecystectomy [5, 21].

Intraoperative cholangiography [22] or indocyanine green fluorescent imaging [21–24] is used to visualize the ductal zone. Modified cholangiography is also used. For this purpose, a bulldog forceps is applied on the supposed intersection site of the bile duct, and cholangiography is performed through the cystic duct stump. In this way, the safety of duct intersection is confirmed [15].

LIVER PARENCHYMAL DISSECTION

To determine the optimal plane of resection when performing hemihepatectomy, clamping of afferent blood flow to the left or right lobe of the liver using vascular clamps is performed. A parenchyma dissection line is marked with a harmonic scalpel along the line of demarcation, and then the vascular clamps are removed [25].

In some transplant centers, just before parenchyma dissection is done, the hepatoduodenal ligament structures are taken onto a turnstile to apply the Pringle maneuver – clamping of afferent blood flow to the liver in the event of massive bleeding, although this technique is not routinely used in some transplant centers [60, 62, 84]. It should be noted that the Pringle maneuver was not used in any of the reports described when performing laparoscopic left lateral sectionectomy [1–3, 6, 9, 26].

Parenchymal dissection is performed using an ultrasonic or water-jet dissector, bipolar and monopolar coagulation, or argon [1–3, 6, 9]. Some authors argue that large vessels will never be injured by light maneuvers as long as the vessels are in the surgeon's field of vision. Even during parenchymal dissection, intraparenchymal structures can be visualized using magnification on a laparoscope, and minor bleeding can be controlled by raising the intra-abdominal pressure [27].

When resecting the left lateral segment, the parenchymal resection line is defined towards the medial wall of the left hepatic vein and goes slightly to the right of the falciform ligament. The dissection is also carried out according to the caudal approach, i.e. from the bottom to up. According to a study in Hungary, the optimal parenchymal dividing line for the left lateral segment should be about 1 cm to the right of the falciform ligament, except for deviant biliary anatomy of the left lateral segment, when the level of segmental bile duct fusion according to MR cholangiography is to the right or left of the intended level [6, 28]. This is due to the need to obtain a minimum number of bile ducts on the graft to reduce the number of biliary complications in the recipient. In hemihepatectomy, the resection line follows the demarcation line as previously described.

It is very important to note that in laparoscopic hemihepatectomy, after dividing the caudate lobe, a nylon tube is passed into the anterior part of the Glisson's right posterior foot in order to raise the residual parenchyma. Thus, the hanging maneuver is performed, which helps to complete the parenchymal dissection most safely, although some authors consider this maneuver as optional [21, 23]. A somewhat similar maneuver has been described for laparoscopic resections of the LL and left lobe in living donors. So, for the convenience of paren-

chymal dissection at the junction of the left and median hepatic veins, the following maneuver is applied: this area is circumferentially bypassed with a webbing and pulled upward, thereby improving visualization during dissection, and providing additional vascular safety [29].

In the parenchymal transsection process, the portal plate, in which the bile duct and paraductal vessels pass, is exposed. These elements are crossed with scissors, and a careful hemo- and biliostasis with suturing and clipping is performed on the donor's side. At some transplant centers, the portal plate is clipped with Hem-o-lock clips (TFX Medical Ltd., RTP Durham, NC, USA) and then crossed with scissors between the clips [9, 30, 31].

GRAFT REMOVAL

After the graft remains connected only by afferent vessels and hepatic veins, the Pfannenstiel incision is performed with installation of a port for manual assistance. Then, the graft is removed directly: the afferent vessels of the graft are clipped and transected (in some transplant centers, the portal vein is transected with a stapler [32, 33]), the hepatic veins are transected using a stapler. The obtained graft is removed using manual assistance through the previously installed port and it is then transferred for perfusion with a preservative solution [8].

After the liver fragment has been extracted, a thorough revision for hemo- and biliostasis is carried out, and, if necessary, electrocoagulation, stitching or clipping of suspicious areas is performed. A silicon drainage is placed to the wound surface of the liver [11, 14], though some authors believe that with "ideal" liver resection, there are no indications for safety drainage [34].

CONCLUSION

Donor safety is of paramount importance in donor liver surgery. This very important aspect is still the main obstacle to the spread of minimally invasive approaches in living liver donation.

This is probably why the approach to laparoscopic liver resection in living donors is significantly different among different transplant centers. Nevertheless, further evaluation of the standardization of methods is needed to improve intermediate surgical outcomes for these surgical procedures.

The authors declare no conflict of interest.

REFERENCES

1. *Kim KH, Jung DH, Park KM, Lee YJ, Kim DY, Kim KM, Lee SG*. Comparison of open and laparoscopic live donor left lateral sectionectomy. *British Journal of Surgery.* 2011; 98 (9).
2. *Troisi RI, Wojcicki M, Tomassini F, Houtmeyers P, Vanlander A, Berrevoet F et al*. Pure Laparoscopic Full-Left Living Donor Hepatectomy for Calculated Small-for-Size LDLT in Adults: Proof of Concept. *American Journal of Transplantation*. 2013; 13 (9): 2472–2478.
3. *Broering DC, Elsheikh Y, Shagrani M, Abaalkhail F, Troisi RI*. Pure Laparoscopic Living Donor Left Lateral Sectionectomy in Pediatric Transplantation: A Propensity Score Analysis on 220 Consecutive Patients. *Liver Transplantation*. 2018; 24 (8).
4. *Goumard C, Soubrane O, Brustia R, Scatton O*. Laparoscopic right hepatectomy for living donation. *Annals of Laparoscopic and Endoscopic Surgery.* 2017; 2: 81–81.
5. *Han HS, Cho JY, Yoon YS, Hwang DW, Kim YK, Shin HK, Lee W*. Total laparoscopic living donor right hepatectomy. *Surgical Endoscopy.* 2015; 29 (1).
6. *Cherqui D, Soubrane O, Husson E, Barshasz E, Vignaux O, Ghimouz M et al*. Laparoscopic living donor hepatectomy for liver transplantation in children. *Lancet*. 2002; 359 (9304): 392–396.
7. *Soubrane O, Cherqui D, Scatton O, Stenard F, Bernard D, Branchereau S et al*. Laparoscopic left lateral sectionectomy in living donors: Safety and reproducibility of the technique in a single center. *Annals of Surgery*. 2006; 244 (5).
8. *Troisi R, Debruyne R, Rogiers X*. Laparoscopic Living Donor Hepatectomy for Pediatric Liver Transplantation. *Acta Chirurgica Belgica*. 2009; 109 (4): 559–562.
9. *Gautier S, Monakhov A, Gallyamov E, Tsirulnikova O, Zagaynov E, Dzhanbekov T et al*. Laparoscopic left lateral section procurement in living liver donors: A single center propensity score-matched study. *Clinical Transplantation*. 2018; 32 (9).
10. *Troisi RI, Elsheikh YM, Shagrani MA, Broering D*. First fully laparoscopic donor hepatectomy for pediatric liver transplantation using the indocyanine green near-infrared fluorescence imaging in the Middle East: a case report. *Annals of Saudi Medicine*. 2014; 34 (4): 354–357.
11. *Samstein B, Cherqui D, Rotellar F, Griesemer A, Halazun KJ, Kato T et al*. Totally laparoscopic full left hepatectomy for living donor liver transplantation in adolescents and adults. *American Journal of Transplantation*. 2013; 13 (9).
12. *Zhu X, Shen Z, Zhang Y, You B, Dong J*. Laparoscopic or abdominal left extrahepatic lobectomy of donor liver in pediatric living donor liver transplantation: a report of 17 cases. *International Journal of Clinical and Experimental Medicine*. 2019; 12 (4): 4116–4123.
13. *Lee J, Shehta A, Suh K, Hong SK, Yoon KC, Cho J et al*. Guidance for Optimal Port Placement in Pure 3-Dimensional Laparoscopic Donor Right Hepatectomy. *Liver Transplantation*. 2019; 25 (11): 1714–1722.
14. *Wakabayashi G, Cherqui D, Geller DA, Buell JF, Kaneko H, Han HS et al*. Recommendations for laparoscopic liver resection: A report from the second international consensus conference held in morioka. *Annals of Surgery*. 2015; 261 (4).
15. *Samstein B, Klair T*. Living Donor Liver Transplantation: Donor Selection and Living Donor Hepatectomy. *Current Surgery Reports*. 2015; 3 (9).
16. *Kwon C.H.D., Choi G.-S., Joh J.-W*. Laparoscopic right hepatectomy for living donor. *Current Opinion in Organ Transplantation*. 2019; 24 (2): 167–174.

17. *Hong SK, Shin E, Lee K-W, Yoon KC, Lee J-M, Cho J-H et al*. Pure laparoscopic donor right hepatectomy: perspectives in manipulating a flexible scope. *Surgical Endoscopy*. 2019; 33 (5): 1667–1673.
18. *Lu L, Wang Z, Zhu W, Shen C, Tao Y, Ma Z et al*. Left Hepatic Vein Preferential Approach Based on Anatomy Is Safe and Feasible for Laparoscopic Living Donor Left Lateral Sectionectomy. *Liver Transplantation*. 2020. C.lt.25793.
19. *Pereskokov SV, Dmitriev AV, Groshilin VS, Tareeva DA, Kozyrevskiy MA*. Khirurgiya pecheni: ot istokov razvitiya do sovremennykh vozmozhnostey. *Sovremennye problemy nauki i obrazovaniya*. 2017; 5.
20. *Vettoretto N, Saronni C, Harbi A, Balestra L, Taglietti L, Giovanetti M*. Critical View of Safety During Laparoscopic Cholecystectomy. *JSLS: Journal of the Society of Laparoendoscopic Surgeons*. 2011; 15 (3): 322–325.
21. *Hong KSSSK, Yi KWLNJ, Ahn HSKSW, Choi KCYJY, Kim DOH*. Pure laparoscopic living donor hepatectomy: Focus on 55 donors undergoingright hepatectomy. 2018; April 2017: 434–443.
22. *Chen K, Siow TF, Chio U, Wu J, Jeng K*. Laparoscopic donor hepatectomy. 2018; 11: 112–117.
23. *Lee KW, Hong SK, Suh KS, Kim HS, Ahn SW, Yoon KC et al*. One Hundred Fifteen Cases of Pure Laparoscopic Living Donor Right Hepatectomy at a Single Center. 2018: 1878–1884.
24. *Han JR, Han YS, Chun JM, Hwang YJ*. Indocyanine green near-infrared fluorescence cholangiogram during pure laparoscopic living donor hepatectomy for optimal bile duct division. *Transplantation*. 2020; 104 (S3): S498–S498.
25. *Au KP, Siu K, Chok H*. Minimally invasive donor hepatectomy, are we ready for prime time? 2018.
26. *Hong SK, Suh K, Kim KA, Lee J, Cho J, Yi N, Lee K*. Pure laparoscopic versus open left hepatectomy including the middle hepatic vein for living donor liver transplantation. *Liver Transplantation*. 2020; 26 (3): 370–378.
27. *Takahara T, Wakabayashi G, Beppu T, Aihara A, Hasegawa K, Gotohda N et al*. Long-term and perioperative outcomes of laparoscopic versus open liver resection for hepatocellular carcinoma with propensity score matching: A multi-institutional Japanese study. *Journal of Hepato-Biliary-Pancreatic Sciences*. 2015; 22 (10).
28. *Kiss M, Deshpande RR, Nemeskéri Á, Nguyen TT, Kürti Z, Kovács S et al*. Optimal line of hepatotomy for left lateral living donor liver transplantation according to the anatomical variations of left hepatic duct system. *Pediatric Transplantation*. 2015; 19 (5).
29. *Wing K, Cheung TT*. Standardizing Laparoscopic Left Lateral Sectionectomy for Hepatocellular Carcinoma. 2016.
30. *Monakhov A, Semash K, Tsiroulnikova O, Djanbekov T, Khizroev K, Kurtak N, Gautier SV*. Laparoscopic left lateral sectionectomy in living liver donors: from the first experience to routine usage. *Transplantation*. 2020; 104 (S3): S241–S241.
31. *Gautier SV, Monakhov AR, Miloserdov IA, Arzumanov S, Tsirulnikova OM, Semash KO, Dzhanbekov TA*. Simultaneous laparoscopic left lateral sectionectomy and nephrectomy in the same living donor: The first case report. *American Journal of Transplantation*. 2019; 19 (6).
32. *Kim JM, Ha SY, Joh JW, Sinn DH, Jeong WK, Choi GS et al*. Predicting hepatic steatosis in living liver donors via noninvasive methods. *Medicine (United States)*. 2016; 95 (7).
33. *Hong Q, Wang J, Wang Y, Fu B, Fang Y, Tong Q et al*. Clinical outcomes of laparoscopic versus open right hepatectomy for liver tumors: A meta-analysis. *Medicine (United States)*. 2020; 99 (1).
34. *Gavriilidis P*. Re-appraisal of prophylactic drainage in uncomplicated liver resections: a systematic review and meta-analysis. *HPB*. 2017; 19 (1).

The article was submitted to the journal on 16.10.2020

DOI: 10.15825/1995-1191-2020-4-154-161

METHODS OF ARTERIAL RECONSTRUCTION FOR PANCREATIC GRAFT

N.S. Zhuravel, I.V. Dmitriev, A.V. Pinchuk

Sklifosovsky Research Institute of Emergency Care, Moscow, Russian Federation

About 2,400 pancreas transplantations are performed every year worldwide, mainly pancreaticoduodenal transplantations. Most clinics use the classical revascularization technique using a Y-shaped vascular prosthetic implant. However, it is not always possible to restore full blood supply to the graft in this way. Therefore, other options for arterial reconstruction are being developed – from isolated blood supply to the graft via the splenic artery to full blood flow restoration through all the main vessels of the organ to ensure the most physiological blood supply to the pancreas. This review is devoted to analysis of the used arterial reconstruction methods and pancreaticoduodenal graft revascularization techniques.

Keywords: pancreas transplantation, pancreaticoduodenal graft, arterial reconstruction, Y-shaped vascular graft, isolated blood supply via the splenic artery.

INTRODUCTION

According to the World Health Organization (WHO), about 200 million people in the world are currently suffering from diabetes. In Russia, 256,200 patients have type 1 diabetes with an annual increase of about 10,000 new cases [1]. WHO predicts that the number of people living with diabetes will rise to 552 million by 2030. This undoubtedly makes diabetes a pandemic of non-infectious etiology.

Simultaneous pancreas-kidney (SPK) transplantation is one of the options for surgical treatment of diabetes in end-stage diabetic nephropathy. This treatment method allows to arrest kidney failure, achieve true insulin independence and significantly improve the patient's quality of life. According to the Global observatory on donation and transplantation (GODT), 2,338 transplants were performed in the world in 2018, of which only 17 were in Russia [2]. Such a small (in comparison to other solid organs) number of operations is due to shortage of suitable donor organs, very stringent requirements for organ quality, and relatively high frequency of loss of pancreas graft due to surgical and immunological complications.

Hendon was the first to attempt pancreas transplant surgery in 1913 in an animal experiment [3]. The first successful human pancreas transplant was performed by William D. Kelly and Richard C. Lillehei on December 17, 1966 at the University of Minnesota (USA). They performed a single-stage transplant of a kidney and pancreatic segment with a ligated main pancreatic (Wirsung) duct on a 28-year-old female patient with end-stage diabetic nephropathy. They developed and applied a method for arterial graft reconstruction with a Y-shaped vascular alloprosthesis (Y-graft), i.e. a technique still used in most transplant centers as a conventional technique for revascularization of a pancreaticoduodenal graft [4].

Given the fact that the native pancreas gets blood supply from 3 main arteries, some surgeons seek to modify this technique to achieve the most physiological organ revascularization. Others, on the other hand, seek to simplify the arterial reconstruction scheme by proposing to minimize the number of vascular anastomoses during operation. Meanwhile, methods have been proposed that would allow the use of those organs that were previously recognized as non-transplantable due to the impossibility of performing Y-graft reconstruction. There are also cases where surgeons have to modify the conventional technique due to the physiological characteristics of the donor organ or recipient.

This review is devoted to analysis of the types of arterial reconstruction and methods of revascularization of pancreatic grafts from the moment of first transplantation in 1966 to the present time at various transplant centers.

METHODS OF RECONSTRUCTION OF THE SPLENIC AND SUPERIOR MESENTERIC ARTERIES

More than 50 years have passed since the first pancreas transplant was performed, but Y-graft reconstruction of the arterial bed is still relevant today. In this technique, at the preoperative preparation stage, a single arterial suture is formed between the superior mesenteric and splenic arteries of the graft using Y-shaped alloprosthesis. Typically, the Y-graft is the bifurcation site of the donor's common iliac artery. Bifurcation of the common carotid or femoral artery can also be used. At the stage of transplantation, anastomosis is formed between the Y-graft and the common iliac, less often the external, recipient

Corresponding author: Nikita Zhuravel. Address: 3/2, Bolshaya Sukharevskaya Ploshchad, Moscow, 129090, Russian Federation. Phone: (906) 703-05-42. E-mail: zhuravelns@gmail.com

artery. This technique of revascularization of the pancreaticoduodenal segment is considered conventional at most transplant centers. At the University of Minnesota clinic, where pancreas transplant was performed for the first time in the world, about 2256 pancreas transplants were performed from 1966 to 2016 using this technique [5, 6]. According to a published report, the incidence of serious arterial complications at this center was 1.1% (10 arteriointestinal fistulas with gastrointestinal bleeding, 3 arteriovesical fistulas, 3 arteriovenous fistulas, 1 arterioureteral fistula, and 7 false aneurysms) [7].

Agnieszka Surowiecka-Pastewka *et al.* analyzed 200 pancreas transplants performed in a single center. They used a classical graft revascularization technique, with the incidence of arterial complications being 3% (2 deaths). In one patient, the revision revealed a ruptured section of the external iliac artery with massive bleeding. Due to dense infiltration, it was difficult to apply open suturing, so endovascular stenting of this area was performed. Control CT scan revealed no evidence of bleeding. In one case, arteriocystic fistula was formed 6 months after transplantation. Later, the patient developed gastrointestinal bleeding, which could not be stopped by endoscopic method, so the pancreaticoduodenal graft was removed. In another case, a patient with repeated transplantation in the early postoperative period was found to have common iliac artery stenosis proximal to the anastomosis; therefore, endovascular stenting of the artery was performed. No recurrent stenosis was detected in a follow-up study [8].

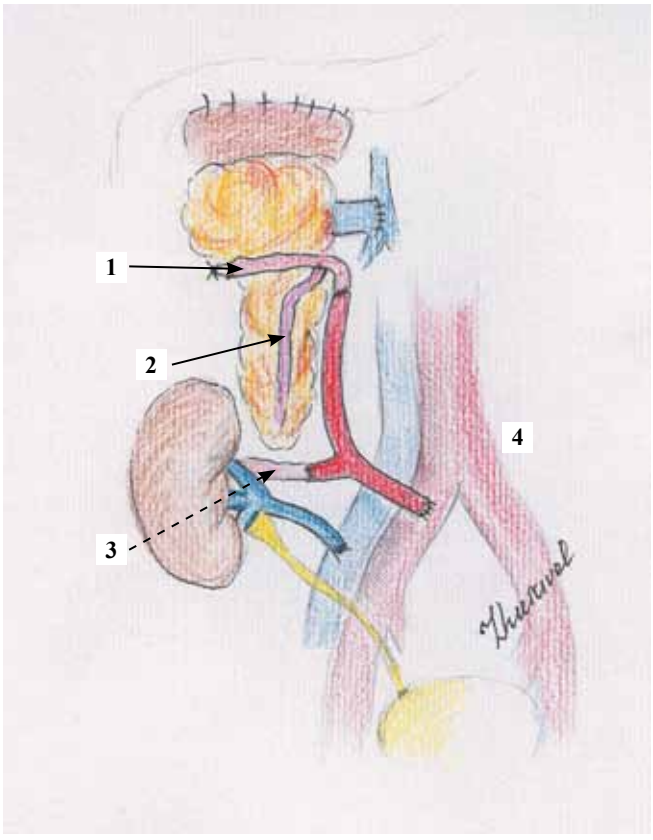

Fig. 1. Graft revascularization in patients with severely calcified iliac arteries: 1 – Donor superior mesenteric artery; 2 – Donor splenic artery; 3 – Donor renal artery; 4 – Aorta

At their center, L. Grabowska-Derlatka *et al.* use the classical graft revascularization technique with abdominal multispiral computed tomography (MSCT) for all recipients at day 6–8 after SPK transplantation. Out of the 60 patients, there were 9 cases of small intragraft vessel thrombosis and 17 cases of large vessel thrombosis. Half of these cases required graft removal [9].

At Brotzu Hospital, from 2005 to 2014, 27 pancreas transplants were performed using the classical revascularization technique. No vascular complications were noted in any case [10].

An interesting surgical technique has been described by Paul L. Tso *et al.* In 5 recipients with total superior vena cava thrombosis and severe iliac calcification, a tunneled central hemodialysis venous catheter was inserted into the left iliac vein. While performing SPK transplantation in these patients, the authors used an original modification of the classical technique: during back table preparation of the kidney, the renal transplant artery was anastomosed in end-to-end fashion to the internal iliac limb of the donor iliac artery Y graft (Fig. 1). The superior mesenteric artery of the pancreatic graft was anastomosed to the external iliac artery Y-graft also in an end-to-end manner. Then, an end-to-side anastomosis was formed between the splenic and superior mesenteric arteries of the graft [11]. Afterwards, an anastomosis was made between the single arterial conduit of the grafts and a small calcification-free area of the recipient's external iliac artery. Out of the 5 patients who underwent transplantation by this method, 1 patient developed a pseudoaneurysm of the allograft at the anastomosis of the splenic and superior mesenteric arteries manifested by gastrointestinal bleeding. This complication required pancreatectomy. The rest of the recipients had no serious complications, and the graft function was satisfactory [12].

In some cases, during pancreas transplantation, the reasons of why it is not possible to use the classical technique are revealed. In such cases, surgeons use various modifications of the classical method. For instance, a curious clinical observation was described by David F. Mercer. During simultaneous transplantation after reperfusion of the pancreaticoduodenal complex, surgeons had to perform immediate transplantatectomy due to ischemia of the donor pancreaticoduodenal segment and abrupt disturbance in blood supply in the recipient's external iliac artery. The cause was an extended atherosclerotic plaque in the anastomotic region. The affected portion of the artery was excised, while the arterial wall defect was repaired with a Gore-Tex® synthetic patch (W.L. Gore and Associates, Flagstaff, AR, USA). Five days later, the patient underwent a pancreas

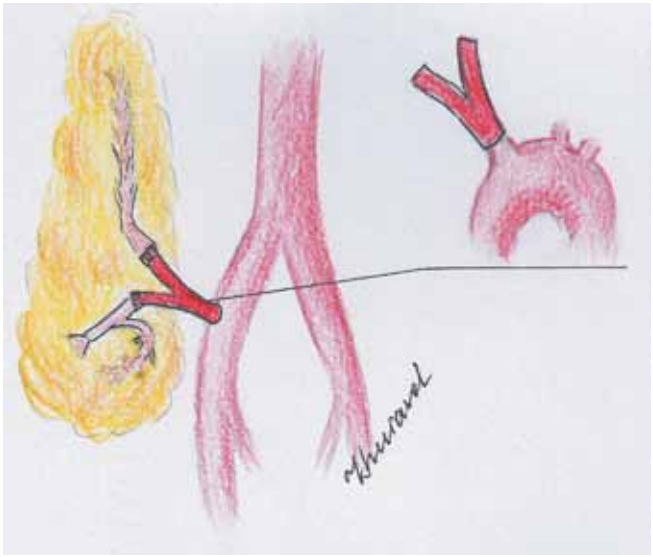

Fig. 2. Formation of a Y-shaped graft using bifurcation of brachiocephalic trunk

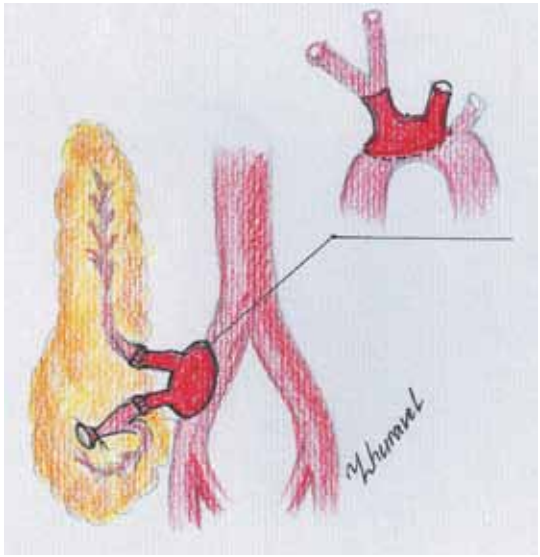

Fig. 3. Formation of a Y-shaped graft using a section of the aortic arch with the brachiocephalic trunk and the left common carotid artery

re-transplantation, during which the synthetic prosthesis was removed. In order to close the arterial defect, the following method was used: the external iliac artery of the donor Y-graft was cut off from the common iliac artery bifurcation and dissected along a linear incision. Thus, from the donor Y-graft, the surgeons obtained a 6-cm allogenic patch, which was used to restore the integrity of the recipient's external iliac artery. In turn, the Y-graft was used to form the common arterial orifice of the pancreatoduodenal graft, which was subsequently successfully anastomosed with an allogeneic arterial patch [13]. Ciancio *et al.* used a section of the brachiocephalic trunk with the subclavian and common carotid arteries as a Y-graft, since the donor's iliac arteries were calcified and unsuitable for reconstruction. At the pre-transplant preparation stage, anastomoses were formed between the superior mesenteric and subclavian arteries, and between the splenic and common carotid arteries (Fig. 2). During transplantation, anastomosis was formed between the base of the donor brachiocephalic trunk and the recipient's common iliac artery [14]. In a similar case, de Miranda *et al.* used as a Y-graft a section of the aortic arch with the brachiocephalic trunk and the left common carotid artery (Fig. 3) [15]. Mizrahi *et al.* performed revascularization of the pancreas without Y-graft. They made an anastomosis between the superior mesenteric artery of the graft and the common iliac artery of the recipient, having previously connected the splenic and superior mesenteric arteries of the pancreatoduodenal complex in an end-to-side manner (Fig. 4) [16]. Troppmann *et al.* reported the possibility of forming separate arterial anastomoses with the external and internal iliac arteries of the recipient, also without the use of Y-graft [17]. In cases where during transplantation, the venous outflow is carried out into the portal vein system, it becomes

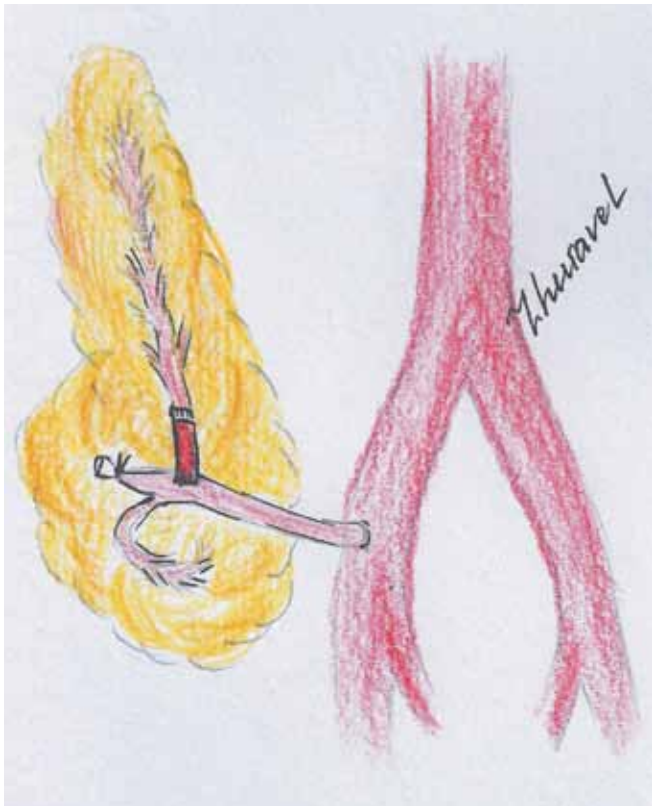

Fig. 4. Graft revascularization through the superior mesenteric artery with preliminary end-to-side connection of the splenic to superior mesenteric artery

difficult to use the Y-graft due to its insufficient length. In such cases, Bigam proposed forming an additional anastomosis between the donor brachiocephalic trunk and the recipient's iliac artery, and then restoring blood supply to the graft using the brachiocephalic joint and Y-graft in an end-to-end manner (Fig. 5) [18].

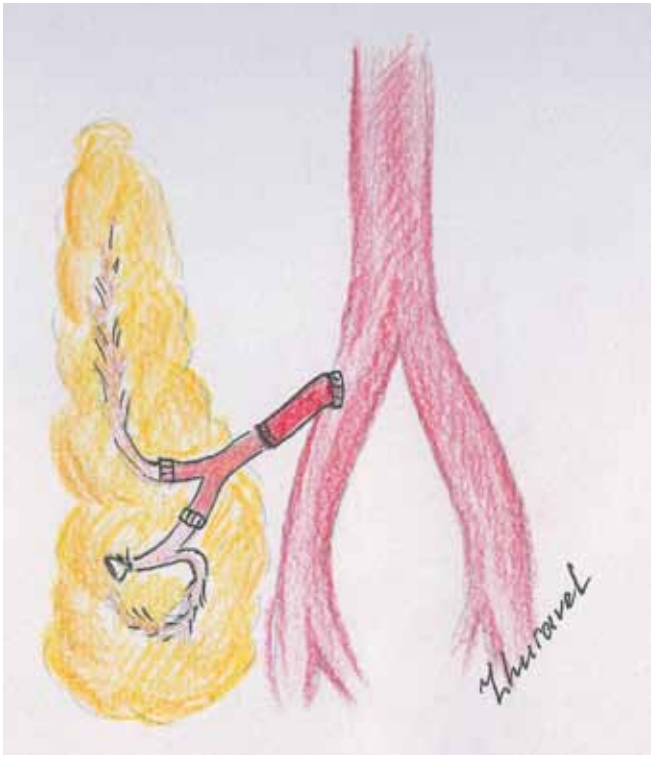

Fig. 5. Using an additional section of the brachiocephalic trunk to lengthen the vascular Y-shaped graft

ARTERIAL REVASCULARIZATION OF PANCREATICODUODENAL GRAFT USING THE CARREL PATCH

To reduce the incidence of vascular complications and the number of arterial anastomoses in pancreatic transplantation, Wen-wei Liao *et al.* modified vascular organ reconstruction based on international experience. In September 2019, they published a paper suggesting that vascular reconstruction should not be performed at the pre-transplantation stage. During multi-organ harvesting, surgeons transected the common hepatic artery after splitting the celiac trunk, allowing them to leave the splenic and superior mesenteric arteries with the celiac trunk in the same location as the aortic site (Fig. 6). This harvesting technique made it possible to perform donor organ revascularization, forming one arterial anastomosis, without prior formation of a Y-graft. The authors believe that this modification can theoretically reduce the incidence of vascular complications caused by thrombosis, bleeding and prolonged cold ischemia, since instead of three (in the classical version), one arterial anastomosis is formed, which reduces the number of risk zones and the time for pre-transplant preparation of the pancreatoduodenal complex. Of the 12 recipients who underwent pancreatic transplantation using this technique, no vascular complications were identified in any case. Graft function in all 12 cases was found to be satisfactory [19].

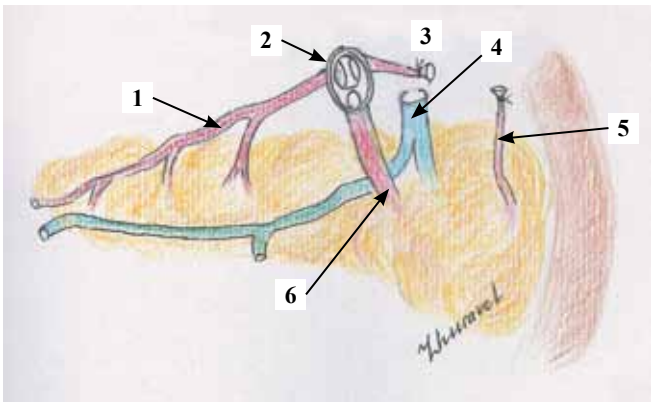

Fig. 6. Graft revascularization using the Carrel patch: 1 – Splenic artery; 2 – Carrel patch; 3 – Common hepatic artery; 4 – Portal vein; 5 – Gastroduodenal artery; 6 – Superior mesenteric artery

Earlier, a similar technique was described by J. Paulino et al. In their work, they focused on the "transverse pancreas" transplantation technique. But no less important is the graft revascularization technique applied by the authors. In 64 surgical interventions, they formed an anastomosis between the common area of the donor's aorta, with the celiac trunk and superior mesenteric artery, and the recipient's common iliac artery. Pancreas graft loss was 7.1%, and the main cause was venous thrombosis. That notwithstanding, there were no complications from arterial anastomosis [20].

ISOLATED BLOOD SUPPLY TO THE PANCREATICODUODENAL COMPLEX VIA THE SPLENIC ARTERY

In some cases, after harvesting the liver graft, the superior mesenteric artery supplying the pancreas remains too short for typical arterial reconstruction, since the orifice of the inferior pancreaticoduodenal artery is inevitably compromised during vascular anastomosis. Previously, in such cases, the pancreas was considered unsuitable for transplantation. At the same time, MSCT of recipients with a successfully functioning pancreaticoduodenal complex usually reveals a well-developed network of vascular collaterals between the basins of the splenic and superior mesenteric arteries. Due to the high occurrence of such vascular architectonics, a technique for isolated revascularization of the pancreaticoduodenal complex through the splenic artery was suggested and tested in practice. A special test was proposed to determine whether there is sufficient number of collaterals; if it gives a positive result, the graft can be successfully transplanted with restoration of arterial blood supply only through the splenic artery. From 2012 to 2018, out of 21 recipients who underwent SPK transplantation, surgery was performed using this technique in 6 cases. The control group of recipients underwent revascularization using the classical arterial reconstruction technique. No

vascular complications were detected in recipients of both groups. There were no statistically significant differences in the volume blood flow characteristics revealed by control MSCT of the pancreaticoduodenal graft in the control and comparison groups [21].

COMPLETE RECONSTRUCTION OF THE MAIN ARTERIES SUPPLYING BLOOD TO THE PANCREAS

In some transplantation centers, surgeons during pancreatic transplantation consider it reasonable to restore blood supply to the graft through all the three main arteries supplying blood to the pancreas – gastroduodenal, splenic and inferior pancreaticoduodenal (i.e. superior mesenteric) arteries. One of the practical ways to implement this reasonable aspiration is to insert a Y-graft between the gastroduodenal and splenic arteries, followed by formation of a common site with the superior mesenteric artery (Fig. 7). This technique makes it possible to transplant even the organs with iatrogenic arterial injuries without ischemia injury to the graft due to insufficiency of intraorganic circulation [22]. C. Socci *et al.* assessed the treatment outcomes of 199 patients who underwent pancreatic transplantation. In 60% of cases, blood supply to the graft was restored through the gastroduodenal artery using Y-graft. In other cases, the classical vascular reconstruction technique was used. Among the complications that developed in the postoperative period, the authors describe the occurrence of gastrointestinal bleeding, while, in 85% of cases of their development, revascularization of the pancreas was done using the classical technique [23].

DISCUSSION

Three main arteries are involved in supplying blood to the pancreas. When using the classical revascularization technique, blood supply to the pancreas is restored through two of the arteries – the inferior pancreaticoduodenal (first branch of the superior mesenteric artery) and the splenic. In this case, blood supply to the graft parenchyma goes through the inferior anterior and posterior pancreaticoduodenal arteries, the dorsal pancreatic artery, the pancreas tail artery, and the greater pancreatic artery. In this respect, due to insufficient revascularization of the gastroduodenal artery, blood supply through the superior anterior and posterior pancreaticoduodenal arteries and, in some cases, the superior duodenal artery, is carried out retrogradely, from intraorgan vascular collaterals. Theoretically, this can lead to circulatory insufficiency in the region of the pancreas head and donor duodenal stump. Given the presence of anastomoses between the superior and inferior pancreaticoduodenal arteries, the Y-graft method is recognized by most experts as sufficient and the most optimal. Having said that, formation of three arterial anastomoses can increase the risk

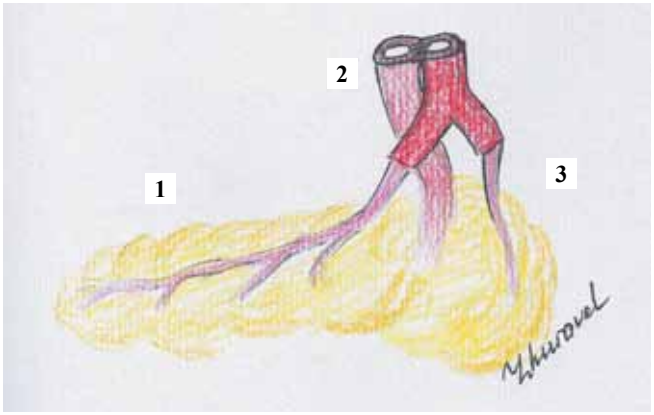

Fig. 7. Graft revascularization via 3 main arteries: 1 – Splenic artery; 2 – Superior mesenteric artery; 3 – Gastroduodenal artery

of vascular complications, such as stenosis, thrombosis, and anastomotic aneurysm. The technique for forming an anastomosis between the aortic site (carrel patch) of the graft and the recipient's iliac artery reduces the risk of developing vascular complications and reduces the warm ischemia time. However, in multi-organ harvesting, the portion of the aorta required for the arterial site is used in most cases during liver transplantation.

Gastroduodenal artery repair can improve blood supply to the pancreas head and duodenum, preventing ischemia. However, this method increases the number of anastomoses, which increases the ischemia time and number of potentially dangerous, "weak" sites for occurrence of vascular complications. The technique involving restoration of isolated blood supply to the graft along the splenic artery has also proved to be effective in cases where the length of the superior mesenteric artery does not allow forming an anastomosis using any other technique. However, this technique can be safely used only with intensive development of arterial collaterals in the graft parenchyma.

During organ harvesting and pre-transplant preparation, one should also not forget about the importance of the dorsal pancreatic artery, which can extend not only from the splenic artery, but also from the common hepatic artery, and even the celiac trunk. When it is damaged, blood supply to the organ is disturbed so significantly that it can lead to ischemia of a large part of the parenchyma with corresponding severe complications and consequences [24]. Besides, in a number of cases, there is a variant anatomy of the pancreas, including, in addition to the dorsal artery, a doubling of the splenic artery. In this case, for sufficient graft revascularization, a modification of the Y-graft technique can be used, in which two splenic arteries are connected side-to-side to form a single arterial orifice, which is then anastomosed with the internal iliac artery Y-graft. The dorsal artery can also be attached to the Y-graft end-to-side (Fig. 8) [25].

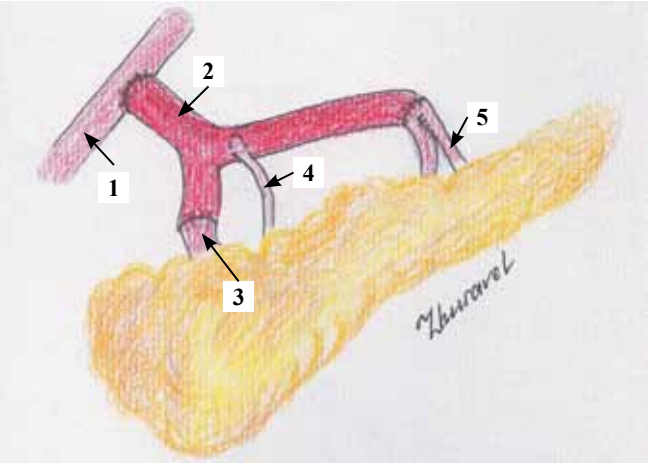

Fig. 8. Additional revascularization of the dorsal pancreatic artery and accessory splenic artery: 1 – Native external iliac artery; 2 – Common iliac artery; 3 – Superior mesenteric artery; 4 – Dorsal pancreatic artery; 5 – Syndactylized splenic arteries

CONCLUSION

At present, quite a lot of variants have been proposed for donor pancreas revascularization during transplantation. Each technique has its own advantages and disadvantages; even the classical technique comes with rather many complications from arterial anastomoses. This has made surgeons around the world to develop and implement new graft revascularization modifications and variants. The final choice of a particular technique depends on the anatomical features of the graft, the specific surgical situation, and the preferences of the surgeons performing the pancreas transplantation.

The authors declare no conflict of interest.

REFERENCES

1. *Shestakova MV, Vikulova OK, Zheleznyakova AV, Isakov MA, Dedov II*. Diabetes epidemiology in Russia: what has changed over the decade? *Terapevticheskii arkhiv*. 2019; 91 (10): 4–13. (in Russ, English abstract). https://doi.org/10.26442/00403660.2019.10.000364.
2. Global observatory on donation and transplantation – 2018 [Internet] [updated 2020 August 11]. Available from: http://www.transplant-observatory.org/summary/.
3. *Starzl T, Thai N, Shapiro R.* The history of pancreas transplantation. In: Corry RJ (ed.) *Pancreatic transplantation*. New York: Springer; 2006: 21–31.
4. *Kelly WD, Lillehei RC, Merkel FK, Idezuki Y, Goetz FC.* Allotransplantation of the pancreas and duodenum along with the kidney in diabetic nephropathy. *Surgery*. 1967; 61 (6): 827–837. PMID: 5338113.
5. *Gruessner RWG, Sutherland DER*. (eds.) Transplantation of the Pancreas. New York: Springer; 2004.
6. *Sutherland DE, Gruessner RW, Dunn DL, Matas AJ, Humar A, Kandaswamy R et al*. Lessons learned from more than 1,000 pancreas transplants at a single institution. *Ann Surg*. 2001; 233 (4): 463–501. PMID: 11303130. https://doi.org/10.1097/00000658-200104000-00003.
7. *Yadav K, Young S, Finger EB, Kandaswamy R, Sutherland DER, Golzarian J, Dunn TB.* Significant arterial complications after pancreas transplantation – A single-center experience and review of literature. *Clin Transplant*. 2017; 31 (10). PMID: 28787529. https://doi.org/10.1111/ctr.13070.
8. *Surowiecka-Pastewka A, Matejak-Górska M, Frączek M, Sklinda K, Walecki J, Durlik M*. Endovascular Interventions in Vascular Complications After Simultaneous Pancreas and Kidney Transplantations: A Single-Center Experience. *Ann Transplant*. 2019; 24: 199–207. PMID: 30975974. https://doi.org/10.12659/AOT.912005.
9. *Grabowska-Derlatkaa L, Grochowiecki T, Pacho R, Rowiński O, Szmidt J.* Role of 16-Multidetector Computerized Tomography in Evaluation of Graft Failure Risk in Patients with Pancreatic Graft Thrombosis After Simultaneous Pancreas and Kidney Transplantation. *Transplant Proc*. 2014; 46 (8): 2822–2824. PMID: 25380927. https://doi.org/10.1016/j.transproceed.2014.09.073.
10. *Tondolo V, Manunza R, Pellegrino RA, Zamboni F*. Pancreas Transplantation: Small-Center Experience in Type 1 Diabetes Mellitus in a High-Incidence Region. *Transplant Proc*. 2015; 47 (7): 2169–2172. PMID: 26361670. https://doi.org/10.1016/j.transproceed.2014.11.070.
11. *Troppmann C, Gruessner AC, Benedetti E, Papalois BE, Dunn DL, Najarian JS et al*. Vascular graft thrombosis after pancreatic transplantation: univariate and multivariate operative and nonoperative risk factor analysis. *J Am Coll Surg*. 1996; 182 (4): 285–316. PMID: 8605554.
12. *Tso PL, Cash MP, Pearson TC, Larsen CP, Newell KA*. Simultaneous Pancreas-Kidney Transplantation Utilizing a Common Arterial Conduit: Early Experience and Potential Applications. *Am J Transplant*. 2003 Nov; 3 (11): 1440–1443. PMID: 14525607. https://doi.org/10.1046/j.1600-6135.2003.00236.x.
13. *Mercer DF, Rigley T, Stevens RB*. Extended donor iliac arterial patch for vascular reconstruction during pancreas transplantation. *Am J Transplant*. 2004; 4 (5): 834–837. PMID: 15084183. https://doi.org/10.1111/j.1600-6143.2004.00422.x.
14. *Ciancio G, Olson L, Burke GW*. The use of the brachiocephalic trunk for arterial reconstruction of the whole pancreas allograft for transplantation. *J Am Coll Surg*. 1995; 181 (1): 79–80. PMID: 7599778.
15. *De Miranda MP, Genzini T, Gil AO, Tacconi M, Gama-Rodrigues J*. Use of a donor aortic cross for arterial reconstruction of the pancreaticoduodenal allograft. *Clin Transplant*. 1998; 12 (3): 165–167. PMID: 9642505.
16. *Mizrahi S, Boudreaux JP, Hayes DH, Hussey JL*. Modified vascular reconstruction for pancreaticoduodenal allograft. *Surg Gynecol Obstet*. 1993; 177 (1): 89–90. PMID: 8322161.
17. *Troppmann C, Gruessner AC, Benedetti E, Papalois BE, Dunn DL, Najarian JS et al*. Vascular graft thrombosis after pancreatic transplantation: univariate and multivariate operative and nonoperative risk factor analysis. *J Am Coll Surg*. 1996; 182 (4): 285–316. PMID: 8605554.

18. *Bigam DL, Hemming AW, Sanabria JR, Cattral MS.* Innominate artery interposition graft simplifies the portal venous drainage method of pancreas transplantation. *Transplantation*. 1999; 68 (2): 314–315. PMID: 10440410. https://doi.org/10.1097/00007890-199907270-00029.
19. *Liao W-W, Ling X-C, Zhang C, Liu F-R, Zhu X-F, He X-S, Hu A-B.* Novel surgical technique and efficacy analysis of donor pancreas preparation without vascular reconstruction in pancreas transplantation. *J Int Med Res*. 2019; 47 (12): 6182–6191. PMID: 31500486. https://doi.org/10.1177/0300060519870894.
20. *Paulino J, Martins A, Vigia E, Marcelino P, Nobre AM, Bicho L et al.* Simultaneous Kidney-Pancreas Transplantation With an Original "Transverse Pancreas" Technique: Initial 9 Years' Experience With 56 Cases. *Transplant Proc*. 2017; 49 (8): 1879–1882. PMID: 28923641. https://doi.org/10.1016/j.transproceed.2017.04.015.
21. *Pinchuk AV, Dmitriev IV, Anisimov YA, Storozhev RV, Balkarov AG, Kondrashkin AS et al.* Pancreas transplantation with isolated splenic artery blood supply – Single center experience. *Asian J Surg*. 2020; 43 (1): 315–321. PMID: 31301933. https://doi.org/10.1016/j.asjsur.2019.06.011.
22. *Miyagi S, Shimizu K, Miyazawa K, Nakanishi W, Hara Y, Tokodai K et al.* A Case of Successful Simultaneous Pancreas-Kidney Transplantation Using the Injured Pancreas Graft. *Transplant Proc*. 2017; 49 (10): 2315–2317. PMID: 29198668. https://doi.org/10.1016/j.transproceed.2017.10.017.
23. *Socci C, Orsenigo E, Zuber V, Caldara R, Castoldi R, Parolini D et al.* Triple arterial reconstruction improves vascularization of whole pancreas for transplantation. *Transplant Proc*. 2006; 38 (4): 1158–1159. PMID: 16757294. https://doi.org/10.1016/j.transproceed.2006.02.020.
24. *Baranski AG, Lam HD, Braat AE, Schaapherder AF*. The dorsal pancreatic artery in pancreas procurement and transplantation: anatomical considerations and potential implications. *Clin Transplant*. 2016; 30 (10): 1360–1364. PMID: 27555344. https://doi.org/10.1111/ctr.12814.
25. *Adamson D, Holzner ML, Wadhera V, Shapiro R*. Reconstruction of a Pancreatic Allograft With Variant Arterial Anatomy for Transplantation. *Transplant Direct*. 2019; 5 (2): e425. PMID: 30882029. https://doi.org/10.1097/TXD.0000000000000863.

The article was submitted to the journal on 13.08.2020

DOI: 10.15825/1995-1191-2020-4-162-167

TREATMENT OF EXPIRATORY TRACHEAL STENOSIS IN COMBINATION WITH BRONCHIECTASIS IN A LUNG RECIPIENT (INITIAL REPORT IN THE RUSSIAN FEDERATION)

I.V. Pashkov, A.V. Nikulin, D.O. Oleshkevich, M.T. Bekov, R.A. Latypov, E.F. Shigaev, A.G. Suchorukova, V.N. Poptsov, E.A. Spirina, E.V. Lebedev, Ya.S. Yakunin

Shumakov National Medical Research Center of Transplantology and Artificial Organs, Moscow, Russian Federation

Lung transplantation is the final treatment option for end-stage lung failure. In 2019, 63,530 lung transplants were performed worldwide [13]. Due to the variety of diseases causing patients to resort to lung transplant surgeries, there is a wide range of different complications and conditions that are subject to an individual clinical approach to determine treatment tactics. Each case is of great clinical interest due to the small amount of these operations and the complexity of postoperative rehabilitation, which requires a multidisciplinary approach [12]. We present a report on a surgical treatment of expiratory tracheal stenosis in combination with bronchiectasis in a lung recipient.

Keywords: lung transplantation, multidisciplinary approach, expiratory tracheal stenosis, bronchiectasis.

INTRODUCTION

Lung transplant recipients have an increased risk of developing infectious complications, particularly bronchiectasis, due to impaired blood supply to the bronchial tree and immunosuppressive drugs. The main factors in the development of the latter are local inflammatory processes in the bronchi and obstructive atelectasis. Progression of the inflammatory process is promoted by bronchial lumen obstruction. In view of the increase in inflammatory changes, the ciliated epithelium is rearranged towards replacement by stratified squamous epithelium, which in turn impairs mucociliary clearance processes. Microcirculation disorder leads to degeneration and dystrophic degeneration of smooth muscle fibers and the bronchial cartilaginous plate, followed by its replacement by connective tissue. Under these conditions, increased intrabronchial pressure, for example, when coughing, leads to stretching of the bronchial wall and promotes formation of bronchiectasis [11].

The incidence of expiratory stenosis is 0.4–21.0% [4]. To date, there is no generally accepted theory of the origin of expiratory tracheal stenosis, but it is often accompanied by chronic inflammatory processes in the lungs. It is not always possible to assert unequivocally which of the pathophysiological processes is primary. Difficulty coughing up phlegm exacerbates chronic inflammation, which in turn produces sputum, increases coughing, and stretches the tracheal walls. Thus, thinning and excessive mobility of the posterior wall of the trachea develop, leading to expiratory stenosis [1]. Conservative treatment of this condition is aimed at improving sputum discharge and prescribing anti-inflammatory drugs [5].

Attempts to find a surgical solution to the problem of expiratory tracheal stenosis have been made since the middle of the 20th century. R. Nissen in 1954 for the first time used a bone graft to strengthen the membranous wall of the trachea [7]. At the same time, H. Herzog suggested using the aponeurosis of the rectus abdominis muscle [2, 3]. The outcomes of surgical treatment of this category of patients are not always satisfactory, and, given that such operations are performed quite rarely, each case is of clinical interest [1]. Currently, synthetic materials such as polypropylene meshes [8, 9] or polytetrafluoroethylene sheets [10] are most often used for posterior tracheal wall plasty. Besides, these operations are usually performed using posterolateral thoracotomy [6].

There are few reports on video-assisted thoracoscopic surgery for expiratory tracheal stenosis. R. Machino et al. in 2020 demonstrated a clinical observation of thoracoscopic plication of the membranous tracheal wall with interrupted sutures in an elderly patient with crescent-shaped tracheobronchomalacia with a positive effect. The patient was discharged on day 126 after surgery [6].

Our observation presents the first experience in the Russian Federation on surgical treatment of expiratory tracheal stenosis in combination with bronchiectasis in the lung graft.

MATERIALS AND METHODS

Description of clinical observation

Patient P., male, 61 years old, since 2018 has been under observation at Shumakov National Medical Research Center of Transplantology and Artificial Organs with the following diagnosis: chronic obstructive pulmo-

Corresponding author: Ivan Pashkov. Address: 1, Shchukinskaya str., Moscow, 123182, Russian Federation. Phone: (495) 190-35-62. E-mail: dr.pashkov.ivan@gmail.com

nary disease (COPD), pulmonary emphysema, extremely severe course, type 2 respiratory failure, mixed form. In August 2018, the patient was included in the waiting list for deceased donor lungs.

In September 2018, bilateral sequential lung transplantation from a deceased donor was carried out.

The donor was a 33-year-old man. Mechanical ventilation (MV) lasted for 1 day. Plain chest x-ray showed no focal or infiltrative changes. Arterial blood oxygenation index pO_2/FiO_2 was 252. Video-assisted bronchoscopy showed a moderate amount of mucous sputum. Cold preservation was carried out using Celsior solution (IGL, France) by anterograde and retrograde method.

Lung transplantation was performed according to the standard technique. The patient was extubated and transferred to spontaneous breathing after 24 hours. The patient stayed in the intensive care unit for 8 days. Drains from pleural cavities were removed on day 8. Immunosuppressive therapy included tacrolimus, methylprednisolone, and mycophenolate mofetil.

The early postoperative period on day 24 was complicated by the development of right lower lobe pneumonia; therefore, tacrolimus dosage was reduced for the patient. Based on the results of a bacteriological study of bronchoalveolar lavage, according to which the growth of Ps. aeruginosa was noted, multicomponent antibacterial therapy (polymyxin, meropenem, sodium colistimethate, ceftazidime) was started with a positive effect – normalization of inflammatory markers and resolution of the clinical and radiological picture of pneumonia.

Control transbronchial biopsy on day 30 revealed the presence of antibody-mediated acute low-intensity graft rejection for which 5 sessions of plasmapheresis and correction of immunosuppressive therapy were carried out. The control transbronchial biopsy of the graft after treatment showed no signs of rejection. The patient was discharged from the hospital in a stable condition on day 54 after transplantation.

On June 10, 2020, patient P. was re-hospitalized at Shumakov National Medical Research Center of Transplantology and Artificial Organs with complaints of severe cough with discharge of copious amounts of viscous purulent sputum. Saturation was 92%, there was a need for continuous oxygen insufflation through nasal cannulas with a 7 L/min flow. Multidetector chest CT scan revealed bronchiectasis of the lower and middle lobes of the right lung (Fig. 1).

Control video-assisted bronchoscopy revealed expiratory stenosis of the lower third of the membranous trachea, which significantly complicated sputum evacuation (Fig. 2).

A multicomponent antibiotic therapy selected according to the sensitivity of the bacterial flora, and multiple sanitation bronchoscopies with a short-term positive effect were administered at the transplant center. Noninvasive ventilation of the lungs was contraindicated in

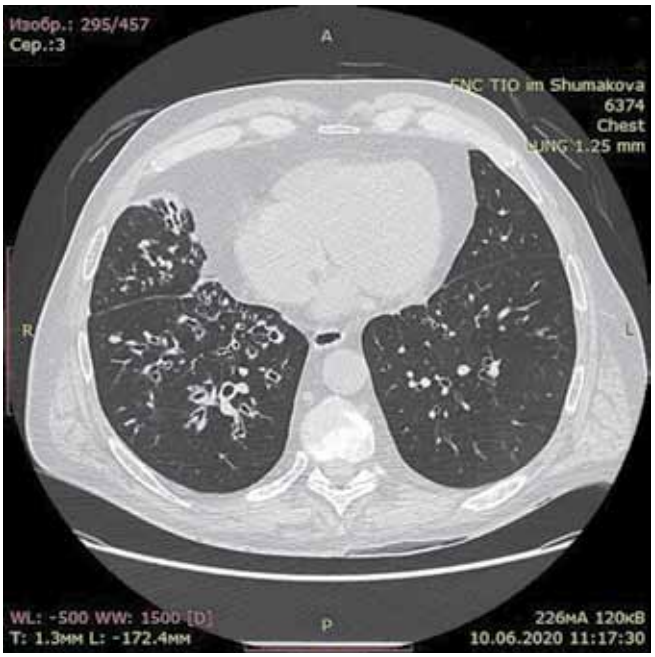

Fig. 1. CT before operation

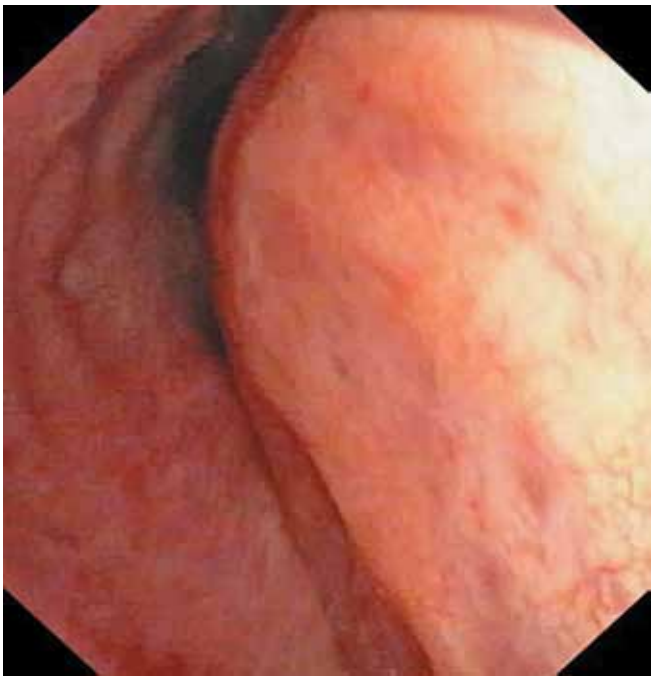

Fig. 2. Expiratory tracheal stenosis in the lower third

the patient due to the presence of bronchiectasis in the middle and lower lobes of the right lung and a large amount of hard-to-separate purulent sputum.

In order to eliminate the expiratory prolapse of the lower third of the trachea, the method developed by M.I. Perelman in 1987 was applied; it consists in phased sclerosis of the membranous trachea by injecting a glucose solution (40%) and the patient's plasma in a 1/1 ratio [14]. Injections were performed at 14-day intervals.

After two stages of endoscopic sclerotherapy, there were some positive dynamics – visual decrease in the

prolapse of the membranous part of the lower third of the trachea, decreased cough intensity, and improved sputum discharge. However, a few days later, the patient re-developed a clinical and laboratory picture of infectious process exacerbation and increased respiratory insufficiency. Bronchoscopy conducted showed a relapse of expiratory prolapse of the membranous wall of the trachea (Fig. 3).

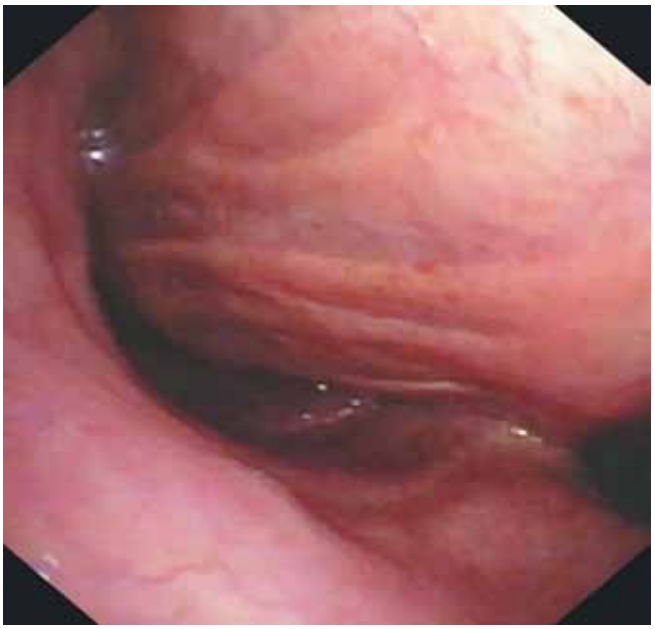

Fig. 3. Recurrence of expiratory prolapse of the membranous wall of the trachea

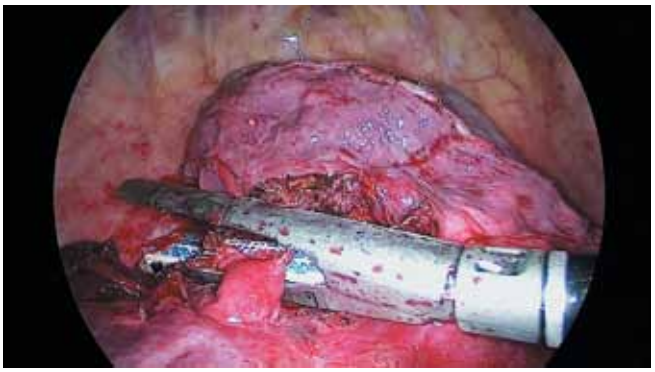

Fig. 4. Transection of basal part of the right pulmonary artery with a linear cutter

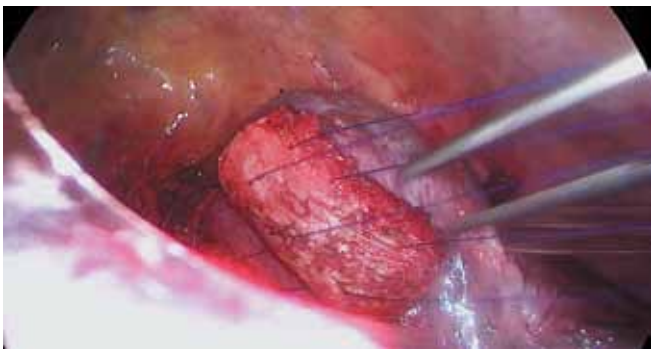

Fig. 5. Suturing the bone allograft to the posterior wall of the trachea

Given the increasing respiratory insufficiency and presence of a persistent infectious process, we decided to perform a surgical operation for vital indications. The purpose was to eliminate the focus of chronic infection and strengthen the membranous wall of the trachea.

On July 30, 2020, video-assisted thoracoscopic lower bilobectomy on the right side was performed with simultaneous plasty of the lower third of the membranous wall of the trachea with bone allograft (Fig. 4, 5, 6).

Course of operation

The patient position was on the left side. Separate intubation with a double-lumen orotracheal tube. An optics was inserted into the 7th intercostal space along the mid-axillary line, and a minithoracotomy (3 cm) was performed in the 5th intercostal space between the anterior and mid-axillary lines. Thoracoscopic inferior bilobectomy on the right side was performed as the first step, after the lung had been isolated from the adhesions using an ultrasonic harmonic scalpel (Fig. 4).

During the surgical access in the 5th intercostal space, a 4 cm long section of the 5th rib was resected to form a bone allograft, cut lengthwise, and a bone plate was formed; its edges were rounded. Suture holes were formed in the resulting bone plate.

In order to prevent damage to the endotracheal tube cuff, the trachea was reintubated using a single-lumen tube under endoscopic guidance. The trachea was mobilized in the middle and lower thirds, taken on a holder. The bone allograft was sutured to the membranous part of the trachea in its lower third with separate interrupted sutures (Prolen 4/0) (Fig. 5).

Multiple bronchiectasis in the lung tissue was found in the macropreparation cut (Fig. 6).

The early postoperative period was complicated by prolonged alveolar insufficiency, which required an artificial pneumoperitoneum (5 sessions of 600 mL each). Drainage was removed on day 5. Control bronchoscopy found no prolapse of the membranous trachea (Fig. 7). Multidetector chest CT scan found that the upper lobe of the right lung completely filled the right hemithorax. The patient subjectively noted significant improvement in his condition. Oxygen demand was reduced to 1–2 L/min. After 7 days, the patient stopped oxygen therapy, arterial blood saturation by atmospheric air was 91%. The patient was discharged in a stable condition on day 21 after the operation. Control CT after 2.5 months showed that the operated right lung was fully expanded, and there were no additional focal-infiltrative changes (Fig. 8). A comparative analysis of objective indicators over time is presented in Table.

Table

Comparative analysis of objective indicators

RF indicators (% of the norm)	Preoperative	Postoperative	After 1 month	After 2.5 months
FEV_1 (% of the norm)	22	23	25	30
FVC (% of the norm)	36	37	45	46
Tiffno's index (%)	47	62	55	65
sO_2 in atm. air (%)	85	88	92	92
sO_2 in oxygen (%)/Vflow (L/min)	92/10	94/7	98/2	98/2

Fig. 6. Gross specimen of multiple bronchiectasis in the lung tissue

Fig. 7. Bronchoscopy after surgery

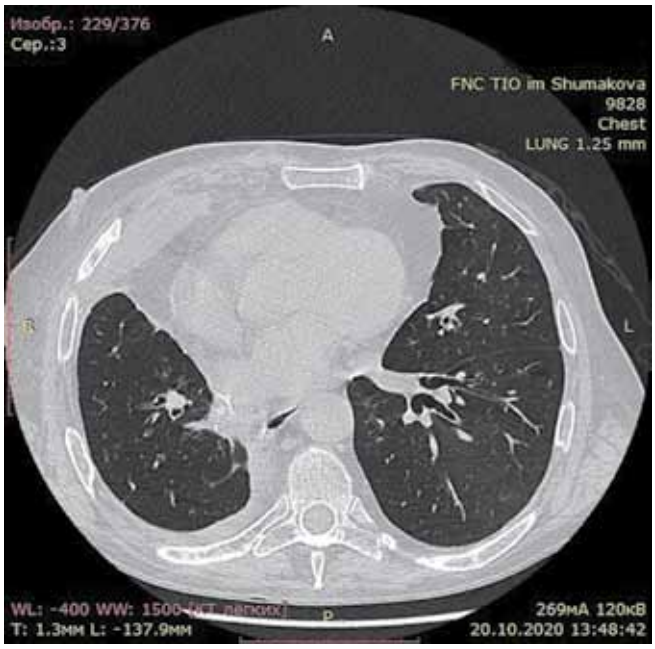

Fig. 8. Multispiral CT scan 2.5 months after surgery

DISCUSSION

Bronchiectasis in lung recipients is a serious issue due to the high risk of developing severe infectious complications against the background of immunosuppressive therapy. A combination of bronchiectasis and expiratory tracheal stenosis, causing impaired ventilation function, leads to rapid progression of respiratory insufficiency and significant deterioration in the patient's condition.

Surgical treatment of patients who have undergone bilateral lung transplantation is associated with a number of difficulties (pronounced adhesions in the pleural cavity, "altered anatomy", frequent exacerbations of chronic infections amidst immunosuppression, in some cases low functional reserves, difficulties in predicting the functional status in the early postoperative period). However, surgery is the only treatment that can significantly improve the quality of life of the patients.

In this clinical case, surgical treatment was the only treatment due to the ineffectiveness of conservative therapy. The increase in pulmonary function (PV) indicators was due to elimination of expiratory tracheal stenosis. Improved blood oxygenation was due to cessation of blood shunting through poorly ventilated as a result of bronchiectasis) lobes of the lung.

CONCLUSION

This clinical case indicates the need for a comprehensive multidisciplinary approach to the treatment of post-lung transplant complications, depending on the specific case. Video-assisted thoracoscopic surgical access, in

the absence of total adhesion, is the method of choice when performing surgical interventions in patients with low functional status. This is due to low trauma and, as a consequence, increased rehabilitation potential of the patient. Plasty of the membranous wall of the trachea in the presence of expiratory stenosis is an effective method of surgical treatment if other methods of correction are ineffective and/or impossible.

The authors declare no conflict of interest.

REFERENCES

1. *Parshin VD et al.* Surgical treatment of a female patient with tracheomalacia and expiratory tracheal stenosis. *Russian Pulmonology.* 2018; 5: 626–631. [In Russ, English abstract]. doi: 10.18093/0869-0189-2018-28-5-626-631.
2. *Herzog H.* Relaxation and expiratory invagination of the membranous portion of the intrathoracic trachea and the main bronchi as cause of asphyxia attacks in bronchial asthma and the chronic asthmoid bronchitis of pulmonary emphysema. *Schweizerische Medizinische Wochenschrift.* 1954; 84: 217–221.
3. *Herzog H.* Expiratory stenosis of the thrachea and great bronchi by loosening of the membraneous portion; plastic chip repair. *Thoraxchirurge.* 1958; 4: 281–319.
4. *Dambaev GC et al.* Eksperimentalnoe obosnovanie sposoba hirurgicheskogo lecheniya ekspiratornogo stenosa trahei i glavnih bronhov. *Bulleten sibirskoi medicini.* 2011; 6.
5. *Bisenkov LN.* Torakalnaya hirurgiya. M.: 2002: 755–759.
6. *Machino R, Tagawa T.* Thoracoscopic plication of the membranous portion of crescent-type tracheobronchomalacia in an elderly patient: a case report. *Surgical Case Reports.* 2020; 1: 1–5.
7. *Nissen R.* Tracheoplastik zur Beseitigung der Erschlaffungdes membraneosen Teils der intrathorakalen Luftrohre. *Schweiz Med Wochenschr.* 1954; 84: 219–221.
8. *Wright CD, Grillo HC, Hammoud ZT, Wain JC, Gaissert HA, Zaydfudim V et al.* Tracheoplasty for expiratory collapse of central airways. *The Annals of Thoracic Surgery.* 2005; 80: 259–266.
9. *Wright CD.* Tracheobronchomalacia and expiratory collapse of central airways. *Thoracic Surgery Clinics.* 2018; 28: 163–166. doi: https://doi.org/10.1016/j.thorsurg.2018.01.006.
10. *Takazawa S et al.* External stabilization for severe tracheobronchomalacia using separated ring-reinforced ePTFE grafts is effective and safe on a long-term basis. *Pediatric Surgery International.* 2013; 11: 1165–1169. doi 10.1007/s00383-013-3383-8.
11. *Samsonova MV, Chernyaev AL, Lemenkova OS.* Modern Aspects of Diagnosis and Treatment of Bronchiectasis. *Practical Pulmonology.* 2017; 1.
12. *Decaluwe H et al.* Thoracoscopic lobectomy after bilateral lung transplantation. *Interactive Cardiovascular and Thoracic Surgery*. 2014; 19: 515–517. doi: https://doi.org/10.1093/icvts/ivu144.
13. Ishltregistries.org [Internet]. The International Society for Heart and Lung Transplantation. Available from: https://ishltregistries.org/.
14. *Alimov AT, Perelman MI.* Skleroziruyuschaya endoscopicheskaya terapiya ekspiratornogo stenoza trahei i glavnih bronhov. *Grudnaya hirurgiya*. 1989; 1: 40–43.

The article was submitted to the journal on 23.10.2020

DOI: 10.15825/1995-1191-2020-4-168-172

HEART TRANSPLANT IN A PATIENT WITH PERSISTENT LEFT SUPERIOR VENA CAVA

G.V. Aniskevich, G.A. Sadrieva, V.N. Poptsov, E.A. Spirina, V.I. Orlov, R.Sh. Saitgareev

Shumakov National Medical Research Center of Transplantology and Artificial Organs, Moscow, Russian Federation

Objective: to present our own experience of heart transplantation in a patient with persistent left superior vena cava (PLSVC). A clinical case of successful orthotopic heart transplantation using the biatrial technique in a patient with PLSVC drainage into the right atrium is presented. The clinical effect achieved as a result of the treatment fully justifies the chosen surgical tactics and allows us to recommend the proposed tactics for treatment of such a rare anomaly. **Conclusion.** The clinical effect achieved as a result of the treatment fully justifies the chosen surgical tactics and allows us to recommend the proposed tactics for treatment of such a rare anomaly.

Keywords: congenital malformation, cardiovascular system, persistent left superior vena cava, heart transplantation.

Persistent left superior vena cava (PLSVC) is a rare congenital vascular anomaly. The incidence is 0.3–0.5% of the general population with a normal heart and in 4.5% of people with congenital heart disease [1]. In most cases (80–90%), PLSVC is associated with a right superior vena cava (SVC) [2], and may also be accompanied by other cardiac anomalies, such as abnormal pulmonary vein connections, coarctation of the aorta, tetralogy of Fallot, transposition of the great vessels, and patent ductus arteriosus (PDA) [3]. At the same time, cardiac arrhythmias are observed.

PLSVC usually flows into the right atrium (in 80–92%) through the dilated coronary sinus [5], but in 10–20% of cases, it flows into the left atrium [7]. The PLSVC can drain directly into the left atrium or coronary sinus, causing a right-to-left cardiac discharge. Most patients with PLSVC are asymptomatic. Only patients with abnormal drainage and right-to-left discharge have a clinical picture. Abnormal venous return via PLSVC can cause cardiac arrhythmias, decreased exercise tolerance, progressive fatigue, chest discomfort, palpitations, fainting, or cyanosis [6].

The presence of PLSVC is important for central venous catheter placement, pacemaker implantation, and cardiac catheterization. PLSVC is also a relative contraindication for retrograde cardioplegia during cardiac surgery [6].

To date, the choice of optimal tactics and the extent of the proposed surgical intervention remains an open question. In this paper, we present the experience of heart transplantation in a recipient with an abnormal left SVC performed by surgeons at the cardiac surgery department No. 1.

CASE STUDY

Patient K., 52 years old, has considered himself ill since 2004, when, without a previous coronary history, he suffered inferior wall acute myocardial infarction (AMI) with the development of early post-infarction angina pectoris. Coronary artery stenting was performed on the background of acute coronary syndrome. In 2008, examination revealed thrombophilia, anticoagulants were prescribed. In 2010, he underwent coronary artery bypass grafting of the right coronary artery and the circumflex branch off the left coronary artery. According to the Holter monitoring data, paroxysmal supraventricular tachycardia (PSVT) was registered. In 2014, a dual-chamber cardioverter-defibrillator was implanted. In 2018, battery depletion was detected and a dual-chamber cardioverter-defibrillator was reimplanted. On July 10, 2019, electrophysiological examination and radiofrequency ablation of the right isthmus and ectopic foci were performed. Control coronarography revealed shunt stenosis, balloon angioplasty with shunt stenting were performed on December 18, 2019 to the circumflex branch. From February 2020, there was an increased frequency of tachycardia attacks, cardioverter defibrillator activation, numerous syncopal episodes. The patient was admitted at the cardiology department of the Shumakov National Medical Research Center of Transplantology and Artificial Organs for examination under the program for potential heart recipients with a ***clinical diagnosis:*** *ischemic cardiomyopathy. Coronary artery disease: Stenosing coronary sclerosis. Postinfarction cardiosclerosis (2004, 2008). Operation: balloon-assisted vasodilation with right coronary artery stenting, anterior interventricular branch, circumflex artery bran-*

Corresponding author: Guzaliya Sadrieva. Address: 1, Shchukinskaya str., Moscow, 123182, Russian Federation. Phone: (937) 790-55-09. E-mail: sadrieva.guzaliya@gmail.com

ches of 2005, 2006, 2007. Left marginal artery, May 28, 2018. Coronary artery bypass grafting of the right coronary artery and circumflex artery in 2010. Shunt restenosis to circumflex artery 80%. Balloon angioplasty with stenting. Coronary artery bypass grafting of the right coronary artery on December 18, 2019.

Main complication: *Arrhythmias: Paroxysmal supraventricular tachycardia. Cardioverter defibrillator implantation in 2014 Battery depletion and reimplantation of cardioverter defibrillator in 2018. Radiofrequency ablation of the right isthmus and ectopic foci on July 10, 2029. Relative mitral regurgitation. Relative tricuspid valve insufficiency. Chronic heart failure, stage 2A circulatory insufficiency, NYHA Class III heart failure.*

Concomitants: *Multifocal atherosclerosis with coronary and carotid artery lesions. Consequences of ischemic stroke of April 2015. Thrombophilia. Chronic cholecystitis. Multiple small cysts in the liver parenchyma. Diffuse nodular goiter. Iodine-induced subclinical thyrotoxicosis.*

Objectively: *a state of moderate severity. Skin and visible mucous membranes of physiological color. There were no peripheral edemas. In the lungs, breathing was rigid, occurring in all parts, no wheezing. Respiratory rate – 17 breaths per min. Examination showed that the boundaries of relative cardiac dullness were not expanded, the cardiac impulse was not determined, the apical impulse was determined in the fifth intercostal space along the left midclavicular line. Clear heart sounds, regular rhythm, a single extrasystole. Heart rate was 72 beats/min. Blood pressure 100/70 mm Hg. The abdomen was soft and painless on palpation. The liver was not enlarged. Murphy's punch sign was negative. There were no dysuric disorders. There were no acute focal symptoms.*

General blood test, biochemical blood test, coagulogram without any peculiarities.

ECG at rest had normal sinus rhythm with a heart rate of 70/min. Myocardial scarring at the posterior diaphragmatic region of the left ventricle. Decreased blood supply in the scarring area, apical-lateral wall.

Frontal chest X-ray: moderate increase in pulmonary vascular pattern was noted.

Preoperative echocardiographic data: *Aorta: at the level of the annulus fibrosus 2.7 cm. Valsalva sinus 4.2 cm. Ascending aorta 3.9 cm. Left atrium: 3.9 cm (anteroposterior dimension); Left atrial volume 60 mL. Right atrium: Right atrial volume 48 mL. Right ventricle: 2.7 cm (anteroposterior dimension); Right ventricular anterior wall thickness 0.5 cm. Interventricular septum 1.2–1.3 cm. Left ventricular posterior wall 1.0 cm. End-diastolic volume 197 mL; End-systolic volume 123 mL; Stroke volume 54 mL. Ejection fraction 37%. Left ventricular local contractility: diffuse hypokinesis. Inferior wall akinesis, posterior part, interventricular septal dyskinesia. No pathological formations. Electrodes are in the right heart chambers. Valve apparatus: Aortic valve: 3-cusp leaflet: sealed with Pgr 9.2 mmHg. Regurgitation degree 1. Mitral valve: Leaflets: sealed, calcium at the base of the posterior valve of the MC. Regurgitation 1 degree. Tricuspid valve: no features of the leaflets. Regurgitation degree 1. Pulmonary artery: Leaflets: no particularities. Pulmonary artery trunk diameter 2.4 cm, Pgr 4.5 mmHg, degree 0–1 regurgitation. Systolic pressure 32 mmHg.*

Fig. 1. Contrast-enhanced multidetector CT imaging of the heart. The right superior vena cava is typically located. Visualized is a persistent left superior vena cava, enveloping the left atrium along its posterior wall and flowing into the coronary sinus, while the transverse vein is not defined; SVC – superior vena cava. LSVC – left superior vena cava

OPERATION

Longitudinal median sternotomy. Cardiolysis of the aorta and the right heart was performed. The heart was enlarged. Cannulation of the aorta and vena cava. Artificial blood circulation was started, cardiolysis continued. The shunts from the aorta were ligated, stitched and cut off. The ascending aorta was clamped, the recipient's heart was excised with technical difficulties due to the pronounced adhesion process. PLSVC was revealed, which entered the pericardium at the left superior pulmonary vein level and flowed into the coronary sinus. The PLSVC was isolated from the adhesions, mobilized, and clamped with a turnstile. A left atrial cavity was formed. The cardiac graft was placed in the pericardial cavity. External cooling of the graft. The left atria of the donor and the recipient were anastomosed with a twisted suture, then the right atria of the donor and recipient. Given the long SVC stump of the donor heart, an end-to-end anastomosis was applied between the donor SVC stump and the recipient's PLSVC. The anastomosis was laid in the transverse sinus, behind the aorta and pulmonary artery. The donor and recipient aorta and the donor and

recipient pulmonary arteries were anastomosed with continuous twisted prolene suture 5-0. The clamp was removed from the aorta to prevent air embolism. Cardiac activity was restored after defibrillation. Drainage was removed from the left ventricular cavity. Cardiotonic support was selected. On the background of inotropic drugs, artificial blood circulation was completed routinely. Decannulation. Thorough hemostasis. The anterior mediastinal cavity was drained. The pericardial and the enclosed left pleural cavity were drained with a single drain. A pacemaker electrode was sutured to the right ventricle. Implantable cardioverter defibrillator with 2 electrodes was removed from a separate incision in the right subclavian region. The sternum was sutured with 6 wire sutures. Layer-by-layer suturing of the surgical wound and a wound in the right subclavian region.

Postoperative course: *The patient was extubated on postoperative day 1. The early postoperative period was accompanied by myocardial insufficiency requiring inotropic support, metabolic disorders requiring renal replacement therapy. On postoperative day 9 against the background of regressive myocardial and respiratory failure, and regression of metabolic disorders, the patient was transferred to the department. The further postoperative period was uneventful. He was discharged on day 23 in a satisfactory condition.*

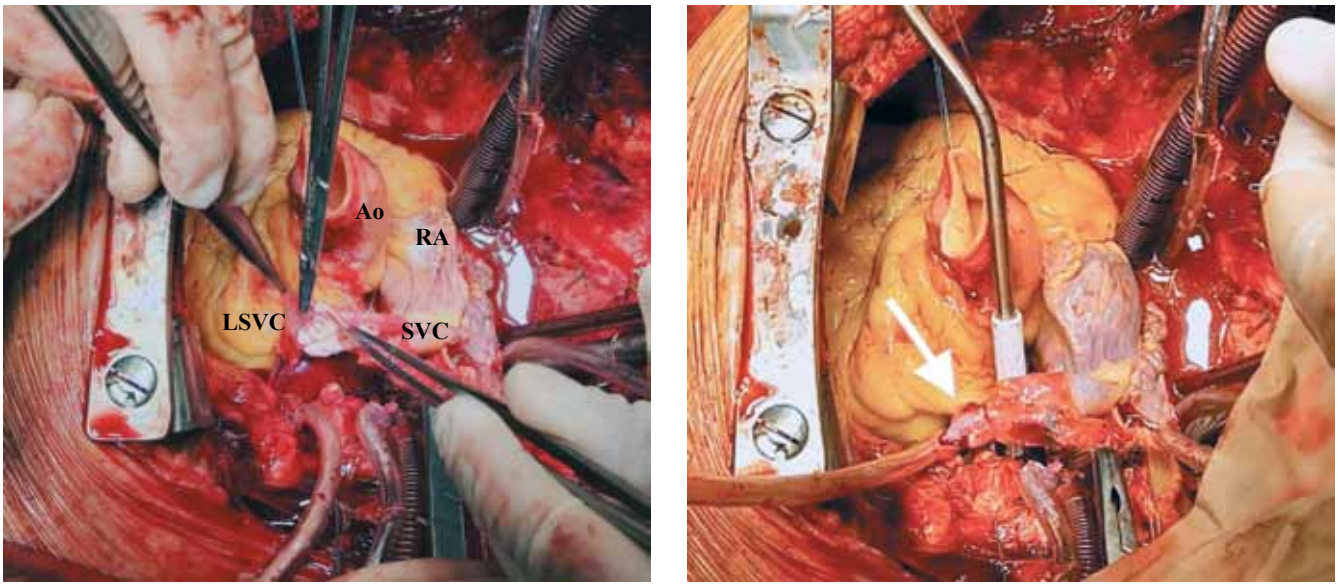

Fig. 2. An end-to-end anastomosis of the donor SVC to the recipient persistent LSVC was performed. The anastomosis is laid in the transverse sinus, behind the aorta and pulmonary artery. The white arrow indicates the patency and tightness of the anastomosis. Ao – aorta; RA – right atrium; SVC – donor superior vena cava; LSVC – persistent recipient left superior vena cava

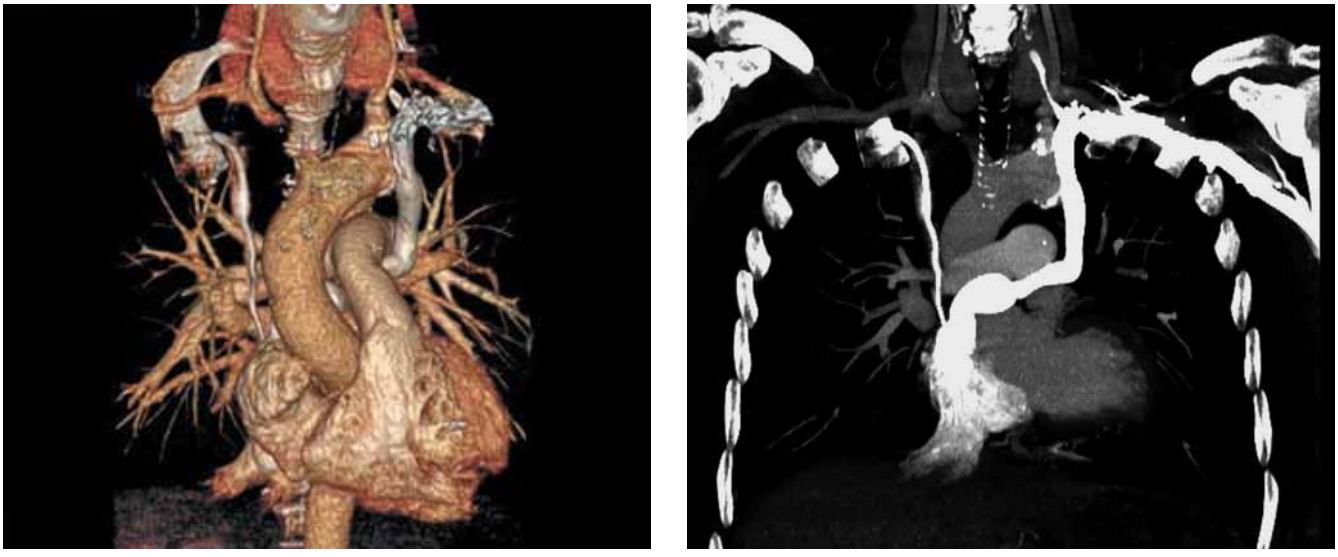

Fig. 3. Contrast-enhanced multispiral CT imaging of the heart. The right superior vena cava is typically located, and it is of small diameter. The persistent left superior vena cava is visualized, anastomosis of the recipient left superior vena cava and the donor superior vena cava is patent

Postoperative echocardiographic results: *Aorta: at the level of the annulus 2.2 cm. Sinuse of Valsalva 3.5 cm. Ascending aorta 3.2 cm. Left atrium: 4.5 cm (anteroposterior dimension) 6.5 × 3.8 (from the apical approach). Right atrium: 5.7 × 3.8 (from the apical approach); Right ventricle: 2.9 cm (anteroposterior dimension); Left ventricle: End-diastolic volume 114 mL; End-systolic volume 37 ml; Stroke volume 77 mL; Ejection fraction 68%. No pathological formations. Valve apparatus: Aortic valve: 3 leaflets, valves are sealed with Pgr/MGr 10.0/– mmHg. 0–1 degree regurgitation. Mitral valve: Leaflets: sealed. M-shaped leaf movement. No peak A. Degree 1 regurgitation. Tricuspid valve: Leaflets: no particularities. 1–2 degree regurgitation. Pulmonary artery: Leaflets: no particularities. Pulmonary artery trunk diameter 2.3 cm, Pgr 7.5 mmHg, degree 1 regurgitation. Systolic pressure 46.0 mmHg. Inferior vena cava 1.9 cm, collapses >50% on inspiration. Pulmonary hypertension group 1.*

DISCUSSION

In cardiac transplantation, PLSVC deserves special attention due to the peculiarities of venous return during the operation of the heart-lung machine and formation of the superior vena cava anastomosis.

If a well-developed unnamed vein is present, occlusion of the PLSVC by simple ligation creates sufficient venous drainage through the innominate vein. However, if the innominate vein is small or absent, PLSVC ligation may increase the risk of neurovascular complications [8].

Several surgical techniques during orthotopic heart transplantation can preserve PLSVC. These surgical approaches include end-to-end anastomosis of the left superior vena cava to the donor's right superior vena cava, end-to-end anastomosis of the PLSVC to the right atrial appendage (direct anastomosis or conduit anastomosis) [8–10].

This paper presents a case of orthotopic heart transplantation in a patient with PLSVC. For direct anastomosis of the PLSVC with the SVC stump of the graft, it was decided to use the biatrial heart transplantation technique, which made it possible to preserve, of sufficient length, the donor heart's SVC stump. When laying the anastomosis in the transverse sinus behind the aorta and the pulmonary artery, there were no significant kinks of the anastomosis, which was confirmed by postoperative examination and the absence of clinical symptoms of venous stasis. In this case, the absence of the innominate vein and complete ligation of the PLSVC could lead to irreversible neurovascular complications. This technique excluded the use of artificial conduits due to the sufficient length of the donor heart's SVC.

CONCLUSION

The clinical effect achieved from treatment fully justifies the chosen surgical tactics and allows us to recommend the proposed tactics for treatment of such a rare anomaly.

The authors declare no conflict of interest.

REFERENCES

1. *Zhong YL, Long X-M, Jiang L-Y, He B-F, Lin H, Luo P et al.* Surgical treatment of dextroversion, isolated persistent left superior vena cava draining into the left atrium. *J Card Surg*. 2015; 30 (10): 767–770.
2. *Ruano CA, Marinho-da-Silva A, Donato P.* Congenital thoracic venous anomalies in adults: morphologic MR imaging. *Curr Probl Diagn Radiol*. 2015; 44 (4): 337–345.
3. *Kula S, Cevik A, Sanli C, Pektas A, Tunaoglu FS, Oguz AD et al.* Persistent left superior vena cava: experience of a tertiary health-care center. *Pediatr Int*. 2011; 53 (6): 1066–1069.
4. *Buirski G, Jordan SC, Joffe HS, Wilde P.* Superior vena caval abnormalities: their occurrence rate, associated cardiac abnormalities and angiographic classification in a paediatric population with congenital heart disease. *Clin Radiol*. 1986; 37 (2): 131–138.
5. *Granata A, Andrulli S, Fiorini F, Logias F, Figuera M, Mignani R et al*. Persistent left superior vena cava: what the interventional nephrologist needs to know. *J Vasc Access*. 2009; 10 (3): 207–211.
6. *Goyal SK, Punnam SR, Verma G, Ruberg FL*. Persistent left superior vena cava: a case report and review of literature. *Cardiovasc Ultrasound*. 2008; 6: 50–50.
7. *Dinasarapu CR, Adiga GU, Malik S.* Recurrent cerebral embolism associated with indwelling catheter in the presence of anomalous neck venous structures. *Am J Med Sci*. 2010; 340 (5): 421–423.
8. *Hammon J, Bender HW*. Major anomalies of pulmonary and thoracic systemic veins. *Sabiston DC, Spencer FC, Gibbon JH, editors. Surgery of the chest*. 5th ed. Philadelphia: Saunders; 1990: 1274–96.
9. *Raisky O, Tamisier D, Vouhe PR*. Orthotopic heart transplantation for congenital heart defects: anomalies of the systemic venous return. *Multimed Man Cardiothorac Surg*. 2006 2006:mmcts.2005.001578.
10. *Joo S, Kim GS, Lim JY et al.* Orthotopic cardiac transplantation after inter-caval anastomosis in a patient with hypertrophic cardiomyopathy and persistent left superior vena cava. *Korean J Thorac Cardiovasc Surg*. 2010; 43: 522–524.

The article was submitted to the journal on 2.09.2020

DOI: 10.15825/1995-1191-2020-4-173-182

VERIFIED CHRONIC SEVERE GIANT CELL MYOCARDITIS: AN INEVITABLE CHOICE FOR HEART TRANSPLANTATION

O.V. Blagova[1], Yu.A. Lutokhina[1], D.H. Ainetdinova[1], V.P. Sedov[1], A.N. Volovchenko[1], D.A. Parfenov[1], N.P. Mozheiko[2]

[1] Sechenov University, Moscow, Russian Federation
[2] Shumakov National Medical Research Center of Transplantology and Artificial Organs, Moscow, Russian Federation

Myocarditis has polymorphic clinical manifestations and is one of the main causes of heart transplantation. We present a clinical case of a 43-year-old female patient who was admitted to the clinic with biventricular heart failure (NYHA class 3–4). She periodically noted exacerbations of bronchitis against the background of prolonged smoking. Twenty-one months prior to hospitalization, she first noted a shortness of breath without an obvious connection with the infection. Her ejection fraction (EF) decreased to 34%, pleural and pericardial effusion was revealed. Coronary angiography found no abnormalities. However, MRI showed subendocardial contrasting of the left ventricular (LV) apex. The diagnosis was myocarditis. Within six months, the patient received therapy with 30 mg/day prednisolone and cardiotropic therapy. Her shortness of breath intensified, and the lower extremities swelled. Examination in the clinic showed a sharp decrease in QRS voltage, QS complexes in the V1–V6 leads, dilation of all heart chambers, thrombus in the LV apical aneurysm, 16% EF, 3.9 cm VTI, 454 mmHg dp/dt, and a sharp increase in anticardiac antibody titers (up to 1:320). Endomyocardial biopsy was not performed due to the patient's rapidly deteriorating condition, the need for cardiotonics, and signs of multiple organ failure. She was transferred to Shumakov National Medical Research Center of Transplantology and Artificial Organs, where extracorporeal membrane oxygenation was performed; orthotopic heart transplant was successfully performed. The patient's condition was stable for the next year. Investigation of the explanted heart revealed a picture of giant cell myocarditis. Issues of diagnosis, possibility of a long-term chronic course, as well as methods of treatment of this variant of myocarditis, including the key role of heart transplantation, are discussed.

Keywords: giant cell myocarditis, heart failure, left ventricular aneurysm, anticardiac antibodies, heart transplantation.

INTRODUCTION

Myocarditis is an inflammatory lesion of the myocardium. It has various origins and it is one of the main causes of heart failure in young people, including incurable heart failure and requiring heart transplantation (HT). Unrecognized myocarditis is often what lies behind the diagnosis "dilated cardiomyopathy" (DCM), which competes on equal terms with coronary heart disease (CHD) as a reason for referral to HT, and according to some reports, it is ahead of it [1]. At the same time, myocarditis is a potentially curable disease, and its timely detection can be critically important for patient prognosis.

The main problem of myocarditis diagnosis in clinical practice, including in Russia, is the almost complete inaccessibility of endomyocardial biopsy (EMB), an invasive interventional technique that is often indispensable for verifying myocarditis diagnosis and determining the scope of therapy. European experts, the authors of the first guidelines on myocarditis in 2013, consider EMB to be absolutely necessary in all cases of suspected myocarditis [2]. American experts recommend performing EMB in acute DCM syndrome with intact coronary arteries, inotropic support if necessary, in the presence of 2nd-degree and 3rd-degree AV block, sustained ventricular tachycardia or treatment failure within 1–2 weeks, i.e. if not in all, then in very many cases of suspicion of severe chronic myocarditis [3].

The main advantages that distinguish EMB from all non-invasive techniques (including the best among them – contrast-enhanced magnetic resonance imaging of the heart) are the ability not only to make myocarditis diagnosis reliable, but to determine its morphological type and the presence/absence of a viral genome in the myocardium, which largely determines the treatment [1]. If myocarditis diagnosis (most often lymphocytic) can be made with a high degree of probability based on non-invasive comprehensive examination, including the use of the proposed and tested algorithm [4], then non-invasive diagnosis of rare and prognostically most unfavorable histological variants without biopsy is absolutely impossible.

Corresponding author: Olga Blagova. Address: 6/1, B. Pirogovskaya str., Moscow, 119992, Russian Federation. Phone: (499) 248-62-33. E-mail: blagovao@mail.ru

These variants include, first of all, giant cell myocarditis (GCM), which was described by S. Saltykov in 1905. Its distinctive morphological feature lies in the presence of inflammatory lymphocytic infiltrates, including giant cells and eosinophils, and cardiomyocyte necrosis, but without formation of sarcoid granulomas [4]. The true incidence of this type of myocarditis is unknown due to the difficulties of its in vivo diagnosis; as a rule, only descriptions of individual clinical cases are given. The largest multicenter registries include a few dozen patients, and transplant surgeons are the most likely to have such observations. Each case is unique and presents physicians with the challenge of aggressive diagnosis and therapy, as well as timely determination of indications for HT [5–7].

We present a clinical case of a patient with severe chronic myocarditis, which illustrates the long-term course of unrecognized GCM and the current possibilities of saving the patient's life through surgery quickly even in the end stage of the disease.

CLINICAL CASE

Patient L., female, 43 years old, was admitted to the Vinogradov Faculty Therapeutic Clinic at Sechenov University on November 11, 2019, presenting with general weakness, shortness of breath at minimal exertion, nausea, swelling of the legs and feet, and increased abdominal volume.

From medical history. *Family history of cardiomyopathy is not burdened. The patient is a psychologist by profession, lives in Krasnoyarsk, travels a lot, smokes up to 30 cigarettes a day for a long time, periodically notes exacerbations of bronchitis with prolonged (up to a month) cough, has not taken antibiotics, no other bad habits. Over 20 years ago, post-tuberculous changes were detected in her lungs; X-rays were regularly performed; there were no dynamics, and she did not need any treatment. She had a history of two spontaneous vaginal deliveries (the last one at the age of 39), there were no heart complications. Until 2018, she considered herself healthy. In February, she felt unwell, difficulty breathing without apparent fever, and regarded it as another exacerbation of bronchitis. For 2 weeks, while on vacation, she noted a decrease in tolerance of previously habitual physical activities. In March 2018, she for the first time noted the emergence of severe shortness of breath, cough, a feeling of lack of air, mainly at night, and progressive weakness. She consulted cardiologists on an outpatient basis, no adequate examination and treatment was carried out.*

In April, due to further deterioration in her health, the ambulance team took her to the hospital, where she was hospitalized. Initially, her condition was treated as pneumonia. However, her ever-first EchoCG revealed a decreased ejection fraction (EF) to 34% or less, diffuse left ventricular (LV) hypokinesis, mitral regurgitation grade 3, increased pulmonary artery systolic pressure (PASP) to 54 mm Hg., pleural and pericardial effusion. Coronarography showed no abnormalities. MRI revealed delayed gadolinium accumulation mainly in the LV apex; there was no evidence of thrombosis. The condition was regarded as myocarditis; therapy with oral prednisolone was administered per os 30 mg/day for 6 months (there were no recommendations on the duration of treatment), torsemide, beta-blockers and angiotensin-converting enzyme (ACE) inhibitors. Against this background, she noted decreased shortness of breath. According to EchoCG from April and June 2018, EF was 37–39%. However, cushingoid manifestations appeared (visceral obesity, "moon-shaped face", "hump"), she on her own gradually withdrew prednisone. Outpatient examinations revealed elevated cytomegalovirus (CMV) IgG antibody titers, and other herpetic viruses were detected.

In February 2019, she noted a deterioration in her health in the form of increased shortness of breath and increasing general weakness. The condition was regarded as DCM. Ivabradine 10 mg/day, sacubitril-valsartan 200 mg/day (withdrawn due to episodes of blood pressure dropping to 60/30 mmHg), digoxin 0.125 mg/day, torsemide 20 mg/day, nicorandil 20 mg/day, eplerenone 50 mg/day were administered. Despite feeling unwell, she went on vacation three times a year, tolerated the trips relatively satisfactorily, and attempted unconventional remedies. In October 2019, she noted renewed dyspnea with minimal physical exertion, a constant feeling of shortness of breath and nausea, increasing edema of the legs and feet. An EchoCG test performed on October 22, 2019 revealed LV apex aneurysm, EF did not exceed 18–20%. The patient was hospitalized for further examination and treatment.

On admission, *her condition was severe. Height 180 cm, weight 76 kg, BMI = 23.46 kg/m^2. Body temperature 36.50 °C. Her skin was moderately pale with normal moisture. Moderate swelling of the legs, feet, thighs. Respiratory rate (RR) 20/minutes, hard breathing, $SatO_2$ 95%. In the lungs, breathing was vesicular in all parts of the lungs, there was no wheezing. Dull heart sounds, systolic murmur at the apex. Heart rate 84/min, correct rhythm, blood pressure 70/40 mm Hg. The abdomen was somewhat tense, painless, moderately enlarged due to ascites. The liver and spleen were not enlarged.*

Blood tests showed *slight leukocytosis (10.9 × 10^9/L, lymphocytes 33.3%, neutrophils 53.2%, eosinophils 2.3%), Hb 156 g/L, platelets 273 × 10^9/L, ESR 5 mm/hour, minimal increase in AST (49 U/L), total bilirubin (27.3 μmol/L) due to direct bilirubin (11.2 μmol/L), normal albumin (35 g/L), creatinine (103.3 μmol/L), lipids, electrolytes, hyperuricemia (606 μmol/l). Blood group AB (IV), Rh factor positive.* ***Urine tests*** *showed decreased specific gravity (1010), urobilinogen 3+.*

ECG *(Fig. 1) revealed a sharp decrease in QRS voltage in standard leads and almost complete absence of R*

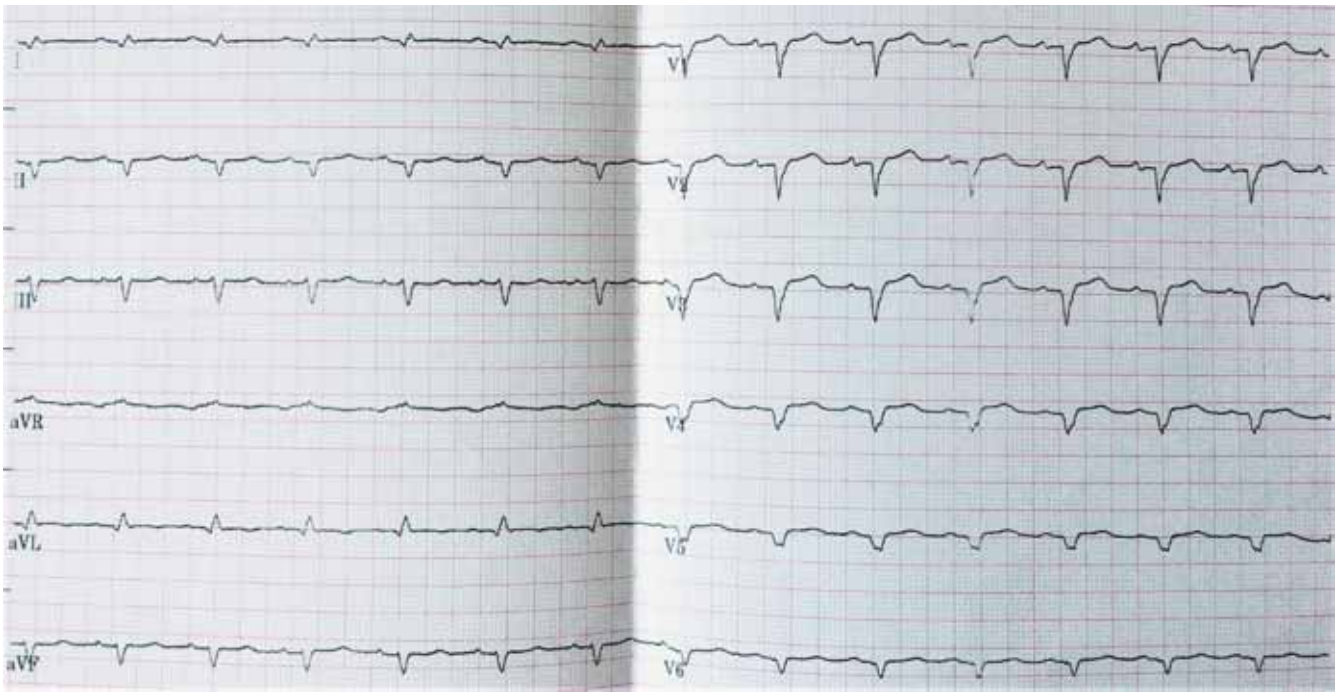

Fig. 1. Patient's ECG upon admission at the hospital. Recording speed 25 mm/s. Sinus rhythm, sharp decrease in QRS voltage in standard leads, QS complexes in the V1–V6 leads, minimum R waves in the II, III, aVF leads, QRS duration 120 ms, PQ 190 ms

waves (QS complexes in V1–V6 leads, minimal R in leads II, III, aVF); QRS lasted for 120 ms, PQ 190 ms, which indicated a pronounced decrease in viable myocardial volume. Holter ECG monitoring revealed no significant ventricular arrhythmias.

***EchoCG** (Fig. 2) confirmed expansion of all heart chambers (LV end-diastolic diameter 6.2 cm, end-diastolic volume 155 mL, end-systolic volume 129 mL, left atrium 4.4 cm, 87 mL, right atrium 103 mL, right ventricle 3.5 cm), LV apex aneurysm lined with thrombus (3.3 × 1.2 cm), a sharp decrease in LV contractility (EF not exceeding 16%, VTI 3.9 cm, dp/dt 454 mm Hg), impaired LV diastolic function according to the pseudonormal type (E/A = 1.17, E/Em 9.2 at the norm <8) in the absence of hypertrophy of its walls (interventricular septal thickness 8 mm, posterior wall thickness 9 mm), mitral and tricuspid regurgitation grade 3, pulmonary hypertension (PASP 45 mmHg), small amount of fluid in the pericardial cavity (posterior wall 1.2 cm, lateral wall 0.7 cm, front wall 0.4 cm, in the right atrium 0.7 cm).*

***Chest X-ray** showed an enlarged heart, a calcified focus with 7 mm in diameter in the right lung, no effusion in the pleural cavities. **Ultrasound** confirmed the presence of free fluid in all parts of the abdominal cavity, the liver at the upper limit of the norm.*

*An **MRI** conducted in May 2018 showed no signs of non-compact myocardium, a scar in the LV apex is clearly defined, no blood clots. Cardiac MRI could not be repeated due to the deterioration of the patient's condition.*

So, there was no doubt about severe myocardial injury with the development of DCM syndrome and biventricular heart failure. But the nature of the lesion was not completely clear. Emergence of dyspnea more than 2 years after her second birth did not allow us to speak of peripartum cardiomyopathy, although we could not completely rule out delayed decompensation of primary (genetically determined) cardiomyopathy. Regular exacerbations of chronic bronchitis and not quite distinct connection of the onset of the disease and one of the exacerbations of chronic bronchitis, as well as a winter trip to India, could become a background (trigger) for myocarditis development. Taking into account the severity of decompensation in April 2018 with clinical of anginal pain, severe dyspnea, ECG (QS complexes in all chest leads), EchoCG (LV apical akinesis and thrombus), and MRI (subendocardial contrasting of the apex over 50% of myocardial thickness), infarct-like debut of severe myocarditis with its subsequent chronicity seemed to be the most likely.

Myocarditis was also supported by a clear positive response to medium-dose prednisolone therapy (clinical and echocardiographic) in the anamnesis. However, insufficient improvement and rapid loss of effect could indicate insufficient monotherapy doses, a particular myocarditis severity, its viral nature, and the presence of an initial genetic myocardial disorder. For the first time, blood tests for anti-cardiac antibodies revealed a concomitant sharp increase in antibody titers to most heart antigens, including cardiomyocyte antigens (Table), which indicated in favor of a highly immune component

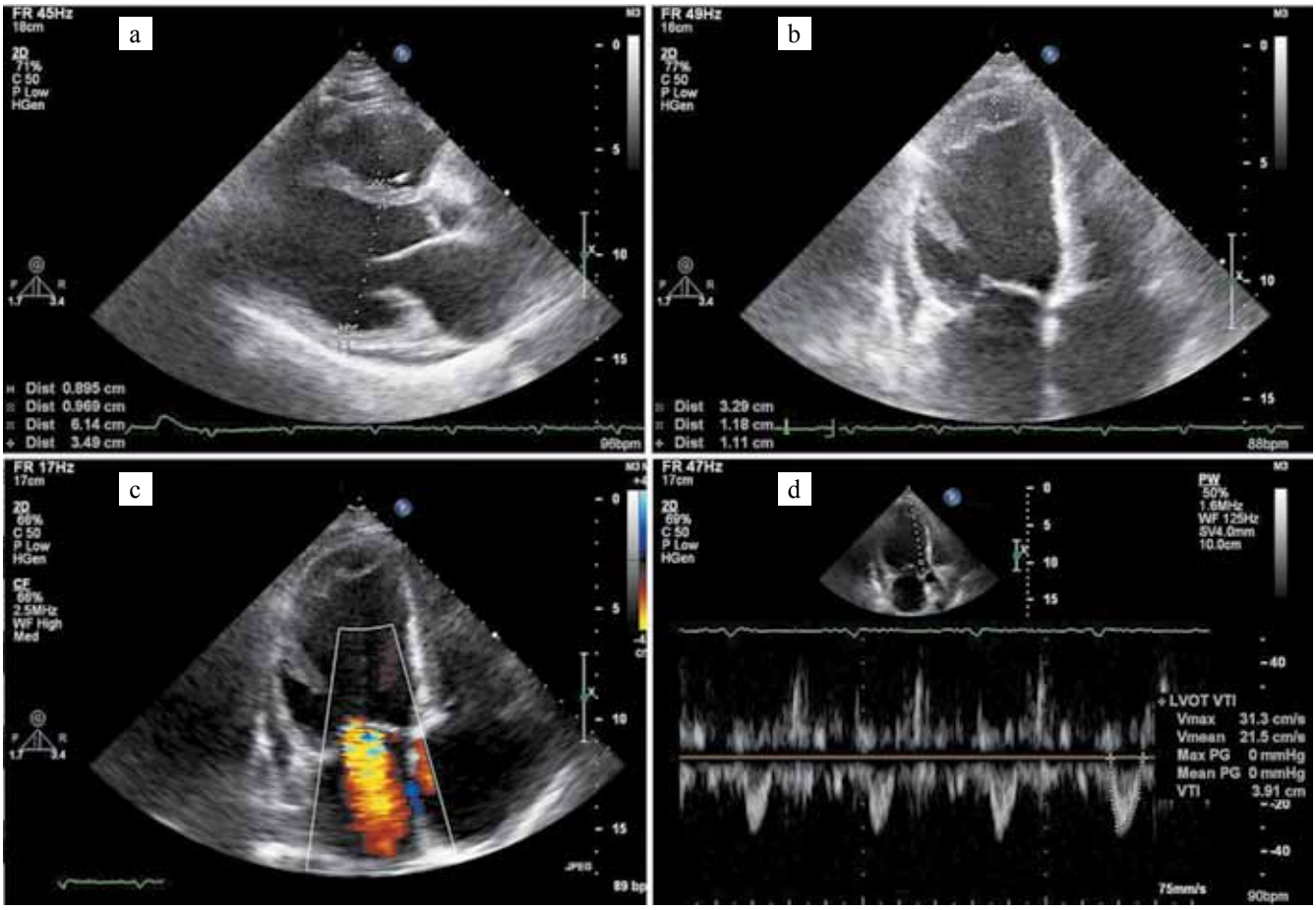

Fig. 2. Patient's ECG upon admission at the hospital. a) two-chamber position, increase in the size of the left and right ventricles; b) four-chamber position underlying thrombus in the left ventricular apical aneurysm; c) color flow Doppler, flow of grade 3 mitral regurgitation (up to the left atrial roof); d) low cardiac output syndrome (sharp decrease in VTI)

of myocarditis. However, this did not allow to completely rule out active viral infection in the myocardium or determine the extent of immunosuppressive therapy.

The only study that could have answered the question about further drug treatment tactics is EMB. However, the severity of the patient's condition increased the risk of this study and made the prospects for baseline therapy for myocarditis questionable, especially given the age of the disease. Despite the high likelihood of active myocarditis, the time for its treatment was obviously missed, the only way to avoid an unfavorable outcome seemed to be HT.

Table

Titers of various anti-heart antibodies in the blood

Indicator	Result	Norm
Antibodies to cardiomyocyte nuclear antigens	none	none
Antibodies to endothelial antigens	1:40	1:40 antibody titer
Antibodies to cardiomyocyte antigens	1:320	1:40 antibody titer
Antibodies to smooth muscle antigens	1:320	1:40 antibody titer
Antibodies to antigens of fibers of the cardiac conduction system	1:160	1:40 antibody titer

Despite attempts at complex cardiotropic therapy (enoxaparin, furosemide, eplerenone), the patient's condition did not improve during her stay in the clinic. Due to pronounced oliguria (100–150 mL of urine for two days) against the background of persistent hypotension (80/60 mmHg or less), which persisted despite complete discontinuation of bisoprolol, she was transferred to the intensive care unit, where, as a result of constant infusion of low doses of dopamine and administration of lasix 240 mg/day resulted in positive diuresis (3900 mL per day) with some reduction in dyspnea. However, diuresis decreased to 700 mL again after dopamine withdrawal and lasix infusion continuation. EchoCG (on November 18, 2019) showed no positive dynamics (EF less than 20%, VTI 3 cm, severe valve regurgitation).

Infusion of dobutamine, lasix and potassium chloride (due to progressive hypokalemia) was resumed, followed by addition of norepinephrine. However, hypotension, oliguria persisted, nausea and vomiting appeared (regarded as a manifestation of ischemic hepatitis); there was an increase in the level of liver enzymes (by November 22, the AST level was 826 IU/L, ALT – 678 U/L). Asym-

Fig. 3. Patient's ECG in the intensive care unit. Bedside monitor recording, speed 25 mm/s. An episode of nonsustained ventricular tachycardia

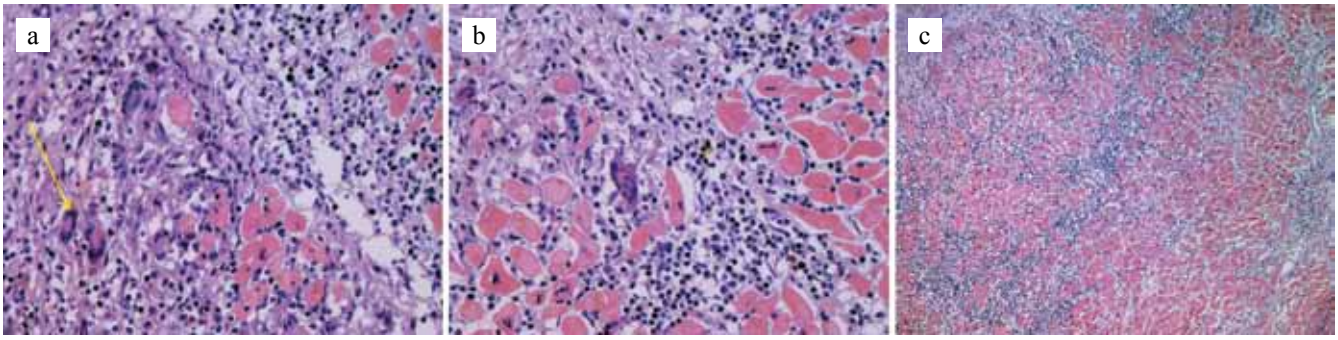

Fig. 4. Results of morphological examination of the explanted heart. a) giant multinucleated cells among diffuse inflammatory infiltration in loose fibrous connective tissue in the interstitium and between cardiomyocytes; b) giant multinucleated cell among diffuse inflammatory infiltration in loose fibrous connective tissue in the interstitium and between cardiomyocytes; c) diffuse focal mononuclear inflammatory infiltration in the edematous interstitium and in sclerosis zones; among inflammatory cells there are multinucleated giant cells. H&E stain. 200× (a, b), 100× (c) microscope magnification

ptomatic episodes of unstable ventricular tachycardia were recorded on the monitor screen (Fig. 3).

*Multi-slice computed tomography (**MSCT**) of the brain and abdominal organs revealed no volumetric lesions; thoracic examination revealed a group of calcified foci, a zone of severe fibrosis, and pleural adhesions in the upper lobe of the right lung. There was emergency consultation with a phthisiatrician: residual changes after spontaneously healed tuberculosis of the upper lobe of the right lung. Performing HT was not contraindicated. When prescribing immunosuppressive therapy, it was rational to administer a course of preventive chemotherapy with isoniazid (0.6/day) against the background of vitamin B_6 (0.06/day) and pyrazinamide 1.5/day.*

After consultation at the Shumakov National Medical Research Center of Transplantology and Artificial Organs with clinical diagnosis of DCM of unspecified genesis, she was on November 22, 2019 transferred to the intensive care unit of the Center, where extracorporeal membrane oxygenation (ECMO) was immediately initiated. Clinical picture at the time of transfer: myocardial infarction (necrosis) of the anterior apical localization of April 2018. Chronic infectious-immune (viral-immune?) myopericarditis, severe course, high degree of immunological activity, in the acute phase? Left ventricular apex thrombosis. Low ejection syndrome. Arrhythmia: ventricular extrasystole, unstable ventricular tachycardia. Relative mitral and tricuspid insufficiency grade 3. Moderate pulmonary hypertension. Chronic heart failure, NYHA FC 3–4, stage IIB: peripheral edema, bilateral hydrothorax, ascites. Acute ischemic hepatitis. CKD stage 3b. Hyperuricemia. Chronic bronchitis without exacerbation. Post-tuberculous changes in the right lung.

Orthotopic HT was performed on the first day of stay at the Shumakov National Medical Research Center of Transplantology and Artificial Organs (on the night of November 23, 2019). Morphological examination of the explanted heart revealed highly active giant cell myocarditis (Fig. 4). During the following year, the patient's condition remained stable, there were no signs of graft rejection.

DISCUSSION

The presented case demonstrates a number of peculiarities of the course and management of myocarditis in general (and GCM, in particular), the analysis of which seems to be very instructive for the entire team of doctors handling such patients.

The debut of the disease and the diagnosis of myocarditis during that period deserve discussion. The following were the clinical grounds for the diagnosis of myocarditis in March 2018: highly probable association with a respiratory infection (another exacerbation of chronic bronchitis, rapid development of severe myocardial dysfunction with increasing dyspnea, ECG changes that were retrospectively (but not at the first visit to the doctor) considered as infarction-like and became one of the grounds for immediate hospitalization. At the same time, there were no data on troponin levels in the blood during that period, no thrombus was detected (including by MRI) in the LV.

Given the complete absence of CHD risk factors, diagnosis of myocardial infarction was rejected at the place of residence (which was also confirmed by normal coronarograms), although the development of infarction with unchanged coronary arteries (so-called MINOCA) could be discussed. MRI findings indirectly confirmed the diagnosis of myocarditis; there were no other possibilities (EMB, determination of the anti-cardiac antibody levels).

With an infarct-like onset of myocarditis, there are several possible courses – quite favorable, typical for young patients, easily diagnosed without the use of EMB, does not lead to a significant drop in LV contractility even in an acute period, does not leave irreversible consequences and is not prone to chronicity and is completely different, having a particularly severe course from the very beginning, with a diffuse drop in contractility and a persistent EF decrease [8], as it happened in our patient. In severe infarct-like onset of myocarditis, along with "banal" lymphocytic myocarditis, several special nosological forms should be considered, namely eosinophilic myocarditis, myocarditis within sarcoidosis, systemic vasculitis (eosinophilic granulomatosis with polyangiitis), and in this series – GCM. However, with GCM, this type of opening is described only in 6–9% of cases [9, 10]. Even less common are LV aneurysms [11], which are considered more characteristic of sarcoidosis and are characterized by high arrhythmogenicity (which was not the case in our case). Thrombus formation in the LV indicates a particular severity of inflammation with necrosis and endocardial involvement. In our case, delayed thrombus formation is likely to reflect a prolonged inflammatory process that remains highly active.

In any variant of myocarditis, the development of persistent cicatricial changes is an unfavorable prognostic factor, which in most cases does not allow counting on a persistent improvement in LV function as an outcome of immunosuppressive therapy (IST) [12]. In the absence of EMB data, several treatment options could be considered – only cardiotropic therapy (which had been used for some time, but did not give sufficient effect); immediate referral to HT (which is practiced in such patients, but cannot be considered optimal tactics in the absence of an accurate diagnosis); implantation of artificial LV in order to buy time and wait for the possible effect of drug treatment (hardly feasible); and, finally, use of IST (in fact, ex juvantibus therapy), which has been undertaken.

This tactic is at variance with the recommendations by European experts, but consistent with Russian realities. In many cases, such treatment gives the desired effect, since lymphocytic myocarditis is the most common option, and among about half of virus-positive cases, myocarditis (associated not with herpes or enteroviruses, but with parvovirus B19, whose impact on IST prognosis and effectiveness remains unclear) predominates. In our case, administration (essentially uncontrolled) of medium-dose prednisolone gave only short-term and insufficient clinical improvement. Further treatment tactics could not be determined without EMB.

Its implementation was one of the main objectives of hospitalization; however, upon admission it became obvious that the degree of myocardial dysfunction had reached a critical level. Diagnosis of highly immune myocarditis remained the most likely, especially based on the results of a blood test for anti-cardiac antibodies. EMB was not possible due to the patient's constant need for cardiotonic support and an increased risk of complications from the procedure. Thus, the decision to carry out immediate HT was the only possible one; retrospective GCM diagnostics confirmed the correctness of rejection from further attempts to verify the diagnosis and IST at this end stage.

Naturally, the question arises whether a timely EMB and GCM diagnostics at the onset of the disease with administration of an adequate IST could change the prognosis and allow avoiding HT or performing it in a less urgent mode. GCM is one of the rarest and probably the most malignant forms of myocarditis. The registry of the Shumakov National Medical Research Center of Transplantology and Artificial Organs contains only four cases of GCM [13]. One of the first multicenter studies of GCM included only 63 cases, patients' mean age was 43 years, men and women had the disease equally often [8]. The only transplant center in Finland with HT facilities has experience diagnosing 46 cases of GCM from 1991 to 2015, with rates increasing significantly every five years; women were twice as likely to have the disease, with a mean age of 51 years [9].

GCM is considered to be an idiopathic autoimmune variant of myocarditis, although virus-positive cases have also been described, e.g. fatal GCM induced by cytomegalovirus infection [12]. In our patient, GCM may have been supported by maximal anti-cardiac antibody titers (despite IST performed a year ago), but this sign is not absolutely specific for GCM, it only suggests the potential benefit of aggressive IST. GCM may indicate the presence of other autoimmune diseases, which are associated with GCM in 15–19% of cases [4, 8, 9] – primarily thymomas with the development of myasthenia gravis, which is characterized by the appearance of antibodies to a wide range of muscle antigens (to acetylcholine receptors, titin, myosin, smooth muscles, [14]), as well as ulcerative colitis, rheumatoid arthritis, polymyositis, Graves' disease, lymphoma, etc. The high activity of the disease with massive myocardial injury explains the high sensitivity of MRI (100%) and positron emission tomography (93%) [9]. However, there is no visual pattern specific to GCM.

The optimal extent of IST in the treatment of GCM has not been determined, although there is no doubt about its feasibility – GCM is one of the few myocarditis options for which IST is definitely recommended [2]. European and American experts also agree that GCM requires a more aggressive IST than other myocarditis options.

Over 20 years ago, an international GCM study group recommended the use of a 3-component combination (prednisolone, azathioprine and cyclosporine), although HT remained the method of choice [8]. Taking into account the importance of T cells in the pathogenesis of GCM, the use of muromonab-CD3 and antithymocyte globulin in addition to cyclosporine is being developed [15]. Attempts are being made to use cytostatics and bioactive drugs (methotrexate, mycophenolate mofetil, sirolimus, tacrolimus, rituximab, basiliximab, [16]), many of which are also used in transplantology.

However, according to various data, adverse outcomes (death and/or HT) can be avoided only in 11–42% of cases, depending on the extent of IST [4]. In a 1997 study, there were 89% adverse outcomes (with a mean time of just 5.5 months from symptom development) [8]. A five-year graft-free survival of 42% in a recent Finnish study was achieved with combined IST (70% of patients), ICD implantation in 57%, and was associated with less necrosis and fibrosis on EMB, as well as baseline troponin levels (also reflecting the severity of necrosis) of <85 ng/L and a positive response to treatment – an increase in EF by 5% or more, a decrease in NT-proBNP levels by 1000 ng/L or more [9].

Unusual for GCM is the prolonged chronic course with periods of improvement observed in our patient. In typical cases, GCM proceeds as fulminant, i.e. it requires intensive cardiotonic and respiratory support already in the acute period [5]. Its most common manifestations are acute heart failure, ventricular arrhythmias, blockages, and cardiogenic shock. Most often, it is in the acute period of GCM that the use of mechanical circulatory support is required, including ECMO, which is one of the most effective technologies for GCM. In the French intercenter register of fulminant GCM, it was applied in 85% of cases and ended with HT in 8 out of 11 patients; in 87% of fulminant GCM cases, HT or death was not avoided. However, EMB and IST were performed in a smaller proportion of patients, which brings this register closer to our observation [17]. We should refer to the experience of E. Ammirati from Milan, who conducts EMB even in patients on ECMO and total anticoagulation, understanding the critical importance of accurate GCM diagnosis for determining further treatment tactics [4].

Our patient required ECMO only in the end stage of the disease as a bridge to successful HT, which reflects a more favorable course of her GCM for almost two years. Regarding the possibility of a long course of GCM, it is worth noting the encouraging results obtained in a recent multicenter study, which included 26 patients with GCM. After 1 year, the 5-year survival rate without transplantation was 72%, the maximum period reached 20 years. However, the work does not contain information about patients who died or underwent HT in the first year of the disease [5]. In any case, it can be judged that the successful experience of the first year is a favorable prognostic sign. Cases of more than 10-year course of GCM with maintenance of EF at 30–35% level through cardiotropic therapy and IST, but still HT in the outcome of the disease have been described [18]. With timely diagnosis of GCM and adequate IST, one could hope for a similar variant of the course in our patient.

The special significance of GCM in the practice of transplantologists depends on the possibility of its recurrence in a transplanted heart (which once again proves its autoimmune nature). The relapse rate in 1997 was 26%. In 1 case out of 9, GCM recurrence resulted in death [9]. Probably, no other myocardial disease has such a malignant course. At the same time, improvement in IST protocols after HT, including in patients with GCM, has led to significant decrease in the number of relapses. Thus, in the French registry (the results were published in 2018), not a single case of GCM development in the transplanted heart was reported [18, 19]. An increased risk of acute rejection has also been reported in patients with GCM compared with DCM (16% vs 5%, $p = 0.021$), but 1.5 and 10-year survival rates do not differ from those for other HT reasons (94%, 82% and 68%, respectively) [20].

Our patient showed no signs of GCM rejection or recurrence by the end of the first year.

CONCLUSION

Giant cell myocarditis is one of the rarest and most severe forms of myocarditis that cannot be definitely diagnosed by any method (including MRI) other than endomyocardial biopsy. Acute development of severe heart failure, up to cardiogenic shock, is typical for GCM. Auxiliary blood circulation is often required in the first days of the disease; much less typical is the infarction-like debut with aneurysm formation, noted in the presented case. Its feature was a weak and short-lived, but distinct positive response to monotherapy with medium doses of prednisolone, which are usually completely insufficient for GCM treatment, and a long (almost two years) relatively favorable course of the disease. The particular severity of myocarditis and the need for aggressive immunosuppression could be indicated by sharply increased titers of anti-cardiac antibodies. However, the time for performing EMB and conducting an adequate IST was missed, which made HT the only reasonable and possible way out. The severity of the patient's condition at the time of transfer to the Shumakov National Medical Research Center of Transplantology and Artificial Organs made it necessary to immediately connect ECMO and perform urgent HT on the first day of hospitalization. Despite the risk of recurrence in the transplanted heart, HT remains the treatment of choice for the majority of patients diagnosed with GCM both preoperatively and retrospectively.

The authors declare no conflict of interest.

REFERENCES

1. *Gautier SV, Poptsov VN, Koloskova NN, Zakharevich VM, Shevchenko AO, Muminov II et al*. Heart transplantation waiting list of V.I. Shumakov National Medical Research Center of Transplantology and Artificial Organs. Trends from 2010 to 2017. *Russian Journal of Transplantology and Artificial Organs*. 2018; 20 (4): 8–13. [In Russ., English abstract]. doi.org/10.15825/1995-1191-2018-4-8-13.
2. *Caforio AL, Pankuweit S, Arbustini E et al*. European Society of Cardiology Working Group on Myocardial and Pericardial Diseases. Current state of knowledge on aetiology, diagnosis, management, and therapy of myocarditis: a position statement of the European Society of Cardiology Working Group on Myocardial and Pericardial Diseases. *Eur Heart J*. 2013; 34 (33): 2636–2648, 2648a–2648d. doi: 10.1093/eurheartj/eht210.
3. *Bozkurt B, Colvin M, Cook J, Cooper LT, Deswal A, Fonarow GC et al*. American Heart Association Committee on Heart Failure and Transplantation of the Council on Clinical Cardiology; Council on Cardiovascular Disease in the Young; Council on Cardiovascular and Stroke Nursing; Council on Epidemiology and Prevention; and Council on Quality of Care and Outcomes Research. Current Diagnostic and Treatment Strategies for Specific Dilated Cardiomyopathies: A Scientific Statement From the American Heart Association. *Circulation*. 2016; 134 (23): e579–e646. PMID: 27832612, doi: 10.1161/CIR.0000000000000455.
4. *Blagova OV, Osipova YV, Nedostup AV, Kogan EA, Sulimov VA*. Clinical, laboratory and instrumental criteria for myocarditis, established in comparison with myocardial biopsy: A non-invasive diagnostic algorithm. *Ter Arkh.* 2017; 89 (9): 30–40. [In Russ., English abstract]. doi: 10.17116/terarkh201789930-40.
5. *Ammirati E, Camici PG*. Still poor prognosis for patients with giant cell myocarditis in the era of temporary mechanical circulatory supports. *Int J Cardiol*. 2018; 253: 122–123. doi: 10.1016/j.ijcard.2017.10.124.
6. *Maleszewski JJ, Orellana VM, Hodge DO, Kuhl U, Schultheiss HP, Cooper LT.* Long-term risk of recurrence, morbidity and mortality in giant cell myocarditis. *Am J Cardiol*. 2015 Jun 15; 115 (12): 1733–1738. doi: 10.1016/j.amjcard.2015.03.023.
7. *Elamm CA, Al-Kindi SG, Bianco CM, Dhakal BP, Oliveira GH*. Heart Transplantation in Giant Cell Myocarditis: Analysis of the United Network for Organ Sharing Registry. *J Card Fail*. 2017; 23 (7): 566–569. doi: 10.1016/j.cardfail.2017.04.015.
8. *Blagova OV, Nedostup AV*. Contemporary masks of the myocarditis (from clinical signs to diagnosis). *Russian Journal of Cardiology*. 2014; (5): 13–22. [In Russ., English abstract]. doi.org/10.15829/1560-4071-2014-5-13-22.
9. *Cooper LT Jr, Berry GJ, Shabetai R*. Idiopathic giant-cell myocarditis – natural history and treatment. Multicenter Giant Cell Myocarditis Study Group Investigators. *N Engl J Med*. 1997; 336 (26): 1860–1866. doi: 10.1056/NEJM199706263362603.
10. *Ekström K, Lehtonen J, Kandolin R, Räisänen-Sokolowski A, Salmenkivi K, Kupari M*. Long-term outcome and its predictors in giant cell myocarditis. *Eur J Heart Fail*. 2016, 18: 1452–1458. doi: 10.1002/ejhf.606.
11. *Ammirati E, Roghi A, Oliva F, Turazza FM, Frigerio M, Pedrotti P*. Ventricular aneurysm as a complication of giant cell myocarditis. [Article in Italian]. *G Ital Cardiol (Rome)*. 2015; 16 (6): 389–390. doi: 10.1714/1934.21040.
12. *Blagova OV, Nedostup AV, Kogan EA, Sedov VP, Donnikov AE, Kadochnikova VV et al*. DCMP as a clinical syndrome: results of nosological diagnostics with myocardial biopsy and differentiated treatment in virus-positive and virus-negative patients. *Russian Journal of Cardiology*. 2016; 21 (1): 7–19. [In Russ., English abstract]. doi.org/10.15829/1560-4071-2016-1-7-19.
13. *Gautier SV, Shevchenko AO, Kormer AYa, Poptsov VN, Saitgareev RSh, Shumakov DV, Zakharevich VM*. Three decades of heart transplantation in the Shumakov center: long-term outcomes. *Vestnik transplantologii i iskusstvennyh organov*. 2015; XVII (2): 70–73. doi.org/10.15825/1995-1191-2018-4-8-13.
14. *Gkouziouta A, Miliopoulos D, Karavolias G, Lazaros G, Kaklamanis L, Kelepeshis G et al*. Acute cytomegalovirus infection triggering fatal giant cell myocarditis. *Int J Cardiol*. 2016; 214: 204–206. doi: 10.1016/j.ijcard.2016.03.202.
15. *Zhou Z, Chen X, Liu G, Pu J, Wu J*. Presence of Multiple Autoimmune Antibodies Involved in Concurrent Myositis and Myocarditis and Myasthenia Gravis Without Thymoma: A Case Report. *Front Neurol*. 2019; 10: 770. doi: 10.3389/fneur.2019.00770.
16. *Suarez-Barrientos A, Wong J, Bell A, Lyster H, Karagiannis G, Banner NR*. Usefulness of Rabbit Anti-thymocyte Globulin in Patients With Giant Cell Myocarditis. *Am J Cardiol*. 2015; 116 (3): 447–451. doi: 10.1016/j.amjcard.2015.04.040.
17. *Patel AD, Lowes B, Chamsi-Pasha MA, Radio SJ, Hyden M, Zolty R*. Sirolimus for Recurrent Giant Cell Myocarditis After Heart Transplantation: A Unique Therapeutic Strategy. *Am J Ther*. 2019; 26 (5): 600–603. doi: 10.1097/MJT.0000000000000796.
18. *Shevchenko AO, Nikitina EA, Koloskova NN, Shevchenko OP, Gautier SV*. Controlled arterial hypertension and adverse event free survival rate in heart recipients. *Cardiovascular therapy and prevention*. 2018; 17 (4): 4–11. doi: 10.15829/1728-8800-2018-4-4-11.
19. *Montero S, Aissaoui N, Tadié JM, Bizouarn P, Scherrer V, Persichini R et al*. Fulminant giant-cell myocarditis on mechanical circulatory support: Management and outcomes of a French multicentre cohort. *Int J Cardiol*. 2018; 253: 105–112. doi: 10.1016/j.ijcard.2017.10.053.
20. *Fallon JM, Parker AM, Dunn SP, Kennedy JLW*. A giant mystery in giant cell myocarditis: navigating diagnosis, immunosuppression, and mechanical circulatory support. *ESC Heart Fail*. 2020; 7 (1): 315–319. doi: 10.1002/ehf2.12564.
21. *Elamm CA, Al-Kindi SG, Bianco CM, Dhakal BP, Oliveira GH*. Heart Transplantation in Giant Cell Myocarditis: Analysis of the United Network for Organ Sharing Registry. *J Card Fail*. 2017; 23 (7): 566–569. doi: 10.1016/j.cardfail.2017.04.015.

The article was submitted to the journal on 1.10.2020

DOI: 10.15825/1995-1191-2020-4-183-191

SUCCESSFUL TREATMENT OF VANISHING BRONCHUS INTERMEDIUS SYNDROME FOLLOWING LUNG TRANSPLANTATION

I.V. Pashkov[1], M.T. Bekov[1], R.A. Latypov[1], D.O. Oleshkevich[1], E.F. Shigaev[1], E.V. Lebedev[1], K.S. Smirnov[1], S.V. Gautier[1, 2]

[1] Shumakov National Medical Research Center of Transplantology and Artificial Organs, Moscow, Russian Federation

[2] Sechenov University, Moscow, Russian Federation

The vanishing bronchus intermedius syndrome is a type of peripheral bronchial stenosis that develops in lung recipients within two to nine months after transplantation. Lack of timely diagnosis and effective treatment leads to increased mortality and poor quality of life. The clinical case presented demonstrates the successful long-term treatment of vanishing bronchus intermedius syndrome in a lung recipient using interventional bronchoscopy.

Keywords: lung transplantation, cystic fibrosis, bronchial stenosis, vanishing bronchus intermedius syndrome.

INTRODUCTION

According to leading transplant centers, bronchial complications following a lung transplantation develop in 2–18% of cases [1–8]. Among the complications, the most common is bronchial stenosis, whose frequency varies from 1.4 to 32% [9, 10], which undoubtedly demonstrates a high interest in methods aimed at timely diagnosis and correction.

Bronchial stenosis most often develops within 2–9 months after surgery, but sometimes they can be diagnosed even several years after transplantation [11]. According to the International Society for Heart and Lung Transplantation, bronchial stenosis in the lung graft is divided into central and peripheral. Central bronchial stenosis is located at the bronchial anastomosis or within 2 cm of the anastomosis, while peripheral is at a distance of more than 2 cm from the suture line, in the proximal direction [5].

Bronchus intermedius stenosis is one of the varieties of peripheral stenosis, which is observed in 2–5% of donor lung transplant cases. A condition characterized by a recurrent course due to the absence of a long-term effect of treatment, resulting in intermedius bronchus atresia, is called the vanishing bronchus intermedius syndrome (VBIS) [5, 12–14]. According to S. Shah et al., the mean survival of lung recipients after VBIS diagnosis is about 25.3 months [15]. According to S. Murthy et al, recurrent stenosis after endoscopic correction occurs in 35% of cases, and with repeated intervention can reach up to 70% [3].

Due to the emergence of new transplant centers in Russia and the dynamic development of lung transplantation programs in leading clinics, the VBIS has become undoubtedly a pressing issue, which makes it necessary to systematize the accumulated experience and demonstrate cases of effective treatment. The paper describes a case of successful long-term treatment of recurrent bronchus intermedius stenosis (vanishing bronchus intermedius syndrome), which developed 2 months after lung transplantation, using multimodal interventional bronchology methods.

CLINICAL CASE

In September 2017, a woman born in 1988 (29 years old) was referred to the Shumakov National Medical Research Center of Transplantology and Artificial Organs in Moscow. Her diagnosis was cystic fibrosis (F508del/F508del/3272-16T>A), mixed form, severe course. Chronic suppurative obstructive bronchitis. Diffuse bronchiectasis. Diffuse pneumosclerosis. Type 3 respiratory failure. Chronic pancreatitis. Polypoid rhinosinusitis with nasal polyps, grade 2 – for examination to clarify the indications and exclude contraindications for lung transplantation.

From the patient's medical history, frequent episodes of respiratory diseases were known from early childhood. Cystic fibrosis was diagnosed at the age of 14. Since that time, chronic respiratory infection with Pseudomonas aeruginosa has been diagnosed. In 2005 and 2012, the patient gave birth to two healthy children. Since 2009, chronic respiratory infection with the Burkholderia cepacia complex has been diagnosed. In the period from 2016 to 2017, there was a sharp deterioration in the condition, in the form of progression of respiratory failure phenomena with a need for constant oxygen insufflation (up to 3–4 L/min flow).

Corresponding author: Robert Latypov. Address: 1, Shcukinskaya str., Moscow, 123182, Russian Federation. Phone: (968) 819-27-09. E-mail: livertranspl@gmail.com

Examination results confirmed the lung injury to be in its end stage. Chest CT scan revealed a bullous-cystic transformation of both lungs with multiple bronchiectasis. Assessment of external respiratory function (ERF) showed: vital capacity (VC) – 1.77 L (47%), forced expiratory volume (FEV_1) – 0.66 (21%), Tiffeneau-Pinelli index – 37.2. Analysis of arterial blood gas composition showed pronounced hypoxemia stage 2–3: pO_2 – 42 mm Hg, pCO_2 – 65 mm Hg. Microbiological analysis of sputum culture revealed a multidrug-resistant Burkholderia cepacia complex. Due to the progressive course of the underlying disease, lack of other effective treatment methods and futility of further conservative therapy, the patient was in September 2017 waitlisted for a deceased-donor lung transplantation. The waiting time for an organ from a deceased donor was 12 months.

On October 2, 2018, bilateral sequential lung transplantation was performed without the use of artificial circulation techniques.

The donor was a 38-year-old woman diagnosed with brain death as a result of acute hemorrhagic cerebral circulation disorder. Brain death was established on the basis of the current legislation (order No. 908n of the Ministry of Health of the Russian Federation, dated December 25, 2014). The donor's lungs were under artificial ventilation for 24 hours; blood gas composition (100% oxygen fraction) in arterial blood – pO_2 – 520 mm Hg., pCO_2 – 36 mm Hg.; there were no episodes of hypotension and cardiac arrest during the donor conditioning period. The donor lungs were harvested according to the standard technique within the framework of multi-organ explantation. Celsior (IGL, France) with a 4-liter volume was used as a preservative solution.

Lung transplantation surgery lasted for 10 hours 3 minutes. The intraoperative period was uneventful. Cold preservation of the right and left lung graft lasted for 6 hours 20 minutes and 9 hours 50 minutes respectively. Due to pronounced mismatch between the diameters of the donor's and recipient's bronchi, bronchial anastomoses were performed telescopically, by intussusception of the donor's bronchial stump into the recipient's main bronchus.

The patient was extubated on postoperative day 2. The early postoperative period was uneventful and without significant clinical events. The drains were removed on postoperative day 3 and day 5. There were no signs of graft dysfunction. During hospitalization, sputum microbiological analysis showed occasional spread in Klebsiella pneumoniae without Burkholderia serasia complex isolation. Laboratory and imaging indicators by the end of postoperative week 3: ERF: VC – 1.88 L (54%), FEV_1 – 1.79 (59%), Tiffeneau-Pinelli index – 83.4; Capillary blood pH (in atmospheric air): pO_2 – 79 mm Hg, pCO_2 – 38 mm Hg, SpO_2 in atmospheric air 96–97%. The patient was discharged on postoperative day 28 in a satisfactory condition with three-component immunosuppressive therapy (tacrolimus, methylprednisolone, mycophenolate mofetil). Concomitant therapy included: antibacterial, antiviral, antifungal and inhaled bronchodilators, gastroprotective therapy. The patient was regularly examined according to the donor lung recipient monitoring protocol.

Two months after transplantation, the patient complained of cough with difficult discharge of scanty amount of sputum, recurrent fever up to febrile digits, and shortness of breath during physical exertion. Outpatient examination revealed a slight decrease in external respiration indicators: (VC – 2.03 L (54%), FEV_1 – 1.76 L (55%), Tiffeneau-Pinelli index – 87). Bronchoscopy revealed cicatricial occlusion of the bronchus intermedius (Fig. 1, a). Chest CT scan revealed an X-ray picture of inflammatory infiltration of the middle and lower lobes of the right lung (Fig. 1, b). Laboratory tests demonstrated an increase in inflammation markers: C-reactive protein 154 mg/L, leukocytosis of up to 12,000 with a left shift in leukocyte formula. Microbiological examination of bronchoalveolar lavage revealed respiratory tract reinfection with Burkholderia cepacia complex and Klebsiella pneumoniae.

Taking into account the clinical and radiological picture of middle and lower lobe obstructive pneumonia, endoscopic balloon bougienage of the intermediate bronchus stenosis (Endo-Flex dilation balloon, 7 Fr, three-step, Germany) was performed in the operating room using rigid bronchoscopy on December 17, 2018. Antimicrobial therapy included antibiotics (meropenem, co-trimoxazole, piperacillin + tazobactam), antifungal drugs (fluconazole), inhalation therapy (colistin, amphotericin). In order to prevent recurrent stenosis, mofetil mycophenolate was converted to everolimus with the target concentration of 4–5 ng/mL. Against the background of the treatment, bronchoscopy and computed tomography showed positive dynamics in the form of formation of a stable bronchus intermedius lumen 5–6 mm in diameter, reduced area and intensity of inflammatory infiltration of the middle and lower lobe of the right lung (Fig. 2, a, b). The patient was discharged on day 12 after balloon bronchoplasty for bronchus intermedius stenosis in a state of positive clinical, laboratory and imaging dynamics. ERF indicators at the time of discharge from the hospital: VC – 2.04 l (58%), FEV_1 – 1.83 L (60%), Tiffeneau-Pinelli index – 89.7.

Four months after transplantation and 2 months after balloon dilatation for cicatricial stenosis, the patient noted renewed signs of respiratory failure. Bronchoscopy (outpatient examination) revealed recurrent bronchus intermedius stenosis of up to 3–4 mm (Fig. 3, a). Chest CT scan showed the areas of inflammatory infiltration in the middle and lower lobes of the right lung (Fig. 3, b). According to ERF data: VC – 1.85 L (52%), FEV_1 – 1.74 L (54%), Tiffeneau-Pinelli index – 85.9.

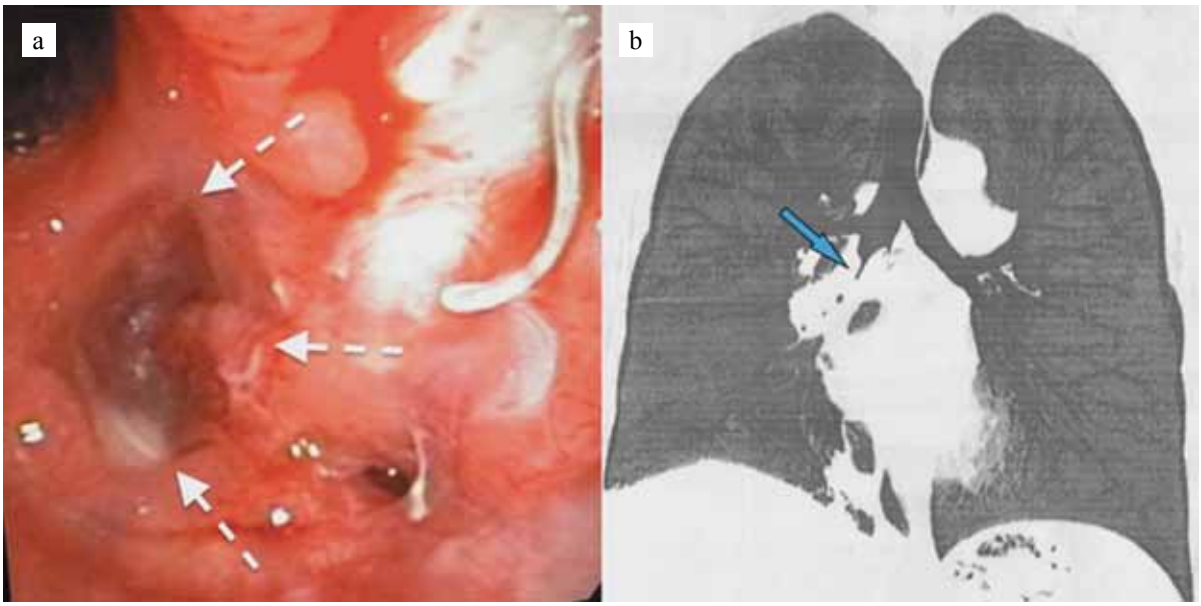

Fig. 1. Cicatricial occlusion of the bronchus intermedius: a – endoscopic picture of the occlusion of the bronchus intermedius (indicated by arrows); b – CT signs of occlusion (indicated by an arrow)

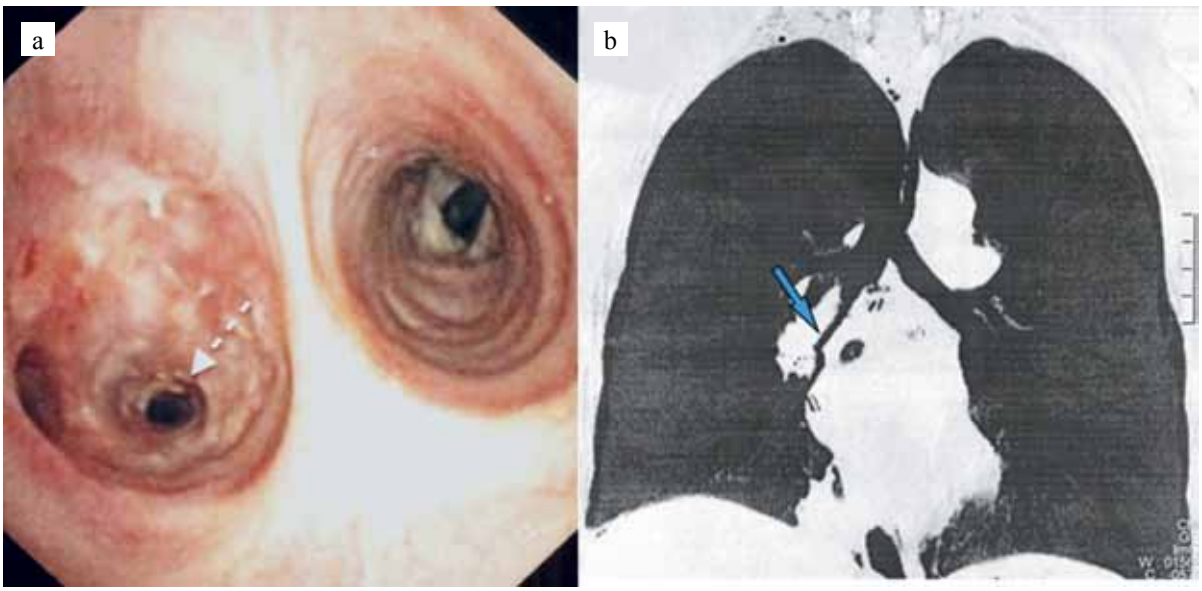

Fig. 2. Resolution of bronchus intermedius stenosis; a, b – lumen of the bronchus intermedius (indicated by arrows)

As part of complex treatment, antibacterial therapy was prescribed according to the scheme: meropenem, cotrimoxazole, piperacillin + tazobactam. Under general anesthesia, with rigid bronchoscopy, two consecutive endoscopic balloon bougienage of stenosis in the bronchus intermedius area were performed on January 31, 2019 and February 11, 2019 in combination with argon-plasma coagulation of scar tissue, until a lumen of 5–6 mm in diameter was achieved.

Within the next month after stenosis correction, while in hospital, the patient suffered recurrent right-sided middle and lower lobe pneumonia associated with multidrug-resistant Burkholderia cepacia complex, complicated by type 2 respiratory failure symptoms (up to 58 mm Hg arterial blood hypoxemia, up to 90% desaturation in the open air).

Six months after lung transplantation and four months after manifestation of recurrent bronchus intermedius stenosis, which required a series of balloon bronchoplasty, it was decided to stent the bronchus intermedius with an uncoated balloon-expanding nitinol stent due to the unstable effect of treatment. This type of stent was chosen due to persistent Burkholderia cepacia – associated pneumonia and the need to maintain effective mucociliary clearance in the stenting area. Stent implantation performed with rigid bronchoscopy (Fig. 4, a, b), made

it possible to carry out long-term scheduled sanitation of the bronchial tree, which was necessary due to persisting right-sided lower and middle lobe pneumonia.

Prolonged implantation of the uncoated bronchial stent (1.5 months) resulted in its partial obstruction due to the growth of scar-granulation tissue in its lumen. On May 27, 2019, the stent was extracted with rigid bronchoscopy (Fig. 5, a, b).

During dynamic observation, the bronchus intermedius with preserved skeletal function and a lumen passable for a 6-mm bronchoscope, which, together with positive clinical, laboratory and imaging dynamics, allowed the patient to be discharged for outpatient observation.

Nine months after lung transplantation, 7 months after the onset of vanishing bronchus intermedius syndrome and 1 month after removal of the uncoated nitinol stent, the patient again began to experience shortness of breath during moderate physical activity. Bronchoscopy revealed recurrent bronchus intermedius stenosis of up to 2 mm (Fig. 6, a). On September 1, 2019, using rigid bronchoscopy, repeated endoscopic restenting of the bronchus intermedius was performed with a self-

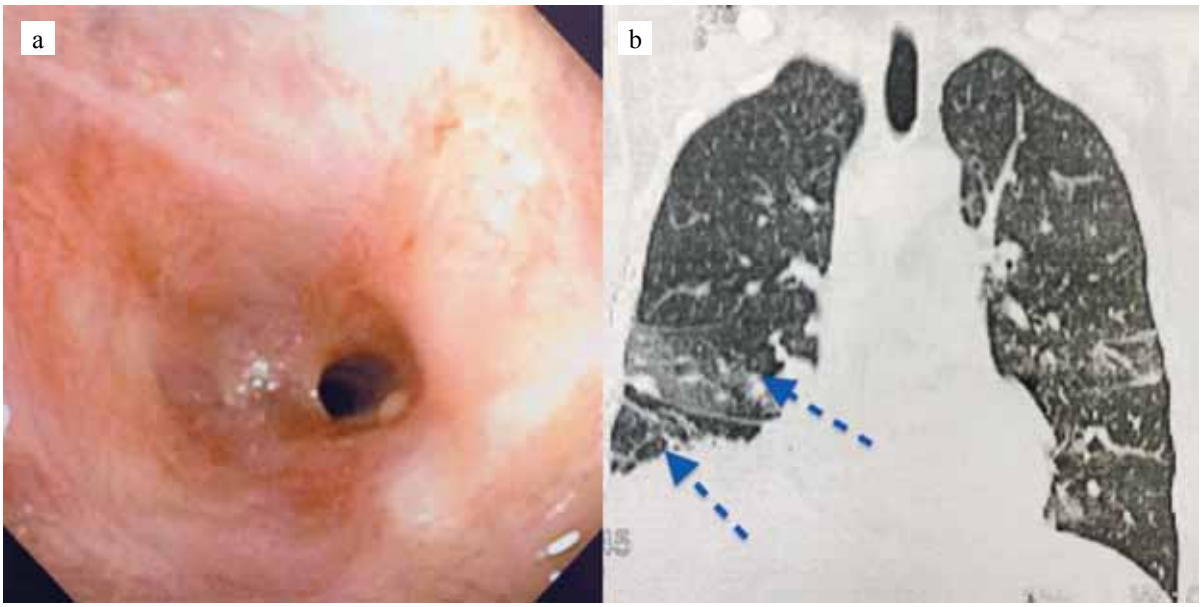

Fig. 3. Development of restenosis after balloon dilatation; a – narrowing of the lumen of the bronchus intermedius; (d ~ 3–4 mm); b – CT signs of pneumonia (indicated by arrow)

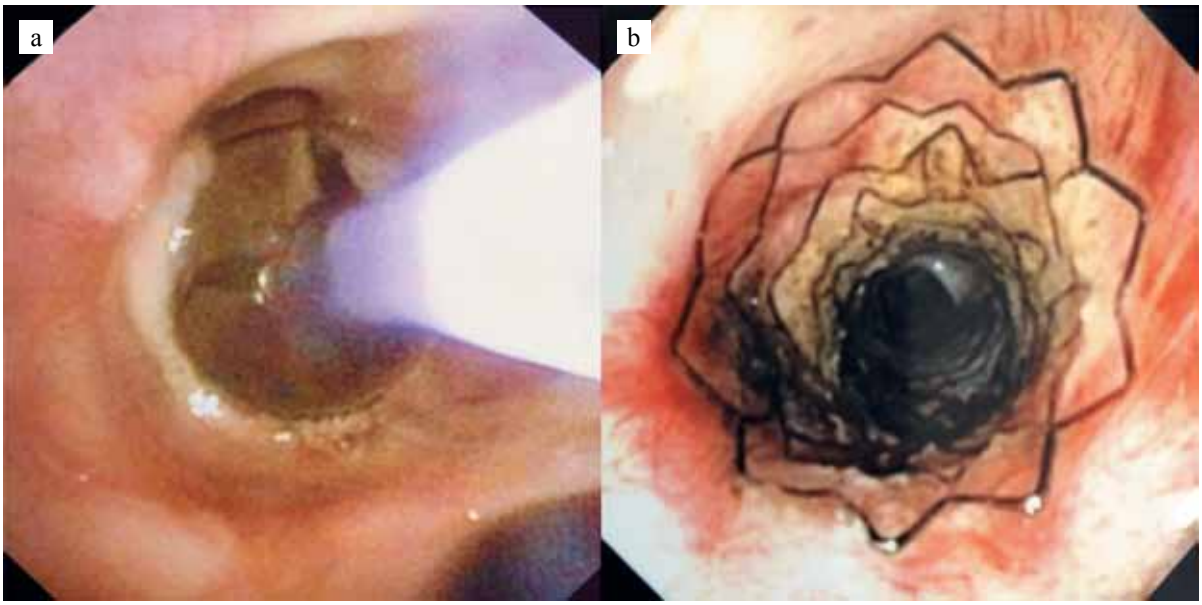

Fig. 4. Stenting of the bronchus intermedius with an uncoated self-expanding nitinol stent; a – balloon dilatation of the bronchus intermedius; b – stent in the bronchus intermedius

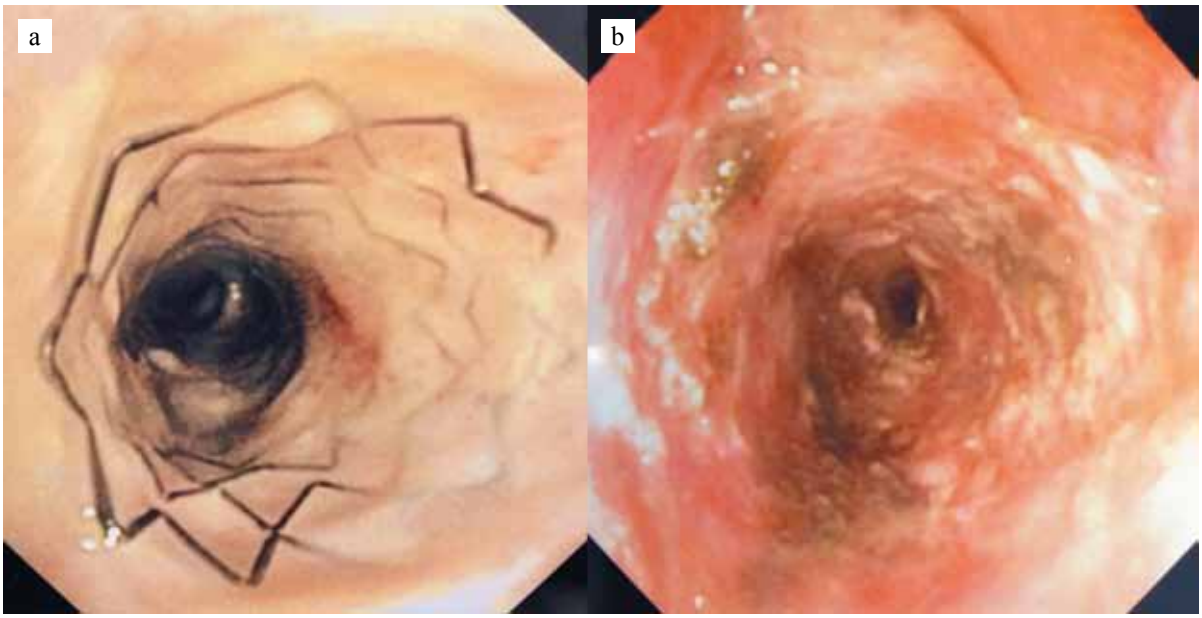

Fig. 5. Extraction of uncoated nitinol stent; a – cicatricial-granulation tissue in the stent lumen; b – after stent extraction

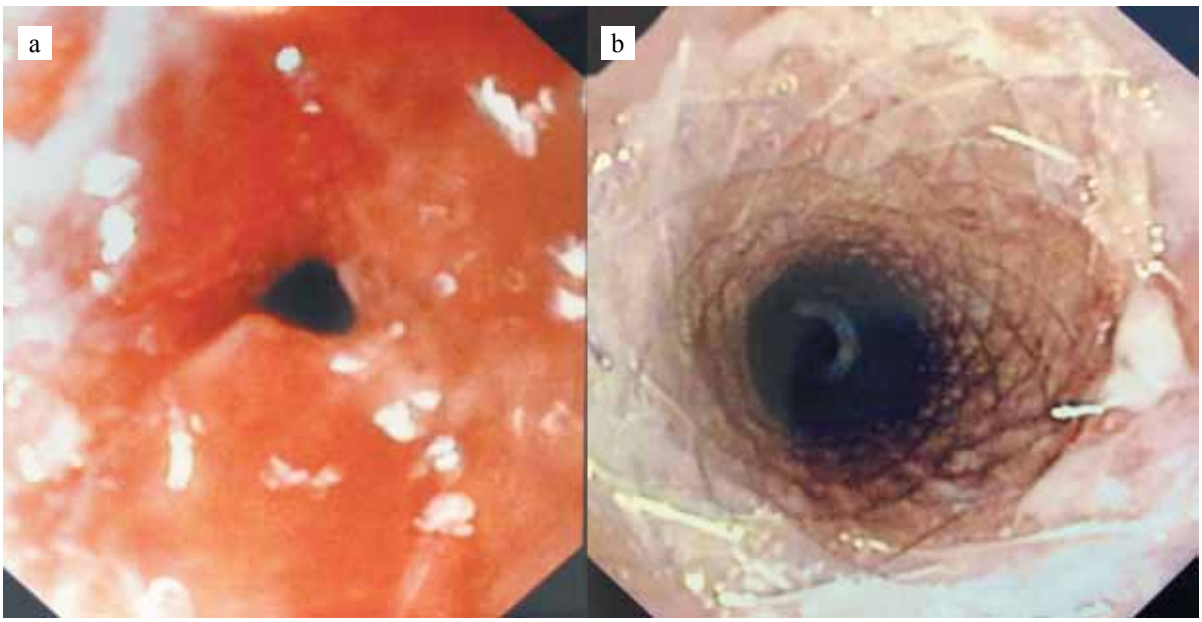

Fig. 6. Stenting of bronchus intermedius restenosis; a – up to 2 mm bronchus intermedius restenosis; b – re-stenting of the bronchus intermedius with a self-expanding nitinol stent d = 8 mm

expanding nitinol stent with 8 mm diameter and 19 mm length (Boston Ultraflex, USA) (Fig. 6, b).

For 6 months after restenting, the patient's condition remained stable, with no signs of respiratory failure. Regular endoscopic examinations showed adequate lumen throughout the bronchus intermedius.

At 16 months after lung transplantation, 14 months after the onset of vanishing bronchus intermedius syndrome, and 7 months after repeated restenosis with routine endoscopic follow-up, signs of recurrent stenosis were revealed in the proximal edge of the previously implanted stent (Fig. 7, a, b).

On February 1, 2020, with rigid bronchoscopy, the stent was removed from the bronchus intermedius, cryoablation of the cicatricial stenosis area was performed. In order to achieve hemostasis after stent extraction, we used electrosurgical methods. After 5 days, after achieving clear positive dynamics in the bronchial mucosa repair processes after application of electrosurgical methods of hemostasis, repeated stenting was performed using a similar self-expanding nitinol stent with a 10 mm diameter (Fig. 7, c).

Within six months after the last restenting, there were no signs of recurrent bronchus intermedius stenosis du-

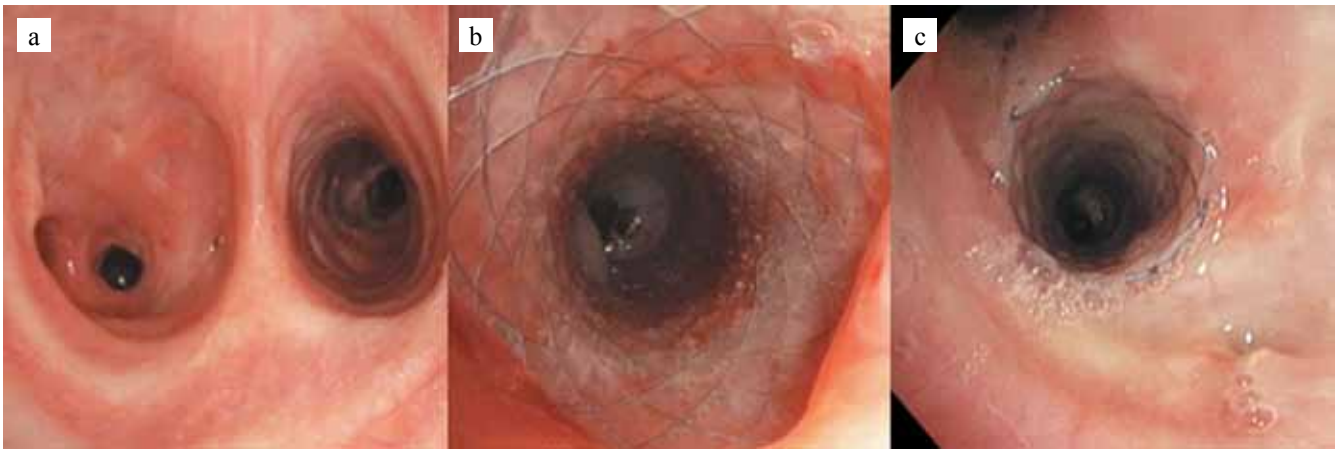

Fig. 7. Conversion of an 8 mm-diameter nitinol stent to a 10 mm-diameter nitinol stent; a – proximal edge of the stent (d ~ 4–5 mm); b – distal and middle third of the stent (d ~ 8 mm); c – after placement of a self-expanding nitinol stent (d = 10 mm)

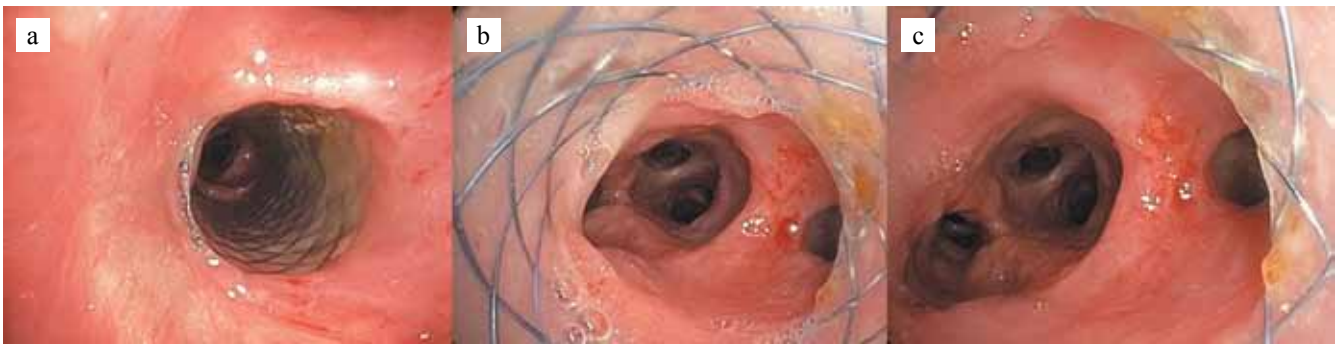

Fig. 8. View of the stent in the bronchus intermedius 6 months after implantation; a – proximal edge of the stent; b – distal edge of the stent; c – area of bifurcation of the bronchus intermedius

ring routine examinations, the function of the transplanted lungs was satisfactory (VC – 2.93 L (84%), FEV1 – 2.16 L (71%), Tiffeneau-Pinelli index – 74%), clinical, laboratory and imaging parameters were within normal range. During endoscopic examination, the stent in the bronchus intermedius was correctly positioned, the stent lumen was passable, there were no marginal scar and granulation changes (Fig. 8).

DISCUSSION

Stenoses are the most common type of bronchial complications in the long term after lung transplantation [9, 16, 17]. To date, there is no consensus and comprehensive understanding of the mechanisms of development of bronchial stenosis and, in particular, vanishing bronchus intermedius syndrome. The opinion of the majority of authors leans in favor of telescoping bronchial anastomosis and highly virulent infection persisting in the tracheobronchial tree as the main factors in the development of bronchus intermedius stenosis. Other authors note the importance of such factors as duration of artificial ventilation, duration of cold ischemia of the lung graft, ischemia-reperfusion injury of the graft, impaired blood supply to the tissues of the bronchial tree as a result of bronchial artery transection [2, 4, 16, 18].

The main causes for the development of VBIS in our observation were: telescoping bronchial anastomosis (used due to marked differences in the lumen diameters of the recipient's bronchus and the donor's bronchus) and presence of chronic respiratory infections Pseudomonas aeruginosa and Burkholderia cepacia, and later Klebsiella pneumoniae.

Within 2 months after VBIS manifestation in the form of obstructive pneumonia, our treatment strategy was limited to staged balloon bougienage. Shortening of the duration of the positive effect of the interventions threatened the re-development of bronchial obstruction with an outcome of middle and lower lobe pneumonia. In order to preserve an adequate bronchus intermedius lumen, providing effective evacuation of the airway contents of the middle and lower lobes of the right lung, stenting of the recurrent stenosis area with an uncoated nitinol stent was performed. Despite the risks of infiltration, up to complete obstruction, uncoated metal stent was chosen, which made it possible to maintain effective mucociliary clearance in the implantation area and thereby avoid aggravating the course of the infectious process and achieve

resolution of inflammatory-infiltrative changes in the right lung. Removal of an uncoated metal stent partially overgrown with cicatricial-granulation tissue naturally required the use of endoscopic electrosurgical methods of hemostasis. Repeated interventions in the form of staged balloon or electrosurgical bronchoplasty with implantation of stents made it possible to achieve stable long-term effect in the form of preserving the bronchus intermedius lumen, sufficient for satisfactory external respiration indicators. Thus, as of August 2020, the duration of effective correction of the vanishing bronchus intermedius syndrome is 21 months. Clinical, laboratory and imaging assessment showed no signs of respiratory failure and graft dysfunction.

Strict outpatient and remote monitoring, together with active use of observational and interventional bronchology techniques, are effective measures for the timely diagnosis and surgical correction of severe bronchial complications threatening the development of lung graft dysfunction and reduction in the quality and life expectancy of lung recipients.

The authors declare no conflict of interest.

REFERENCES

1. *Frye L, Machuzak MS*. Airway complications after lung transplantation. *Clinics in Chest Medicine*. 2017; 38 (4): 693–706. doi: 10.1016/j.ccm.2017.07.010.
2. *Santacruz JF, Mehta AC*. Airway complications and management after lung transplantation: ischemia, dehiscence, and stenosis. *Proceedings of the American thoracic society*. 2009; 6 (1): 79–93.
3. *Murthy SC, Blackstone EH, Gildea TR, Gonzalez-Stawinski GV, Feng J, Budev M et al.* Impact of anastomotic airway complications after lung transplantation. *The Annals of thoracic surgery*. 2007; 84 (2): 401–409. doi: 10.1016/j.athoracsur.2007.05.018.
4. *Murthy SC, Gildea TR, Machuzak MS*. Anastomotic airway complications after lung transplantation. *Current Opinion in Organ Transplantation*. 2010; 15 (5): 582–587. doi: 10.1097/MOT.0b013e32833e3e6e.
5. *Crespo MM, McCarthy DP, Hopkins PM, Clark SC, Budev M, Bermudez CA et al.* ISHLT Consensus Statement on adult and pediatric airway complications after lung transplantation: Definitions, grading system, and therapeutics. *The Journal of Heart and Lung Transplantation*. 2018; 37 (5): 548–563. doi: 10.1016/j.healun.2018.01.1309.
6. *Van Berkel V, Guthrie TJ, Pur V, Krupnick AS, Kreisel D, Patterson GA et al.* Impact of anastomotic techniques on airway complications after lung transplant. *The Annals of thoracic surgery*. 2011; 92 (1): 316–321. doi: 10.1016/j.athoracsur.2011.03.031.
7. *Yserbyt J, Dooms C, Vos R, Dupont LJ, Van Raemdonck DE, Verleden GM.* Anastomotic airway complications after lung transplantation: risk factors, treatment modalities and outcome – a single-centre experience. *European Journal of Cardio-Thoracic Surgery*. 2016; 49 (1): e1–e8. doi: 10.1093/ejcts/ezv363.
8. *FitzSullivan E, Gries CJ, Phelan P, Farjah F, Gilbert E, Keech JC et al*. Reduction in airway complications after lung transplantation with novel anastomotic technique. *The Annals of thoracic surgery*. 2011; 92 (1): 309–315. doi: 10.1016/j.athoracsur.2011.01.077.
9. *Fonseca HV, Iuamoto LR, Minamoto H.* Stents for bronchial stenosis after lung transplantation: should they be removed? *Transplantation proceedings*. 2015; 47 (4): 1029–1032.
10. *Schweiger T, Nenekidis I, Stadler JE, Schwarz S, Benazzo A, Jaksch P et al.* Single running suture technique is associated with low rate of bronchial complications after lung transplantation. *The Journal of Thoracic and Cardiovascular Surgery*. 2020. doi: 10.1016/j.jtcvs.2019.12.119.
11. *Choong CK, Sweet SC, Zoole JB, Guthrie TJ, Mendeloff EN, Haddad FJ et al.* Bronchial airway anastomotic complications after pediatric lung transplantation: incidence, cause, management, and outcome. *The Journal of thoracic and cardiovascular surgery*. 2006; 131 (1): 198–203. doi: 10.1016/j.jtcvs.2005.06.053.
12. *Hayes Jr D, Mansour HM*. Vanishing bronchus intermedius syndrome in a pediatric patient with cystic fibrosis after lung transplantation. *Pediatric transplantation*. 2012; 16 (8): E333–E337. doi: 10.1111/j.1399-3046.2012.01682.x.
13. *De Gracia J, Culebras M, Alvarez A, Catalán E, De la Rosa D, Maestre J et al.* Bronchoscopic balloon dilatation in the management of bronchial stenosis following lung transplantation. *Respiratory medicine*. 2007; 101 (1): 27–33. doi: 10.1016/j.rmed.2006.04.019.
14. *Marulli G, Loy M, Rizzardi G, Calabrese F, Feltracco P, Sartori F et al*. Surgical treatment of posttransplant bronchial stenoses. *Transplantation proceedings*. 2007; 39 (6): 1973–1975. doi: 10.1016/j.transproceed.2007.05.021.
15. *Shah SS, Karnak D, Minai O, Budev MM, Mason D, Murthy SC et al.* Symptomatic narrowing or atresia of bronchus intermedius following lung transplantation vanishing bronchus intermedius syndrome (VBIS). *Chest Meeting Abstracts*. 2006; 130 (4): 236S.
16. *Fallis RJ, Jablonski L, Moss S, Axelrod P, Clauss H.* Infectious complications of bronchial stenosis in lung transplant recipients. *Transplant Infectious Disease*. 2019; 21 (4): e13100. doi: 10.1111/tid.13100.
17. *Mahajan AK, Folch E, Khandhar SJ, Channick CL, Santacruz JF, Mehta AC et al.* The diagnosis and management of airway complications following lung transplantation. *Chest*. 2017; 152 (3): 627–638. doi: 10.1016/j.chest.2017.02.021.
18. *Alraiyes AH, Inaty H, Machuzak MS*. Vanishing Bronchus After Lung Transplantation. The Role of Sequential Airway Dilatations. *Ochsner Journal*. 2017; 17 (1): 71–75. doi: 10.1043/1524-5012-17.1.71.

The article was submitted to the journal on 31.08.2020

DOI: 10.15825/1995-1191-2020-4-192-196

MORPHOLOGY OF TRANSPLANTED LIVER IN RECURRENT PROGRESSIVE FAMILIAL INTRAHEPATIC CHOLESTASIS TYPE 2

I.M. Iljinsky[1], N.P. Mozheiko[1], O.M. Tsirulnikova[1, 2]

[1] Shumakov National Medical Research Center of Transplantology and Artificial Organs, Moscow, Russian Federation

[2] Sechenov University, Moscow, Russian Federation

Progressive familial intrahepatic cholestasis type 2 (PFIC-2), formerly known as Byler's syndrome, is an autosomal recessive disorder. In infancy or early childhood, this disease leads to end-stage hepatic disease, in which liver transplantation is the only radical treatment. In general, liver transplantation outcomes are good, but in the long term, PFIC-2 may reoccur. We present a case where a girl, aged 28 months, who suffered from cirrhosis resulting from PFIC-2, underwent a related transplantation of the left lateral sector of the liver (her grandmother as the donor). Punch biopsy was performed 8 years after the liver transplant due to graft dysfunction. Histopathology revealed a recurrent PFIC-2. F4. Increased liver failure was the reason for retransplantation of the left lobe of the liver also from a related donor (mother). Pathological pictures in the biopsy specimen and in the liver removed during retransplantation were identical, which once again confirmed PFIC-2 recurrence.

Keywords: recurrent progressive familial intrahepatic cholestasis, PFIC-2, hepatocyte dystrophy, multinucleated cells.

Progressive familial intrahepatic cholestasis (PFIC) is a heterogeneous group of diseases with an autosomal recessive inheritance. In PFIC, bile formation is impaired and hepatocellular cholestasis develops. Currently, there are six known types of pyelonephritis [1, 2]. Among them, PFIC type 2 (PFIC-2), formerly known as Byler disease, is characterized by a mutation in the ABCB11 gene, which encodes the BSEP transport protein. Its absence in the canalicular membrane of hepatocytes causes cholestasis and leads to liver fibrosis and end-stage disease in the first decade of life [3].

In PFIC-2, the main clinical symptoms are cholestasis, pruritus, and jaundice. In the blood serum, the activity of gamma-glutamyl transferase is within the normal range [4, 5]. Diagnosis is based on clinical manifestations, liver ultrasound, cholangiography, and liver histology [5]. An analysis of the results of palliative operations in children showed a decrease in pruritus and cholestasis [6–8]. However, liver transplantation remains the uncontested radical treatment method.

In general, the outcomes of liver transplantation in patients that have had PFIC-2 are good [9]. However, more recently, there have been reports that PFIC-2 patients after liver transplantation develop recurrent cholestasis along with clinical and histological signs of primary disease. Recurrence of the disease is associated with the emergence of autoantibodies against the BSEP protein, which inhibits the transport activity of the bile salt pump and causes severe cholestasis [3, 10–13].

This study reports on one of the cases where histological signs of recurrent PFIC-2 were found while examining transplanted liver biopsy specimens.

OWN OBSERVATION

On November 26, 2009, a 28-month-old girl with PFIC-2 cirrhosis underwent a related orthotopic left lateral liver transplantation from her grandmother. The removed native liver weighed 630 g, measured 19 × 15 × 11 × 6 cm, and had a brown-green surface, slightly granular. In the cut, the liver was greenish-brown, the bile ducts, mainly in the area of the gate, were dilated, filled with thick bile and sand.

Histological examination. *The hepatic beam and lobular structure is disturbed. Hepatocytes were 2–3 times enlarged compared to the norm, in a state of marked protein degeneration, necrosis of individual cells (Fig. 1). There was a large number of multinucleated giant cells. Intracellular cholestasis. There was stagnation of bile in the dilated bile capillaries. Foci of accumulation of polynuclear leukocytes and their debris in sinusoids. In the sclerosed portal tracts, the bile ducts were preserved, vascular congestion (Fig. 2). Porto-portal and porto-central septa with insignificant infiltration of lymphoid cells, with an admixture of polynuclear leukocytes and moderately pronounced ductuloneogenesis.* ***Histological diagnosis:*** *liver cirrhosis resulting from PFIC-2.*

The early postoperative period was uneventful. The patient was discharged in a satisfactory condition under outpatient supervision. Graft function remained satis-

Corresponding author: Igor Iljinsky. Address: 1, Shchukinskaya str., Moscow, 123182, Russian Federation. Phone: (999) 877-60-95. E-mail: iiljinsky@mail.ru

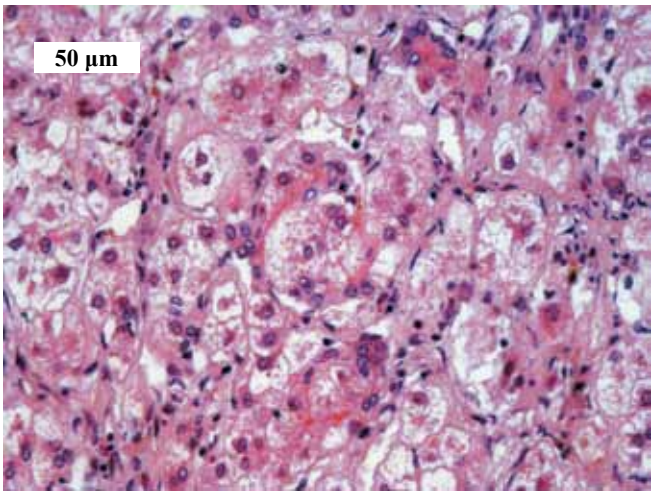

Fig. 1. The girl is 28 months old. Native liver. Giant hepatocyte dystrophy. Visible among them are multinucleated cells. H&E stain. 400× magnification

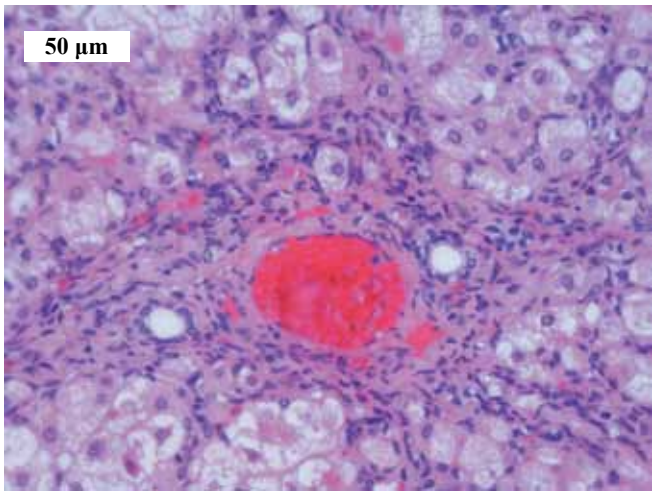

Fig. 2. The girl is 28 months old. Native liver. Red thrombus in the vein of the sclerosed portal tract. Lymphocytic infiltration of the portal tract and septa. F4 (by METAVIR). H&E stain. 400× magnification

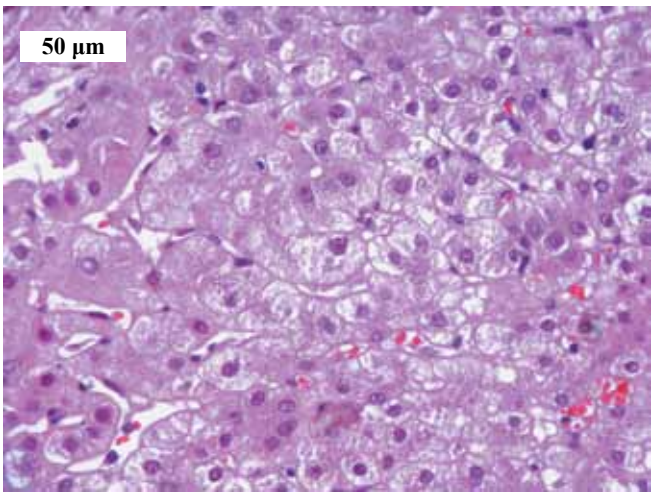

Fig. 3. At 2 years and 8 months after liver transplant. Needle biopsy of the transplanted liver. Giant hepatocyte dystrophy. H&E stain. 400× magnification

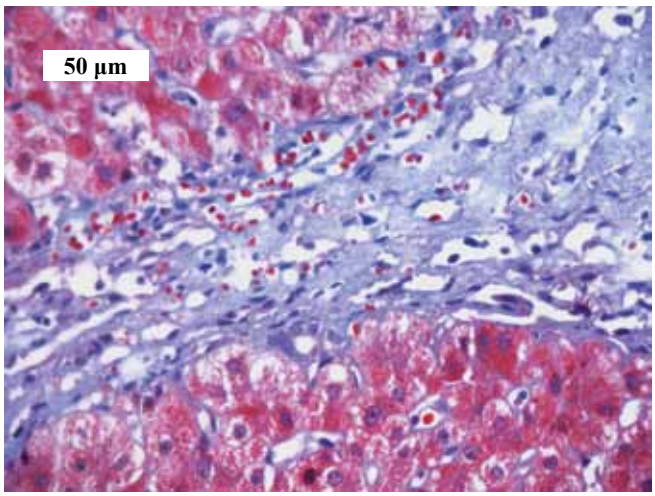

Fig. 4. At 2 years and 8 months after liver transplant. Needle biopsy of the transplanted liver. Sclerosis of the portal tract and septal sclerosis. F2 (by METAVIR). H&E stain. 400× magnification

factory. There were episodes of intercurrent infectious diseases (acute respiratory and intestinal). Routine therapy was administered.

The patient's condition was satisfactory until August 2012. Her immunosuppressive therapy included prograf 1.5 mg per day, methylprednisolone 6 mg per day, and CellCept 500 mg per day. Plasma creatinine level was 19.6 mmol/L, blood plasma urea 2.57 mmol/L, bilirubin 150 mmol/L, AST 67.8, and ALT 59.6. The patient's body weight was 21 kg. The blood level of prograf was 8.8 mg/mL.

Transcutaneous needle biopsy of the transplanted liver was performed on August 2, 2012 due to signs of dysfunction of the transplanted liver. The biopsy specimen showed abnormal lobular and beam structure of the liver, pronounced diffuse protein dystrophy and micro-focal necrosis of hepatocytes (Fig. 3). Porto-portal and porto-central septa with hemorrhages, moderate inflammatory infiltration, mild proliferation of the bile ducts (Fig. 4). Severe perivenular fibrosis of the central vein wall. Focal small-droplet fatty degeneration of hepatocytes.

The patient developed itchy skin from October 2018, with increasing severity. The itching was ruled out to have allergic, mechanical, or infectious origin. By February 13, 2019, clinical-laboratory and imaging signs of liver graft dysfunction were identified. Cytolysis level 1044/1444, total bilirubin level 84, direct bilirubin 44, albumin 28 g/L. Immunosuppression: tacrolimus 2 × 2 times a day. The patient's body weight was 33 kg.

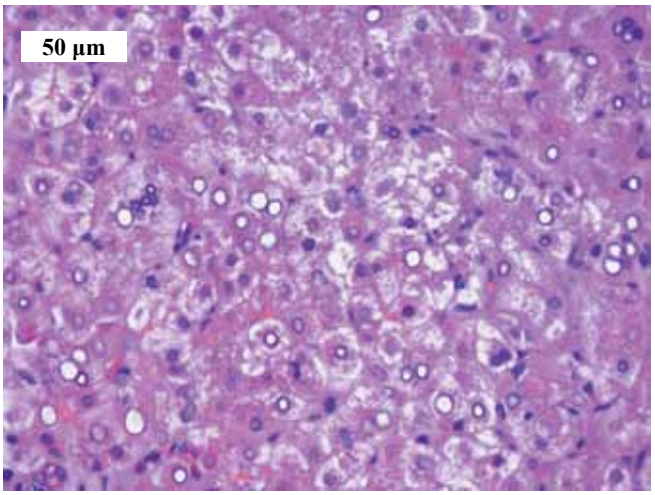

Fig. 5. Material from a needle biopsy of the transplanted liver 8 years and 11 months after surgery. Dystrophic changes not only in the cytoplasm of giant hepatocytes, but also in the nuclei, which look like an "hourglass". H&E stain. 400× magnification

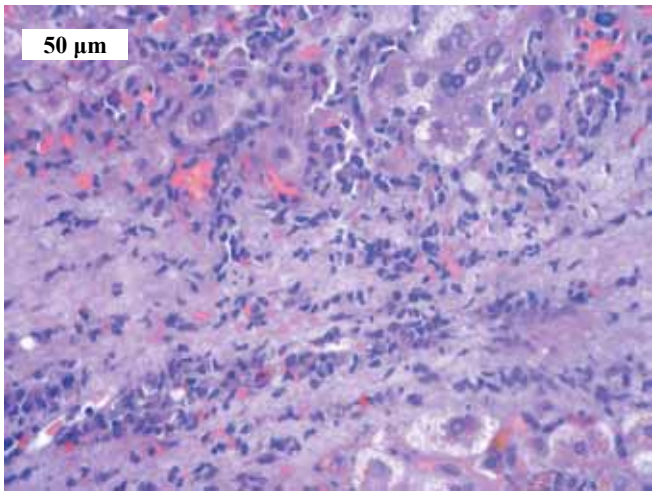

Fig. 6. Material of percutaneous needle biopsy of the transplanted liver at 8 years and 11 months after surgery. Lymphocytic infiltration of the portal tract and septa. F4 (by METAVIR). On the periphery of the septum are giant and multinucleated hepatocytes. H&E stain. 400× magnification

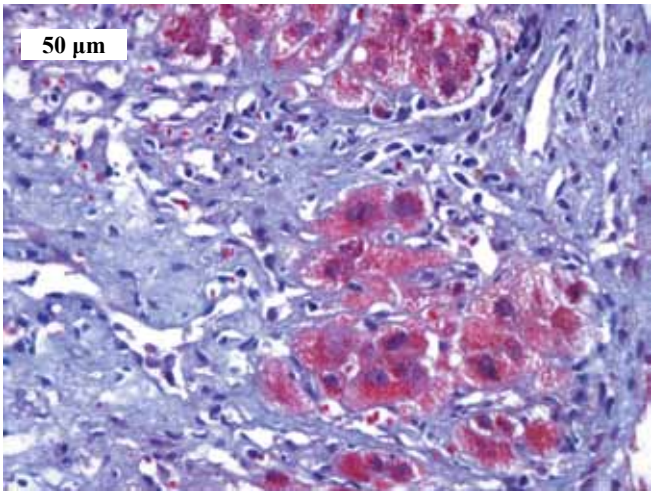

Fig. 7. Material from percutaneous needle biopsy of the transplanted liver at eight years and 11 months after surgery. Dystrophic changes in giant hepatocytes in the false lobules. F4 (by METAVIR). H&E stain. 400× magnification

A second biopsy of the transplanted liver was performed on February 14, 2019. Histological examination found that the changes in the graft were similar to those described in the material of the previous biopsy. The beam and lobular structure of the liver was abnormal. There were severe granular and focal ballooning degeneration of hepatocytes, multinucleated hepatocytes. Unlike the previous biopsy, there was a large number of cells with "sandy" nuclei (Fig. 5). Severe portal tract fibrosis, formation of varying width of porto-portal septa. Portal triads were infiltrated by mononuclear cells, with single newly formed bile ducts; bile duct epithelium was preserved (Fig. 6, 7). There was intracellular accumulation of bile pigment granules, mainly in hepatocytes located periportally, bile stagnation in single small bile ducts. Immunofluorescence revealed small granular deposits of the C4d complement fragment in the portal tracts and in single sinusoids.

Based on the clinical picture and results of needle biopsies of the transplanted liver, a histological diagnosis was made: recurrent PFIC-2. F4.

Thus, the study results showed that 8 years after the liver transplant, the graft developed changes similar to the pathology of its own liver. In this regard, as well as in connection with the increase in liver failure, the girl underwent retransplantation of the left lobe of the liver, also from a related donor (mother) on June 19, 2019. The pathological picture in the biopsy specimen and in the liver removed during retransplantation was identical, which once again confirmed recurrent PFIC-2.

DISCUSSION

Recurrent PFIC-2 is a rare post-liver transplant complication. Only one relatively old publication [14] reported on 6 patients with PFIC-2 who developed a recurrence of the disease. The rest of the publications on this topic are devoted to single cases [3, 10–13].

In our case, it is not possible to determine the timing of the onset of recurrent PFIC-2, since the first clinical signs of transplanted liver failure appeared 2 years and 8 months after the operation. At the same time, the first percutaneous needle biopsy of the graft was performed. Histological examination of a biopsy specimen of the transplanted liver revealed a several-fold increase in the size of hepatocytes due to edema, which was associated with the absence of the BSEP protein, which ensures transport of bile salts from hepatocytes [3, 10–13]. There were also multinucleated hepatocytes, which, according

to literature [13], are a distinctive histological feature of PFIC-2. Intracellular accumulation of bile acids led to development of portal tract sclerosis and appearance of septa (F2). The peculiarity of our case is that the end stage of liver failure developed six and a half years after the appearance of its first signs, when the second biopsy revealed cirrhosis of the graft. Interestingly, hepatocyte pathology in the second biopsy was similar to hepatocyte changes in the much earlier, first biopsy. A distinctive feature was the appearance of a large number of hepatocytes with "sandy nuclei", which, in our opinion, indicates a more severe degeneration.

MAIN PROVISIONS BASED ON THE ABOVE CASE

- Typical histological changes in the transplanted liver upon return of PFIC-2: severe hepatocyte degeneration, a several-fold increase in hepatocyte size, multinucleated hepatocytes.
- Upon return of PFIC-2, the first clinical signs of transplanted liver failure appear according to the histological changes in hepatocytes and the presence of liver fibrosis of at least F2 (according to METAVIR).
- Upon return of PFIC-2, the end-stage of the transplanted liver failure corresponds to the histological picture of liver cirrhosis.

The authors declare no conflict of interest.

REFERENCES

1. *Sticova E, Jirsa M, Pawłowska J.* New Insights in Genetic Cholestasis: From Molecular Mechanisms to Clinical Implications. *Can J Gastroenterol Hepatol*. 2018 Jul 26; 2018: 2313675. doi: 10.1155/2018/2313675.
2. *Henkel SA, Squires JH, Ayers M, Ganoza A, Mckiernan P, Squires JE.* Expanding etiology of progressive familial intrahepatic cholestasis. *World J Hepatol*. 2019 May 27; 11 (5): 450–463. doi: 10.4254/wjh.v11.i5.450.
3. *Kubitz R, Dröge C, Kluge S, Stross C, Walter N, Keitel V et al.* Autoimmune BSEP disease: disease recurrence after liver transplantation for progressive familial intrahepatic cholestasis. *Clin Rev Allergy Immunol*. 2015 Jun; 48 (2–3): 273–284. doi: 10.1007/s12016-014-8457-4.
4. *Davit-Spraul A, Gonzales E, Baussan C, Jacquemin E.* Progressive familial intrahepatic cholestasis. *Orphanet J Rare Dis*. 2009 Jan 8; 4: 1. doi: 10.1186/1750-1172-4-1.
5. *Jacquemin E.* Progressive familial intrahepatic cholestasis. *Clin Res Hepatol Gastroenterol*. 2012 Sep; 36 Suppl 1: S26–35. doi: 10.1016/S2210-7401(12)70018-9.
6. *Wang KS, Tiao G, Bass LM, Hertel PM, Mogul D, Kerkar N et al.* Childhood Liver Disease Research Network (ChiLDReN). Analysis of surgical interruption of the enterohepatic circulation as a treatment for pediatric cholestasis. *Hepatology*. 2017 May; 65 (5): 1645–1654. doi: 10.1002/hep.29019.
7. *Saha H, Tapanjyoti G, Biswas S, Mishra PK, Basu KS, Chatterjee U.* Two Cases of Progressive Familial Intrahepatic Cholestasis Type 2: Role of Surgery with Brief Review of Literature. *J Indian Assoc Pediatr Surg*. 2019 Jan–Mar; 24 (1): 75–77. doi: 10.4103/jiaps.JIAPS_235_17.
8. *Kamath BM, Stein P, Houwen RHJ, Verkade HJ.* Potential of ileal bile acid transporter inhibition as a therapeutic target in Alagille syndrome and progressive familial intrahepatic cholestasis. *Liver Int*. 2020 Jun 3; 40 (8): 1812–1822. doi: 10.1111/liv.14553.
9. *Squires JE.* Protecting the allograft following liver transplantation for PFIC1. *Pediatr Transplant*. 2016 Nov; 20 (7): 882–883. doi: 10.1111/petr.12787.
10. *Keitel V, Burdelski M, Vojnisek Z et al. De novo* bile salt transporter antibodies as a possible cause of recurrent graft failure after liver transplantation: a novel mechanism of cholestasis. *Hepatology*. 2009; 50 (2): 510–517.
11. *Masahata K, Uehara S, Ibuka S, Nakahata K, Hasegawa Y, Kondou H et al.* Recurrence of Progressive Familial Intrahepatic Cholestasis Type 2 Phenotype After Living-donor Liver Transplantation: A Case Report. *Transplant Proc*. 2016 Nov; 48 (9): 3156–3162. doi: 10.1016/j.transproceed.2016.02.067.7.
12. *Stindt J, Kluge S, Dröge C, Keitel V, Stross C, Baumann U et al.* Bile salt export pump-reactive antibodies form a polyclonal, multi-inhibitory response in antibody-induced bile salt export pump deficiency. *Hepatology*. 2016 Feb; 63 (2): 524–537. doi: 10.1002/hep.28311.
13. *Kang HJ, Hong SA, Oh SH, Kim KM, Yoo HW, Kim GH, Yu E.* Progressive Familial Intrahepatic Cholestasis in Korea: A Clinicopathological Study of Five Patients. *J Pathol Transl Med*. 2019 Jul; 53 (4): 253–260. doi: 10.4132/jptm.2019.05.03.
14. *Siebold L, Dick AA, Thompson R, Maggiore G, Jacquemin E, Jaffe R et al.* Recurrent low gamma-glutamyl transpeptidase cholestasis following liver transplantation for bile salt export pump (BSEP) disease (posttransplant recurrent BSEP disease). *Liver Transpl*. 2010 Jul; 16 (7): 856–863. doi: 10.1002/lt.22074.

The article was submitted to the journal on 1.10.2020

DOI: 10.15825/1995-1191-2020-4-197-201

COVID-19 IN DECOMPENSATED CIRRHOSIS

O.V. Tashchyan, M.G. Mnatsakanyan, A.P. Pogromov, I.V. Kuprina, Yu.F. Shumskaya
Sechenov University, Moscow, Russian Federation

Elderly patients with diabetes, hypertension and obesity are at risk of severe course of the novel coronavirus infection COVID-19. Patients with chronic liver disease are also at high risk of severe course and death due to SARS-CoV-2. **Case report.** Patient D., 65 years old, since 2010, was observed for Child-Pugh class B-C cirrhosis of mixed etiology (alimentary and metabolic), type 2 diabetes. He was hospitalized on May 17, 2020 due shortness of breath, increased encephalopathy and CT signs of bilateral polysegmental pneumonia, involving about 75% of the lung tissue (CT-scan indicates possible COVID-19-associated pneumonia). Despite repeated negative results of PCR test targeting SARS-CoV-2 viral RNA, the clinical picture and CT scans pointed at the novel coronavirus infection COVID-19 (virus not identified). Because of decompensated cirrhosis, the patient decided to refrain from antiviral and anticytokine therapy. Oxygen therapy, positional therapy, antithrombotic therapy (fondaparinux sodium), antibacterial therapy (ceftriaxone, then levofloxacin), infusion of 20% albumin solution and fresh frozen plasma were carried out. Due to increasing hypoxemia, the patient was transferred to the ICU and placed under mechanical ventilation. Despite all measures, he developed symptoms of multiple organ failure and died of asystole. **Discussion.** Mortality in chronic liver diseases, including cirrhosis, under the novel coronavirus infection caused by SARS-CoV-2, reaches 40% [4]. Factors aggravating the novel coronavirus disease in such patients include immune-mediated liver cell damage, direct cytotoxicity resulting from viral replication in hepatocytes, hypoxia, drug-induced liver injury, and reactivation of previously latent liver diseases (including hepatitis B and C virus). **Conclusion.** In the above clinical case, end-stage lung disease (CT stage 3–4), complicated by disseminated intravascular coagulation (DIC) syndrome, with progressive respiratory and multiple organ failure, led to the death of the patient suffering from cirrhosis and COVID-19.

Keywords: COVID-19, cirrhosis, pneumonia.

The relevance of the study of the clinical picture and features of coronavirus infection COVID-19 caused by the SARS-CoV-2 virus in patients with chronic diseases is beyond doubt. It is known that elderly patients, as well as patients with diabetes, hypertension and obesity, are at risk for severe course of the novel coronavirus disease COVID-19. There are few literature data on the relationship between chronic liver disease and COVID-19 infection [1–3].

It is obvious that patients with severe fibrosis and cirrhosis and liver transplant recipients are also a rather vulnerable group with increased risk of infection and severe course of COVID-19. Experts from the University of Oxford, UK and the University of North Carolina, USA argue that patients with cirrhosis and chronic liver disease have an overall mortality rate of up to 40% after COVID-19 infection, which is several dozen times higher than the standard mortality rate for this disease [4].

In this regard, the following clinical observation is of interest.

Patient D., 65 years old, was followed up in the clinic for 10 years from September 2010 with the following diagnosis: cirrhosis of mixed (alimentary, metabolic) genesis, Child-Pugh class B, C. Portal hypertension. Esophageal varices, gastric varices, small and large bowel varices. Splenomegaly, hypersplenism (deep thrombocytopenia, leukopenia (neutropenia), erythropenia. Ascitic-edematous syndrome. Hepatic encephalopathy grade 2. Anemia of mixed origin – iron deficiency, B_{12} deficiency. Type 2 diabetes mellitus, compensated.

During the follow-up period, he was hospitalized at the clinic almost every year due to decompensated cirrhosis. Numerous therapies included aldosterone inhibitors, Heptral, Hepa-Merz, repeated transfusions of albumin solutions and fresh frozen plasma, which made it possible to reduce liver cell failure manifestations for a short time. The issue of liver transplantation of which the patient opted out, was repeatedly discussed. After discharge from the hospital on April 10, 2020, the patient was asked to adhere to a strict self-isolation regime. After 2 weeks, his body temperature increased to 38.0 °C without chills and catarrhal events. This was accompanied by pain in the right ear. He was consulted on an outpatient basis by an ENT doctor, otitis media was diagnosed, antibiotic therapy was recommended (azithromycin 500 mg per day for 3 days). Against this background, the pain in the ear decreased, his condition somewhat improved, and a slight subfebrile condition persisted. After a few days, encephalopathy increased (the patient's mood changed, he started having disrupted night sleep). The condition

Corresponding author: Olga Tashchyan. Address: 6/1, B. Pirogovskaya str., Moscow, 119991, Russian Federation. Phone: (499) 248-63-85. E-mail: Olgatash1@rambler.ru

was considered in the program of complications of cirrhosis, large intestinal decontamination was carried out, his diet was limited (thermally unprocessed foods were excluded and animal proteins were limited), and oral intake of mixture with 1000 mg kanamycin was started. After 2–3 days, his health improved, night sleep normalized, subfebrile condition – up to 37.30 °C maximum. Shortness of breath, cough, catarrhal phenomena were not observed. On May 10, 2020, the patient's daughter fell ill (high evening fever, cough, weakness), then his wife (a similar clinical picture). Over the next 10 days, with the persisting subfebrile condition, his weakness increased significantly, a dry cough and growing symptoms of respiratory failure appeared. On May 17, 2020, the patient underwent an outpatient multislice computed tomography (MSCT) of the chest, which revealed a picture of community-acquired bilateral polysegmental pneumonia, the lesion volume was up to 75% of the lung tissue on each side (CT-3). The patient was taken by an ambulance team and was admitted at the department for treatment of patients with coronavirus infection of Clinical Hospital No. 1 at Sechenov University.

The patient's condition was severe on admission. His Glasgow Coma Scale (GCS) score was 15. Muscle tone and peripheral sensitivity were fully preserved. Focal neurological and meningeal symptoms were not identified. The skin is icteric, pale, and cyanotic. No peripheral edema was detected. Body temperature 37.40 °C. Spontaneous breathing, mouth-nose. Auscultation was not performed according to pandemic requirements. Respiratory rate = 24–26/min. Sat 02 – 75% when breathing atmospheric air. Against the background of respiratory support – low-flow oxygen therapy with humidified oxygen through a face mask (oxygen flow rate 10–12 L/min) in a prone position, oxygen saturation increased to 93%. Hemodynamics was stable, with a tendency to hypotension. Blood pressure 100/55 mmHg. The abdomen was enlarged due to bloating and ascites, painless on palpation. Stool 2 times a day, loose stool, without pathological impurities. No dysuric disorders were noted.

During laboratory examination: (on May 18, 2020) prothrombin by Quick method: 42% (70–130); INR: 1.98 (0.9–1.16); Prothrombin time: 22 sec (10.4–12.6); Fibrinogen: 1.29 g/L (1.8–4.0). Hematocrit: 28.6% (35–52); Hemoglobin: 90 g/L (117–180); Platelets: 93 × 10^9/L (150–450); Erythrocytes: 3.41 × 10^{12}/L (3.8–6.1); Leukocytes: 3.95 × 10^9/L (4–11) (Basophils: 0.04 × 10^9/L (0–0.1); Lymphocytes: 0.44 × 10^9/L (1.0–3.7); Monocytes: 0.42 × 10^9/L; Neutrophils: 2.88 × 10^9/L; Eosinophils: 0.1 × 10^9/L; Unclassified quantity: 0.07 × 10^9/L); Erythrocyte sedimentation rate 29 mm/h; Color index: 0.79 (0.8–1.5). Total protein: 66.8 g/L (57–82); Albumin: 19.8 g/L (32–48); Glucose: 5.8 mmol/L (4.1–5.9); Creatinine: 65 μmol/L (44–115); Cholesterol: 1.7 mmol/L (3.2–5.6); Triglycerides: 0.62 mmol/L (0.41–1.7); Iron: 6 μmol/L (9–20); Total bilirubin: 28.3 μmol/L (3–21); Direct bilirubin: 13.4 μmol/L (0–5); Uric acid: 320 μmol/L (145–415); Potassium: 4.6 mmol/L (3.5–5.0); Sodium: 135 mmol/L (136–145); ALT: 12 IU/L (10–49); AST: 46 IU/L (0–34); GGT: 34 units/L (0–73); KFK: 232 units/L (0–190); C-reactive protein: 57.78 mg/L (0–8.0); Ferritin: 63.9 μg/L (7.0–200.0). Urinalysis – no abnormalities. Imaging: non-contrast chest CT scan on May 18, 2020: Conclusion: Bilateral hydrothorax. The CT scan of lung changes is highly likely to correspond to bilateral polysegmental COVID 19-associated pneumonia. Cirrhosis. Ascites. Severity according to CT-CT-4 (critical). Damage to 100% of the lung tissue of both lungs. Abdominal ultrasound (of May 19, 2020): ECHO signs of ascites, diffuse dystrophic changes in the liver parenchyma (cirrhotic by type), diffuse changes in the pancreatic parenchyma. RNA SARS-Cov-2 test results: May 17, 2020 – not found; May 19, 2020 – not found; May 23, 2020 – not found.

Thus, the patient with cirrhosis, Child-Pugh class C, was diagnosed with coronavirus infection caused by the COVID-19 virus. The virus was not identified (COVID-19 is diagnosed clinically). Community-acquired bilateral polysegmental pneumonia of an extremely severe course (CT-4). Type 2 respiratory failure. Hydrothorax.

Given the concomitant pathology, it was decided to abandon etiological therapy with antiviral drugs. The patient underwent oxygen therapy (insufflation of humidified oxygen through a face mask), antibacterial therapy with ceftriaxone 1000 mg per day (intravenous drip), planned therapy continued (Hepa-Merz, Inspro, Lasix, Rabeprazole). However, there was a gradual increase in respiratory failure, rapid desaturation of the patient persisted when respiratory support was turned off.

A remote meeting of the council of physicians was held at the Coronavirus Center, where it was decided to abstain from biological anti-cytokine therapy. According to the recommendations of the council, the patient was transfused with 1 dose of fresh frozen plasma.

Despite ongoing therapy, the patient's condition progressively worsened, symptoms of respiratory failure increased, and weakness progressed. On May 24, 2020, the patient was transferred to the ICU of Sechenov University. The patient was in a very serious condition when he was admitted at the ICU. His GCS score was 13–14. The patient is agitated. OD = OS, photoreaction is preserved, vivid, symmetrical. Muscle tone and peripheral sensitivity are fully preserved. No focal neurological and meningeal symptoms were identified. The skin is icteric, pale, cyanotic. No peripheral edema was detected. Body temperature 37.40 °C, shortness of breath (RR = 31–34/min). Sat 02 – 50% when breathing atmospheric air. The patient was transferred to a prone position. Against the background of prone position and insufflation of humidified oxygen at 15 L/min, no increase in oxygenation was observed. A decision was made to carry out tracheal intubation. The trachea was

intubated with an endotracheal tube No. 8.0. The patient was placed on mechanical ventilation in SIMV-PC mode, with the following ventilation parameters: Pinsp 15 cmH20, against this background Vt: 490–520 mL, PEEP of 11 cmH20, FiO_2 of 75%, Sat 02 – 92%. Hemodynamics is stable without vasopressor and inotropic support. In a repeated coagulogram on the 6th day of stay, prothrombin according to Quick was 36%; aPTT was 1.52; D-Dimer was 126.65 μg/ml!!! INR was 2.26; Prothrombin time was 25.2 sec. Complete blood count was Hematocrit 35.5%; Hemoglobin 107 g/L Platelets 168 × 10^9/L (with time – 50,000, 37,000, 47,000, 87,000, 91,000); Erythrocytes: 3.91 × 10^{12}/L; Leukocytes: 21 × 10^9/L (with time – 7,900, 5,300, 5,700, 5,900); (Lymphocytes #: 0.8 × 10^9/L; Neutrophils #: 19.1 × 10^9/L); ESR 43 mm/h; Color index: 0.82. Biochemical blood test on May 24, 2020: Albumin: 25 g/L; Urea nitrogen: 10.3 mmol/L; Total bilirubin: 32.4 μmol/L; Direct bilirubin: 16.9 μmol/L; Creatinine: 92.11 μmol/L; ALT: 14 IU/L; AST: 46 IU/L; GGT: 24 IU/L; creatine phosphokinase (CPK): 29 /L; Lactate dehydrogenase (LDH): 896 IU/L (2–250); C-reactive protein: 130.4 mg/L!!! Biochemical blood test of May 25, 2020: Total protein 68.2 g/L; Albumin 23.5 g/L; Urea nitrogen 17.8 mmol/L; Total bilirubin 31.8 μmol/L; Direct bilirubin 18 μmol/L; Glucose 10.8 mmol/L; Potassium 3.8 mmol/L; Sodium 141 mmol/L; Creatinine 96.6 μmol/L; Uric acid 467 μmol/L; ALT 10 IU/L; AST 29 IU/L; GGT 27 IU/L; CPK 32 IU/L; LDH 632 IU/L; C-reactive protein 173.81 mg/L!!! Ferritin 115.9 μg/L.

Bronchial fibroscopy: Diffuse bilateral catarrhal endobronchitis with level 2 inflammatory activity with severe obstruction at the segmental level.

Pulsed Doppler ultrasound of the tibial veins: Echo signs of non-occlusive deep vein thrombosis in both legs, without signs of flotation. Echo-KG of May 25, 2020: Sinus rhythm, heart rate 68–70 per min. The patient is in the ICU on mechanical ventilation. Visualization is extremely limited. There is no ultrasound window in the parasternal and apical positions. Partial visualization in subcostal projection only. The right chambers of the heart are not dilated. Right ventricle (RV) – 3.5 cm, right atrium (RA) – 60 mL. A moderate increase in left atrium (LA) – up to 84 mL cannot be ruled out. Left ventricle (LV) – not increased, end-diastolic dimension (EDD) – 4.0 cm, end diastolic volume (EDV) approx. 60–70 mL, ejection fraction (EF) approx. 60–68%. No significant LV hypertrophy was detected (interventricular septum (IVS) approx. 1.2 cm). Type 1 LV diastolic dysfunction. Valve device without rough defects. Sclerotic changes in aortic valve (AV) – peak gradient up to 11.6 mmHg are likely, divergence in AV leaflets is sufficient. No aortic regurgitation was revealed. No significant mitral and tricuspid regurgitation was detected. Possibly, up to stage 1 tricuspid regurgitation. Systolic pulmonary artery pressure – approx. 24 + 5 = up to 29 mmHg. Pulmonary hypertension was not detected. Inferior vena cava (IVC) not expanded – at the liver level, about 5.0 cm from the RA 2.3–2.5 cm, 1.6 cm closer to the RA, 1.4 cm when it flows into the RA, reacts to respiration by over 50%. No fluid was found in the pericardial cavity.

In the ICU, in addition to mechanical ventilation, the following therapy was carried out: Infusion therapy with glucose solutions and saline solutions; positional therapy; nutritional therapy; gastroprotective therapy (omez 40 mg twice/day); antibiotic therapy (levofloxacin 500 mg twice/day); Anticoagulant therapy (arixtra 2.5 mg once/day). Despite the complex ongoing therapy, the patient's condition gradually deteriorated with the development of multiple organ failure. The patient died as a result of asystole. Resuscitation measures were carried out in full, without any effect.

DISCUSSION

Based on the data published in Russia in June 2020, fatty degeneration of varying severity, more likely hypoxic and metabolic, possibly iatrogenic, was detected in the liver of the deceased. Characteristic petechial hemorrhages, lymphocytic infiltration of the portal tracts, similar to reactive interstitial hepatitis. In some cases, extensive liver necrosis was found [5].

The following are considered among the possible mechanisms of liver injury in COVID-19:

1. Immune-mediated liver injury as a result of severe inflammatory response, as inflammatory biomarkers, such as C-reactive protein (CRP), serum ferritin, LDH, D-dimer, Interleukin-6, and Interleukin-2 are significantly increased in COVID-19 [6].
2. Direct cytotoxicity as a result of active viral replication in liver cells: SARS-CoV-2 binds to target cells through ACE-2 receptors. Since ACE-2 is abundantly expressed in the liver and particularly in biliary epithelial cells, the liver is a potential target for direct infection [7].
3. Hypoxia (anoxia): Respiratory failure is the hallmark of COVID-19. That is why hypoxic hepatitis due to anoxia is often found in severe cases [8].
4. Drug-induced liver injury: Initial clinical guidelines recommended antiviral drugs for COVID-19, with some of them, including lopinavir/ritonavir, remdesivir, chloroquine, hydroxychloroquine, uminefovir, potentially hepatotoxic in some patients (and some have since been proven ineffective).
5. Reactivation of preexisting liver disease: Patients with preexisting chronic liver disease may be more susceptible to liver injury from SARS-CoV-2.18 biologic therapies, such as tocilizumab and baricitinib, can also cause hepatitis B virus (HBV) reactivation and thus lead to decreased liver function. On the other hand, it is still unknown whether SARS-CoV-2 infection aggravates cholestasis in individuals with underlying cholestasis [9].

With regard to the described observation, it is our opinion that end-stage COVID pneumonia and anoxia, complicated by DIC syndrome, were the leading factors in development of the disease that led to the patient's death.

The authors declare no conflict of interest.

REFERENCES

1. *Gong Feng, Kenneth I Zheng, Qin-Qin Yan, Rafael S Rios, Giovanni Targher, Christopher D Byrne et al*. COVID-19 and Liver Dysfunction: Current Insights and Emergent Therapeutic Strategies. *J Clin Transl Hepatol*. 2020 Mar 28; 8 (1): 18–24.
2. *Jian Wu, Shu Song, Hong-Cui Cao, Lan-Juan Li.* Liver diseases in COVID-19: Etiology, treatment and prognosis. *World J Gastroenterol*. 2020 May 21; 26 (19): 2286–2293.
3. *Isabel Garrido, Rodrigo Liberal, Guilherme Macedo*. Review article: COVID-19 and liver disease – what we know on 1st May 2020. *Aliment Pharmacol Ther*. 2020 Jun 2: 10.1111/apt.15813.
4. Journal of Hepatology. 2020; 05.
5. Patologicheskaya anatomiya COVID-19. Atlas / Pod obshchej red. O.V. Zajrat'yanca. 2020: 21.
6. *Liu J, Li S, Liu J et al.* Longitudinal characteristics of lymphocyte responses and cytokine profiles in the peripheral blood of SARS-CoV-2 infected patients. *EBioMedicine*. 2020. doi: 10.1016/j.ebiom.2020.102763.
7. *Chai X, Hu L, Zhang Y et al.* Specific ACE2 expression in cholangiocytes may cause liver damage after2019-nCoV infection. *bioRxiv*. 2020. doi: https://doi.org/10.1101/2020.02.03.931766.
8. *Jian Sun, Alessio Aghemo, Alejandro Forner, Luca Valenti.* COVID-19 and liver disease. *J Liver International*. 2020 Apr. doi: 10.1111/LIV.14470.

The article was submitted to the journal on 2.07.2020

INSTRUCTIONS FOR AUTHORS

Submitted articles should contain original work that has not been previously published and is not under consideration for publication elsewhere. We do not charge any publication fee.

The paper size should be A4 (1 copy, 1.5 pt line spacing). The text of the body of the paper should be in Times New Roman with font size 12 pt. The paper should be presented in the form of an identical Microsoft Word file on electronic media (attached CD or via e-mail).

Structure of the paper

The Title page must contain:

– Title of the paper.
– Author names (list the author's initials before listing his or her last name).
– Institutional affiliation, city and country. Spell out the name of the institution fully.

Note: List all authors in one line. Then list the institutional affiliations of all the authors below the author names. Affiliations corresponding to the author names are denoted using superscript numbers/letters.

Details about authors

Indicate the full name of each author and his or her position in at the relevant department/institution.

Corresponding author

Indicate the full name of the author, who will be communicating with the journal. Also indicate his or her address (including postal code), telephone, fax number, and e-mail address.

Abstract

Each article must have an abstract of no more than 300 words for a literature review, and no more than 200 words for clinical observation. The abstract should be a concise summary of the entire content of the paper. It is a fully self-contained, capsule description of the paper. Avoid using abbreviations and acronyms in the abstract.

The abstract of ***the original article*** should contain the following sections: ***Aim***, ***Materials and methods***, ***Results***, ***Conclusion***. The abstract should present the most important results of the research.

Do not write: "*A comparative analysis of sensitivity and specificity was conducted ...*"

Should write: "*The sensitivity was ... % and ...%, p = , specificity, respectively ...% and ...%, p = *".

Keywords

Keywords must be given at the end of the abstract. Keywords should be selected from the Medical Subject Headings (MeSH) thesaurus – a comprehensive vocabulary created and updated by the United States National Library of Medicine at http://www.ncbi.nlm.nih.gov/mesh.

Conflict of interest

All authors must disclose any actual or potential conflict of interest by including such information on the appropriate section of the article. If there is no conflict of interest, the author should also report this by writing: "The author declares no conflict of interest."

This information is indicated before the text of the article.

Text of article

Original article should include the following sections:

- Introduction
- Materialsandmethods
- Results
- Discussion
- Conclusion
- References

Review article should include literature review and analysis, with the presentation of modern sources (mainly in the last 5 years).

Clinical observation should be well illustrated (to reflect the essence of the problem) and include discussion with the use of literature data.

Reference citation numbers should be placed in square brackets: [1], [2, 5], [14–18]. ***The reference list should be arranged in the order of appearance of the in-text citations***, beginning with [1], and continuing in an ascending numerical order, from the lowest number to the highest. All values contained in the paper should be expressed or duplicated in **SI** units.

References

The author is solely responsible for the accuracy of their references to others' works. "Unpublished" or "in press" references are not allowed.

References are presented on a separate page.

The names of journals may be abbreviated in accordance with the abbreviation adopted by the particular journal.

If the cited paper has a DOI (digital object identifier) and/or PMID (Pub Med identifier), it/they must be indicated at the end of the reference text. The National Library of Medicine (NLM) writing style guide is used as the standard referencing style – (http://www.nlm.nih.gov/bsd/uniform_requirements.html. If a reference has 6 or fewer authors, display all the author names in the citation. If a reference has more than six authors, display

the names of the first six authors followed by 'et al' in the citation.

Tables and Fig.ures

Tables should be placed in the text. They must all be labeled with numbered captions clearly labeled columns and rows, convenient and simple to read. Data contained in tables must correspond to the numbers indicated in the text of the article but should not contain duplicate data. References to tables are required in the text.

Illustrations and diagrams should be submitted in electronic format (JPEG or TIFF extension with a resolution of at least 300 dpi and no smaller than 6 × 9 cm in size). Each must not exceed 1 MB in size. Diagrams must include all copyright symbols – arrows, numbers, signs, etc. Fig.ure captions should be submitted in a separate file with the **.doc* extension. First, the name is given, then all numeric and alphabetical characters (lettering) are explained.

All manuscripts should be sent to the Editor to the address:
Russian Journal of Transplantology and Artificial Organs
V.I. Shumakov National Medical Research Center of Transplantology and Artificial Organs
1, Shchukinskaya street., Moscow 123182, Russian Federation
Or by email: vestniktranspl@gmail.com

Издание зарегистрировано в Госкомпечати РФ, № 018616 от 23.03.99 г.

Подписано к печати 18.01.21.

Тираж 1000 экз.

ООО «Издательство «Триада».
ИД № 06059 от 16.10.01 г.
170034, г. Тверь, пр. Чайковского, 9, оф. 514,
тел./факс: (4822) 42-90-22, 35-41-30
E-mail: triadatver@yandex.ru
http://www.triada.tver.ru

Отпечатано в ООО «Тверская фабрика печати».
170006, г. Тверь, Беляковский пер., 46.

Заказ 0294